GEOTECHNOLOGIES AND THE ENVIRONMENT

Nancy Hoalst-Pullen · Mark W. Patterson (Eds.)

Geospatial Technologies in Environmental Management

Geotechnologies and the Environment

Volume 3

Series Editors:

Jay D. Gatrell, *School of Graduate Studies and Department of Geography, Geology, and Anthropology, Indiana State University, Terre Haute, IN, USA*

Ryan R. Jensen, *Department of Geography, Brigham Young University, Provo, UT, USA*

The "Geotechnologies and the Environment" series is intended to provide specialists in the geotechnologies and academics who utilize these technologies, with an opportunity to share novel approaches, present interesting (sometimes counter-intuitive) case studies, and most importantly to situate GIS, remote sensing, GPS, the internet, new technologies, and methodological advances in a real world context. In doing so, the books in the series will be inherently applied and reflect the rich variety of research performed by geographers and allied professionals.

Beyond the applied nature of many of the papers and individual contributions, the series interrogates the dynamic relationship between nature and society. For this reason, many contributors focus on human-environment interactions. The series are not limited to an interpretation of the environment as nature per se. Rather, the series "places" people and social forces in context and thus explore the many socio-spatial environments humans construct for themselves as they settle the landscape. Consequently, contributions will use geotechnologies to examine both urban and rural landscapes.

For further volumes:
http://www.springer.com/series/8088

Nancy Hoalst-Pullen · Mark W. Patterson
Editors

Geospatial Technologies in Environmental Management

Springer

Editors
Dr. Nancy Hoalst-Pullen
Dept. Geography & Anthropology
Kennesaw State University
Chastain Road 1000
30144 Kennesaw Georgia
USA
npullen@kennesaw.edu

Dr. Mark W. Patterson
Dept. Geography & Anthropology
Kennesaw State University
Chastain Road 1000
30144 Kennesaw Georgia
USA
mpatters@kennesaw.edu

ISBN 978-90-481-9524-4 e-ISBN 978-90-481-9525-1
DOI 10.1007/978-90-481-9525-1
Springer Dordrecht Heidelberg London New York

Library of Congress Control Number: 2010935177

Cover image: USGS/NASA Landsat Program

Printed on acid-free paper

Springer is part of Springer Science+Business Media (www.springer.com)

Foreword

Geotechnologies and the Environment: Environmental Applications and Management presents an engaging and diverse array of physically-oriented GIScience applications that have been organized using four broad themes. While the book's themes are by no means mutually exclusive, Hoalst-Pullen and Patterson provide an elegant overview of the field that frames the collection's subsequent thematic structure – Wilderness and Wildlife Response; Glaciers; Wetlands and Watersheds; and Human Health and the Environment. Over the course of the volume, the contributing authors move beyond basic (and in some respects clichéd) landscape ecology of land use change to explore human-environment dynamics heretofore not emphasized in the applied literature. In doing so, the collection presents a compelling case for the importance of developing new physically-oriented GIScience applications that reside at the nexus of social and natural systems with the explicit intent of informing public policy and/or the decision making practices of resource managers.

Individually, the chapters themselves are intentionally diverse. The diversity of the approaches, their spatial context, and emphases on management applications demonstrate the many ways in which geotechnologies can be used to address small and big problems in both developed and developing regions. The collection's internal coherence is derived – *like the book series* – from its explicit appeal to a wide variety of human-environment interactions with potential policy linkages. At its most basic level, the chapters illustrate the importance of identifying, mapping, assessing, and inventorying natural landscape features using GIS and remote sensing as a cost effective and accessible means of assessing risk, and observing change across space. Whether the reader is interested in utilizing spatial technologies to assess wildlife response of natural disasters, or to address the human element in environmental health, the individual chapters equip researchers with methodological roadmaps to design and implement GIScience applications.

Beyond the scale and scope of the projects, the constituent chapters demonstrate that in order to advance GIScience, researchers need to construct multi-disciplinary teams. As the affiliations of the authors demonstrate, GIScience researchers need to leverage the disciplinary expertise of many fields to effectively and efficiently investigate complex human-environment interactions. In turn, these teams will need to develop and deploy new inter-disciplinary methods in order to unpack the emerging problems facing researchers at a variety of scales from the local to the global.

While the book series is inherently applied, this collection moves beyond mere applications and expands the methodological frame of spatial science and geography. The chapters utilize innovative methods, often borrowed from other fields that have the potential to broaden the conceptual and methodological landscape of GIScience. For example, one chapter uses geographically weighted regression (an econometric technique more often associated with the social sciences) to assess water quality. Another contribution demonstrates that survey research methods can be used to unlock the socio-spatial dynamics of bio-solids across space. In doing so, the chapters reinforce the importance of utilizing and integrating novel techniques into enhance GIScience. Similarly, the papers demonstrate the inherent flexibility of spatial science and geotechnologies.

In conclusion, Hoalst-Pullen and Patterson have successfully recruited a diverse collection of high-quality novel applications from across physical geography and allied fields. The papers and collection represent one of the first attempts to engage a broader audience that in the process establishes the relevance of applied physical research and geotechnologies to the broader community – as well as the work of researchers situated well beyond the traditional boundaries of GIScience. Finally, Hoalst-Pullen, Patterson, and the contributors have produced a work that is not only consistent with the objectives of the series but one that will inevitably serve as a template for future volumes.

Department of Earth & Environmental Systems,
Indiana State University, Terre Haute, IN, USA

Jay D. Gatrell, Ph.D.

Acknowledgements

A well deserved thank you to Jay Gatrell for graciously introducing us to this opportunity, and for his sincere enthusiasm in our work. Thanks to Angela Lands for her help with the little details. And to our spouses, thank you for your constant support and understanding.

GIS techniques
in a management context
Nature is spatial

Contents

Contributors

Bhuiyan Alam Department of Geography and Planning, The University of Toledo, Toledo, OH 43606, USA

April Ames Department of Geography and Planning, The University of Toledo, Toledo, OH 43606, USA

José Araos Centro de Estudios Avanzados en Zonas Áridas (CEAZA), La Serena, Chile, jose.araos@gmail.com

Bereket Araya Purdue Terrestrial Observatory, Rosen Center for Advanced Computing, Information Technology at Purdue (ITaP), Purdue University, and School of Civil Engineering, Purdue University, West Lafayette, IN 47907, USA, mbereket@purdue.edu

Timothy W. Ault Department of Geography and Planning, The University of Toledo, Toledo, OH 43606, USA

Antonio Bellisario Department of Earth and Atmospheric Sciences, Metropolitan State College of Denver, Denver, CO 80217, USA, abellisa@mscd.edu

Louis C. Bender Departments of Extension Animal Sciences and Natural Resources, Animal and Range Sciences, and Fisheries and Wildlife, New Mexico State University, Las Cruces, NM 88003, USA, lbender@nmsu.edu

Teresa Benko Department of Geography and Planning, The University of Toledo, Toledo, OH 43606, USA

Larry L. Biehl Purdue Terrestrial Observatory, Rosen Center for Advanced Computing, Information Technology at Purdue (ITaP), Purdue University, West Lafayette, IN 47907, USA, biehl@purdue.edu

Michael Bisesi College of Public Health, The Ohio State University, Columbus, OH 43210, USA

Leonardo Chapa-Vargas Instituto Potosino de Investigación Científica Institute y Tecnológica, División de Ciencias Ambientales, San Luis Potosí, SLP CP 78216 México, lchapa@ipicyt.edu.mx

James Coss Department of Geography and Planning, The University of Toledo, Toledo, OH, USA

Matthew Crawford Kentucky Geological Survey, University of Kentucky, Lexington, KY 40506, USA, mcrawford@uky.edu

David Czajkowski Department of Geography and Planning, The University of Toledo, Toledo, OH 43606, USA

Kevin P. Czajkowski Department of Geography and Planning, The University of Toledo, Toledo 43606, OH, USA, kevin.czajkowski@utoledo.edu

Patti R. Dappen New Mexico Forest and Watershed Restoration Institute, New Mexico Highlands University, Las Vegas, NM 87701, USA, prdappen@nmhu.edu

Ronald W. Davis Department of Geosciences and Natural Resources, Western Carolina University, Cullowhee, NC 28723, USA, rdavis@email.wcu.edu

Souleymane Fall Department of Earth and Atmospheric Sciences, Purdue University, West Lafayette, IN 47907 USA, sfall@purdue.edu

Songlin Fei Department of Forestry, University of Kentucky, Lexington, KY 40546, USA, songlin.fei@uky.edu

Brian Fink Department of Public Health and Preventive Medicine, The University of Toledo, Toledo, OH 43606, USA

Sohaib Ghani Purdue Terrestrial Observatory, Rosen Center for Advanced Computing, Information Technology at Purdue (ITaP) and School of Electrical and Computer Engineering, Purdue University, West Lafayette, IN 47907, USA, sghani@purdue.edu

Darion Grant Purdue Terrestrial Observatory, Rosen Center for Advanced Computing, Information Technology at Purdue (ITaP), and School of Civil Engineering, Purdue University, West Lafayette, IN 47907, USA, dsgrant@purdue.edu

Nancy Hoalst-Pullen Kennesaw State University, Department of Geography and Anthropology, Kennesaw, GA 30144, USA, npullen@kennesaw.edu

Jason R. Janke Department of Earth and Atmospheric Sciences, Metropolitan State College of Denver, Denver, CO 80217, USA, jjanke1@mscd.edu

Jinha Jung Purdue Terrestrial Observatory, Rosen Center for Advanced Computing, Information Technology at Purdue (ITaP), and School of Civil Engineering, Purdue University, Lafayette, IN 47907, USA, jinha@purdue.edu

Wonkook Kim Purdue Terrestrial Observatory, Rosen Center for Advanced Computing, Information Technology at Purdue (ITaP), and School of Civil Engineering, Purdue University, West Lafayette, IN 47907, USA, wkkim@purdue.edu

Sadik Khuder Department of Public Health and Preventive Medicine, The University of Toledo, Toledo, OH 43606, USA

Brian D. Lee Department of Landscape Architecture, University of Kentucky, Lexington, KY 40546, USA, blee@uky.edu, http://www.uky.edu/Ag/LA/KLEAR/KLEAR.htm

Jorge Marín Centro de Estudios Avanzados en Zonas Áridas (CEAZA), La Serena, Chile, jorge.marin@ceaza.cl

Chetan Maringanti Purdue Terrestrial Observatory, Rosen Center for Advanced Computing, Information Technology at Purdue (ITaP), and Department of Agricultural and Biological Engineering, Purdue University, West Lafayette, IN 47907, USA, cmaringa@purdue.edu

Abdur Rahman M. Maud Purdue Terrestrial Observatory, Rosen Center for Advanced Computing, Information Technology at Purdue (ITaP), Purdue University, and School of Electrical and Computer Engineering, Purdue University, West Lafayette, IN 47907, USA, amaud@purdue.edu

Paul W. Mausel Department of Earth and Environmental Systems, Indiana State University, Terre Haute, IN 47809, USA, paul.mausel@indstate.edu

Bertin Hilaire Mbongo Purdue Terrestrial Observatory, Rosen Center for Advanced Computing, Information Technology at Purdue (ITaP) and Department of Agricultural and Biological Engineering, Purdue University, West Lafayette, IN 47907, USA, bmbongo@purdue.edu

Wendy McNulty Department of Geology, Bowling Green State University, Bowling Green, OH 43403, USA

Michael J. Medler Department of Environmental Studies, Huxley College, Western Washington University, Bellingham, WA 98225, USA, michael.medler@wwu.edu

James W. Merchant Center for Advanced Land Management Information Technologies (CALMIT), School of Natural Resources, University of Nebraska, Lincoln, NE 68583, USA, jmerchant1@unl.edu

Sheryl Milz Department of Public Health and Preventive Medicine, The University of Toledo, Toledo, OH 43606, USA

Krishnakumar Nedunuri International Center for Water Resources Management (ICWRM), Central State University, Wilberforce, OH 45384, USA

Stanislov Nikolov Department of Geography and Planning, The University of Toledo, Toledo, OH 43606, USA

Mark W. Patterson Kennesaw State University, Department of Geography and Anthropology, Kennesaw, GA 30144, USA, mpatters@kennesaw.edu

Joseph E. Quansah USGS National Wetland Research Center (NRWC), IAPWS, Leetown Science Center, Kearneysville, WV 25430, USA, jquansah@usgs.gov

Lova Rakotomalala Woodrow Wilson School of Public and International Affairs, Princeton University, Princeton, NJ 08544, USA; Purdue University Cytometry Lab. (PUCL), Cytometry for Life (C4L)-Africa, Bindley Bioscience Center, West Lafayette, IN 47907, USA, lova.rakotomalala@gmail.com, http://www.cytometryforlife.org/index.htm

Gilbert L. Rochon Purdue Terrestrial Observatory, Rosen Center for Advanced Computing, Information Technology at Purdue (ITaP), Purdue University, Lafayette, IN 47907, USA, rochon@purdue.edu

Hildred S. Rochon Alpert School of Medicine, Brown University, Providence, RI 02912, USA; Purdue University Cytometry Lab. (PUCL), Cytometry for Life (C4L)-Africa, Bindley Bioscience Center, West Lafayette, IN 47907, USA, hildred_rochon@brown.edu, http://www.cytometryforlife.org/index.htm

Joe Schibig Division of Mathematics and Science, Volunteer State Community College, Gallatin, TN 37066, USA, jschibig@volstate.edu

Alison Spongberg Department of Environmental Sciences, The University of Toledo, Toledo, OH 43606, USA

Subramania Sritharan International Center for Water Resources Management (ICWRM), Central State University, Wilberforce, OH 45384, USA

Thierno Thiam Purdue Terrestrial Observatory, Rosen Center for Advanced Computing, Information Technology at Purdue (ITaP), Purdue University, West Lafayette, IN 47907, USA, tthiam@purdue.edu

Jun Tu Department of Geography and Anthropology and the Interdisciplinary Program of Environmental Studies, Kennesaw State University, Kennesaw, GA 30144, USA, jtu1@kennesaw.edu

Angel Torres Valcarcel Department of Earth and Atmospheric Sciences, Purdue University, West Lafayette, IN 47907, USA, atorresv@purdue.edu

Robert Vincent Department of Geology, Bowling Green State University, Bowling Green, OH, USA

Richard E. Warner Office of Sustainability, University of Illinois at Urbana-Champaign, Champaign, IL 61820, USA, dickw@illinois.edu

Jason Witter Department of Environmental Sciences, The University of Toledo, Toledo, OH 45384, USA

Demetrio P. Zourarakis Kentucky Division of Geographic Information, Commonwealth Office of Technology, Frankfort, KY 40601, USA, demetrio.zourarakis@ky.gov, http://technology.ky.gov/gis/

Chapter 1
Geotechnologies in Environmental Management

Mark W. Patterson and Nancy Hoalst-Pullen

1.1 About This Series

This edited collection, as a continuation of the "Geotechnologies and Environment" series, delves into the applications of geotechnologies for researchers, academics and end users interested in the real-world applications of geospatial technologies. While the previous two volumes focused predominately on the urban environment, particularly planning and socioeconomic applications (Gatrell and Jensen 2009) and urban hazards and disaster analysis (Showalter and Lu 2010), this volume's focus is more aligned with aspects of the physical environment, and the role environmental management and natural resource practices (and to an extent its associated policies) impact physical landscapes and human-environment interfaces.

Although this volume is inherently scientific and research-oriented in nature, we argue that it still appeals to a broad audience interested in environmental applications of geospatial technologies, thus making this collection applicable to the fields of GIS, remote sensing, geography, environmental science, and forestry, among others. The local, national, and international case studies help to underscore the diffusion of geospatial applications around the world.

As Gatrell and Jensen (2009) state, the chapters in this series inherently have an applied nature to them. However, unlike some literature with an applied focus, this series (thus far) has not focused extensively on methodology. Rather, an overarching theme in the three volumes is the socio-environmental context in which geotechnologies are employed. The examples contained in this edited collection showcase work from collaborations within and among geotechnology-oriented practitioners and environment-oriented researchers; and while the majority of authors hail from academia, there are an important few that represent government agencies and various research institutions. Likewise, not all authors possess educations

M.W. Patterson (✉)
Kennesaw State University, Department of Geography and Anthropology, Kennesaw, GA 30144, USA
e-mail: mpatters@kennesaw.edu

N. Hoalst-Pullen, M.W. Patterson (eds.), *Geospatial Technologies in Environmental Management*, Geotechnologies and the Environment 3, DOI 10.1007/978-90-481-9525-1_1,

(at times inferred by current positions) within the purer "environmental" disciplines (e.g. GIS, geography, ecology, forestry etc.); however, their contributions provide innovative or distinct approaches regarding the use of geotechnologies within the framework of environmental and natural resource management. The result is a series we believe holds interest to both the physical and social science communities, and to both academia and professional practitioners. However, like previous volumes, the material also will be of interest to upper division undergraduate and graduate students, especially those looking for examples of environmental applications of geotechnologies.

1.2 About This Book

Applications of geotechnologies range from the pure social to the pure scientific. Those interested in human-environment interactions use geotechnologies to study, report and model the interrelationships between environmental phenomena and human induced factors that may exist. Arguably, nearly every agency charged with the management, assessment, measurement, modeling, preservation or conservation of natural resources employs geotechnologies.

The use of geotechnologies for environmental management can be traced to the 1960s, with separate groups from Canada and US striving to automate and digitize mapping (Goodchild 2000). Fast forward a half century later, and the literature has grown appreciably rich with examples of how geospatial technologies are used for environmental purposes. Yet notwithstanding the growth of literature and complexity of research in this area of study, there still is ample room in the literature for examples that explicitly connect applications of geotechnology with management decision making. Indeed, the inherently spatial nature of environmental and natural resources lends themselves to the use of geotechnologies, with subsequent results ideally contributing to sound management and policy decisions. In other words, an adoption of geotechnologies in environmental management is an example of research that spans the physical and social sciences.

A little over decade ago, Rindfuss and Stern (1998) speculated two possible reasons why the purer social sciences did not widely embrace spatial technology: (1) social scientists (particularly outside the discipline of geography) did not value the "spatial explicitness" provided by such technology; and (2) scientists and researchers using remote sensing imagery had little in common with social scientists regarding their techniques, theories and epistemologies (p. 2). However, considering the scientific, social, and spatial aspects of environmental management, geotechnologies have propagated – and continue to propogate – the collaborative nature of geospatial knowledge regarding the environment and its resources. As Skidmore (2002) notes, the environment is linked not only to human economic activity and well-being, but to its own inherent worth. As a result, the integration of the physical science with social science is essential to address aspects of management, including but not limited to sustainable land use and development, and its influence and impact on society from societal, political, economic and cultural perspectives.

In response, social scientists are adopting geotechnologies in their research, while physical scientists are recognizing the significant contributions their work can make in environmental decision-making processes. Indeed, the application of geotechnologies does not occur in a vacuum (as there are reasons for applying these technologies), nor does sound management decisions occur without the input of scientifically rigorous data and analyses. Likewise, agencies that fund research using or emphasizing geotechnologies are also encouraging multidisciplinary studies between scientists, both social and physical. To that end, social scientists and physical scientists have learned (and continue to learn) how to speak with each other – and not just "to" each other – using a common geospatial language that is arguably becoming ubiquitous in the literature.

However, the levels in which geotechnologies are employed still vary considerably (see Lyon and McCarthy 1995). At the fundamental level, geotechnologies aid in the basic inventory, information storage, and quantification of spatially-referenced data. At the highest level, geotechnologies can create complex, spatially integrated models of a given phenomena. At whatever level, however, the importance of the geospatial component in understanding the geography of human-environment interactions is essential to managing environmental systems.

One of the strengths of this book is all authors have explicitly linked their use of geotechnologies to environmental management implications. All chapters provide a compelling discussion on how the management of resources can benefit from information produced through the application of geotechnologies. The main focus (and resultant strength) of these case studies is the fact that all incorporate the causative and resultant roles of environmental management practices, policies or decision making perspectives within a geospatial context. Moreover, authors explicitly state the type of geotechnology (e.g. GIS, remote sensing, GPS, statistical analysis, etc.) used in their chapter, making it easy for readers to find studies using particular types of geotechnologies. Topics covered in this book range thematically from forest fires (Medler) to wetlands management (Merchant and Dappen) and range geographically from the Americas (Marín and Araos; Janke and Bellisario) to Africa (Rochon et al.). Table 1.1 provides a synopsis of the chapters in this book.

Table 1.1 Summary of topics per chapter

Chapter	Author(s)	Topic
2	Davis et al.	Wildlife Habitat and Management
3	Medler	Forest Fire Modeling
4	Fei et al.	Habitat Classification and Management Plans
5	Janke and Bellisario	Glaciers, Climate Change and Mountain Hazards
6	Marín and Araos	Glacier Inventory and Water Management
7	Merchant and Dappen	Wetlands Management and Soil Erosion
8	Zourarakis and Lee	Watershed Imperviousness and Land Cover Change
9	Tu	Urbanization and Water Quality
10	Czajkowski et al.	Human Health and Biosolids Management
11	Rochon et al.	Human Health and Environmental Applications

We have divided this book into 4 sections, namely, wilderness and wildlife, glaciers, wetlands and watersheds, and human health and the environment. Undoubtedly, some debate will ensue over our section titles and the placement of chapters, considering the nature of environmental resources and the use of geotechnolgies are not mutually exclusive. The following sections provide a brief overview of each chapter section.

1.2.1 Wilderness and Wildlife Response

The following three chapters in this section focus on the applications of geotechnologies regarding the natural environment; predominantly, the role of disturbance on the physical landscape and the wildlife found within. In Chapter 2, Davis et al. examines the black-tailed deer in relation to disturbance patterns and resultant habitat changes within and adjacent to the blast zone of Mt. St. Helens, Washington State, USA. The authors analyzed remotely sensed imagery to develop post eruption habitat maps and models for predicting deer population densities, and conducted GIS modeling to determine the impact of habitat change and road building on the deer population. From one scarred wilderness landscape to another, Medler's chapter (re)introduces us to pyrogeography, the study of the distribution and behavior of wildfires. Medler provides an overview of the advances of the field, which is heavily dependent on geotechnologies and discusses how information gleaned from computer models aid in managing fire in forest ecosystems. The section concludes with a chapter by Fei et al. and the use of geotechnologies to compile, organize and analyze data used in formulating management plans for the once dominant American chestnut (*Castanea dentata*) in Mammoth Cave National Park. Specifically, the authors provide a case study that uses geotechnology to identify existing American chestnut stands and to locate potential areas where restoration of this tree may be undertaken.

1.2.2 Glaciers

Although glaciers are not as commonly studied as an environmental resource, particularly with respect to geotechnologies, this book presents two highly complementary chapters on this portion of the cryosphere and its connection to natural resource management. Chapter 5 is a case study by Janke and Bellisario that study California rock glacier in Colorado to assess geomorphic hazards of mountainous areas. Using geotechnologies to measure flow rates and comparing these rates to regional climate data, the authors identified an area on the glacier deemed sensitive to changing climate conditions that could lead to an increase in rock falls. As the authors note, the geotechniques and associated geotechnologies used in their case study in Colorado are applicable for use in other mountainous areas. The authors then change scale and discuss potential applications and management implications of this research as related to the Andes. They recognize the significant contribution of Andean glaciers regarding water supply for humans, agriculture and industry and

note that as glaciers rapidly disappear, the possibilities for hazards increase. They issue a call for more glacier inventory studies as a start to mitigation planning. In Chapter 6, Marín and Araos seem to answer Janke and Bellisario's call for more glacier inventories. Although most glacier inventories in Chile focus on the southern regions (e.g. Patagonia) of the country, Marín and Araos point out how glaciers are a vital source of water in the arid north and do so with their case study in the Huasco watershed in northern Chile. While their chapter examines how they conducted a glacier inventory using geotechnologies, they discuss the management implications of knowing the quantity of water available (as estimated from the inventories) for economic activities such as mining and agriculture.

1.2.3 Wetlands and Watersheds

This section introduces three different applications of geotechnologies, each with a focus on water resources (excluding glaciers). In Chapter 7, Merchant and Dappen examine the Rainwater Basin, a complex of wetlands in southern Nebraska that plays a critical staging area for migratory fowl. Using geotechnologies, they present how various spatial datasets are integrated and use to create models of the wetlands. Specifically, they implement the Revised Universal Soil Lose Equation to determine the impact of increased sedimentation in the study area. Overall, the authors note how the resultant datasets and models are used to improve decision support and create priorities for wetlands management. In Chapter 8, Zourarakis and Lee use geotechnologies to compare two methods of calculating impervious surface within a watershed in Kentucky. Increases in this surface type are linked to increases in land cover change. Findings from their research are discussed in the context of watershed and stormwater management. In Chapter 9, Tu investigates the impact of urbanization on water quality in Massachusetts. Using GIS to create a spatial dataset, he applies geographically weighted regression (GWR) to analyze the spatial relationships between water quality and urbanization; the findings imply that areas deemed "urban sprawl" have a greater impact on water quality that areas deemed "highly urbanized." He concludes with a discussion on the use of GWR for environment research, policy and management practices concerning human-environment interfaces.

1.2.4 Human Health and the Environment

This final section provides two chapters that focus on the environment with respect to human health. Such a correlation is important in environmental management, as toxins, diseases, and disasters influencing the physical landscape (via air, water and land) contribute to health hazards and risks on the human landscape. In Chapter 10, Czajkowski et al. address the dumping of biosolids on agricultural lands in Ohio, in conjunction with a self-reported human health survey. The authors were interested in modeling the associated runoff from the fields and the proximity to where

respondents lived. Results showed that out of the 25 symptoms listed in the survey, 7 symptoms and 3 acute diseases (out of 14) had statistically significant relationships to the proximity to biosolid dumping locations. Like Czajkowski et al. who link location to processes and phenomena, Rochon et al. explore how geography is related to public health, environmental conditions, and disaster phenomena. They present a review of geotechnologies and its applications for public health and disaster management, including the use of remote sensing for identifying habitat conducive for infectious disease vectors, the integration of GPS and HIV/AIDS testing devices, as well as a review of relevant hydrologic models. The review explores how geotechnologies can be can generate data and information, which then lends, ultimately, to spatially informed management decisions and decision making practices and policies.

1.3 Closing Remarks

While the applied approach is a strength of the book, we are also aware that there are many more opportunities, methods and resources on which physical and social scientists can collaborate, particularly with regard to environmental management. Multidisciplinary collaborations cannot be underscored enough, as the literature is (unfortunately) littered with examples showcasing research that negates spatial patterns or processes, conclusions that disregard the location or geography in question, or policies that misinterpret intricate findings or complex results. Of these examples, the latter is of most concern to us, as there exists the propensity for poor decision making to occur among scientists (physical and social), public servants (federal to local), and policy makers due to misunderstandings in data and conclusions. Indeed, the fundamental flaw that scientists (social and physical), public servants (federal to local), and other interested parties habitually partake in is the practice of talking past each other rather than with each other.

We believe that geotechnologies help bridge the policy vs. science divides by helping both policy makers and scientists to make sense of the increasingly complex interface that exists between the human (built) and physical (natural) landscapes. We are encouraged by the applied examples in which geoeotechnologies tackle unique or complex problems; but moreso, we applaud those that integrate data from sometimes disparate sources, use sophisticated programs and analysis, and then make every effort to simplify the findings in ways that maintain scientific validity yet are logical and meaningful to decision makers. A future direction for scientists (both academic and non-academic) who study environmental or natural resources is to continue working in concert with each other and with those outside the science realm, so that the end result has the broader impacts and influence necessary for environmental management and policy decisions and practices.

Regrettably, no single volume can do adequate justice in presenting the breadth of geotechnology applications used in and for environmental management. Although we believe that this book contributes to this increasingly important body of work,

we recognize that there are many others examples with their stories waiting to be told. For now, enjoy the read.

References

Gatrell JD, Jensen RR (eds) (2009) Geotechnologies and the environment: planning and socioeconomic applications. Springer, Heidelberg.

Goodchild MF (2000) The current status of GIS and spatial analysis. J Geo Sys 2:5–10.

Lyon JG, McCarthy J (1995) Introduction to wetland and environmental applications of GIS. In: Lyon JG, McCarthy J (eds) Wetland and environmental applications of GIS. CRC Press LLC, Boca Raton, FL

Rindfuss R, Stern P (1998) Linking remote sensing and social sciences: the need and the challenges. In: Liverman D, Moran E, Rindfuss R, Stern P (eds) People and pixels: linking remote sensing and social science. National Academy Press, Washington, DC

Showalter P, Lu Y (eds) (2010) Geotechnologies and the environment: geospatial techniques in urban hazard and disaster analysis. Springer, Heidelberg

Skidmore A (2002) Introduction. In: Skidmore A (ed) Environmental modeling with GIS and remote sensing. Taylor and Francis, London

Part I
Wilderness and Wildlife Response

Chapter 2
Modeling Post-Eruption Habitat Changes for Deer at Mount St. Helens using Remote Sensing and GIS

Ronald W. Davis, Louis C. Bender, Paul W. Mausel, Leonardo Chapa-Vargas, and Richard E. Warner

Abstract GIS and remote sensing are essential tools in evaluating wildlife habitat quality. Ultimately, habitat evaluations should relate quality measures to population dynamics particularly when habitat conditions are changing. Following the 1980 eruption, populations of Columbian black-tailed deer (*Odocoileus hemionus columbianus*) (hereafter BTD) increased rapidly but quickly declined. Similar declines have been historically attributed to a predominance of even-aged closed canopy forest and low forage biomass. The link between forage and BTD population dynamics has been shown but to our knowledge no study has applied geospatial tools to quantify landscape forage conditions and relate this to population changes for BTD. We used 6 dates of post-eruption Landsat imagery (1984, 1988, 1991, 1996, 1999, and 2002) to map forest successional patterns and estimate subsequent changes in winter forage for a portion of the Mount St. Helens blast zone. We used forest maps as inputs into a GIS model estimating the supportable density of deer as an indicator of nutritional carrying capacity (NCC). To simulate potential road and cover effects on habitat use, we reduced habitat values based upon published effects of distance to roads and the ratio of forage to cover vegetation. We created 1000 randomly placed simulated home ranges to provide a bootstrap data set for model comparisons and to characterize potential uncertainty around model estimates. We compared model estimates to actual deer population estimates in the study area. Habitat models indicated a pattern of rapid forest succession and decrease in forage which closely followed the estimated population trends for the study area. Closed canopy forest dominated the landscape after 1991, and by 1996 comprised 70% of the winter range. The combined effects of roads and cover reduced estimated habitat values by over 70% ($P < 0.02$) in all years although NCC models alone were closer to actual population estimates in 1984 and 1988. By 1991, NCC reduced by road and cover effects was closer to actual trends although NCC was most highly

R.W. Davis (✉)
Department of Geosciences and Natural Resources, Western Carolina University, Cullowhee, NC 28723, USA
e-mail: rdavis@email.wcu.edu

N. Hoalst-Pullen, M.W. Patterson (eds.), *Geospatial Technologies in Environmental Management*, Geotechnologies and the Environment 3, DOI 10.1007/978-90-481-9525-1_2,

correlated ($r = 0.72$) with estimated deer numbers. Confidence intervals around NCC estimates indicated a considerable amount of variability in all years although a statistically significant decline in forage biomass was predicted between 1991 and 2002 ($P < 0.03$). Even given high variation, estimated declines in habitat quality were similar to actual population declines indicating a predictable link between habitat changes and population dynamics. Our models did detect relevant changes in habitat quality similar to population changes observed and indicate that management interspersion of early successional forests will be required for successful deer management in this region.

Keywords Mount St. Helens · Deer · Habitat quality · Remote sensing · GIS · Uncertainty · Forest Succession · Forrage · Carrying Capacity

2.1 Introduction

In evaluating habitat quality for wildlife, ecologists must often rely on geospatial modeling, adaptive management, or natural disturbances to simulate experimental conditions (Turner et al. 2001). The 1980 eruption of Mount St. Helens (MSH) provided a dramatic natural disturbance and the opportunity to study vegetation changes and wildlife recovery over time. The eruption devastated over 500 km^2 of forested landscape (Franklin et al. 1985; Frenzen and Crisafulli 1990) leaving a seemingly sterile landscape in its wake. Despite fears that recovery would take years, it began soon after the eruption (Dale et al. 2005) and included not only early successional plants and small animals, but also predators and grazing mammals including elk (*Cervus elaphus*) and BTD.

By the time of the 1980 eruption, ungulate populations in the Mount St. Helens area were considered stable. The Washington Department of Game (1983) estimated that 1600 elk and up to 5000 BTD were killed in the eruption, although natural vegetation recovery and seeding in selected areas provided high quality forage and ungulate populations recovered quickly in the years following the blast (Merrill et al. 1986). By the early 1990's ungulate populations at MSH were declining, a trend seen throughout much of the Pacific Northwest (PNW) as far back as the 1960's (Carpenter 1998).

Regional population declines for deer and elk have been attributed to an increase in even-aged regenerating forests and the subsequent decrease in forage production (Brown 1961; Taylor and Johnson 1976; Scharpf 1985; Davis 1999). Management in the industrial forests of the PNW consists of patch clear-cutting followed by a combination of herbicide treatments, slash burning (Taylor and Johnson 1976), and replanting to a single species. In productive areas, closed canopy conditions can be reached in as little as 12 years and understory biomass levels drop dramatically by this time (Taylor and Johnson 1976).

Despite the impact of even-aged forest management on deer populations, few studies exist relating landscape-scale forest changes to population dynamics

of BTD. Gilbert et al. (2007) used forest harvest records to estimate forage biomass in western Washington and found forage to be a critical determinant of the population dynamics of female deer. This was likely the first study to connect landscape forage conditions and population dynamics specifically for this species, although general applicability would depend upon the availability of forest harvest records. Remote sensing evaluations of forest conditions are common (e.g. Cohen et al. 1995) yet to our knowledge no study has used such data to relate forest conditions to population dynamics for BTD. Because it allows efficient mapping of large land areas (Skovlin et al. 2002; O'Neil et al. 2005) geospatial data is often the most practical means of quantifying habitat features for large ranging animals (Glenn and Ripple 2004) and could greatly facilitate evaluations of the potential links between habitat quality and BTD population declines.

For deer and other ungulates, population success is a direct function of the quantity and quality of available forage (Cook 2002; Cook et al. 2004), which is mostly obtained from early successional habitats on the landscape (Heffelfinger et al. 2003). In the PNW, such habitat is becoming increasingly rare due to management for later successional habitats on state and federal lands (Lutz et al. 2003). Despite this management focus, deer populations remain an economically important resource to many communities and state agencies are facing an increasing demand from constituents to restore deer populations. Given decreased logging on state and federal lands, successful habitat management for deer will increasingly depend upon cooperation between private industry and wildlife managers to develop forest management practices which produce conditions capable of supporting larger deer populations.

In relating habitat to population dynamics, wildlife managers require detailed knowledge of habitat carrying capacity (Beck et al. 2006). Generally, this is quantified from some measure of critical habitat resources such as forage. However, even given such measures, relating the quantity and distribution of habitat components to population dynamics is often difficult because the underlying mechanisms are either unknown or not incorporated into models (Morrison 2001). Such mechanistic links are critical if habitat quality is to be meaningfully evaluated (Hobbs and Hanley 1990; Eberhardt 2002), particularly in areas where habitat conditions are changing rapidly.

2.1.1 Purpose and Objectives

Our purpose was to evaluate post-eruption changes in habitat composition and structure within a portion of the MSH blast zone and to compare these trends with changes in the size of the BTD population. Specific objectives included: (1) use Landsat TM imagery to develop landcover classifications depicting forest successional stages from 1984–2002; (2) estimate the available biomass of winter forage as an indicator of habitat carrying capacity; (3) incorporate the potential mitigating effects of roads and cover; and (4) compare model estimates to estimates of population size of BTD in the study area.

2.2 Study Area

Our study was conducted within the Washington Department of Fish and Wildlife Game Management Unit (GMU) 524 and included approximately 22,300 ha to the north and northwest of Mount St. Helens (Fig. 2.1). It was bounded on the North by the Green River and on the south by portions of the North Fork Toutle River, Hoffstadt Creek, and Coldwater Lake. Physiographically, most of the area belongs in the southern Western Cascade Province (Franklin and Dyrness 1988), is located in the western Cascade Mountains, and consists of steep mountainous terrain to the east and rolling foothills to the west. Elevation ranges from 240 to 1200 m and the climate is Pacific maritime wet. Mean annual precipitation ranges from 162 cm in the Cowlitz River valley north of the study area to over 350 cm on the slopes of Mount St. Helens to the south. Approximately 45% of the annual precipitation falls as snow between November and January and summers are typically dry and cool.

Prior to the 1980 eruption, much of the study area was dominated by mature coniferous forests, with occasional scattered openings and riparian corridors. Based on elevation and moisture gradients, Franklin and Dyrness (1988) described two major forest zones in the area; the Western Hemlock (*Tsuga heterophylla*) zone at lower elevations and the Pacific Silver Fir (*Abies amabilis*) zone at middle elevations.

Approximately 3/4 of the study area was affected by the 1980 eruption with damage consisting mostly of forest blow down from the lateral blast, though some areas of forest were scorched and left standing. The western 1/4 of the study area was largely undamaged by the blast as was a small pocket of forest protected by topography directly north of Mount St. Helens (Fig. 2.1). The formation of the Mount St. Helens National Volcanic Monument (hereafter Monument) in 1982 (Fig. 2.1) allowed much of the devastated area to recover naturally. Following the eruption, lands outside the monument, mostly private industrial forest, were salvage logged and quickly replanted, accelerating forest succession in many areas (Harrington et al. 1998).

According to the Washington Department of Fish and Wildlife (WDFW), deer populations in this study area were largely wiped out in 1980, but by 1988 had reached levels similar to pre-eruption numbers of just over 5000 deer estimated in 1974. By the year 2000 estimated numbers declined to less than 500 animals.

2.2.1 Habitat Requirements for Deer

Habitat evaluations for ungulates center on estimates of available forage and, in forested environments, overstory attributes such as canopy cover are dominant factors affecting understory plant dynamics (Alaback 1982; Pieper 1990; Canham et al. 1994; Nabuurs 1996; Robinson and McCarthy 1999; Jules et al. 2008). In the western Cascades, forage habitats occur in natural and manmade openings typically less than 10 years of age and canopy closure less than 60% (Brown 1961; Crouch 1981; Witmer et al. 1985).

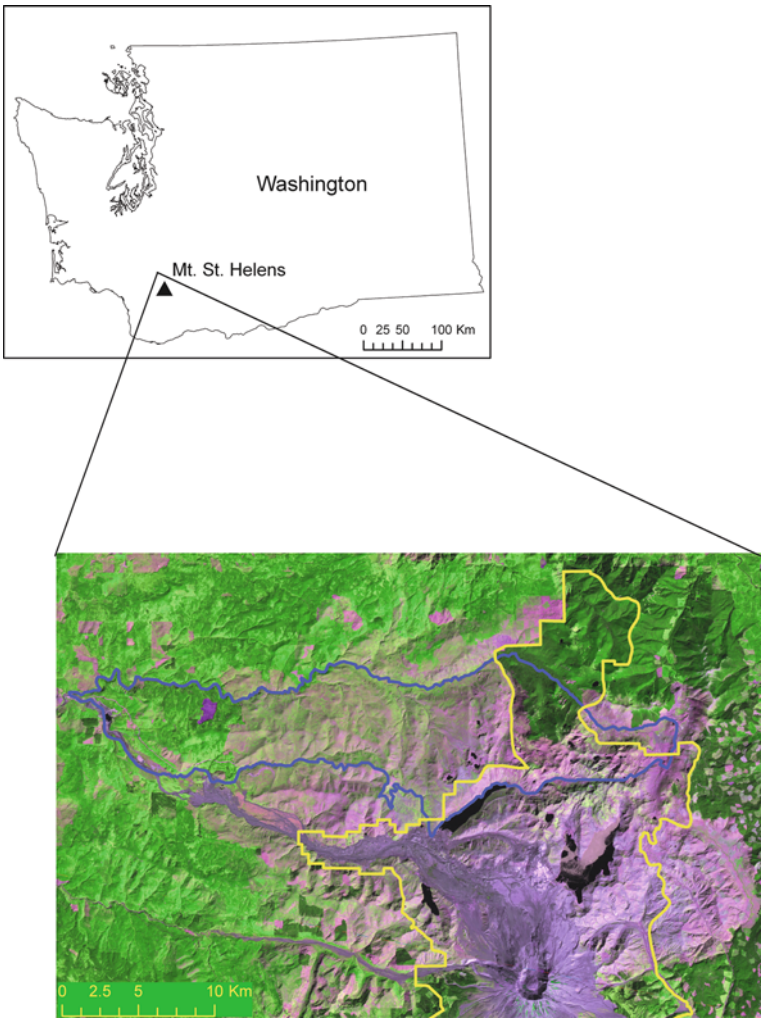

Fig. 2.1 Game management unit 524 (*blue line*) lies to the north and west of Mount St. Helens in the southwestern portion of Washington State. A 1988 Landsat TM color composite scene with the Mount St. Helens National Volcanic Monument indicated (*yellow line*). The approximate limits of the blast zone can be seen in the marked boundary distinguishing more dense green vegetation from early successional stages. The western $^{1}/_{4}$ of the study area was basically undamaged by the eruption as was a small portion in the northeastern region now contained inside the monument

Habitat capability is often defined as the biological carrying capacity of a habitat in the most extreme environmental conditions such as winter. While summer-fall forage nutrition is critical to ungulate productivity (Cook et al. 2004) this can vary greatly through the season, and thus can require extensive sampling effort. Consequently, estimates of winter forage biomass are often used as an indicator

of habitat carrying capacity, since the availability of resources during this season likely establishes the upper limit of population size, particularly during harsh winters (Scharpf 1985; Gilbert et al. 2007). The level of forage available at the end of the growing season is directly related to forest succession and canopy cover and, unless covered with snow, early successional stages provide the greatest amount of forage biomass (Scharpf 1985).

In addition to forage, habitat use can be limited by the availability of security cover and degree of disturbance from roads (e.g. Witmer et al. 1985). Disturbance associated with roads can reduce habitats and can increase disturbance and mortality in both hunting and non-hunting seasons (Cole and Smith 1983; Farmer et al. 1982). Road disturbance has been estimated to reduce elk habitat use as far as 1.8 km from the road (Rowland et al. 2000), though smaller values have been reported for elk in the Cascades (Witmer and de Calesta 1985; McCorquodale 2003) and for mule deer (*Odocoileus heminous*) (Rost and Bailey 1979).

2.2.2 Remote Sensing-GIS Based Habitat Evaluations

Remote sensing has been successfully applied in estimating forest structural attributes such as stand age or canopy cover (Cohen and Spies 1992; Cohen et al. 1995; Collins and Woodcock 1996; Mirik 2005), and has been used specifically to estimate understory forage biomass (Davis 1999; Peek et al. 2002; Davis 2005). The use of remote sensing allows the mapping of landcover over large extents which can be an invaluable resource for managers. However, even given estimates of forest seral stage, forage biomass, cover vegetation, and road density it is unlikely that simply aggregating overall values will be sufficient to predict animal population responses (e.g. see Hobbs 2003). Like many animals, ungulates make habitat selection decisions at multiple spatial scales (Senft et al. 1987, Boyce et al. 2003) and while management often occurs at landscape scales, for evaluation it is important to consider scale(s) appropriate to the ecology of foraging animals (i.e. Roloff and Kernohan 1999).

Although widely applied, geospatial data modeling can introduce potential error and uncertainty particularly when multiple data layers are used (see Fassnacht et al. 2006; Van Niel and Austin 2007). For managers, it is ultimately the degree of certainty in output map estimates which is perhaps of most use for decision making. The integration of GIS and remote sensing tools is essential in the analysis of habitat at multi-spatial and multi-temporal scales, yet issues of error and uncertainty are often not addressed. This is generally due to a lack of field data but, to the extent possible, these issues should be considered in geospatial modeling efforts.

2.3 Methods

To develop landcover classifications we used 4 Landsat TM and 2 ETM images from June 17, 1984, August 31, 1988, July 7, 1991, August 21, 1996, September 7, 1999, and August 18, 2002, respectively. Image date was based upon growing season,

availability, and cloud cover. To minimize the potential effects of topographic shadowing in vegetation classifications we calculated the NDVI (Normalized Difference Vegetation Index) to enhance vegetation signatures and provide some shadow correction in all images (Lillesand and Kiefer 2004), and then incorporated these as a layer into each multiband image. In doing this, the original spectral patterns of the various features could be examined, with the NDVI values incorporated into the spectral signature as another band. This allowed the NDVI values to be compared to other spectral values for any pixel simultaneously and thus identify some areas where shadowing may have lowered vegetation signatures within the same class.

We processed images using the isocluster algorithm for unsupervised cluster classification in Erdas Imagine 8.3. To ensure all spectral variability was captured, analyses were repeated with increasing numbers of clusters until the number of requested classes exceeded the number derived from cluster statistics. This resulted in between 45 and 90 unsupervised classes which we identified based upon spectral signatures and supportive field data available for some years. Supportive data used to identify and merge classes included a series of ground photos (by Ross Gilcrist of Weyerhaeuser Corporation) taken at the same locations yearly from 1980 to 1999, and an ARC/INFO coverage of tree planting data for a portion of the study area supplied by the Weyerhaeuser Corporation. Aerial photos from 1996 and field work conducted in July 1997 were also used to aid in confirming classifications.

We merged clusters into seven landcover vegetation and non-vegetation classes to represent the major habitat components of deer and elk described by Witmer et al. (1985) and the dominant vegetation and potential forage production (Washington Department of Fish and Wildlife, unpublished data):

- Non-Veg: Non or very low vegetation features including water, bare soil, rock, soil/sparse-vegetation. Estimated forage biomass = 0 kg/ha.
- Soil-Veg: Bare soil areas having some degree of vegetation influence on spectral signatures (or evident in ground photos) but still dominated by bare soil. Estimated forage biomass = 3 kg/ha.
- Grass-Forb: Early successional class following site preparation for replanting. Consists of mostly herbaceous vegetation although very early stands may have a significant (@ 50%) bare soil component. Estimated forage biomass = 11 kg/ha.
- Shrub-Seedling: Follows planting of seedling trees and consists of deciduous shrubs (and conifer species in later stages) overtopping Grass-Forb. Conifer and shrubs are generally less than 1 m tall. Little bare soil influence on spectral signatures. Estimated forage biomass = 56 kg/ha.
- Shrub-Seedling: Representing more advanced regeneration and co-dominance of tall shrubs, conifer saplings, and herbaceous forage. Estimated forage biomass = l97 kg/ha.
- Closed Sapling-Pole (CSP): Consists of forest stands approximately 12 years of age or older and having canopy closure of 60% or greater. Estimated forage biomass = 6 kg/ha.

- Shadow: Designation used when clusters obviously contained multiple vegetation classes or landcover features which because of shadowing could not be distinguished. Estimated forage biomass = 0 kg/ha.

2.3.1 Habitat Carrying Capacity Estimates

Estimated forage biomass was used to estimate the nutritional carrying capacity (NCC) value in a given successional stage at the end of the growing season. Since much higher elevation areas are snow-covered in winter, NCC estimates focused only on areas below approximately 823 m and assumed a season of use by BTD of 165 days (Scharpf 1985). To compute a supportable density of deer, NCC estimates were multiplied by the total area for each class, and then divided by the estimated average daily needs of deer. Estimates vary widely as to daily intake rates so we selected a middle range estimate of 1.8 kg/day (Wickstrom et al. 1984) for 165 days to determine the total number of deer/km^2 that the range could support for the winter time period.

2.3.2 GIS Model Development

The resultant NCC maps were used as inputs for an ArcGIS 9.3.1 (ESRI Redlands CA) based model that incorporated the potential negative impacts of roads (NCC_Rd), effects of forage-cover ratios (NCC_FC), and a combination of both on the NCC of BTD habitat. Models estimating specific road impacts on habitat use in ungulates have largely used the densities of open roads to reduce estimates of habitat quality or use (Witmer et al. 1985; Wisdom et al. 1986). In reality much of the effect of roads actually would depend upon the spatial configuration and degree of use (Rowland et al. 2000). In the more open forests of the west, decreased habitat use for elk has been reported as far as 1.8 km from roads (Rowland et al. 2000) and 200 m for mule deer (Rost and Baily 1979). In the denser forests of the western Cascades, McCorquodale (2003) reported avoidance of roads by elk in winter of at least 147 m, whereas Witmer and de Calesta reported a 50% decline in habitat use by Roosevelt elk (Cervus elaphus rooseveltii) within 60 m of roads but not beyond this distance.

Given that BTD do not range as far as elk, and that roads in this study area were almost entirely private secondary (gravel) roads, we applied an effect distance buffer of 100 m around roads and reduced habitat NCC by 50% to simulate reductions in habitat use. This allowed us to incorporate both a density effect while also including the effects of the spatial pattern of roads.

In evaluating cover effects, management recommendations call forage-to-cover ratios of 40:60 optimal in deer and elk habitats of western Washington (Rodrick and Milner 1991). These ratios may overstate the importance of cover in areas of limited winter severity, where optimal forage-to-cover ratios of 60:40 are more likely (Brown 1961; Thomas 1979). For our modeling we assumed no reduction in usability of forage where ratios fell between these values. Areas having either no

forage or no cover present were assumed to receive only about 10% use (see Witmer 1985) and values in between were scaled proportionally between 0.1 and 1.0. These values were then used as multipliers to reduce NCC estimates.

2.3.3 Model Comparisons

To examine habitat quality at a scale more representative of BTD movements, we used simulated deer home ranges as GIS sub-sampling windows (see Katnik and Wielgus 2005). We created 1000 random points within the winter range of deer for each date. We buffered each point with a circular polygon 1.6 km^2 (see Witmer et al. 1985) and estimated NCC independent of road and forage-cover ratio effects, and NCC as modified by the influences of roads (NCC_Rd), forage-cover ratios (NCC_FC), and both in reducing use of winter range by BTD.

The set of n=1000 home range subsamples provides a distribution for calculating probability values associated with differences between model estimates and for estimating confidence intervals around output means as an indication of variation or uncertainty (Efron and Tibshirani 1993; Bender et al. 1996). To calculate probability values for model comparisons we created difference vectors for each set of 1000 (unranked) model outputs (i.e. 1984 NCC–1988 NCC), ranked the resultant values, and calculated the number of extreme values (i.e., greater than or less than 0 depending upon whether NCC was increasing or declining between the 2 periods) to determine the probability of difference between any two models. For example, if the number of extreme values from the 1984–1988 comparison was 41/1000, then the P value associated with the difference between these two models is 0.041. We calculated 90% confidence intervals for each model by removing the extreme 5% values from each tail of the ranked frequency distribution (Bender et al. 1996).

2.4 Results

The pattern of vegetation change showed a rapid progression of forest succession from west to east (Table 2.1, Fig. 2.2). In the total (summer) range, Non-Veg was dominant in 1984 but decreased steadily as succession proceeded. A similar pattern of succession was observed in the winter range although Grass-Forb and Shrub-Seedling were dominant initially (Table 2.1, Fig. 2.2).

Eastern portions of the study area within the monument zone exhibited the least amount of successional change, with most changes being a shift from non-vegetation to Grass-Forb and Shrub-Seedling by 2002 (Fig. 2.2).

2.4.1 Habitat Quality Estimates

High forage biomass classes (Shrub-Seedling and Sapling) peaked in 1988 and 1991 then declined rapidly. Successional patterns and associated NCC estimates predicted supportable densities of approximately 7 deer/km2 in 1984, increasing to 23 by

Table 2.1 Percent landcover changes in summer and winter ranges within GMU 524 between 1984 and 2002

Summer	1984	1988	1991	1996	1999	2002
Non-Veg	36.49	13.92	7.28	6.69	3.78	2.03
Soil-Veg	1.52	18.39	11.02	9.23	11.16	10.34
Grass-Forb	17.39	15.56	22.95	12.81	11.16	9.47
Shrub-Seedling	20.88	14.03	14.24	13.66	8.89	10.39
Shrub-Seedling	0.00	14.89	18.91	7.19	10.41	10.07
CSP	22.48	22.66	23.64	49.00	53.34	56.42
Shadow	1.25	0.56	1.95	1.42	1.26	1.27
Winter	1984	1988	1991	1996	1999	2002
Non-Veg	12.62	3.37	1.40	1.31	0.86	0.79
Soil-Veg	0.35	6.46	2.73	1.37	6.59	3.47
Grass-Forb	21.49	16.49	13.54	3.77	2.23	3.97
Shrub-Seedling	30.76	16.12	16.02	7.86	3.93	3.42
Shrub-Seedling	0.00	22.71	28.76	7.30	7.10	6.23
CSP	33.42	34.19	37.09	77.88	78.83	81.63
Shadow	1.35	0.65	0.46	0.52	0.48	0.49

1991, and then declining to just under 7 deer/km2 by 2002 (Fig. 2.3). Within individual years, roads and forage-cover ratios reduced NCC values by >50% ($P < 0.02$). NCC models not corrected for roads and/or forage-cover ratios fit actual population changes in BTD in 1984 and 1988 better than did models corrected for road and/or forage-cover ratio effects (Fig. 2.3). In contrast, between 1991 and 2002, NCC_Rd, NCC_FC, and the combined models produced estimates more similar to actual deer population trends (Fig. 2.3) although simple correlations show the NCC model most associated with deer numbers across all years (Table 2.2).

2.4.2 Model Comparisons

NCC and modified estimates for each year along with bootstrap 90% confidence limits are shown in Table 2.3. Variation was high, particularly in 1988 and 1991, with NCC estimates ranging from approximately 5–51 deer/km^2. Variation was somewhat reduced in other years although confidence limits were proportionally high relative to NCC in all models (Table 2.3).

Among-year comparisons revealed no statistically significant differences between 1984 and 1988, while values in 1991, when mean NCC peaked, were marginally greater than in 1984 though not statistically significant ($P < 0.12$) (Table 2.4). A statistically significant decline in NCC occurred between 1991–1999 and 1991–2002 for all models ($P < 0.05$), with the greatest difference seen in the combined model (Table 2.4).

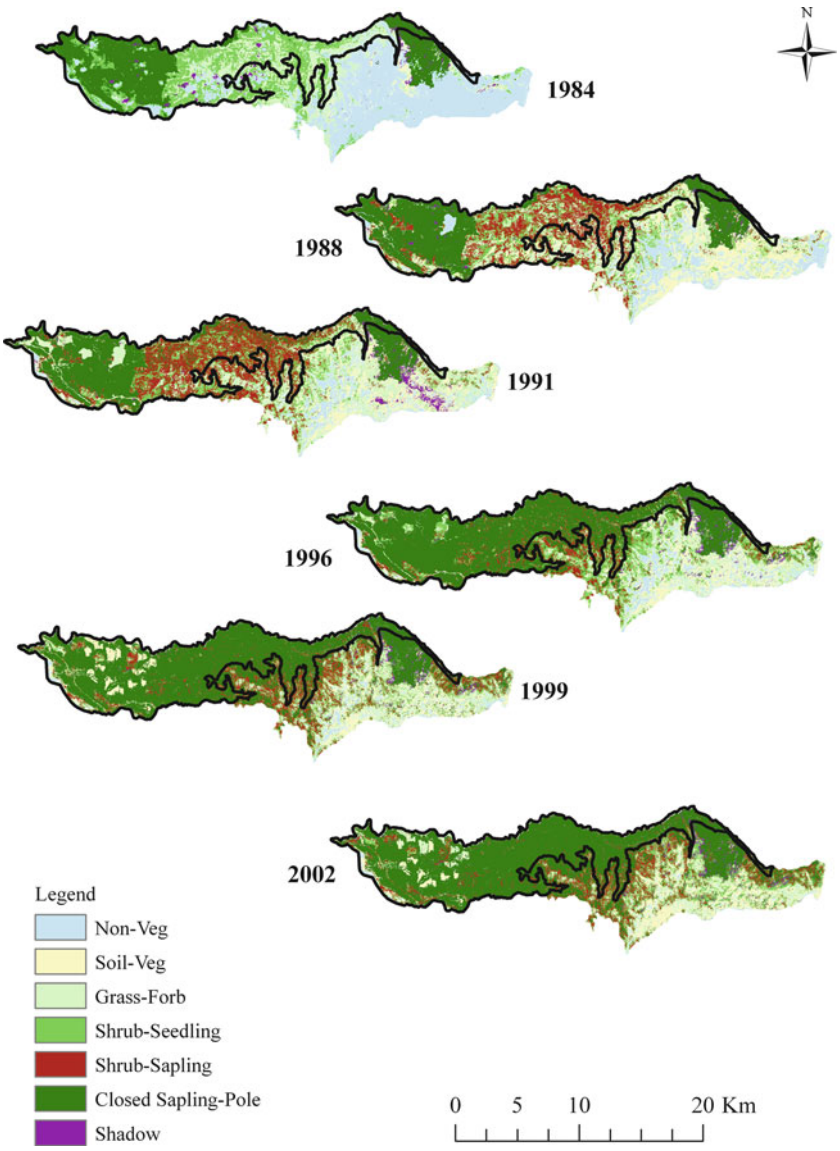

Fig. 2.2 Landcover changes within GMU 524 from 1984 to 2002 with approximate winter range of black-tailed deer indicated (*black line*). Closed canopy forest (CSP) increased markedly between 1991 and 2002 particularly within the approximate winter ranges. In the higher elevations within the monument zone early successional habitats remain dominant

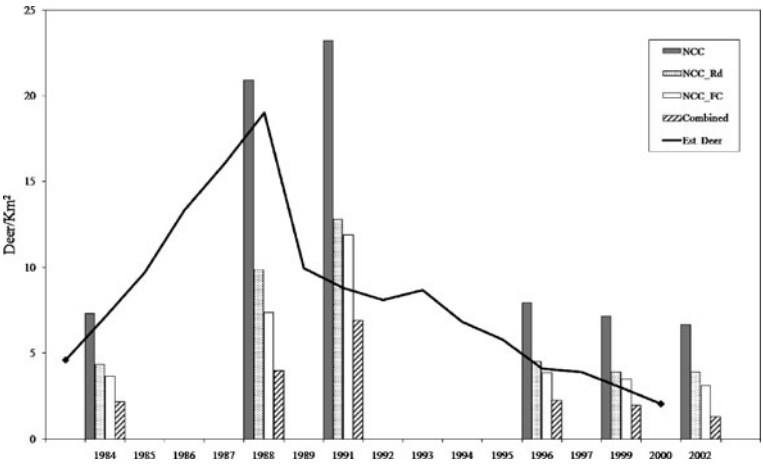

Fig. 2.3 Population changes from 1982 to 2000 (*line*) and habitat nutritional carrying capacity (NCC) estimates and modified estimates for 1984, 1988, 1991, 1999 and 2002

Table 2.2 Pearson correlations between habitat capacity estimates and deer population estimates across all years

Model	Pearson's *r*	*P* > *r*
NCC	0.72	0.16
NCC-Rd	0.62	0.26
NCC-FC	0.45	0.43
Combined	0.41	0.49

Table 2.3 Estimated supportable deer density (Deer/km^2) and 90% confidence limits (CL) under forage only (NCC), forage reduced by road effects (NCC_Rd), forage reduced by cover effects (NCC_FC) and a combined model of forage and roads

Year	NCC	CL	NCC_Rd	CL	NCC_FC	CL	Combined	CL
1984	7.3	2.7–14.5	4.3	1.8–8.2	3.7	1.4–7.3	2.2	0.9–4.1
1988	20.9	4.2–43.9	9.9	1.5–25.4	7.3	0.6–17.9	4.0	0.2–14.3
1991	23.2	5.3–50.9	12.8	3.2–27.7	11.9	1.6–24.8	6.9	1.6–12.9
1996	7.9	3.9–16.0	4.5	2.2–10.5	3.9	1.9–8.0	2.3	1.1–5.2
1999	7.1	3.1–16.2	3.9	1.7–8.5	3.5	1.5–8.4	1.9	0.8–4.3
2002	6.6	1.8–11.2	3.9	2.2–7.6	3.1	0.7–5.5	1.3	0.2–2.9

Table 2.4 Probability values associated with comparisons of habitat models among selected years

Comparison	NCC	NCC_Rd	NCC_FC	Combined
1984–1988	0.16	0.26	0.36	0.41
1984–1991	0.12	0.11	0.12	0.11
1988–1991	0.53	0.31	0.29	0.86
1988–1999	0.09	0.21	0.31	0.33
1988–2002	0.01	0.17	0.11	< 0.001
1991–1996	0.36	0.37	0.33	0.17
1991–1999	0.03	0.03	0.02	< 0.001
1991–2002	0.01	0.01	0.05	< 0.001

2.5 Discussion

The general pattern of forest succession and subsequent increases and declines in NCC in these models were consistent with the pattern suggested by BTD population trends as well as general ungulate population declines in this region (Brown 1961; Taylor and Johnson 1976; Davis 1999; Peek et al. 2002). Forage has previously been associated with population trends of BTD in western Washington (Gilbert et al. 2007), our study provides a widely applicable tool for managers allowing them to predict both the direction and magnitude of BTD population changes in response to management actions and ultimately the proportion of the management area that needs to be in various successional classes to achieve a desired relative density of BTD. Further, remote sensing and GIS allow the opportunity to assess habitats over multiple spatial and temporal scales particularly where detailed timber management data are lacking.

In addition to forage estimates, GIS modeling allowed for incorporation of effects of multiple factors that could affect BTD use of habitat (i.e., roads, forage-cover ratios) and evaluation of landscape variation at a scale potentially more ecologically relevant to BTD than previous stand-level studies. Specifically, it allowed for characterization of the uncertainty around model estimates, which can be critical in habitat studies (Bender et al. 1996). While high variation and overlapping confidence intervals meant that some model comparisons among some years did not differ statistically, all modeled estimates of NCC did demonstrate significant forage declines between 1991 and 2002, which coincided with the general population decline in deer.

To what extent the high degree of variation in annual estimates of NCC reflect actual habitat quality available to deer is unknown, although some of the variation was likely due to the random placement of home range polygons in our analyses. Foraging animals are unlikely to distribute themselves randomly over a landscape; rather, they tend to match the distribution of forage resources (see Fretwell and Lucas 1970; Stephens and Krebs 1986; Senft et al. 1987). Distribution of forage was highly variable across the landscape (Fig. 2.2), and consequently some random

polygons fell onto areas of very poor habitat that likely would have been avoided by BTD. While our use of random placement was necessary to satisfy statistical requirements, the high degree of variation in habitat quality estimated here may well have exceeded that in habitats actually selected by deer. Decoupling of statistically sound sampling requirements from the biology of animals, such as behaviors associated with foraging and use of cover by BTD (both of which, for example, would result in avoidance of sparsely vegetated habitats such as rock faces), continues to be a challenge in wildlife-habitat modeling (e.g. Yoccoz 1991) and certainly introduce variation into habitat models not present in resource selection decisions of the animals themselves.

Despite high variation, however, at least 1 model form in each year was reasonably close to deer population estimates (Fig. 2.3) and all models followed the general pattern of population increases and declines. Whether, as our models suggest, roads and cover were of less importance during early successional years (Fig. 2.3) is unknown although NCC values were most closely associated with deer numbers (Table 2.3). Despite a lack of cover immediately after the eruption, there is evidence that ungulates made significant use of early successional habitats in the blast zone (Merrill et al. 1986), likely because limits on human access, including road closures, mitigated the lack of security cover available. Early use of the area despite a lack of security cover likely allowed BTD to achieve a high quality diet, which in turn allowed for a rapid increase in population despite the lack of cover.

Using such general forage biomass estimates ultimately limits any ability to estimate anything beyond general patterns. Given time lags between changing forage quality and deer population dynamics (e.g. Gill et al. 1996; Gilbert et al. 2007) it is often the forage conditions in preceding seasons which affect population demographics (Farmer et al. 1982). The population peak in 1988 was certainly influenced by vegetation conditions prior to this time. An abundance of Shrub-Seedling resulted in the estimates of NCC peaking in 1991, yet may have represented an overestimate of forage quantity. By 1991, some Shrub-Seedling stands were surpassing 10 years of age and likely had canopy cover values exceeding 60% and thus the level of available forage in these stands was already declining (see Taylor and Johnson 1976).

Even considering high variation around model estimates, closed canopy forests clearly began to dominate this landscape within a decade of the 1980 eruption. This successional trajectory resulted in loss of understory forage and declines in BTD populations in the MSH area. Such patterns in forest succession are also occurring across the PNW region in response to state and federal management emphasis on late-successional (old growth) forests. If management to increase BTD numbers is to be successful in the PNW, then the maintenance or establishment of early successional habitats, either by natural or man-induced disturbance, needs to be integrated into forest management plans at far greater levels than at present. Similarly, appreciation of the deleterious effects of maintaining large areas of even-aged closed canopy forest on deer and other species dependent upon early-successional habitats needs increased consideration in forest planning across the PNW.

2.6 Conclusions

Effective environmental management requires detailed knowledge of resource distribution and wildlife management requires the ability to relate these resources to species ecology and population changes. The study presented here successfully estimated forest successional changes and habitat carrying capacity changes for deer at Mount St. Helens between 1984 and 2002. Like any modeling effort, the integration of multiple data layers and various model assumptions increases potential uncertainty in output estimates. This may be unavoidable in many cases, yet some estimate of potential uncertainty could improve the value of habitat models for management decision making (Davies et al. 2010). Our efforts to introduce random variation indicated a high degree of uncertainty around specific model estimates, but still indicated statistically significant declines in habitat quality. The patterns of changed indicated by our models were similar to those observed in actual deer population changes and strongly suggest that a more even interspersion of closed and open canopy forests will be essential for successful deer management in this region.

Acknowledgments We would like to thank the Weyerhaeuser Corporation for the use of forest management data. In particular we thank Ross Gilcrist for sharing his ground photos and Janette Bach helping compile GIS data. This work was partially supported by a NASA Technology Transfer grant to Indiana State University 1995–1999.

References

Alaback PB (1982) Dynamics of understory biomass in Sitka spruce-western hemlock forests of southeast Alaska. Ecol 63:1922–1948

Beck JL, Peek JM, Strand EK (2006) Estimates of elk summer range nutritional carrying capacity constrained by probabilities of habitat selection. J Wildl Manag 70:283–294

Bender LC, Roloff GJ, Haufler JB (1996) Evaluating confidence intervals for habitat suitability models. Wildl Soc Bull 24:347–352

Boyce MS, Mao JS, Merrill EH, Fortin D, Turner MG, Fryxell J, Turchin P (2003) Scale and heterogeneity in habitat selection by elk in Yellowstone National Park. Ecosci 10:421–431

Brown ER (1961) The black-tailed deer in Washington state. Biological Bulletin 13 Washington State Game Department, Olympia, WA

Canham CD, Finzi AC, Pacala SW, Burbank DH (1994) Causes and consequences of resource heterogeneity in forests: interspecific variation in light transmission by canopy trees. Can J For Res 24:337–349

Carpenter LH (1998) Deer in the west. In: deVos JC (ed) Proceedings of the 1997 Deer/Elk workshop, Rio Rico, Arizona 1–10. Arizona game and fish department, Phoenix

Cohen WB, Spies TA (1992) Estimating structural attributes of douglas-fir/western hemlock forest stands from landsat and spot IMAGERY. Remote Sens Environ 41:1–17

Cohen WB, Spies TA, Fiorella M (1995) Estimating the age and structure of forests in a multi-ownership landscape of Western Oregon, USA. Int J Remote Sens 16:721–746

Cole CA, Smith RL (1983) Habitat suitability indices for monitoring wildlife populations-evaluation. Trans N Am Wildl Nat Resour Conf 48:367–375

Collins JB, Woodcock CE (1996) An assessment of several linear change detection techniques for mapping forest mortality using multitemporal Landsat TM data. Remote Sens Environ 56:66–77

Cook JG (2002) Nutrition and food. In: Toweill DE, Thomas JW (eds) North American elk: ecology and management, 2nd edn. Smithsonian, Washington, DC, 962 p, pp 259–349

Cook JG, Johnson BK, Cook RC, Riggs RA, Delcurto V, Bryant LD, Irwin LL (2004) Effects of summer-autumn nutrition and parturition date on reproduction and survival of elk. Wildl Monogr 155: 61

Crouch GL (1981) Coniferous forest habitats: part 1 food habits and nutrition. In: Wallmo OC (ed) Mule and black-tailed deer of North America. University of Nebraska Press, Lincoln, pp 423–433

Dale VH, Swanson FJ, Crisafulli CM (2005) Disturbance, survival and succession: understanding ecological responses to the 1980 eruption of mount St Helens. In: Dale VH, Swanson J, Crisafulli CM (eds) Ecological responses of the 1980 Eruption of mount St. Helens, Springer, New York, NY

Davis RW (1999) Black-tailed deer habitat changes in a portion of the Mount St Helen's blast zone. (thesis) Indiana State University, Terre Haute, IN

Davis RW (2005) A GIS-based habitat model predicting elk nutritional condition in the Pacific Northwest (thesis) University of Illinois, Urbana, IL

Davis RW, Bender LC, Cook JG, Cook R, Warner RE (2010) Uncertainty in habitat quality maps for elk: implications for estimates of carrying capacity. In: Tate N, Fisher PF (eds) Proceedings of the 9th international symposium on spatial accuracy assessment in natural resources and environmental sciences, Leicester, UK, pp 365–368

Eberhardt LL (2002) A paradigm for population analysis of long-lived vertebrates. Ecol 83:2841–2854

Efron B, Tibshirani RJ (1993) An introduction to the bootstrap. Chapman and Hall, New York, NY

Fassnacht KS, Cohen WB, Spies TA (2006) Key issues in making and using satellite-based maps in ecology: a primer. For Ecol Manag 222:167–181

Farmer AH, Armbruster MJ, Terrell JW, Schroeder RL (1982) Habitat models for land-use planning: assumptions and strategies for development. Trans N Am Wildl Nat Resour Conf 47:47–56

Franklin JF, MacMahon JA, Swanson FJ, Sedell JR (1985) Ecosystem responses to the eruption of mount Saint Helens. Natl Geogr Res 1985:198–216

Franklin JF, Dyrness CT (1988) Natural vegetation or Oregon and Washington. Oregon State University Press, Corvallis, OR

Frenzen PM, Crisafulli CM (1990) Mount Saint Helens ten years later: past lessons and future promise. Northwest Sci 64:263–267

Fretwell SD, Lucas HL (1970) On territorial behaviour and other factors influencing habitat distribution in birds. Acta Biotherotica 19:16–36

Gilbert BA, Raedeke KJ, Skalski JR, Stringerv AB (2007) Modeling black-tailed deer population dynamics using structured and unstructured approaches. J Wildl Manag 71:144–154

Gill RMA, Johnson AL, Francis A, Hiscocks K, Peace AJ (1996) Changes in roe deer (Capreolus capreolus L) population density in response to forest habitat succession. For Ecol and Manag 88:31–41

Glenn EM, Ripple WJ (2004) On using digital maps to assess wildlife habitat. Wildl Soc Bull 31:852–860

Harrington LMB, Harrington JA, Frezen PM (1998) Vegetation change in the Mount Saint Helens (U.S.A.) blast zone, 1979–1992. Geocarto Int 13:75–82

Heffelfinger JR, Carpenter LH, Bender LC, Erickson G, Kirchoff MD, Loft ER, Glasgow WM (2003) Ecoregional differences in population dynamics. In: deVos JC, Conover MR, NE Headrick (eds) Mule deer conservation: Issues and management strategies. Jack H. Berryman Press, Logan, UT

Hobbs NT, Hanley TA (1990) Habitat evaluation: do use/availability data reflect carrying capacity? J Wildl Manag 54:515–522

Hobbs NT (2003) Challenges and opportunities in integrating ecological knowledge across scales. For Ecol Manag 181:223–238

Jules, MJ, Sawyer JO, Jules ES (2008) Assessing the relationships between stand development and understory vegetation using a 420-year chronosequence. For Ecol Manag 255:2384–2393
Katnik DD, Wielgus RB (2005) Landscape proportions versus Monte Carlo simulated home ranges for estimating habitat availability. J Wildl Manag 69:20–32
Lillesand TM, Kiefer RW (2004) Remote sensing and image interpretation. Wiley, New York, NY
Lutz DW, Wakeling BF, Carpenter L, Stroud D, Cox M, McWhirter D, Rosenstock S, Bender LC, Reeve AF (2003) Impacts and changes to mule deer habitat. In: deVos JC, Conover MR, Headrick NE (eds) Mule deer conservation: issues and management strategies. Jack H. Berryman Press, Logan, UT, pp 13–62
Merrill EH, Raedeke K, Knutson KL, Taber R (1986) Elk recolonization and population dynamics in the northwest portion of the Mount St. Helens blast zone. In: Keller SAC (ed) Mount St. Helens: five years later. East Washington University Press, Spokane, WA
McCorquodale SM (2003) Sex-specific movements of elk in relation to roads in the cascade range of Washington. J Wildl Manag 67:729–741
Mirik M (2005) Hyperspectral one-meter-resolution remote sensing in Yellowstone National Park, Wyoming: I forage nutritional values. Rangel Ecol Manag 58:452–458
Morrison ML (2001) A proposed research emphasis to overcome the limits of wildlife-habitat relationship studies. J Wildl Manag 65:613–623
Nabuurs GJ (1996) Quantification of herb layer dynamics under tree canopy. For Ecol Manag 88:143–148
O'Neil TA, Bettinger P, Marcot BG, Luscome BW, Koeln GT, Bruner HJ, Barrett CB, Pollack JA, Bernatas S (2005) Application of spatial technologies in wildlife biology. In: Braun CE (ed) Techniques for Wildlife Investigations and Management, 6th edn. The Wildlife Society, Bethesda, MD
Peek JM, Dennis B, Hershey T (2002) Predicting population trends for mule deer. J Wildl Manag 66:729–736
Pieper RD (1990) Overstory-understory relations in pinyon-juniper woodlands in New Mexico. J Range Manage 43:413–415
Robinson S, McCarthy BC (1999) Potential factors affecting the estimation of light availability using hemispherical photography in oak forest understories. J Torrey Bot Soc 126: 344 349
Rodrick E, Milner R (eds) (1991) Columbian black-tailed deer In: Management recommendations for Washington's priority habitats and species. Washington Department of Fish and Wildlife, Olympia, WA
Roloff GJ, Kernohan BJ (1999) Evaluating the reliability of habitat suitability index models. Wildl Soc Bull 27:973–985
Rost G, Bailey J (1979) Distribution of elk and mule deer in relation to roads. J Wildl Manag 43:634–641
Rowland MM, Wisdom MJ, Johnson BK, Kie JG (2000) Elk distribution and modeling in relation to roads. J Wildl Manag 64:672–684
Scharpf RW (1985) Process paper for calculating deer and elk populations In: Brown ER (ed) Management of wildlife and fish in the forests of western Oregon and Washington. USDA US For Serv Publ R6-F&WL-192-1985:1–13
Senft RL, Coughenour MB, Baily DW, Rittenhouse LR, Sala OE, Swift DM (1987) Large herbivore foraging and ecological hierarchies: landscape ecology can enhance traditional foraging theory. Biosci 37:789–799
Skovlin JM, Zager P, Johnson BK (2002) Elk habitat selection and evaluation In: Toweill DE, Thomas JW (eds) North American elk: ecology and management, 2nd edn. Smithsonian, Washington DC, pp 531–556
Stephens DW, Krebs JR (1986) Foraging theory. Princeton University Press, Princeton, NJ
Taylor RH, Johnson RL (1976) Big game habitat improvement project in western Washington 1967–1976 PR project W-74-R Final Report, Pittman-Robertson Project W-74-R. Washington Department of Game, Olympia, WA

Thomas JW (ed) (1979) Wildlife habitats in managed forests, the Blue Mountains of Oregon and Washington. USDA US For Serv Handb 553: 512

Turner MG, Gardner RH, O'Neil RV (2001) Landscape ecology in theory and practice. Springer, New York, NY

Van Niel KP, Austin MP (2007) Predictive vegetation modeling for conservation: Impact of error propagation from digital elevation data. Ecol Appls 17:266–280

Washington Department of Game (1983) Big Game Status Report, 1980-1981-1982. Olympia, WA

Wickstrom ML, Robbins CT, Hanley TA, Spalinger DE, Parrish SM (1984) Food intake and foraging energetics of elk and mule deer. J Wildl Manag 48:1285–1301

Witmer GW, de Calesta DS (1985) Effect of forest roads on habitat use by Roosevelt elk. Northwest Sci 59:122–125

Witmer GW, Wisdom M, Harshman EP, Anderson RJ, Carey C, Kuttel MP, Luman ID, Rochelle JA, Sharpf RW, Smithey D (1985) Deer and elk. In: Brown ER (ed) Management of wildlife and fish habitats in forests of western Oregon and Washington. USDA, US For Serv Publ R6-F&WL-192-1985, Washington, DC

Wisdom MJ, Bright LR, Carey CG, Hines WW, Pedersen RJ, Smithey DA, Thomas JW, Witmer GW (1986) A model to evaluate elk habitat in western Oregon. USDA, US For Serv Publ R6-F&WL-216-1986, Washington, DC

Yoccoz NG (1991) Use, overuse, and misuse of significance tests in evolutionary biology and ecology. Bull Ecol Soc Am 72:106–111

Chapter 3
Pyrogeography: Mapping and Understanding the Spatial Patterns of Wildfire

Michael J. Medler

Abstract Wildland fires are a significant and growing problem for many communities. Simultaneously, fire is increasingly seen as an important component of natural ecosystems. As human development continues to encroach on wildland areas we will see more conflicts between allowing fire in ecosystems and human development. Geotechnologies such as remote sensing, GIS, and Dendrochronology are increasingly important in improving our understanding of the complex processes involved and the complicated social issues that accompany human interaction with wildland fire. Pyrogeography is an emerging approach that brings together many disciplines and techniques to help elucidate the spatial and temporal patterns that can help us better understand wildland fire. This chapter explores the key concepts necessary to understand current spatial research in fire ecology, spatial computer fire models, and some of the spatial data sets that are used in wildland fire research in the United States.

Keywords Pyrogeography · Wildland Fire · Fire Modeling · LANDFIRE · FARSITE

3.1 Introduction

Large forest fires might seem simple to map using modern geotechnology. Satellites or aircraft can provide good post-fire imagery and all that might seem necessary is to use standard geographic information systems (GIS) to draw polygons around all the newly blackened regions. In fact almost every fire season we see these sorts of simple maps in the news. It is even a common introductory GIS class exercise to produce simple burn perimeter maps from air photos. However, wildland

M.J. Medler (✉)
Department of Environmental Studies, Huxley College, Western Washington University, Bellingham, WA 98225, USA
e-mail: michael.medler@wwu.edu

N. Hoalst-Pullen, M.W. Patterson (eds.), *Geospatial Technologies in Environmental Management*, Geotechnologies and the Environment 3, DOI 10.1007/978-90-481-9525-1_3,

fire is actually an immensely complicated phenomenon with many idiosyncrasies and complexities. Because of these complexities, effective land management and associated fire management requires a much more nuanced and sophisticated understanding of the spatial patterns and processes involved in past, present, and future fires. Therefore, to improve our management of wildland fire we need to improve our spatial understanding of these processes. This chapter is intended to provide experienced GIS and remote sensing professionals with some of the necessary background and information for effective use of geotechnology in support of wildland fire mapping, modeling, and management.

Despite the standard Hollywood portrayal of wildfires, most fires do not burn uniformly across the landscape nor destroy everything in their path, though examples of such extreme fire events do seem to be increasing, (Covington et al. 1997; Stephens and Ruth 2005). Nearly all wildland fires actually result in complicated mosaics of burned and unburned patches, and within those burned patches the effects of fire can range from minimal underbrush scorching to complete removal of most biomass even in the soils. Mapping this complex range of effects after a fire can be useful to land managers. Unfortunately, mapping such complexity can be onerous. Developing effective predictive spatial models of wildland fire is even more problematic. Though such models can be very useful planning tools, they must overcome all the vagaries and inaccuracies of the input datasets while also encountering the difficulties of quantifying such non-linear and complex phenomena as weather, climate, convective pre-heating, and even micro-site winds generated within a fire itself. If we introduce human structures and fire fighting tactics the exercise becomes even more difficult.

Because of the many ecological, geographical, and even social issues involved with wildland fire, developing GIS analysis that promotes effective forest or grassland fire management requires understanding a host of physical and social relationships that are not always easily defined or modeled, much less mapped. For example, many land managers and fire managers are looking to geotechnology to help them understand local fire histories, subtle fire effects on local ecology, likely future fire patterns, or even the impact of smoke on nearby communities. Therefore, geotechnologies such as GIS, GPS, remote sensing, and Dendrochronology can play strong roles in helping us understand the complex relationships between fire and a host of other ecological and policy issues. Beyond simply mapping fires, these techniques can help us with problems ranging from fire's role in spreading invasive species, to fire's influences on groundwater hydrology, or even suburban development patterns and zoning regulations.

Fire brings together such a complex range of phenomena that no single discipline has been able to integrate all the associated spatial, ecological, forestry, and policy issues. Over the last 20 years, however, the subfield of Pyrogeography has developed to help provide a spatial lens through which to approach wildland fire.

In this chapter, I begin with a broad overview of this emerging subfield. Then I discuss the concept of fire regimes, which is a central notion for anyone working with the spatial or temporal distribution of fire. I define and detangle the five traditional elements of fire regimes and use examples to illustrate the geospatial

techniques used to assess each of these elements. I then go on to examine two popular computer models that are used to predict how fire will move across landscapes, and then finish with an exploration of a significant new national level data set that can be used to work with GIS in Pyrogeography.

3.2 Pyrogeography

Almost every year brings new wildfire events that highlight the tragic ways fire continues to impact our society. However, over the course of the 20th century, our scientific understanding of wildland fire changed drastically. Many people no longer see each fire as a disaster, and we now understand that fire is an essential element in most terrestrial ecosystems (Bond and Keeley 2005). Over the last 20 years, a geographical approach to evaluating wildland fire has developed and greatly improved our ability to understand and differentiate the complexities of fire ecology and human interaction with fire. For example, after the Yellowstone fires of 1988 and on into the 1990s developments in remote sensing and GIS allowed many researchers and analysts to make significant strides in mapping wildland fires as well as increasing our understanding of the spatial and ecological complexity of fire. This geographic approach will only continue to develop and be increasingly vital for improved fire management. A broad collection of these spatial analysis activities in fire can now be encompassed by the emerging subfield of Pyrogeography.

The term "Pyrogeography" was coined by the University of Arizona's Dr. Steve Yool and his Geography graduate students in the mid 1990s. For the next few years Pyrogeography sessions were introduced at the annual meetings of the Association of American Geographers (AAG), with early sessions sponsored by the AAG Biogeography Specialty Group, and later sessions co-sponsored by the Remote Sensing and GIS specialty groups. In recent years, the term Pyrogeography has began to surface in many professional and academic meetings, and even in the titles of courses taught at several universities. Some wildland fire professionals are even beginning to use it in their job titles.

Pyrogeography asks questions about the spatial distribution of fire. These questions go far beyond simply what burned or how hot it burned. Rather, Pyrogeography helps us understand the complex interactions between fire and all that interacts with it, and fire interacts with almost everything. Even oceanic chemistry and Antarctic climate are affected by the atmospheric byproducts of wildland fires. Nearly all terrestrial life intersects with fire at some point in its life history, and fire is a pervasive element in the evolution and distribution of almost all land plants and even animals. In essence, Pyrogeography examines the spatial and temporal patterns of fire. However, this simple description fails to encompass all the nuances or even the underlying assumptions and complexity of Geography itself.

Geography, like History, is both a disciplinary approach and a set of organizing principles that helps us make sense of our world. As a discipline, History begins with the notion that time matters, and that understanding a sequence of events can help us understand those events. This construct encompasses the simple notion that

events are affected by the events that came before. From this framework historians can develop entire fabrics of understanding about complex and nuanced situations. Likewise, Geography allows us to examine questions from the starting assumption that location matters. Understanding what is where, and what is near or far from it can also help us understand the underlying process at work and hopefully even help us understand how to better interact with the world, which is the corner-stone of improving environmental management. Pyrogeography strives to bring exactly this sort of spatial understanding to wildland fire management and the social planning necessary for humanity to coexist effectively with this inevitable natural process.

Another central element of Geography is the notion of scale. It is critically necessary that we understand both the temporal and spatial scales of our questions or we risk misunderstanding the meaning of the answers. For an example at the broadest global scale, wildland fires interact with our atmosphere releasing huge amounts of gases and particulates each year. These gasses and particulates affect the climate and interact with the biosphere changing how and where plants grow, which influences future wildland fires. Geotechnical tools such as global remote sensing systems have radically altered our ability to map these processes across many scales. In so doing, these tools have helped us to develop better regional and even global understanding of the impacts of fire (Randerson et al. 2006).

It is the role of Pyrogeography to help us understand these spatial and temporal patterns and by extension to help elucidate and detangle the underlying processes that lead to those patterns, as well as help us understand the implications of our management policies and practices. In this way Pyrogeography goes well beyond ecology or forestry, both which are not suited for integrating such diversity issues. Because fire interacts with so many things in so many places, Pyrogeography is also a continuously expanding enterprise. However, the term tends to refer to wildland fire issues and associated ecological, climate, fire management, and urban wildland intermix (WUI) issues. Though urban and structural fire fighting are obviously both "Pyro" and "Geography" the term has not been extended into these areas. GIS and Geotechnologies have been proving themselves invaluable in the suppression and prevention of fire in the urban environment. However, structural fire is not the topic of this chapter.

3.3 Fire Regimes

To work in wildland fire analysis it is essential to understand the concept of fire regimes. Fire regimes are also one of the central notions in Pyrogeography. We differentiate fire regimes across space because fires in different places are qualitatively and quantitatively different in both how they burn and what that burning changes about ecosystems. The concept of fire regimes was introduced by Malcolm Gill in 1975 (Gill 1975). Any region of the earth with enough vegetation to burn has a fire regime, and these regimes change over space and time as vegetation and climate varies. As with many other ecological and land management concepts there is also debate about the role of humans in the "natural" processes of fire regimes.

For example, it is unclear how to define "natural" fire regimes, while accounting for thousands of years of Native American burning practices in many parts of the Americas. Many ecosystems have clearly co-evolved with continual native burning, though to what degree this burning has changed ecosystems is controversial. Nevertheless, the concept of historical fire regimes remains a useful tool to understand whether fires are changing over time, as well as differentiating types of wildland fires and the systems through which they burn (Swetnam et al. 1999).

To further illustrate the concept of fire regimes, it is helpful to consider two very different sorts of wildland fires and the areas in which they might occur. One wildland fire might sweep through 1000 acres of homogeneous grassland in the late fall, while another might burn through 1000 acres of mountainous forest at the height of summer. While our grassland may be flat with a continuous mix of vegetation, our forest consists of rough topography with 500–800 year old mixed conifers with patches of deciduous aspen and interspersed with small wetlands and meadows.

In the case of the grassland, fires might have occurred in the area every 2–6 years resulting each time in almost complete consumption of all the above ground biomass within the entire perimeter of each fire. However, within a year or two it might be difficult to see much evidence of each fire. In the forest example, a fire might be the first to occur in the area in centuries. The fire might burn in a patchy mosaic with many areas seeing only light surface fire, leaving the entire overstory undisturbed in those patches. Other areas might burn hot enough for the fire to get into the crowns and kill patches of trees for dozens of acres at a time. The evidence of this mixed conifer fire will endure on the landscape for centuries as many surviving trees will carry fire scars, dead snags will persist in other areas providing valuable habitat, and successional cycles will be reset in many forest patches but not others. A few years after the fire, new aspen groves might expand because of their competitive advantages in some of the new openings in the conifer forest, while many of the meadows might expand as small trees in the surrounding areas were killed by the light fire burning through the meadows' grass.

Each of these two hypothetical fires could be traditionally mapped with a single 1000 acre outline on a regional map and most news media would report that each fire "destroyed 1000 acres." However, the vastly different patterns on the landscape illustrate the different elements of fire regimes that would be of interest to anyone looking to better understand the processes or patterns involved with these fires. For example, understanding the subtleties of the historical local fire regimes is critical to understanding whether a given fire falls outside the historical range of variability. If a wildland fire is well outside the historical fire regime of the area, it may indicate other changes are occurring to the systems involved. Fuels may be accumulating because of decades of fire suppression, or climate change might be leading to dryer conditions. The linkages between these sorts of patterns and processes can help analysts understand the processes that are occurring.

Fire regimes are sometimes simplified to aid in mapping. For example, Fig. 3.1 shows a map of simplified computer simulated historical fire regimes. As detailed field data on historical fire frequencies can be difficult to produce, computer simulations can provide a method to map these processes over broad scales. This map

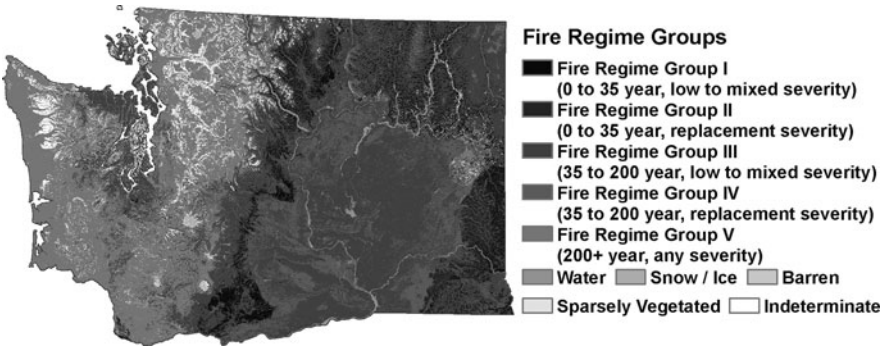

Fig. 3.1 LANDFIRE data mapping Washington State's Fire Regime Groups, which represent an integration of frequency and severity. These groups are intended to characterize the presumed historical fire regimes within landscapes based on interactions between vegetation dynamics, fire spread, fire effects, and spatial context. (Graphics by Jacob Lesser)

categorizes fire regimes into five very simple classes representing combinations of only fire frequency and expected fire severity (Fig. 3.1). However, rather than only two variables, fire regimes traditionally involve five variables that are characterized here as; fuel types and their structures, fire intensity, fire severity, fire timing, and the spatial scale of the fires.

The definitions of each of these variables can be somewhat elusive, and there has been considerable debate about how to understand, quantify, and map each of them. Even the terms themselves have been controversial. For example, Lentile et al. have suggested that "fire intensity" be replaced with "active fire characteristics" and "fire severity" be replaced with "post-fire effects" (Lentile et al. 2006). Additionally, Keeley has recommended differentiating between what he calls "fire severity" and "burn severity." For an excellent history and discussion of several of the terms associated with fire regimes see Keeley (2009). Rather than providing an exhaustive review, this chapter will simply attempt to capture the broad characteristics that make up each of these elements of fire regimes while explaining some of the subtleties and current trends, geotechnical tools, and techniques that are being used in Pyrogeography.

3.4 Fuels and Fuel Models

We often map wildland fuels with raster data sets. Each pixel is assigned a value that represents some particular structure and arrangements of living and dead fuels. However, fire burns fuels not pixels. Mapping, modeling, and understanding the spatial patterns of these fuels can be devilishly complicated. Obviously, the possible combinations of species and structures of biomass are essentially infinite. Therefore, it has been practical to develop sets of "fuel models" that represent a simplified set of all the possible combinations of fuels and species. As these models were originally developed to aid in the prediction of fire behavior, it has also been important that

these models represent easily differentiated fuel types with different expected fire behavior and fire effects.

In 1972, Rothermel introduced 11 "fire behavior fuel models" as inputs for his work with mathematical fire spread modeling (Rothermel 1972). In 1976, Albini added two more fire behavior fuel models (Albini 1976). This set was further refined and codified by Anderson in 1982 (Anderson 1982). Since that time most wildland fire professionals in the U.S. have been familiar with the 13 Anderson fuel models and they are still the basis of many computerized fire models, as well as central to mapping, planning, and even firefighting efforts. Figure 3.2 shows a map of the 13 Anderson Fire Behavior Fuel Models (Fig. 3.2).

These 13 standard models include categories such as model 1 (short grass), model 4 (chaparral), and model 13 (heavy logging slash). Each of the 13 models has assigned values for the amount of available fuels in tons per acre and the depths of those fuels. Those fuels are further divided into expected amounts of fuels in each of three size classes of dead fuels as well as the amount of live fuels. Additionally, each fuel model has an associated level of fuel moisture that is anticipated to extinguish fire in that fuel model. These 13 models greatly simplify the mathematical calculations necessary in developing predictive models of fire spread and behavior, as trying to model the infinite variety of fuels on the ground is prohibitive.

These original 13 fire behavior fuel models were intended to provide a complete set of references to which the fuels in any forest or grassland patch could be assigned. These models were also intended to help predict fire behavior during the severe conditions associated with the peak of fire season. Therefore, each model is parameterized to account for uniformly low fuel moistures. However, many contemporary uses for the fuel models are intended to predict fire behavior in other wetter and cooler conditions, such as the burning conditions when many prescribed fires are ignited.

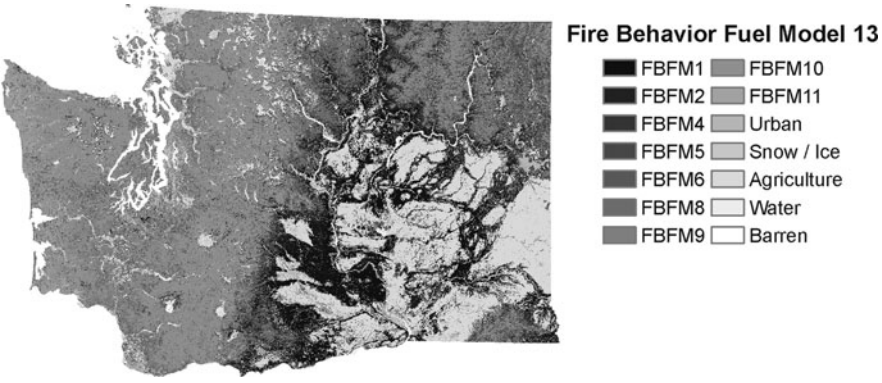

Fig. 3.2 LANDFIRE data mapping the original 13 standard fire behavior fuel models for the State of Washington. Fire behavior fuel models represent distinct distributions of fuel loading found among surface fuel components (live and dead), size classes, and fuel types (Graphics by Jacob Lesser)

Because of the limitations of the original 13 standard fuel models, some fire behavior models (such as the ones discussed later in this chapter) allow users to create custom fuel models that better capture the structures being modeled. Meanwhile there has been considerable effort to develop a new extended set of fuel models that can better capture the full extent of fuels we might find in the field without establishing an infinitely expansive set of models. One commonly used such classification is a new set of 40 fuel models that are an extension of Anderson's original 13 (Scott and Burgan 2005).

Understanding and mapping fuels remains a complicated and elusive activity. Any set of models will underrepresent the variability in the landscape and there is no obvious "correct" pixel size or mapping-unit for analyzing fuels or for mapping the underlying terrain. Even massive governmental efforts (such as the LANDFIRE project) using satellite data to map regions into the standard 13 fire behavior fuel models tend to provide controversial results (Aplet and Wilmer 2003; Provencher et al. 2009).

3.4.1 Intensity

Fire intensity theoretically refers to the amount of energy released by the process of combustion. Therefore, it would seem natural that this important constituent of fire regimes would be quantified and mapped in some measure of energy released per unit area over a specific amount of time. But wildland fire is complicated. In many large fires, thermal sensors, both on the ground and airborne, are used to identify and map hotter parts of the fire. Rather than mapping extreme fire behavior and the hottest temperatures, these tools tend to be used at night to identify areas that have remained hot after the passage of the flaming front of a fire. These are the areas fire fighters worry about extinguishing to avoid further spread of the fire during the following afternoon or in future windy conditions.

Researchers interested in fire behavior might instead be concerned with mapping the internal patterns of fire intensity or perhaps modeling future fire intensity. Depending on their ecological focus they may be interested in the peak temperature reached when the initial flaming front passes or they may be more interested in the length of time the soil was exposed to certain temperatures during the glowing combustion or smoldering phase of fire, which may continue for hours after the flame front passes, resulting in significant changes to the organic materials in soils. However, such measurements are problematic in the field. Therefore, flame height, flame length, or even the rate at which the fire spreads are often used as proxies for the energy released by fire.

Unfortunately, such measures are only able to be tied to specific amounts of energy released when they are tied to specific fuel configurations (Cheney 1990). Also, there is no single system or nomenclature for estimating the intensity of a wildland fire after it has burned. Therefore, analysts tend to look at the degree of change seen on the landscape after the fire to map the associated fire intensity.

However, this degree of change has traditionally been considered a separate and even more elusive phenomenon referred to as fire severity.

3.4.2 Severity

Fire severity is a measure of the ecological impact of fire. However, like intensity, severity is difficult to define in any practical way that can be applied across various ecosystems or at various spatial or temporal scales. We can see some of these difficulties in our previous examples of the fire in the grassland and the fire in the mixed conifer forest. The grassland fire resulted in complete removal of vegetation while in the forested example much of the biomass remained intact after the fire. Therefore, it would seem that the grassland fire was far more severe (and by extension arguably more intense). However, examining changes caused by each fire, we see that the grassland fire has few long term effects on the landscape, while some patches of the forest fire area will carry changes for centuries.

As fire has been increasingly recognized as a natural part of ecosystems rather than a negative disturbance, it has become even more difficult to determine the sorts of negative effects we had traditionally defined as "severe." Because of these sorts of complications and differences we have tended to look at changes in canopy cover to estimate severity in forested areas, while we have tended to look at soil changes in areas without extensive forest canopy. Unfortunately, these two traditions can cause confusion and they can even cause conflicts for analysts trying to map the severity of fire events that burn both forests and grasslands.

In the last decade there have been efforts to refine our understanding of severity and develop both field and remote sensing techniques to better map it. It has also become increasingly clear that mapping fire severity can be accomplished effectively with satellite imagery if we analyze the fire effects on both vegetation and soils that are detectable from above. Thematic Mapper (TM) multispectral data sets have become the standard tools for mapping fire severity (Chuvieco and Congalton 1988; Collins and Woodcock 1996; Medler and Yool 1997; Patterson and Yool 1998; Rogan and Franklin 2001). One of the key capabilities of this type of multispectral data is the production of band ratio images. TM band ratios have been used to map fire effects since at least the early 1990s (Lopez and Caselles 1991).

By the late 1990s, Key and Benson refined a specific band-ratio algorithm that used TM satellite spectral bands to map and quantify the degree to which areas on the ground had undergone vegetation removal and soil changes associated with fire (Key and Benson 1999; Key et al. 2002). This Normalized Burned Ratio differencing algorithm (dNBR, or sometimes simply NBR when using only post fire data) is now widely used in the U.S. by groups including the National Park Service and Forest Service. Key and Benson define burn severity as a "scaled index gauging the magnitude of ecological change caused by fire." However, the dNBR was developed for the forests of western North America and more work is required to develop optimal multispectral algorithms for mapping severity in a broad range of vegetation

types (Roy et al. 2006). Other recent work has also been developing more automated and regionally flexible systems for mapping severity using newer sensors such as the Moderate Resolution Imaging Spectroradiometer (MODIS) (Loboda et al. 2007; Roy et al. 2005).

Along with these developments in remote sensing, it has been necessary to develop systematic protocols for assessing fire severity in the field. Key and Benson have also introduced a measure they call the Composite Burn Index (CBI) that is coordinated with a set of field techniques to provide a field system for assessing vegetation, soil, and even longer term ecological effects of wildland fire (Key and Benson 2006). The CBI is also intended to provide a systematic method for assessing fire severity in the field, that can be directly linked to the phenomena that are being captured by the dNBR. Like the dNBI, the CBI has been developed for the forests of western North America, and developmental forms of the CBI field protocol have been used in the U.S. since 2001.

3.4.3 Timing

Once again our grassland and forest examples can provide starting points for thinking about the importance and complications of understanding the role of timing in fire regimes. In essence we are interested in how often a given place burns as well as in which seasons it tends to burn. In our grassland example we had historical evidence that the area was subjected to fire every 2–6 years. Therefore we might refer to this area having a Mean Fire Return Interval (MFRI) of 4 years. National data sets are now available that map MFRI for the entire U.S.

However, like intensity and severity, the notion of MFRI becomes more complex as we examine it more closely. One statistical problem is that knowing an area's MFRI does not mean we understand the variability around that mean. A 4 year mean might mask the possibility of much longer intervals between fires. It can also remain unclear whether this fire regime is the result of human activities or is in fact a "natural" regime. Additionally, it is unclear whether we expect the entire 1000 acre area to burn every 4 years, or as is the case in many MFRI map products, we are mapping the MFRI at exactly each pixel. For example Fig. 3.3 shows each pixel in a region mapped for expected Mean Fire Return Interval (Fig. 3.3).

One alternative to MFRI is to instead consider Fire Rotation Interval, or the amount of time it would take for an entire region of interest to be visited by fire, regardless of how many individual fires are required. Fire Rotation Interval may be of more interest to many land managers responsible for specific management units, but it is inherently subjective and tied to the size of the area of analysis, while MFRI is a less subjective point measure.

In some cases it may be important to understand the historical seasonality of the fire regime as well. Many organisms co-evolved with fire and have adapted to historical fire seasonality. For example, many plants survive hot summer fires by resprouting from their roots quickly after fire. However, prescribed fires often take place when conditions are cooler and wetter. Paradoxically, the increased soil

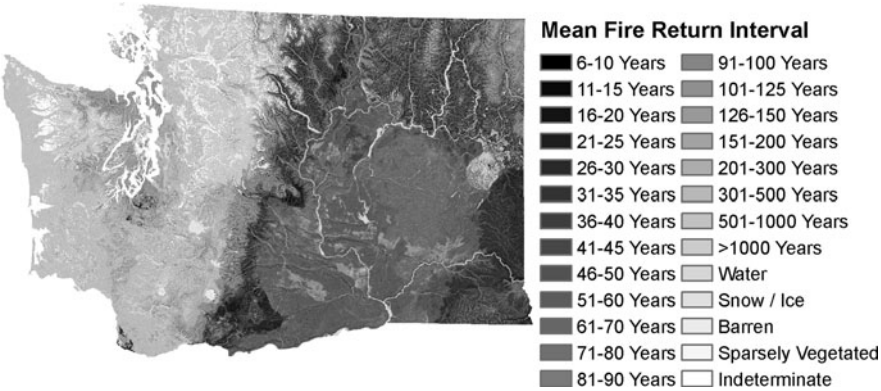

Fig. 3.3 LANDFIRE data mapping Washington State's Mean Fire Return Interval, which quantifies the average period between fires under presumed historical fire regimes. (Graphics by Jacob Lesser)

moisture levels in these seasons may transfer heat far better than dry summer soils, allowing the less intense prescribed fires to kill the roots of plants that would have survived more intense summer fires.

Even in the face of significant climate change, a strong argument can be made that understanding the historical patterns of ecosystems is critical for effective management (Swetnam et al. 1999). However, when historical records are not available, or do not extend long enough to be of use in understanding fire history, the most common tool is Dendrochronology. It is far beyond the scope of this chapter to expand on the field or statistical techniques of Dendrochronologists, but excellent texts are available.

The discipline was developed in the early 20th century by the astronomer A.E. Douglas. Douglas was trying to demonstrate that sunspots affected climate and therefore the width of annual growth rings in trees. He went on to establish the Laboratory of Tree-Ring Research at the University of Arizona in 1937. Dendrochronology has moved far beyond simply estimating the annual growing conditions encountered by single trees. In fact, the discipline has developed into a powerful geographic tool. Not only has it been central in determining the fire return patterns for many areas of the world, it has become a powerful tool in climate reconstruction and was even central in unraveling mysteries such as the nature of the relationship between North American climate and the El Niño Southern Oscillation in the southern Pacific (Swetnam and Betancourt 1990).

3.4.4 Scale

The final element of fire regimes is scale. Fire regimes can be classified by referring to the expected size of fires. Once again, this simple concept can require considerable expansion. Like MFRI, there may be unstated variability around mean fire size

within a particular fire regime. Often our historical information is incomplete and we really know very little about the sizes or internal heterogeneity of fires that occurred before written record keeping. In areas with particularly long MFRIs spanning centuries or even millennia, it can be very difficult to ascertain whether the sizes of a set of fires fall outside the natural range of variability.

In some ecosystems fire patterns remain visible in the landscape for centuries. This is particularly true in higher elevation forests with extremely long MFRIs and forest types that burn in large continuous blocks. As the forests regenerate, going through successional stages, these previous burns can be obvious hundreds of years later, even in satellite imagery. In other areas, the patterns left on the ground by fire are far less obvious, but in some of these areas Dendrochronology can once again be a valuable approach to understanding this element of fire regimes. For example, landscape level tree sampling can allow researchers to identify years in which many trees where scarred by fire. By mapping these trees and dates on a landscape it is sometimes possible to extrapolate the likely size of historical fires (Morgan et al. 2001).

Mapping the internal heterogeneity of historical fires is even more difficult than mapping perimeters. It can even be very difficult to map the internal patterns of last season's fires, much less historical fires. This is made even more difficult by the continuous nature of fire effects. Fires do not burn in a binary way across landscapes. At almost any scale of analysis, or pixel size, it is common to have many pixels that contain a mix of both burned and unburned vegetation. Therefore, most fire maps grossly underestimate the true complexity of the patterns on the ground. To make things even more difficult these patterns may express themselves differentially over time after a fire. For example, trees that seem healthy immediately after a fire can succumb later to processes such as insect infestations that were exacerbated by the fire.

Because of complications like those discussed above, fire regimes can seem impossibly complex and variable. Nevertheless the concept of fire regimes can provide considerable guidance in how we think about fires in any given area. In the same way that complicated variability in fuels can be simplified into the 13 standard fire behavior fuel models, fire regimes are often simplified into a few simple categories. For example, the national LANDFIRE data sets discussed at the end of this chapter has a data set that maps the fire regimes of the entire U.S. into just the five categories seen in Fig. 3.1. Depending on the intended use, such coarse categorization may be acceptable, while for other uses extremely detailed local fire regime information may be necessary.

3.5 Predictive Fire Modeling and Data

There are many exciting developments occurring in fire mapping, geospatial research in fire ecology, and wildland fire management. One of the most engaging of these geotechnical developments is predicative computer modeling of wildland fire behavior and fire effects. Many government agencies, academic researchers, and

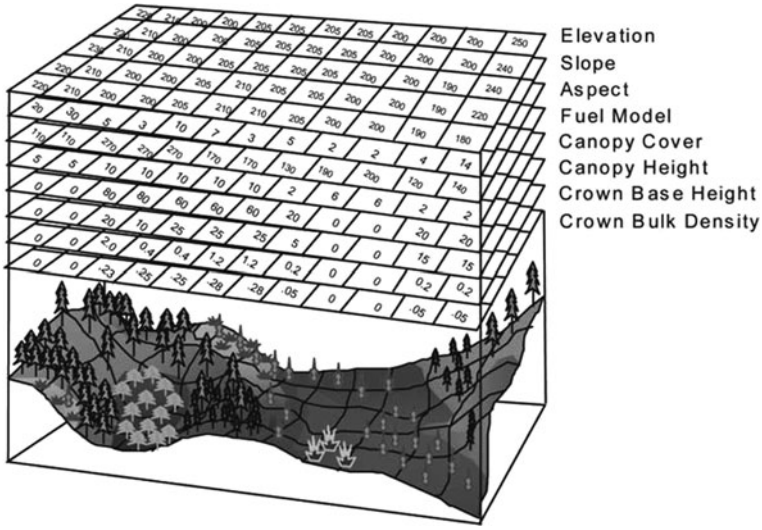

Fig. 3.4 FlamMap and FARSITE share the input data above. All input rasters must be co-registered with a shared extent and pixel size. (From Finney 2006)

private companies have been working for years to develop analytical models and computer based modeling programs to help predict the spatial patterns of wildland fires. All these projects must face the various complications discussed above as well as a host of other technical and ecological issues.

Rather than produce an exhaustive list of the efforts underway, this chapter focuses on just two major modeling packages that are now widely used in the U.S. to model how fires will burn across complex landscapes. One is the PC computer software package FARSITE, which is intended to help land managers and fire managers predict the behavior and growth of active fires with known ignition points and a known set of weather conditions. The other software package FlamMap, uses similar input data sets and algorithms to predict expected fire behavior and fire effects over an entire landscape regardless of ignition point. Rather than modeling the behavior and growth of a single fire, as with FARSITE, FlamMap predicts the expected fire behavior for each pixel in a raster data set assuming fire visits each pixel in a predetermined set of weather and fuel moisture conditions. Figure 3.4 shows an assortment of the input data layers necessary to run each of these programs (Fig. 3.4). Information on both programs and several others is available from www.firemodels.org.

3.5.1 FARSITE, Fire Simulator

The software program FARSITE (Fire Area Simulator) has become a standard tool for wildland fire modeling (Green et al. 1995; Finney 1998). It is widely used by the National Park Service, Forest Service, and other federal and state land management

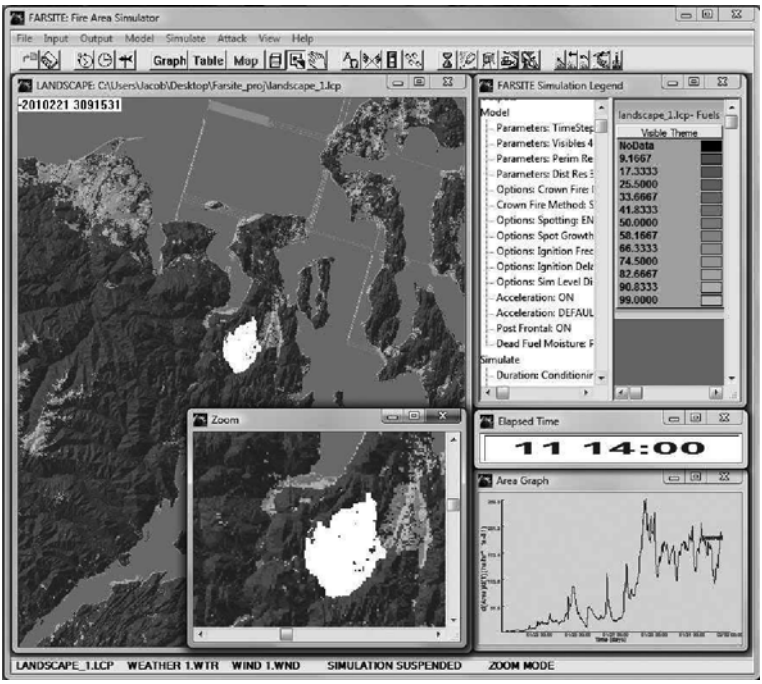

Fig. 3.5 Screen shot of FARSITE software. This is a simulation of a fire on Washington State's Olympic Peninsula. (Graphics by Jacob Lesser)

agencies. FARSITE uses an intuitive graphical user interface and 2-dimensionl fire growth and behavior models that calculate wildfire growth patterns across heterogeneous landscapes (Fig. 3.5). It can even incorporate changing weather conditions and fire suppression activities. This model can be particularly useful for analysts using multiple scenario runs to explore possible outcomes that might result from alternative firefighting strategies or changes in the weather.

FARSITE requires raster terrain data representing slope, elevation, and aspect. In addition this model requires a fuel model data layer using the standard 13 models or some other similar set of fuel models. FARSITE uses a wave propagation algorithm based on ellipses to model the progress of the fire through a set of time steps. There are many other optional inputs including weather variables such as precipitation, temperature, humidity, wind speed, wind direction, and even cloud cover. Other biophysical inputs can include canopy cover and fuel moisture. FARSITE outputs include a set of rasters representing time of arrival, fireline intensity, flame length, rate of spread, heat/area, reaction intensity, crown fire activity, and spread direction. The FARSITE support website lists the following capability of the software:

- Automatically computes wildfire growth and behavior for long time periods under heterogeneous conditions of terrain, fuels, and weather.
- Uses existing fire behavior models for surface and crown fires, post-frontal combustion, and fuel moisture.

- It is a deterministic model, meaning that you can relate simulation results directly to your inputs.
- Produces outputs that are compatible with PC and Workstation graphics and GIS software for later analysis and display.
- Can simulate air and ground suppression actions.
- Can be used for fire gaming, asking multiple "what-if" questions and comparing the results.
- Accepts both GRASS and ARC/INFO GIS raster data themes.

FARSITE also includes a manual rate of spread adjustment that analysts can use to help calibrate the output of the model to better match their expert observations or expectations. Though easily abused, this calibration capability can even be used during a fire to improve the performance of the model based on observed fire behavior in the hopes of improving the outputs of the model. Because of the level of expertise required to understand the model parameters and output, FARSITE is intended to be used by analysts familiar with wildland fire and the associated terminology and the limitations of the available input data sets, and more importantly, the limitations of FARSITE's outputs.

3.5.2 FlamMap, Predicative Fire Effects Mapping

FlamMap is an algorithmic extension of FARSITE (Finney 2006). Using the same input layers as FARSITE, FlamMap computes potential fire behavior characteristics such as spread rate, flame length, fireline intensity, and crown fire behavior for an entire FARSITE landscape. Unlike FARSITE, FlamMap uses constant weather and fuel moisture conditions for the entire landscape. The many output rasters represent expected consequences of fire for each pixel in the entire study area regardless of ignition points.

FlamMap is intended to model fire behavior assuming that fuel moisture, wind speed and wind direction are held constant across the study area. This allows for comparisons between various management scenarios. For example, FlamMap is particularly well suited to preplanning efforts and analyzing the possible ramifications of management activities such as thinning projects designed to remove biomass to reduce fire hazards (Stratton 2004). Once again, this software is also intended to be used by skilled and trained fire analysts.

Like most computer models, FARSITE and FlamMap are limited by the availability and quality of the input data. Reasonably good digital elevation models (DEMs) are now available for many areas and slope and aspect data sets are easily produced from those DEMs. Unfortunately, these fire behavior models also require fuels data, which is far more problematic. Many of the optional data layers that improve the performance of these models are even harder to acquire. Many governmental organizations have been working to gather their own vegetation and fuels data sets, but quality varies widely. Often the less common optional FARSITE input data layers, such as canopy bulk density, or height to base of crown, are simply

unavailable in appropriate input forms. To remedy this problem in the U.S., the national LANDFIRE project was initiated to assure that the fire community had access to consistently mapped, fire modeling and fire ecology data.

3.5.3 LANDFIRE, National Level Data

One of the more bold and interesting geotechnical projects in the last few years is the LANDFIRE project (Rollins 2009). This project has developed a set of 25 data layers. Each of these layers is available for the entire U.S. as raster data with a 30 m pixel resolution. The data can be downloaded from the National Map Program at http://landfire.cr.usgs.gov/viewer.

This multi agency effort has used TM satellite imagery in coordination with groups of regional experts to create a regionally calibrated national data set. The LANDFIRE project and the resulting data sets provide a remarkable number of raster data sets that are already spatially aligned and developed specifically for spatial analysis of wildland fire and other ecological issues. Working at this national scale requires considerable effort and numerous technical problems and issues are inevitable (Aplet and Wilmer 2003; Provencher et al. 2009). The resulting data sets are controversial and many users are still trying to develop locally derived data. But for a majority of the U.S., these data sets represent the only fire regime data available, and at a national level this data represents a remarkable opportunity to do broad scale analyses. Extensive information about this project is available at http://www.landfire.gov. This website explains:

> LANDFIRE, also known as the Landscape Fire and Resource Management Planning Tools Project, is a five-year, multi-partner project producing consistent and comprehensive maps and data describing vegetation, wildland fuel, and fire regimes across the United States. It is a shared project between the wildland fire management programs of the U.S. Department of Agriculture Forest Service and U.S. Department of the Interior.

The website above offers extensive metadata for all 25 data sets, including what each layer represents and how they were developed. Many of these data sets were developed using computationally intense ecological models incorporating a complicated mix of satellite data and expert opinion. The list of outputs from this project include nine fire behavior products, eight fire regime products, six vegetation data products, and two fire effects data products (Table 3.1).

The bold scope of this project is clear from this extensive list of data products. The LANDFIRE project is also planned to continuously refine and update the data sets for perpetuity. If these data sets prove to be adequate for the uses to which they are put, this collection of spatial data will radically alter the range of questions that can be asked in wildland fire and WUI research throughout the country. Similar programs in other countries will also be watching the LANDFIRE project to assess their own data programs. Ultimately LANDFIRE represents a breakthrough in data uniformity and access. It remains to be seen to what degree the wildland fire research and spatial analysis community embrace these data sets.

Table 3.1 LANDFIRE data sets available for the entire U.S.

Fire behavior data products	Fire regime data products	Vegetation and fire effects data products
• 13 Anderson (1982) fire behavior fuel models • 40 Scott and Burgan (2005) fire behavior fuel models • Canadian forest fire danger rating system • Forest canopy bulk density • Forest canopy base height • Forest canopy height • Forest canopy cover • Elevation • Aspect • Slope	• FRCC (fire regime condition class) • FRCC departure index (degree of departure from FRCC) • Fire regime groups • Mean fire return interval • Percent low-severity fire • Percent mixed-severity fire • Percent replacement-severity fire • Succession Classes	• Environmental SITE potential • Biophysical settings • Existing vegetation type • Existing vegetation height • Existing vegetation cover • Vegetation dynamics models • Fuel loading models • Fuel characteristic classification system

Source: http://landfire.cr.usgs.gov/viewer

3.6 Conclusion

Wildland fire is now generally considered a natural process that occurs in ecosystems and we now see more agencies and land managers trying to reintroduce more elements of natural fire regimes, even in areas that have seen decades of fire suppression. It is now also well understood that in many areas we can not entirely exclude fire and even if we were to succeed our efforts would have other undesirable effects on biodiversity and ecosystems. Nevertheless, as more and more human development expands into previously undeveloped land, it is inevitable that we will see wildland fire conflicting with human agendas, sometimes with tragic consequence.

One of the critical questions for Pyrogeography is: how well can we learn to live with fire and how much are we willing to change ecosystems or our practices to improve our species interactions with fire? Answers to this question will require expanding our spatial and temporal understanding of the ecological and human processes that influence and are influenced by wildland fire. Pyrogeography offers an analytical framework that can integrate the biophysical and social factors involved in this sort of complex work, in turn helping the many people who depend on improving our understanding of fire.

Acknowledgments I would like to thank Jacob Lesser for his assistance with the graphics for this chapter.

References

Albini FA (1976) Estimating wildfire behavior and effects. USDA US For Ser Gen Tech Rep INT-30, Ogden, UT

Anderson HE (1982) Aids to determining fuel models for estimating fire behavior. USDA US For Ser Gen Tech Rep INT-122, Ogden, UT

Aplet GH, Wilmer B (2003) The wildland fire challenge: focus on reliable data community protection and ecological restoration. The Wilderness Society, Washington, DC

Bond WJ, Keeley JE (2005) Fire as a global 'herbivore': the ecology and evolution of flammable ecosystems. Trends Ecol Evol 20:387–394

Cheney P (1990) Quantifying bushfires. Math Comput Model 13:9–15

Chuvieco E, Congalton RG (1988) Mapping and inventory of forest fires from digital processing of TM data. Geocarto Int 4:41–53

Collins JB, Woodcock CE (1996) An assessment of several linear change detection techniques for mapping forest mortality using multitemporal Landsat TM data. Remote Sens Environ 56: 66–77

Covington WW, Fule PZ, Moore MM, Hart SC, Kolb TE, Mast JN, Sackett SS, Wagner MR (1997) Restoring ecosystem health in ponderosa pine forests of the Southwest. J For 95:23–30

Finney MA (1998) FARSITE: fire area simulator–model development and evaluation. USDA US For Ser Res Pap RMRS-RP-4, Ogden, UT

Finney MA (2006) An overview of FlamMap fire modeling capabilities. USDA US Forest Service Proceedings RMRS-P-41, Fort Collins, CO

Gill AM (1975) Fire and the Australian flora: a review. Aust For 38:4–25

Green K, Finney MA, Campbell J, Weinstein D, Landrum V (1995) Fire! using GIS to predict fire behavior. J For 93(5):21–25

Keeley JE (2009) Fire intensity, fire severity and burn severity: a brief review and suggested usage. Int J Wildland Fire 18(1):116–126

Key CH, Benson NC (1999) Measuring and remote sensing of burn severity: the CBI and NBR. Poster abstract. In: Neuenschwander LF, Ryan KC (eds) Proceedings joint fire science conference and workshop, Vol. II. Boise, Idaho, pp 15–17

Key CH, Benson NC (2006). Landscape assessment: ground measure of severity, the composite burn index; and remote sensing of severity, the normalized burn ratio. In: Lutes DC, Keane RE, Caratti JF, Key CH, Benson, Sutherland NCS, Gangi LJ (2006) FIREMON: fire effects monitoring and inventory system. USDA For Ser Gen Tech Rep RMRS-GTR-164-CD

Key CH, Zhu Z, Ohlen D, Howard S, McKinley R, Benson N (2002) The normalized burn ratio and relationships to burn severity: ecology, remote sensing and implementation. In: Greer JD (ed) Rapid delivery of remote sensing products. Proceedings of the 9th forest service remote sensing applications conference, San Diego, CA 8–12 April 2002. American Society for Photogrammetry and Remote Sensing, Bethesda, MD

Lentile LB, Holden ZA, Smith AMS, Falkowski MJ, Hudak AT, Morgan P, Lewis SA, Gessler PE, Benson NC (2006) Remote sensing techniques to assess active fire characteristics and post-fire effects. Int J Wildland Fire 15:319–345

Loboda T, O'Neal KJ, Csiszar I (2007) Regionally adaptable dNBR-based algorithm for burned area mapping from MODIS data. Remote Sens Environ 109(4):429–442

López MJ, Caselles V (1991) Mapping burns and natural reforestation using Thematic Mapper data. Geocarto Int 6:31–37

Medler MJ, Yool SR (1997) Improving thematic mapper based classification of wildfire induced vegetation mortality. Geocarto Int 12:49–58

Morgan P, Hardy C, Swetnam TW, Rollins MG, Long DG (2001) Mapping fire regimes across time and space: understanding coarse and fine-scale patterns. Intl J Wildland Fire 10(3–4):329–342

Patterson MW, Yool SR (1998) Mapping fire-induced vegetation mortality using landsat thematic mapper data: a comparison of linear transformation techniques. Remote Sens Environ 65: 132–142

Provencher L, Blankenship K, Smith J, Campbell J, Polly M (2009) Comparing locally derived and LANDFIRE geo-layers in the Great Basin, USA. Fire Ecol 5(2):126–132

Randerson JT, Liu H, Flanner MG, Chambers SD, Jin Y, Hess PG, Pfister G, Mack MC, Treseder KK, Welp LR, Chapin FS, Harden JW, Goulden, ML, Lyons E, Neff JC, Schuur EAG, Zender CS (2006) The impact of boreal forest fire on climate warming. Sci 314(5802): 1130–1132

Rogan J, Franklin J (2001) Mapping wildfire burn severity in southern California forests and shrublands using enhanced thematic mapper imagery. Geocarto Int 16(4):91–106

Rollins MG (2009) LANDFIRE: a nationally consistent vegetation, wildland fire, and fuel assessment. Int J Wildland Fire 18:235–249

Rothermel RC (1972) A mathematical model for predicting fire spread in wildland fuels. USDA US For Ser Gen Tech Rep INT-115, Ogden, UT

Roy DP, Jin Y, Lewis PE, Justice CO (2005) Prototyping a global algorithm for systematic fire-affected area mapping using MODIS time series data. Remote Sens Environ 97(2):137–162

Roy DR, Boschetti L, Trigg S (2006) Remote sensing of fire severity: assessing the performance of the normalized burn ratio. IEEE Trans Geosci Remote Sens Lett 3(1):112–116

Scott JH, Burgan RE (2005) Standard fire behavior fuel models: a comprehensive set for use with Rothermel's surface fire spread model. USDA US For Ser Gen Tech Rep RMRS-GTR-153, Fort Collins, CO

Stephens SL, Ruth LW (2005) Federal forest-fire policy in the United States. Ecol Appl 15: 532–542

Stratton RD (2004) Assessing the effectiveness of landscape fuel treatments on fire growth and behavior. J For 102(7):32–40

Swetnam TW, Allen CD, Betancourt JL (1999) Applied historical ecology: using the past to manage for the future. Ecol Appl 9:1189–1206

Swetnam TW, Betancourt JL (1990) Fire-Southern oscillation relations in the Southwestern United States. Sci 249(4972):1017–1020

Chapter 4
Assisting Natural Resource Management in Mammoth Cave National Park Using Geospatial Technology

Songlin Fei, Matthew Crawford, and Joe Schibig

Abstract Mammoth Cave National Park contains the longest surveyed cave system in the world, recording more than 587 km of mapped passages to date. The park exhibits a delicate connection between the subsurface and the landscape surface, including a unique relationship between geology and plant habitats. A suite of geospatial technologies are available to optimize the management of these natural resources. GIS, GPS, and geospatial modelling and visualization technologies were used in this study to demonstrate the use of geospatial technologies in solving environmental and natural resources related issues. We compiled a variety of geospatial data, such as geology, soil, vegetation, and land use history, in GIS to be used to address the many environmental issues at Mammoth Cave National Park. A detailed case study was conducted to assist the classification of the American chestnut (*Castanea dentata*) habitat at the Park. Geospatial technology provides the capability to solve natural resource issues at difference scales, which help the National Park Service manage their environmental issues, satisfy federal mandates, and present environmental information that is valuable to all citizens who enjoy national parks.

Keywords Geospatial modeling · Habitat classification · Mammoth Cave National Park

4.1 Introduction

Mammoth Cave National Park is located in south-central Kentucky (Fig. 4.1). It was authorized as a national park in 1926 and was fully established in 1941 in order to preserve the cave system, scenic landscape, and diverse flora and fauna of

S. Fei (✉)
Department of Forestry, University of Kentucky, Lexington, KY 40546, USA
e-mail: songlin.fei@uky.edu

N. Hoalst-Pullen, M.W. Patterson (eds.), *Geospatial Technologies in Environmental Management*, Geotechnologies and the Environment 3, DOI 10.1007/978-90-481-9525-1_4,

Fig. 4.1 Geographic location of Mammoth Cave National Park

south-central Kentucky. The park has an area of 21,396 ha that is located on the eastern edge of the Shawnee section of the Interior Low Plateau Province (Fenneman 1938). The Green River flows east to west through the park forming moderately steep valley walls. The ridges and upper slopes of the park are capped with sandstone which produces soils that are usually acidic, sandy, and rocky. Sandstone boulders commonly outcrop on the uppermost slopes. The lower slopes and valleys are composed primarily of limestone, housing many caves and sinkholes that are part of the karst landscape. The park contains most of the longest recorded cave system in the world, with more than 587 km of mapped passages to date. Because Mammoth Cave by itself is so famous, people are often unaware that activities beyond the park boundary have an effect on the park environment.

Geospatial technology is essential for Mammoth Cave National Park needs. Karst environments are dynamic and require GIS practices that convey how these landscapes develop and can be managed. The connection between bedrock geology and other related information, such as springs, sinkholes, surface streams, elevation, vegetation, slope, and aspect will provide a platform for effective geospatial relationships. Mammoth Cave National Park has recently used 1:24,000-scale geologic data along with a variety of GIS data and customized maps to help the park meet their management needs and also provide valuable information to all visitors. In this chapter, we demonstrate the value of geospatial technology in park management by presenting a case study which uses geospatial tools to assist locating and restoring an important tree species, American chestnut (*Castanea dentata*). And we discuss the application of geospatial technologies in solving environmental issues and challenges for the park and beyond.

4.2 Regional Landscape

Geologic and environmental issues in Mammoth Cave National Park are affected by areas far beyond the park boundary. The erosional dynamics between the Green River and tributaries, rocks in the Chester Upland, karst valleys in the park, and the Pennyroyal Plateau all influence the shape of the land, cave development, flora and fauna communities, and human culture.

Erosion is the removal of rock and soil material that has been broken down or dissolved over the years. Erosion by water, whether above or below ground, is the primary agent that sculpts the landscape, and the variable rate of this erosion and the type of rock dictates the shape of the land. This is the reason we have the distinctive Chester Upland caprock sequence, karst valleys connected with the Pennyroyal Plateau, and the Dripping Springs Escarpment, which separates these major physiographic areas. The insoluble rocks, mainly sandstone, of the Chester Upland are more resistant to erosion and are able to remain high above the soluble limestone of the Pennyroyal Plateau. The Pennyroyal Plateau and its underlying limestone are spectacularly pitted with countless depressions called sinkholes. In fact, this area is commonly called the Sinkhole Plain. Sinkholes are formed when openings in the limestone are widened by the dissolving action of water. The karst valleys in between the resistant ridges of the Chester Upland once contained surface streams that drained into the Green River. As the streams eroded through the caprock and encountered the soluble limestone, the water was diverted underground, forming a karst landscape (Fig. 4.2).

A karst landscape is one that is underlain by soluble rocks (mainly limestone) and contains features such as sinkholes, caves, springs, and disappearing streams. Much of Kentucky's farmland, major cities, and recreational lands are underlain by karst, where springs and water wells provide water to thousands of people. About 55% of Kentucky is underlain by limestones that could develop a karst landscape given enough time, and about 38% of the state has at least some development of karst features (Currens 2002). The Pennyroyal Plateau is one of the largest regions

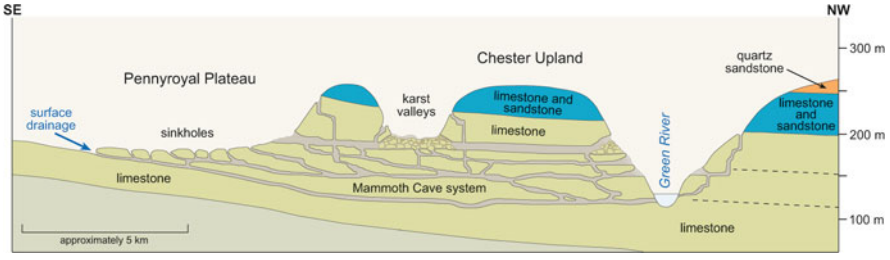

Fig. 4.2 Cross-section through the Mammoth Cave area showing the relationship of the cave to the landscape and geology. Modified from Palmer, A.N. (1981; credit to Authur N. Palmer and Cave Books for its use)

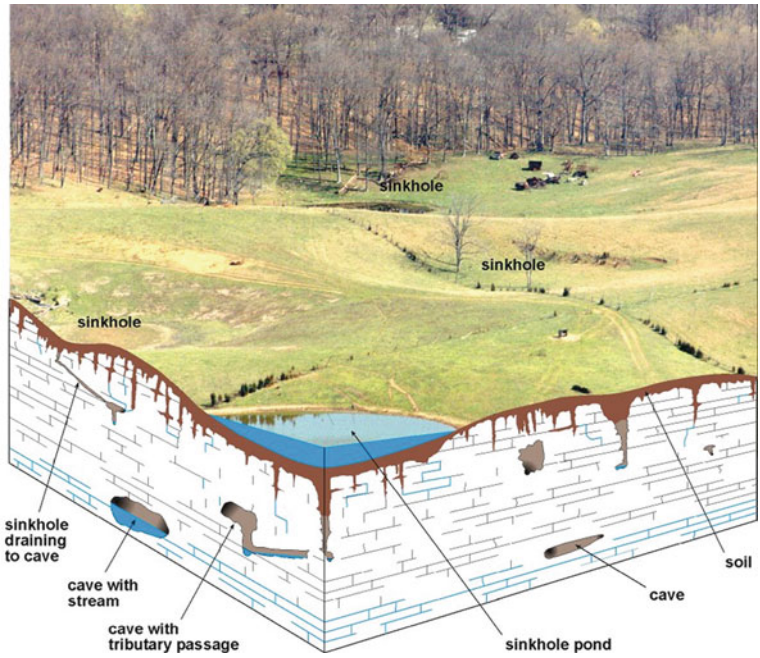

Fig. 4.3 Some important karst features typical of the Mammoth Cave area. The area commonly referred to as the sinkhole plain is in the foreground and the tree-line represents that start of the Dripping Spring Escarpment. Illustration by Collie Rulo, courtesy of the Kentucky Geological Survey

of cavernous rocks in the United States (Palmer, 1981). The karst in Kentucky forms in a continuing process, taking millions of years to develop. As water from precipitation and surface streams moves underground, the limestone bedrock is slowly dissolved away by naturally occurring weak acids. This process results in the beautiful landscape we see today in the Mammoth Cave area (Fig. 4.3).

The types of trees and other plants at any place in the park depend heavily on the slope, aspect, and geology, which in turn strongly influence the type of soil that develops. Aspect, or the direction a slope faces, controls how much sunlight a site receives and how much water is lost to evaporation. Geology also has major effects on moisture loss because in areas underlain with limestone, the water will drain down through the rock. This is why on one limestone site we will find prickly pear cactus (*Opuntia* spp.), and at another we will find maidenhair ferns (*Adiantum* spp.). It is also why some plant communities in the park are fire adapted, and others are not (Olson and Noble 2005).

The physical attributes of karst geomorphic processes above and below the surface requires detailed spatial analysis to understand the scope of the environmental and natural resource issues. Because of the sensitive karst landscape in Mammoth Cave National Park, there are many concerns that require attention. The geology and karst geomorphology of Mammoth Cave also has a profound impact on vegetation and wildlife habitat classification. Different rock types, slope angles, and aspects

generate complex soil development and thus the diversity of flora and fauna that thrive in a particular area. For example, in areas underlain with limestone, surface water will drain down through openings in the rock affecting the moisture content of the soil creating particular habitat types. Classifying the physical attributes of plant and animal communities and understanding the spatial distribution is a challenge. A better understanding of the distribution and abundance can help to more efficiently manage and protect the unique flora and fauna and maintain a healthy ecosystem. In the following case study, we will demonstrate the power of geospatial technology, including GIS, GPS, and geospatial modelling, to analyze and visualize the habitat classification of American chestnut in the special landscape settings of the park.

4.3 Case Study–American Chestnut Habitat Mapping

In recent years, as the development of blight-resistant American chestnut trees by The American Chestnut Foundation's backcross breeding program has been nearing fruition, Mammoth Cave National Park has been a site of intensive field research on this species. American chestnut was historically one of the most ecologically and economically important trees in the eastern U.S. (MacDonald 1978). It is known to have been a component of forests in and around Mammoth Cave National Park based on the documents recorded by European explorers (Hussey 1884) and witness tree data (McEwan et al. 2005). Chestnut blight (*Cryphonectria parasitica*) severely decimated chestnut trees in the park during the 1930s and 1940s, and by the late 1940s nearly all the large chestnut trees were dead (Schibig et al. 2005). Throughout its range, this once dominant canopy tree has been reduced mostly to small trees less than 3 m in height, and its reproduction by seed is now quite rare. The loss of this historically dominant and important forest species is one of the most important events in the history of the eastern North American forest. In this project, we developed and tested a geospatial modeling approach to classify American chestnut habitat in Mammoth Cave National Park which would allow us to efficiently locate new chestnut specimens for the backcross breeding program and to identify suitable sites for chestnut restoration within the park and in other areas with similar site conditions.

4.3.1 Field Inventory

American chestnut sprouts were inventoried in Mammoth Cave National Park from 2003 to 2006 over diverse landscapes during the summer when chestnut sprouts were more easily identifiable. The "Big Woods," a chestnut-rich old growth forest (120 ha) in the northeastern section of the park, was thoroughly sampled. Elsewhere, we searched for chestnut specimens in most sections of the park that were reasonably accessible (usually within a hiking distance of 2 km from a road). For each specimen, geographic coordinates were recorded with a GPS unit.

4.3.2 Geospatial Modeling

4.3.2.1 Input Variables and Geospatial Model

Seven geospatial variables were used in our spatial model (Table 4.1). Slope curvature, elevation, topographic position index (TPI), slope steepness, and topographic relative moisture index modified (TRMIM) were derived from a 10 m resolution digital elevation model (DEM). Slope curvature, elevation, and slope steepness were calculated using tools in ArcGIS 9.2 (ESRI, Redlands, CA, U.S.), TPI was calculated in ArcView 3.2 (ESRI, Redlands, CA, U.S.) using an extension developed by Jenness (2006), and TRMIM was calculated in Arc Grid (ESRI, Redlands, CA, U.S.) based on Parker's (1982) method.

Fine resolution geologic data were also used in the model. Geological formations were classified into sandstone and limestone families, and Euclidean distance from the boundary of the sandstone and limestone formations was then calculated and used in the spatial model. Land use history was reconstructed based on the 1936 vegetation map provided by Mammoth Cave National Park. Based upon the park's history, we classified the non-restocking and restocking categories as historical agricultural areas (previously cultivated fields and pastures) and the other forest types as non-agricultural areas. Because land use history is a human driven factor, we did not include it in the habitat modeling; however, it was incorporated as a mask to build a map to locate surviving American chestnut sprouts.

In this study, only locations that had American chestnut were recorded. Hence, we employed ecological niche factor analysis (ENFA) to compute the habitat suitability map for American chestnut based on the presence-only data in Biomapper 3.1 (Hirzel et al. 2004). Data partitioning was applied to all the 2156 located American chestnut sprouts as a validation technique (Fielding and Bell 1997). Two thirds of the specimens (1437) were used in Biomapper to build the spatial model, and one third (719) were used to validate the model. Distributions of the variables that were recognized by ENFA to have strong association with chestnut were further compared between chestnut locations and random locations (1437 spatially random points generated in GIS) in the study area. Biomapper only provides a range of

Table 4.1 Variables used in spatial modeling of American chestnut habitat at Mammoth Cave National Park, Kentucky, U.S.A.

Variables	Resolution (m)	Description
Curvature	10	Convexity/concavity based on DEM
Elevation	10	Elevation from DEM
Topographic Position Index	10	Topographic position based on DEM (Jenness 2006)
Slope	10	Slope steepness (degree)
Topographic relative moisture index	10	Dryness-wetness index based on DEM (Parker 1982)
Land use history	–	Land use history (based on 1936 vegetation map)
Geology	–	General bedrock formation (1:24,000 scale)

habitat suitability (0–100) and does not provide a threshold of favorable habitat. We used the maximum cumulative frequencies difference method (Browning et al. 2005, Thompson et al. 2006) to estimate the threshold. We first obtained habitat suitability values for both the 1437 chestnut locations and 1437 random locations, calculated the cumulative frequencies of locations by habitat suitability, and then located the maximum difference between the two cumulative frequencies to define the threshold.

The chestnut habitat suitability model derived from ENFA was then evaluated using two approaches. The first approach was a cross-validation conducted in Biomapper 3.1. The study area was partitioned into 10 sub-regions to validate the model. To minimize the spatial-autocorrelation among the partitions, locations of the partitions were randomly assigned. In the second approach, we used the 719 trees that were not included in the habitat modeling process to test the robustness of the model derived from ENFA. Percentages of trees located in each of the probability zones in the habitat model were then calculated.

4.3.2.2 Site Affinity

Land use history had a strong influence on the current distribution of chestnut sprouts. Based on the 1936 vegetation map, about 41% of the area (8057 ha) was classified as abandoned agricultural land. A total of 89% of the chestnut sprouts at Mammoth Cave National Park were located within areas that were classified as non-agricultural land. The remaining 11% of the chestnuts were located within a 10 m buffer around non-agricultural land. Thus, all surviving chestnuts were located in or close to the edge of historically non-agricultural land.

Based on ENFA, chestnut distribution was strongly associated with elevation, geological formation, slope steepness, and TPI (Table 4.2). The three factors derived from ENFA explained 98.3% of the total variance. Factor 1 which explained most of the variance (78.8%) was mainly due to the Euclidean distance from the edge of sandstone and limestone formations. Factor 2 was mainly due to slope steepness and elevation, while Factor 3 was mainly contributed by elevation and TPI. Geological formation, as expressed as the Euclidean distance, had a much stronger association with the distribution of chestnut than the other variables.

Different distribution patterns by variables derived from chestnut locations and random locations further confirmed the strong site affinities of chestnut sprouts. American chestnut sprouts were more frequently located near the border line of sandstone and limestone formations, with a buffer zone of 40 m on each side of the boundary. Chestnut sprouts were distributed in a relative narrow elevation range of 200–240 m. Chestnut sprouts were also more frequently located on steeper slopes between 25 and 40°. The distribution patterns between chestnut locations and random points of TPI do not have an apparent difference compared to the other three variables. However, relatively low chestnut presence on ravine and ridge sites compared to higher presence on steep mid-slopes and upper slopes was observed. A comprehensive view of chestnut distribution on a topographic relief geological map further confirms the association between chestnut sprouts and environmental variables (Fig. 4.4).

Table 4.2 Score matrix of the first three factors derived from ecological niche factor analysis (ENFA) and the percentage of variance explained by each factor

	Factors		
Variables	1	2	3
Curvature	0.008	0.010	–0.012
Elevation	0.024	0.614	–0.596
EucDist[a]	0.997	–0.056	–0.255
Slope	0.056	0.776	–0.251
TPI	–0.041	0.092	–0.513
TRMIM	–0.015	–0.093	0.063
Variance explained (%)	78.8	14.2	3.6

[a]EucDist – Euclidean distance from the boundary of sandstone and limestone formations

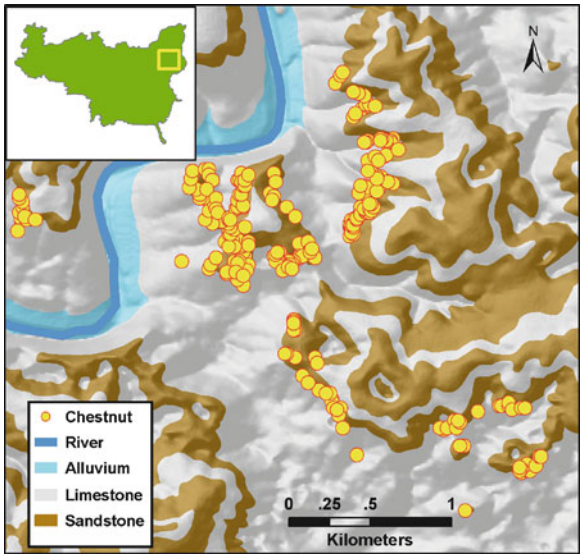

Fig. 4.4 Example of American chestnut spatial distribution on a topographic relief geological map

4.3.2.3 Habitat Map

Two habitat maps were generated for American chestnut (Fig. 4.5). Biomapper 3.1 provided a continuous habitat suitability map with a range of 0–100, but it did not provide a threshold of favorable chestnut habitats. Based on the maximum cumulative frequencies difference method (Browning et al. 2005; Thompson et al. 2006), the threshold of favorable chestnut habitats was around a habitat suitability of 16. To make a conservative prediction, we defined areas as favorable chestnut habitats when habitat suitability was greater than 20. Figure 4.5a is the overall habitat suitability map for American chestnut in Mammoth Cave National Park. About 28% of the areas were predicted as favorable chestnut habitats. Suitable habitat

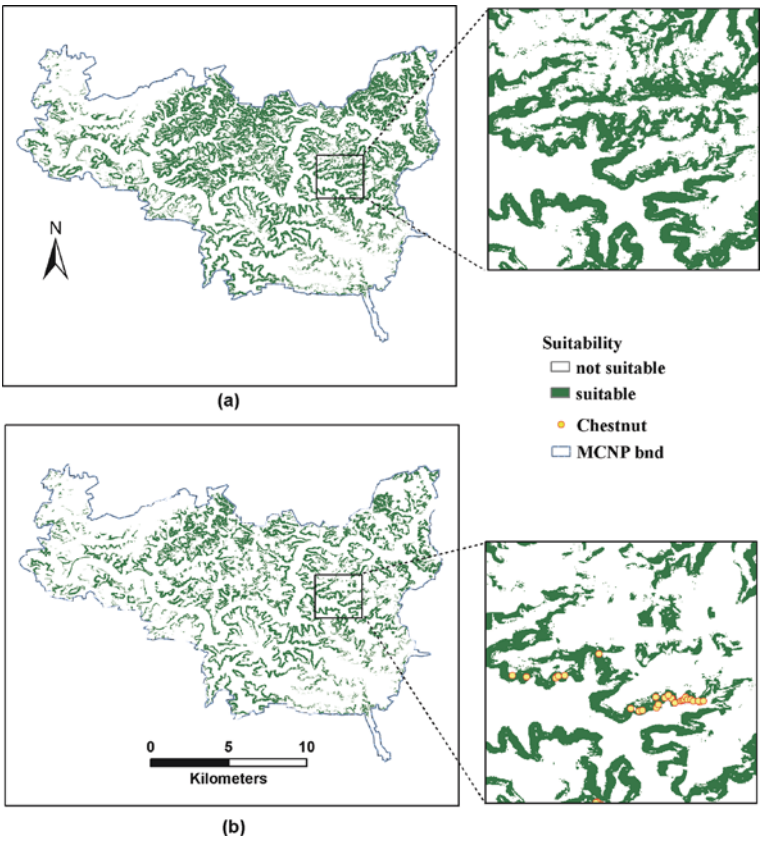

Fig. 4.5 American chestnut habitat suitability map for Mammoth Cave National Park: (**a**) – suitability map for the entire park; and (**b**) – suitability map on the historically non-agricultural lands. Areas with habitat suitability greater than 20 are defined as favorable chestnut habitats

for American chestnut was more concentrated in the north-central and northeastern part of Mammoth Cave National Park. Figure 4.5a provides a spatial reference for future chestnut restoration. On the second map, a mask of land use history was added (Fig. 4.5b). Land use history was superimposed on Fig. 4.5a, and areas classified as historical agricultural lands were masked, because most chestnut sprouts were located on non-agricultural land. With the land use history mask, about 19% of the areas were predicted as favorable chestnut habitat. Figure 4.5b provides a spatial reference for locating more chestnut specimens in the future. Based on the map, there would be a low chance of finding American chestnut sprouts in the western and southeastern portion of Mammoth Cave National Park.

4.3.2.4 Model Validation

Cross-validation was first applied to validate the chestnut habitat model. The Continuous Boyce Index (CBI, Boyce et al. 2002) was 0.97 ± 0.03 for the

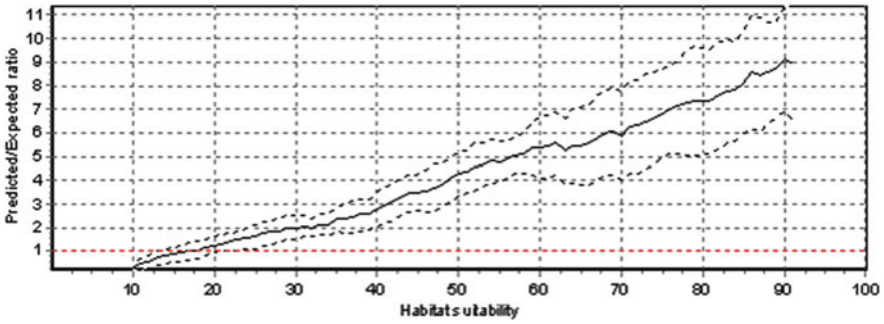

Fig. 4.6 Relationship between F-ratio (predicted chestnut presence/expected chestnut presence) and habitat suitability

cross-validation on the 10 sub-regions random partition. The CBI indicated that our chestnut habitat suitability model was very robust (CBI equal to one indicates a perfect model). In addition, the relationship between the F-ratio (predicted/expected ratio) and probability of habitat suitability derived from the cross-validation also indicated that the chestnut habitat suitability model was robust (Fig. 4.6) because the F-ratio was low when habitat suitability was low, F-ratio was high when habitat suitability was high, and F-ratio was nearly monotonically increasing (Boyce et al. 2002).

We also used partitioning (Fielding and Bell 1997) to validate the model based on locations of the 719 chestnuts that were not included in the habitat suitability model. Over 87% of the chestnuts were located in the areas that were classified as favorable chestnut habitats (Fig. 4.5b), and nearly 90% of the chestnuts were located in the favorable habitats if the habitat suitability map was smoothed by a 3×3 filter with a mean value algorithm. This further indicates that our chestnut suitability model was robust.

Our results indicate that geospatial analysis was effective in determining both the chestnut site affinities and habitat map in Mammoth Cave National Park. American chestnut sprouts have a relatively narrow niche in Mammoth Cave National Park. Strong site affinities were found for American chestnut sprouts in Mammoth Cave National Park. They have a very low presence on relatively young abandoned agricultural lands, but most often occur in less disturbed forests on relatively steep mid to upper slopes near the boundary of limestone and sandstone formations, but with greater preference for the sandstone soils. We believe this model can be a valuable tool for locating surviving American chestnut trees for use in chestnut breeding programs. Another potential use of this model is to identify restoration sites where planted chestnut seedlings may have a good chance to survive. The current distribution of chestnut sprouts appears to be a combined result of land use history and actual chestnut site affinities. The potential restoration sites predicted by the model may be suitable areas for chestnut trees to survive but may not be the best sites for chestnut trees to thrive.

4.4 Future Applications

Geospatial technology may also be used for other purposes in the park. Numerous state, federal, and local government organizations in Kentucky have cooperated to produce GIS data sets such as 1:24,000-scale geology, soils, digital elevation models, surface streams, springs, sinkholes, Karst groundwater basins, groundwater flow routes, transportation networks, high resolution aerial photography, land cover, and various internet map services and static maps. The park can apply geospatial technology with these data sets to analyze environmental and natural resource issues as discussed in the following examples.

One of the challenges for the park is groundwater contamination. Activities from agricultural, urban, and transportation settings can threaten groundwater quality in a well-developed karst terrain. The Mammoth Cave region contains several different groundwater basins many of which cross the park boundary and even drain in park property. Karst landscapes are susceptible to many types of contamination. Human-induced pollution such as animal waste, agricultural chemicals, leakage from underground storage tanks, transportation fuels, and runoff from urban or industrial sites is capable of contaminating groundwater and therefore cave ecosystems. Pollution and waste can easily enter the groundwater system through sinks and then spreads because of the often high velocity of the groundwater. Having the ability to quickly visualize the spatial extent of data, like the list above, in a GIS allows visualizing groundwater systems and planning to protect groundwater quality.

Another important environmental concern is karst hazards in the form of sinkhole collapse and flooding. Cover-collapse sinkholes are sinkholes that occur when a dissolved void space in the limestone bedrock cannot support loose overling soil material. They can vary in width and depth. A karst landscape is somewhat like the plumbing system in your house. If there is a disturbance to part of the plumbing, then the effects are felt somewhere else. Factories and homes built over sinkholes may be damaged as artificial fill moves down into the sinkhole and it collapses. Structures built in sinkholes, or garbage clogging sinkholes, can make adjacent areas vulnerable to flooding. The public in general and planners in particular need to be aware of the vulnerability of a karst landscape, and how it affects both natural and cultural resources (Olson 2001). The spatial analysis of specific layers such as geology, slope, aspect, sinkholes locations, groundwater flow paths, springs, and many other data sets provides a powerful tool to avoid or alleviate karst hazards.

In addition, geospatial technologies can be used in other environmental policy and/or management applications such as land-use planning, energy research, water resources, and fire management in the park and elsewhere. Geospatial analysis and the ability to create customized maps and other data sets allows the park to educate the public in ways were not possible years ago. Creating maps, reports, graphs, and online maps in a GIS can be the means of facilitating awareness of the vulnerability of a karst landscape.

4.5 Conclusion

This study demonstrated the power of geospatial technology in solving and managing environmental and natural resource related issues. Geospatial technology allows effective organization of complex geospatial data, quick visualization of spatial data and related tabular data, and comprehensive analysis of issues and challenges in a spatial context. The availability of geospatial technologies, especially geospatial modeling and visualization, can improve decision-making for a variety of environmental and natural resource issues. Geospatial techniques no doubt will be used more in the management, research, education, and other applications in parks and other places as time goes on.

Acknowledgments We are grateful to the personnel of the Mammoth Cave National Park and students from Volunteer State Community College who provided field assistance. The chestnut inventory at Mammoth Cave National Park was financially supported by the National Park Service and The American Chestnut Foundation.

References

Boyce MS, Vernier PR, Nielsen SE, Schmiegelow FKA (2002) Evaluating resource selection functions. Ecol Model 157:281–300

Browning DM, Beaupre SJ, Duncan L (2005) Using partitioned Mahalanobis D^2 (k) to formulate a GIS-based model of timber rattlesnake hibernacula. J Wildl Manage 69:33–44

Currens JC (2002) Kentucky is karst country! What you should know abound sinkholes and springs: Ky Geol Sur Ser 12 Inf Circ 4, Lexington, Kentucky

Fenneman NM (1938) Physiography of eastern United States. McGraw Hill Book Company, New York, NY

Fielding AH, Bell JF (1997) A review of methods for the assessment of prediction errors in conservation presence/absence models. Environ Conserv 24:38–49

Hirzel AH, Hausser J, Perrin N (2004) Biomapper 3.1 laboratory of conservation biology, department of ecology and evolution, University of Lausanne. http://www.unil .ch/biomapper. Accessed Feb 2009

Hussey J (1884) Report on the botany of barren and Edmonson Counties. Kentucky Geol Surv. Frankfort

Jenness J (2006) Topographic position index (tpi_jen.avx) extension for ArcView 3.x, v. 1.2. Jenness Enterprises. http://www.jennessent.com/arcview/tpi.htm. Accessed Feb 2009

MacDonald WL (1978) Foreward. In: MacDonald WL, Cech FC, Luchock J, Smith C (eds) Proceedings of the American chestnut symposium, p.v. West Virginia University Press, Morgantown

McEwan RW, Rhoades C, Beiting S (2005) American chestnut (Castanea dentata) in the presettlement vegetation of Mammoth Cave National Park, Central Kentucky, USA. Nat Area J 25:275–281

Olson RA (2001) Karst landscapes and the importance of three dimensional data in protection of cave and karst resources. In: U.S. Geological Survey Karst Interest Group Proceedings, pp. 1–7, Kuniansky EL (eds) US Geol Surv Water Resour Investig Rep 01-4011. St. Petersburg, Florida

Olson RA, Noble C (2005) Geodiversity and geoconservation. George Wright Forum 22 (3): 22–28

Palmer AN (1981) A geological guide to Mammoth Cave National Park: Thompson-Shore, Dayton, OH

Parker AJ (1982) The topographic relative moisture index: an approach to soil-moisture assessment in mountain terrain. Phys Geogr 3:160–168

Schibig J, Neel C, Hill M, Vance M, Torkelson J (2005) Ecology of American chestnut in Kentucky and Tennessee. J Am Chestnut Foundation 19:42–48

Thompson LM, van Manen FT, Schlarbaum SC, Depoy M (2006) A spatial modeling approach to identify potential butternut restoration sites in Mammoth Cave National Park. Resto Ecol 14: 289–296

Part II
Glaciers

Chapter 5
Geospatial Techniques to Assess High Mountain Hazards: A Case Study on California Rock Glacier and an Application for Management in the Andes

Jason R. Janke and Antonio Bellisario

Abstract California rock glacier, located in the Sangre de Cristo Mountains of Colorado, was used as a case study to exemplify the geospatial techniques needed to assess geomorphic hazards in mountainous regions. Horizontal and vertical velocities from 1983 to 1998 were calculated using GIS and photogrammetric techniques, and GPS measurements from 2003 to 2008 were used to supplement photogrammetric measurements. From 1983 to 1998, horizontal rates of flow averaged 57 cm/yr (± 3 cm/yr) and vertical thinning averaged 30 cm/yr (± 7 cm/yr) near the head of the rock glacier. GPS measurements from 2003 to 2008 indicate an average horizontal velocity of 52 cm/yr (± 5 cm/yr) for seven points extending from the midsection of the rock glacier to the toe. When comparing mean velocities, the rock glacier has experienced an overall slight deceleration; however, a detailed spatial evaluation of flow indicates GPS points 5–7 show an increase in horizontal velocity from 2003 to 2008 in an isolated section of the toe of the rock glacier. Regional climate data suggest that slightly drier and warmer conditions existed from 2003 to 2008, which may allow ice near the toe to deform more quickly. This region also contains the end of a longitudinal furrow that may funnel and accumulate water in a slightly concave toe. The water could act as a lubricant between shear planes or may warm ice, and allow it to flow more quickly. Although the observed change in horizontal velocity is not significant compared to other rock glaciers that are accelerating to over 300 cm/yr, the analysis has identified a potentially sensitive region of the rock glacier that should be monitored in the future. Mountain hazards, in the form of catastrophic rockfalls, moraine dammed lake outburst floods, avalanches, slumps, slides or others may become more prominent in changing climatic conditions; the GIS, remote sensing, and GPS techniques utilized in this study can easily be replicated or enhanced with other spatial, spectral, or temporal data to evaluate the potential for hazards in mountainous environments. A geospatial application for the Andes is discussed. Increased awareness of hazards and hydrological implications

J.R. Janke (✉)
Department of Earth and Atmospheric Sciences, Metropolitan State College of Denver, Denver, CO 80217, USA
e-mail: jjanke1@mscd.edu

N. Hoalst-Pullen, M.W. Patterson (eds.), *Geospatial Technologies in Environmental Management*, Geotechnologies and the Environment 3, DOI 10.1007/978-90-481-9525-1_5,

associated with receding glaciers could lead to proactive public participation and implementation of adaptive management strategies designed to adjust to short-term climate change.

Keywords Rock glaciers · Mass wasting · Geospatial techniques

5.1 Introduction

Rock glaciers, tongue-shaped or lobate masses of consolidated rock and ice, are abundant in the Colorado Rocky Mountains (Vitek and Giardino 1987; Barsch 1996; Haeberli 2000; Janke 2005a). Although they have not been as intensely studied compared to temperate glaciers, rock glaciers have many important functions in the alpine ecosystem. They serve as a source for construction material, a backdrop for residential areas, dam abutments, drill sites, shaft and tunnel portals, and a water source for urban areas (Giardino and Vick 1987; Burger et al. 1999). Measurements of the movement of rock glaciers provide geomorphologists information about landform development, flow, age, or ice content. Slope failures induced by climate change can increase the hazard potential for nearby communities or roads, modify aquatic ecosystems, or affect drinking water quality by increasing suspended and solute concentrations (Kääb et al. 1997; Konrad et al. 1999; Kääb and Vollmer 2000; Degenhardt and Giardino 2003; Williams et al. 2006; Williams et al. 2007).

The movement of rock glaciers has been measured using field surveying techniques, such as tape measurements, triangulation, or laser ranging (White 1971; Haeberli 1985; Benedict et al. 1986; White 1987; Sloan and Dyke 1998; Konrad et al. 1999; Krainer and Mostler 2000; Leonard et al. 2005; Janke 2005a; Serrano et al. 2006). Recent studies have utilized photogrammetry and computer algorithms to observe flow of the entire surface of rock glaciers, effectively increasing the density of sampling points and extending the period of analysis (Kääb et al. 1997; Kaufmann 1998; Kääb 2002; Kaufmann and Ladstädter 2002; Janke 2005b; Wangensteen et al. 2006). Differential Global Positioning Satellite (GPS) technology has been used on some rock glaciers to detect seasonal motion (Lambiel and Delaloye 2004; Bauer et al. 2005; Krainer and Mostler 2006; Wangensteen et al. 2006). Using a GPS receiver as a reference station and one as a rover (Real Time Kinematics), rapid and accurate measurements of <1 cm can be obtained (Hofmann-Wellenhof et al. 1994; Eiken et al. 1997; Little et al. 2003).

The climatic response of rock glaciers is unique compared to temperate glaciers. Rock glaciers typically have a debris cover (1–3 m thick in some instances), which acts as an insulator and protects internal ice. This debris filters short-term climate anomalies and is not as sensitive to yearly fluctuations in temperature or snowfall compared to temperate glaciers. As internal ice melts, some rock glaciers will experience deceleration because the ice is becoming too thin to flow effectively. Other rock glaciers may show accelerating horizontal velocities as ice warms. Warm

ice can flow more quickly or meltwater can act as a lubricant and reduce friction between internal shear planes (Bucki and Echelmeyer 2004; Krainer and Mostler 2006; Ikeda et al. 2008). Rock glaciers will often show an overall surface thinning because of warming. Some small-scale ridge advection or heaving may be observed; advancing ice may cause compression or overthrusting near the toe (Kääb and Weber 2004; Chueca and Julian 2005; Janke 2005a; Kellerer-Pirklbauer et al. 2008). A variety of geomorphic (internal structure, underlying topography, slope, curvature, etc.) and environmental (snowfall totals, snowmelt timing, temperature change, etc.) variables must be taken into account to properly evaluate the response of a rock glacier to climatic fluctuations.

Climate change will affect high mountain systems by altering geomorphic processes. The increased frequency and magnitude of hazardous events in mountains, such as glacial lake outburst floods or mass movements, such slumps, flows, rockfalls, or others from melting ground ice, will have an economic and ecological impact on the alpine environment (Huggel et al. 2002; Quincey et al. 2005; Thies et al. 2007). In addition, previously unaccounted sources of carbon dioxide and methane could enhance warming as storage sinks in permafrost are released and create a positive feedback that will accentuate hazardous events in mountains.

Remotely sensed and Geographic Information Systems (GIS) data and software provide the proper spatial resolution, spatial coverage, temporal resolution as well as robust operations to assess and manage hazardous events in mountains (Shroder and Bishop 1998; Giardino et al. 2004; Roessner et al. 2005; Saha et al. 2005; Kääb 2008). This paper provides a case study, utilizing the California rock glacier (37.617°N, 105.486°W) in southern Colorado, to illustrate the characteristics of this rock glacier and evaluate the hazard potential in a dynamic alpine environment. A discussion of glacial recession in the more populous Andes is also provided as an example of how geospatial techniques can be used to increase awareness, and in turn, develop proactive adaptive management strategies.

5.2 Study Area

California rock glacier (≈ 3655 m) occupies a portion of the Huerfano River Valley (≈ 3200 m) of the Sangre de Cristo Mountains of Colorado (Fig. 5.1). Blanca Peak (4375 m), the fourth tallest peak in Colorado, marks the southern edge of the north-south trending Huerfano River Valley. California rock glacier is the third largest (0.342 km^2) of about 44 rock glaciers that cover 3.16 km^2 of the massif (Berta 1986; Parson 1987; Janke 2001). The rock glacier flows in an easterly direction and has a subdued surface slope compared to the surrounding topography (Table 5.1). A 0.8 km longitudinal furrow meanders from the head of the rock glacier to its steep front slope that is about 60 m high and has about a 40° slope (Fig. 5.2).

Rocks found on the surface of the rock glacier are part of the Minturn Formation (Middle Pennsylvanian) with gray arkosic sandstone, conglomerates, siltstone,

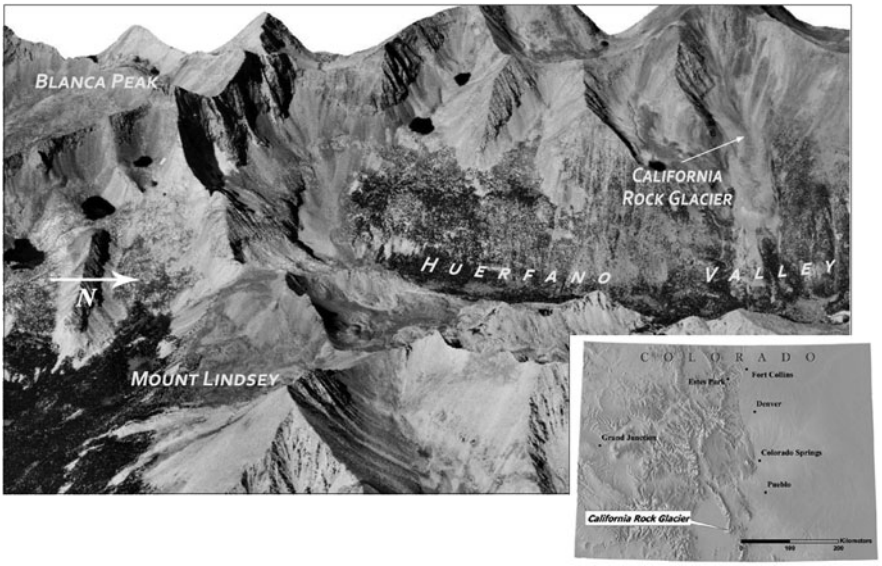

Fig. 5.1 Location of the California rock glacier in the Sangre de Cristo Mountains of southern Colorado

Table 5.1 Geomorphic characteristics of California rock glacier

Variable	Average	Standard deviation
Elevation	3655.8 m	Range: 3856–3,499 m
Aspect	83.2°	35.4°
Slope	18.3°	7.6°
Curvature[a]	0.03	1.11
Plan curvature[b]	0.01	0.69
Profile curvature[c]	– 0.02	0.54

[a] Positive values indicate a convex slope; negative indicate concave
[b] In the direction of the slope
[c] Perpendicular to the slope

shale, and minor amounts of limestone. Tonalite gneiss (Early Proterozoic) metamorphic rocks that are white to light gray green can also be found on the surface. A sequence of thrust faults exist in the free face behind the head of the rock glacier (Parson 1987; Johnson and Bruce 1991).

During the Last Glacial Maximum, the western half of the massif contained relatively straight, narrow, and thin glaciers that emerged from single cirques. On the eastern and northern flanks, the glaciers were thicker and wider and nourished by multiple cirques. The largest glacier, which occupied the Huerfano Valley, extended about 12 km north from Blanca Peak and covered an area of about 1.8×10^7 m^2 (Brugger et al. 2007).

Fig. 5.2 Terrestrial photograph of the California rock glacier

5.3 Methods

5.3.1 Photogrammetric GIS Measurements

A combination of GIS, remote sensing, and field techniques were used to measure horizontal and vertical displacements from 1983 to 2008. USGS digital aerial photographs with a resolution of 0.3 m were obtained for 1983, 1988, and 1998. Leica Photogrammetry Suite (LPS) was used to create DEMs and orthophotos for each image date. Full Ground Control Points (GCP) (x, y, and z) were located in the field (at least 5 per image) and were then digitized on the digital stereopairs. Tie points (non-field points, but points easily identifiable on each image) were generated to improve stereocorrelation estimates. A DEM was then created for a region around California rock glacier using a special filtering strategy for high mountain terrain.

To create orthophotos for each image, the DEMs were used to remove the effects of topography, and a cubic convolution technique was used to resample the image. The corrected images and DEMs were imported into ArcGIS to assess horizontal and vertical change. A cross-correlation technique was used to identify corresponding points on each image. A 27 by 27 cell (8.1 m by 8.1 m) filter was passed over the set of images. Once a correlation of greater than 90% existed on the set of three images, the centers of the filter were identified (0.3 m) and vectors were drawn to connect the centers of each filter. This method is highly dependent upon sufficient image contrast so that corresponding pixels can be identified. Large rocks on

the surface of the rock glacier provided ideal image contrast. Displacement vectors were then divided by the period covered between image sequences to estimate flow (m/yr).

To visualize change, the mid-points of the flow vectors were then converted to a continuous field using ordinary kriging. Because velocities of rock glaciers tend to decrease from the head to the toe, a global trend was removed from the dataset to improve kriging estimates in a west to east direction, following the main axis of the rock glacier. The same interpolation criteria were applied to each image set to avoid misinterpretation from different interpolation techniques. The interpolations were then subtracted using map algebra to visualize horizontal change in the rates of flow between 1983 to 1988 and 1988 to 1998.

Thickness change (vertical displacements) was measured by subtracting the 1983 and 1998 DEMs in ArcGIS. The 1988 DEM was not utilized in this portion of the analysis because uncertainty was too high given a short period of time (5–10 years) between the dates of the images. Uncertainty was measured by averaging horizontal (x and y) and vertical (z) error between stable points surrounding the rock glacier. The average error terms were then divided by the number of years in the record to express uncertainty results in m/yr.

5.3.2 Field GPS Measurements

GPS measurements were taken with a submeter GPS receiver for seven rocks on the surface of California rock glacier. Points were marked with neon paint and photographed in 2003 to aid in relocation. One stable GCP was marked off the surface of the rock glacier to measure the error associated with the recordings. During 2008, the points were relocated and another set of GPS measurements were taken. Points were then post-processed and differentially corrected. Rates of flow (m/yr) were calculated in ArcGIS by measuring the distance between points and dividing by the number of years in the record.

5.4 Results

5.4.1 Photogrammetric GIS Measurements

Photogrammetric measurements indicate that the rates of horizontal flow averaged 57 cm/yr (± 3 cm/yr) from 1983 to 1998 (over the entire period). Velocities generally decrease from the head toward the toe of the rock glacier. An average rate of horizontal flow of 66 cm/yr (± 8 cm/yr) from 1983 until 1988 was calculated (Table 5.2, Fig. 5.3). From 1988 to 1998, average horizontal velocities decreased to 55 cm/yr (± 4 cm/yr) for the entire rock glacier (Table 5.2, Fig. 5.4). Between the two periods, velocities showed the most substantial decrease near the midsection of the rock glacier (Fig. 5.5).

Table 5.2 Average vertical and horizontal velocities

Variable	Time period	Velocity
	1983–1988	0.662 m/yr ± 0.083 m/yr
Mean horizontal velocity	1988–1998	0.548 m/yr ± 0.041 m/yr
	2003–2008	0.520 m/yr ± 0.048 m/yr
Mean thickness change	1983–1998	– 0.299 m/yr ± 0.076 m/yr

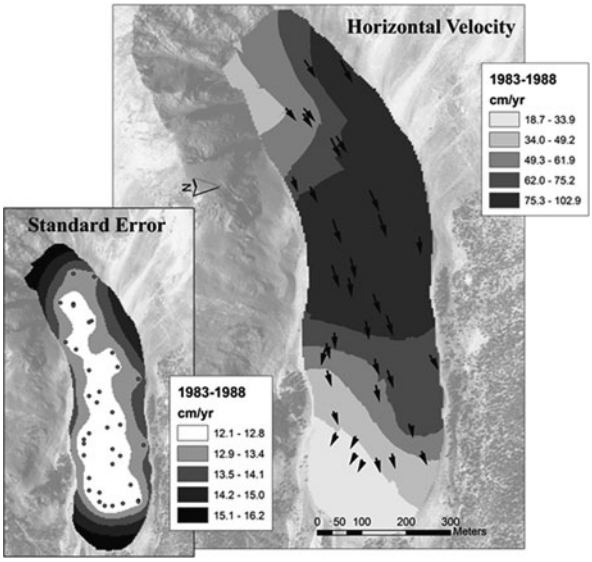

Fig. 5.3 Horizontal rates of flow from 1983 to 1988

Vertical change in thickness, calculated from subtracting DEMs for different image dates, averaged a loss of 30 cm/yr (± 8 cm/yr) from 1983 to 1998 (Table 5.2). A visual inspection of change suggests that thinning was most concentrated near the head and northern edges of the rock glacier (Fig. 5.6).

5.4.2 Field GPS Measurements

GPS surveys indicate a mean horizontal velocity of 52 cm/yr (± 5 cm/yr) from 2003 to 2008. Point 7 near the toe of the rock glacier had the least displacement (30 cm/yr) (Fig. 5.7). Greater displacements were observed near the midsection (63–65 cm/yr). Point 1, located closest to the head of the rock glacier, however, is an exception to this pattern (Fig. 5.7). This point is unique because of local ridge advection or ice thinning.

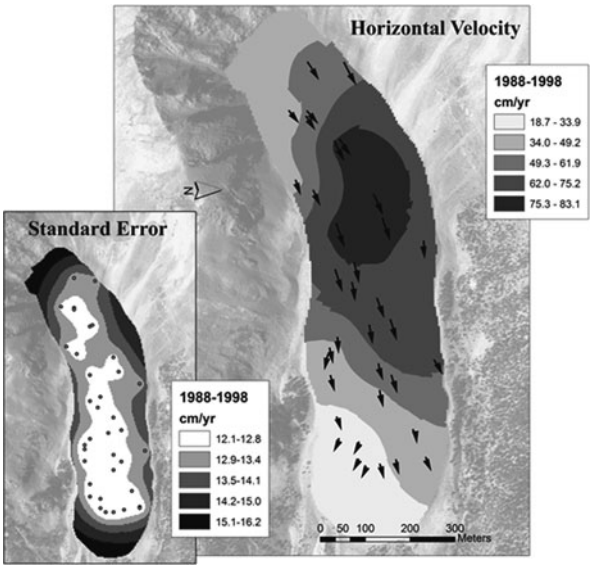

Fig. 5.4 Horizontal rates of flow from 1988 to 1998

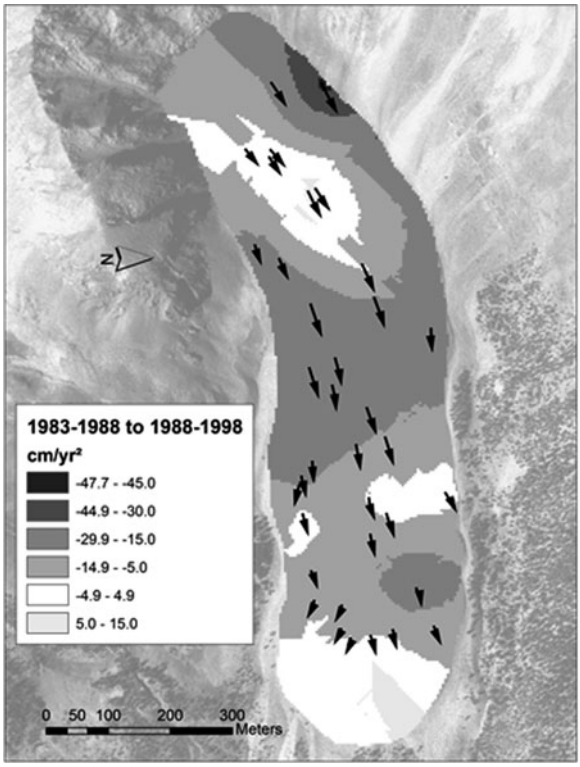

Fig. 5.5 Horizontal change in rates of flow from period 1 (1983–1988) to period 2 (1988–1998)

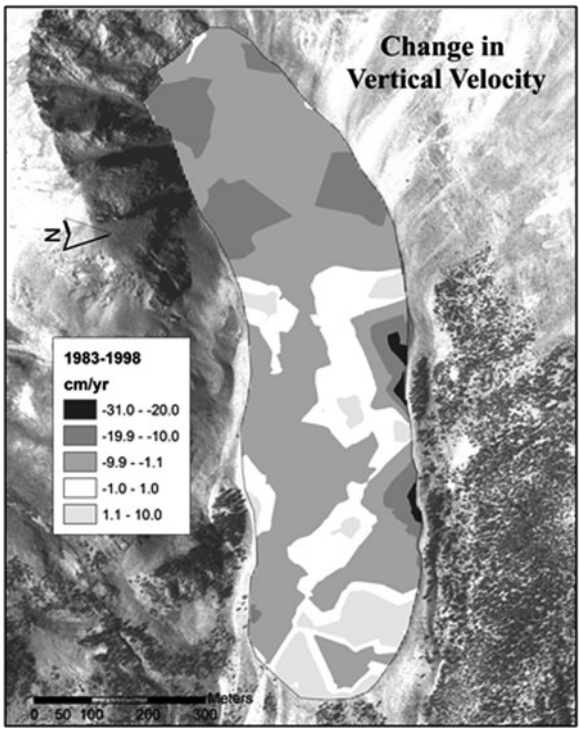

Fig. 5.6 Vertical thickness change from 1983 to 1998

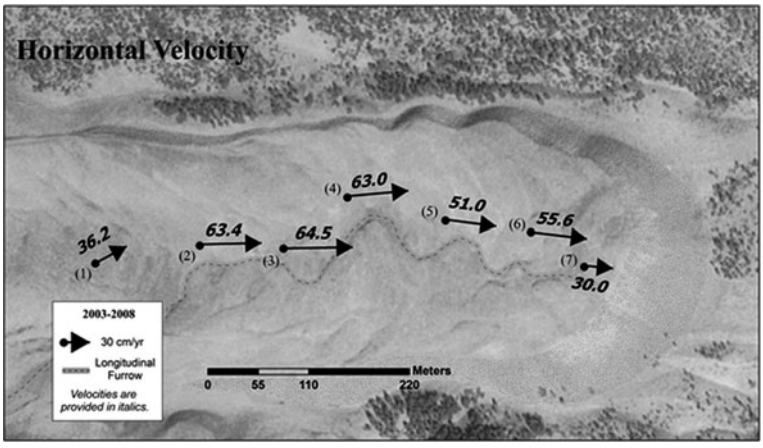

Fig. 5.7 Horizontal rates of flow from 2003 to 2008 obtained using GPS surveys

5.4.3 Geomorphic Variables

Estimates of thickness, volume of rock contained in the rock glacier, rates of cliff retreat, formation age, and average thickness of ice were calculated (Table 5.3). These variables can improve our understanding of the current characteristics and provide some useful information about Holocene erosional processes and recent activity. Based on the surface slope and height of the front slope, the rock glacier has an average thickness of about 54 m. If the debris content (excluding ice and void spaces) is assumed to be 30–50% of the total volume, the volume of rock ranges from 5,540,400 to 9,234,000 m^3 (Table 5.3) (Barsch 1996). When considering the source area of this rock, 17–28 m of rock must have been removed from the cliff walls surrounding the rock glacier. This corresponds to a cliff retreat rate of about 1.7–2.8 mm/yr, assuming the rock glacier began forming 10,000 years ago.

Glen's flow law has been modified to account for the weight of overlying rock; this provides a method to estimate the thickness of ice contained within rock glaciers (Konrad et al. 1999). The equation assumes that basal sliding is not a major component of the flow of the rock glacier. Using this formula, mean ice thickness could range from 1–10 m for California rock glacier, assuming that 2–5 m of surface debris exists over the entire surface of the rock glacier (Table 5.3).

Table 5.3 Geomorphic variables estimated from analysis of GIS data and rates of flow

Variable	Calculation	Formula
Mean thickness	54.1 m	$H_v(\cos\alpha)$, where H_v = height of the front slope, α = slope of upper surface
Volume of debris	5,540,400–9,234,000 m^3	(Arg) (Drg) (T), where A_{rg} = rock glacier area, D_{rg} = debris content (0.3–0.5), T = mean thickness
Thickness of bedrock worm	17.0–28.3 m	(Vrg)/(As), where V_{rg} = volume of the rock glacier, A_s = area of source
Cliff retreat rate	1.70–2.82 mm/yr	$(T_b)/(10{,}000)$, where T_b = thickness of bedrock
Mean ice thickness with 2 m of surface debris	9.8 m	$\left(\frac{v(n+1)}{2A(\rho_i g \sin\theta)^n} + \frac{\rho_d}{\rho_i} d^{(n+1)}\right)^{\frac{1}{n+1}} - \frac{\rho_d}{\rho_i} d$, where v = surface velocity, g = acceleration of gravity, ρ_i = density of ice (900 kg/m^3), ρ_d = surface debris (2700 kg/m^3)
Mean Ice Thickness with 3 m of Surface Debris	6.9 m	
Mean ice thickness with 4 m of surface debris	3.9 m	From Konrad et al. (1999)
Mean ice thickness with 5 m of surface debris	1.0 m	–

5.5 Discussion

5.5.1 Photogrammetric and GIS Analysis of Rates of Flow

Velocities for the California rock glacier fall within the typical range of most published flow rates (1–100 cm/yr) (Barsch 1996). On Galena Creek rock glacier in the Absaroka Mountains of Wyoming, Potter et al. (1998) measured rates of flow between 14–80 cm/yr from the 1960s to 1990s. In the Elk Mountains of Colorado, flow rates averaged 63 cm/yr from 1964–1968 (Bryant 1971). Front Range rock glaciers have rates of flow that typically average 10–20 cm/yr from the late 1970s to late 1990s, much slower compared to an average of 57 cm/yr for California rock glacier from 1983 to 1998 (Janke 2005b). The maximum velocities on California rock glacier, however, are insignificant in comparison with some > 300 cm/yr displacements that have been observed on the Fireweed rock glacier in Alaska and on some rock glaciers in the Austrian Alps (Bucki and Echelmeyer 2004; Krainer and Mostler 2006). If large volumes of rock and ice are moving down slope at greater rates, this could present hazards for nearby alpine communities.

Near the head of California rock glacier, a section of decreasing flow rates showed a marked difference compared to an interior region (Fig. 5.5). Interestingly, the change in velocity seems to reflect two different sources of talus and snow input. The talus source on the southern edge of the headwall is associated with increasing rates of flow, whereas a talus source located on the northern edge of the headwall is experiencing decreasing rates of flow. Thinning is apparent in each of these regions, which may be the result of extensional flow or a decaying internal ice structure (Fig. 5.6). Rates of flow are typically greater near the head of the rock glacier (Benedict et al. 1986; Janke 2005b). This is also the case for the California rock glacier. More loading of rock adds weight to the head. When combined with greater slopes near the head, greater flow rates are produced.

The rock glacier midsection showed a decrease in horizontal velocities over the two periods (Fig. 5.5). This may be the result of ice thinning, which inhibits the rock glacier from flowing as quickly. No significant change in elevation was observed in this region, however, except near the northern edges of the rock glacier (Fig. 5.6). Perhaps ice from the head of the rock glacier, which has shown a slight increase in horizontal velocity, has propagated down glacier and has slowed from compression.

5.5.2 GPS Analysis of Flow Rates

The GPS point measurements were also compared with photogrammetric estimates of flow by overlaying points on the interpolated grids for 1983–1988 and 1988–1998 (Fig. 5.7). Points 1–3 showed a steady decline in surface velocity from 1983 to 2008. Interestingly, points 5–7, which are located near the toe, exhibited an increase in surface velocity from 2003 to 2008. Unlike temperate glaciers, the temperature of ice in a rock glacier has been shown to affect rates of flow more so compared

to slope and thickness (Janke and Frauenfelder 2008). Perhaps a warmer climate is transforming ice near the toe that was previous too cold and rigid to produce greater rates of flow.

Water may also be affecting rates of flow near the toe. Ikeda et al. (2008) found rapid rock glacier acceleration during periods of snowmelt in the Swiss Alps. Air voids in the frozen debris fill with water, which may improve the capability of ice flow (Ikeda et al. 2008). Krainer and Mostler (2006) noted several springs at the base of the rock glaciers in the Austrian Alps in correlation with large displacements that cannot be explained by ice deformation alone. This suggests that water acts as a lubricant between shear planes. On the California rock glacier, water could accumulate in the toe from drainage down a longitudinal furrow (Fig. 5.7). After comparing surface characteristics of a region around points 1–3 (decreasing velocities) versus points 5–7 (increasing velocities), it appears that curvature varies the most between these areas (Table 5.4). More specifically, profile curvature of the surface is slightly negative in the region surrounding points 5–7 (Table 5.4). The concaveness in the direction of the longitudinal furrow suggests potential for water capture. In turn, water may warm ice, fill void spaces, or act as a lubricant between shear planes to increase flow rates.

Although far from comparable environmental conditions exist, an attempt was made to compare climatic data from nearby stations for two periods in which velocities were calculated: the mid-1980s to 1998 and 2003 to 2008. Total precipitation and Mean Annual Air Temperature (MAAT) were averaged for a climate station northwest of the field site (Great Sand Dunes at 2,475 m [37.717°N, 105.533°W]) and a station northeast of the rock glacier (Sheep Mountain at 2,362 m [37.717°N, 105.233°W]). Unfortunately, only two sites are available for comparison because observations are often incomplete or do not correspond to the same period of this study. Average total precipitation has decreased 3.8 cm at Great Sand Dunes and 0.8 cm at Sheep Mountain; average MAAT has shown a 1.0°C increase at Great Sand Dunes and a 1.5°C at Sheep Mountain between the two aforementioned periods. Therefore, increased snowfall and associated melt are less likely to cause greater velocities; however, warmer temperatures may affect the timing and amount of melt from permanent snowbanks located on the rockwalls surrounding the rock glacier, or ice at lower elevations may be melting quicker and produce greater rates of flow. Neither the change in climate nor the change in rates of flow are substantial

Table 5.4 Average topographic variables for regions surrounding GPS survey points

ID	Elevation (m)	Slope (°)	Curvature[a]	Plan curvature[b]	Profile curvature[c]
1–3	3,640	15.2	0.05	0.10	0.05
5–7	3,576	16.0	0.27	0.11	– 0.18

[a]Positive values indicate a convex slope; negative indicate concave
[b]In the direction of the slope
[c]Perpendicular to the slope

compared to observations in other mountain ranges, but the distinct pattern and spatial clustering of increasing displacements warrants future investigation.

5.5.3 Analysis of Geomorphic Variables

California rock glacier is much larger in terms of area and thickness compared to most Front Range rock glaciers (Janke 2005b). Cliff retreat rates for California rock glacier (1.70–2.82 mm/yr) are also greater than the Front Range (0.17–1.33 mm/yr). This illustrates the relative inactivity of physical weathering in the Front Range compared to other mountains (Caine 1974; Humlum 2000). High mountain streams and melt water from snowpack contain a large concentration of ions in their dissolved load. Because dissolved load is not visible, it is often neglected; however, given the continuous nature in which chemical weathering operates, the magnitude may be comparable if not greater than the amount of physical weathering (Vitek et al. 1981).

The California rock glacier most likely contains a notable amount of ice (1–10 m average thickness). Williams et al. (2007) found that seven Rocky Mountain rock glaciers emit higher nitrate concentrations (69 μmoles/L) compared to snow (7 μmoles/L) and rain (25 μmoles/L). At Green Lakes 5 rock glacier, Mg^{2+} concentrations increased to more than 4,000 μeq per L in September; Ca^{2+} were greater than 4000 μeq per L; and SO_4^{2-} reached 7000 μeq per L (Williams et al. 2006).

A more reliable indicator of ice content and thickness could be estimated with geophysical surveys such as those that utilize Ground Penetrating Radar (GPR). GPR has been used on rock glaciers to locate subsurface inclinations, debris rich or supersaturated layers, ice, water flow paths, and bedrock foundations (Berthling et al. 2000; Isaksen et al. 2007; Vonder Mühll et al. 2002; Hausmann et al. 2007; Monnier et al. 2008; Fukui et al. 2008). A better measurement of ice thickness would help better assess the potential impact on nearby aquatic ecosystems.

5.5.4 Hazard Assessment

Although no major slope processes, such as rockfalls, surface collapse features, outburst floods from supraglacial lakes from melting snow or ice, or significant increases in rates of flow were observed, the combination of remote sensing, GIS, and field techniques provides a useful assessment of the current status of the California rock glacier. The region where rates of flow were recently increasing should be examined in more detail; a greater hazard potential could exist if the rock glacier were to advance and override nearby forests as has been observed in the nearby San Juan Mountains of Colorado. In other areas of the world that are experiencing more significant warming and have greater population densities, the fact that a temperature increase can induce rock glacier advance rather than retreat is of concern. Rocks, which are sporadically deposited at angles in excess of 40°, are now

being pushed forward at greater rates. This could increase the volume of rock and the distance of which rocks are being delivered down valley. Regulations should limit hiking in these high-use wilderness areas, or in densely populated regions, policies need to be implemented to restrict development. If drainage is limited as rocks fill pore spaces, water could also accumulate at the surface of the concave toe of the rock glacier. The rock glacier could act as a dam, filling until a breach occurred, flooding nearby communities in populous alpine areas.

If the climate warms and ice is melted, the additional solutes contained in this water source could affect water quality in nearby alpine lakes and streams (Thies et al. 2007). Most urban areas near mountains rely heavily on snowfall and glaciers for a large quantity of water. Increased nitrate deposition because of synthetic agricultural fertilizers or driving cars that release nitrous oxides has been linked to increased eutrophication, or excess algae growth, in alpine areas. Not only is eutrophication of concern because of algae's bad taste or odor, but it is also a problem because increased total organic carbon requires more disinfection which adds more chemicals to the water. Improved regulations may be needed to limit human nitrogen emissions if naturally occurring chemical weathering of rock can also add significant amounts of nitrates to pristine alpine waters.

More importantly, the techniques used to monitor California rock glacier can also be utilized in areas where similar phenomena can have a greater human impact. For instance, similar methods can be used to map, monitor, and assess hazards for roads or major highways that transverse mountain ranges or for alpine cities or towns that rest in valleys that are susceptible to high magnitude, low frequency, geomorphic processes. Debris flows, mudflows, rockfalls, slumps, landslides, avalanches, or other processes that are sensitive to melting ice or permafrost could be monitored using similar techniques to manage sensitive alpine areas.

Ideally, hazard assessment should employ multiple sources of remotely sensed and GIS data, but analysis is often dependent upon what data are available, data quality, and spatial, spectral, and temporal resolution (Giardino et al. 2004). Detailed studies that rely on motion detection should use a combination of aerial photographs, field, Synthetic Aperture Radar (SAR), and Light Detection and Ranging (LiDAR) data sources. At a more regional scale, Advanced Spaceborne Thermal Emission and Reflection Radiometer (ASTER), Satellite Pour l'Observation de la Terre (SPOT), and Landsat Enhanced Thematic Mapper Plus (ETM+) could be used to measure and map the changing extent of glaciers, growing supraglacial lakes, the timing of snowmelt, or historical landslides or avalanche paths (Huggel et al. 2002; Quincey et al. 2005; Roessner et al. 2005; Paul et al. 2007; Kääb 2008). The tradeoff between detailed observations and regional assessment is most easily evaluated on a case-by case basis of hazard type; however, image fusion techniques show much promise to assess hazards at the local and regional scale (Kääb et al. 2005).

5.5.5 Andean Glaciers Application

Current levels and future projections of greenhouse gas emissions in the atmosphere indicate that the planet is experiencing accelerated environmental change (IPCC

2007a). The response of the international community to climate change, largely, is wrestling with the question of how to reduce greenhouse gas emissions and slow the long-term warming trend. The measures being discussed will be implemented over the next decades and their impact will be felt by future generations. However, glacier retreat caused by climatic change is currently happening worldwide and is affecting water supply and triggering devastating natural hazards such as outburst floods, rockfalls, or avalanches (IPCC 2007b). A disconnect exists between the foreseeable future and the present situation where unsustainable practices as well as outdated ideas and methods continue to be practiced. Mitigation planning and capacity building adaptation to address these unavoidable and present hazards are still in their infancy.

The Andes are the only mountain system in the Southern hemisphere with a north-south axis that covers equatorial, tropical, subtropical, temperate, humid, and sub-arctic climates. Due to the importance of glaciers as indicators of climate change, Andean glaciers could provide meaningful observations over a wide-range of environmental and climatic conditions. Gaps remain as to the evolution of Andean glaciers, their associated impact on future water supply, and potential hazards (Casassa et al. 2007). Chile, which contains 75% of the total glacier area of South America, has mapped 1934 glaciers covering an area 15,488 km^2, but there remain 4700 km^2 to be inventoried because of: (1) the vastness of the system; (2) the remoteness and inaccessibility of some areas (especially in Patagonia and Tierra del Fuego); and (3) the economic limitations that exist.

Although South America contains the second largest reservoir of fresh water, its population is vulnerable to water scarcity (The World Bank 2004). Watersheds in the region are dependent on snowfall and glacial melt from the high mountain system. Glaciers release water during the dry-season, a guarantee for year-round water flow for cities, agricultural production, and industry that may not be available in the near future (The World Bank 2004, 2009). Quito, Ecuador; Lima, Peru; La Paz/El Alto, Bolivia; Santiago, Chile; and Mendoza, Argentina are inhabited by millions of people that depend on Andean watersheds for potable water, agriculture, and hydroelectric power generation. Glaciers in the South American high Andean systems are currently receding at alarming rates (Rivera et al. 2002; Casassa et al. 2007; Bown et al. 2008). The glaciers in the tropical Andes (from Venezuela to Bolivia) have lost 15% of their surface area in a period of 30 years (The World Bank 2009). In some cases, glaciers are completely vanishing. In Bolivia, the Chacaltaya glacier has lost 95% of its surface area, while the Ecuadorian glacier, Cotacachi, has disappeared (The World Bank 2009). Andean cities will have to adapt to the challenge of water scarcity while maintaining their ability to sustain urban economies.

Despite future water scarcity, increased glacial melt over the short-term has resulted greater runoff, which has increased the risk of natural disasters such as floods. In the Himalayas, Richardson and Reynolds (2000) have noted that flooding caused by moraine-dammed lake outbursts have become more prevalent. In Latin America, the risk of glacial lake outburst floods has also increased, especially in the tropical Andes, where human settlements in mountainous areas are more common (Carey 2005; Mark 2008). The frequency and severity of glacial lake outburst floods and avalanches should increase with future warming in mountainous environments

worldwide, posing a significant risk for life and property loss. In Latin America, response and recovery activities have traditionally been used to manage disasters; however, proactive approaches that focus on immediate adaptation measures should be implemented. While natural hazards caused by climate change cannot be prevented, their risk to life and property can be greatly reduced through mitigation planning or adaptation to reduce vulnerability. GIS technologies and remote sensing data are reliable tools for mitigation planning; they can be used for identifying hazards, surveying potential risk, assessing vulnerability, and estimating potential losses (Bamber and Rivera 2007). In the Andes, these technologies could be used to develop detailed glacier inventories to assess hazardous risk and to monitor the evolution of glacial lakes and assess their potential for outbursts.

Basic applied-research to document glacier mass, glaciated area, glacial contribution to water supply, and natural hazard risk are needed. The techniques presented in this paper could easily be implemented in the Andes. Temporal, small-scale satellite imagery could first be used to classify glacier extent and identify sensitive areas through change detection techniques. Large-scale, aerial photography or digital satellite imagery could then be used to perform an analysis of recession. Flow, areal loss, volumetric loss, and potential growth of moraine-dammed lakes could all be analyzed using simple GIS digitizing methods and DEM generation techniques. Detailed field measurements could then be used to validate existing measurements or examine geomorphological processes at a finer scale. Estimates could be derived to determine how much water remains locked in a glacier or how much water could be released in a dam failure. Susceptible areas in flood zones could be identified. Current rates of area and volume loss could be extrapolated to predict when glaciers and water will disappear, or sophisticated climate models could be integrated with GIS data to model future scenarios. In less-developed countries, where research funds are scarcely allocated, this methodology provides a straightforward, affordable monitoring technique. Results and possible future impacts could alter public awareness and perceptions of local hazards and climate change. Identification of negative impacts that affect an individual's livelihood could lead a shift to a proactive approach in which adaptive strategies, better management, and potentially regional polices, standards, or guidelines could be designed to manage the Andean high mountain environment.

5.6 Conclusions

GIS, photogrammetric, field, and GPS techniques were used to assess the hazard potential of California rock glacier. Horizontal rates of flow averaged 57 cm/yr (± 3 cm/yr) from 1983 to 1998 according to photogrammetric measurements. Average velocities of surface debris decreased from 66 cm/yr (± 8 cm/yr) to 55 cm/yr (± 4 cm/yr) over the 1983–1988 and 1988–1998 periods. Vertical thinning (– 30 cm/yr ± 8 cm/yr) was concentrated near the head of the rock glacier from 1983 to 1998. Seven GPS measurements from 2003 to 2008 indicated an average horizontal velocity of 52 cm/yr (± 5 cm/yr).

GPS points 5–7 showed a recent (2003–2008) increase in horizontal velocity compared to photogrammetric estimates from 1983 to 1998. The area of increase was isolated in the toe of the rock glacier, a region that has a longitudinal furrow feeding into a slightly concave slope. Snowmelt or water from melting internal ice may flow and accumulate in this region. The excess water may act as a lubricant between shear planes or may warm ice and allow it to flow more quickly.

Although this area is remote, campers and hikers frequently visit this area, which poses some future danger. The frequency of rockfalls could increase with greater rates of flow as rocks are displaced downslope. Water could also accumulate on the rock glacier surface, overcome a threshold, and inundate the surrounding landscape. Coupled with climate change, the frequency and magnitude of mountain processes such as flow, falls, slumps, slides, floods, and avalanches will likely increase and could become hazardous. Although no imminent danger exists from the California rock glacier, the methods utilized in this study can easily be replicated to assess other slope processes in mountainous terrain. The techniques can be used to manage or develop policy for sensitive areas such as those in the Andes. To capture the spatial variability of alpine processes, researchers must use an array of data sources with different temporal, spectral, and spatial resolutions.

Acknowledgments The authors would like to thank Jack Vitek, John Giardino, and Susan Berta for their suggestions and comments which greatly improved this chapter.

References

Bamber JL, Rivera A (2007) A review of remote sensing methods for glacier mass balance determination. Glob and Planet Chang 59:138–148

Barsch D (1996) Rockglaciers: indicators for the present and former geoecology in high mountain environments. Springer, Berlin

Bauer A, Kellerer-Pirklbauer A, Avian M, Kaufman V (2005) Five years of monitoring the front slope of the highly active Hinteres Langtalkar rock glacier using terrestrial laser scanning: A case study in the Central Alps, Austria. 2nd European conference on permafrost terra nostra, Potsdam

Benedict JB, Benedict RJ, Sanville D (1986) Arapaho rock glacier, Front Range, Colorado, USA: a 25 year resurvey. Arct Alp Res 18:349–352

Berta SM (1986) Identification of rock glaciers using enhanced Landsat MSS data. Indiana State University. Terre Haute Dep of Geogr and Geol Prof Pap 18:3–15

Berthling I, Etzelmuller B, Isaksen K, Sollid JL (2000) Rock glaciers on Prins Karls Forland. II: GPR soundings and the development of internal structures. Permafr and Periglac Process 11:357–369

Bown F, Rivera A, Acuña C (2008) Recent glacier variations at the Aconcagua basin, central Chilean Andes. Ann of Glaciol 48:43–48

Brugger K, Refsnider K, Leonard EM, McCalpin JP (2007) Late Pleistocene Equilibrium-line altitudes and climate on the Blanca Massif, Sangre de Cristo Range, Colorado. Geol Soc Am Abs Prog 39:79

Bryant B (1971) Movement measurements on two rock glaciers in the eastern Elk Mountains, Colorado. US Geol Surv Prof Pap 750-B:B108–116

Bucki AK, Echelmeyer KA (2004) The flow of Fireweed rock glacier, Alaska, USA. J Glaciol 50:76–86

Burger KC, Degenhardt JJ, Giardino JR (1999) Engineering geomorphology of rock glaciers. Geomorphol 31:93–132

Carey M (2005) Living and dying with glaciers: people's historical vulnerability to avalanches and outburst floods in Peru. Glob Planet Chang 47:122–134

Casassa G, Haeberli W, Jones G, Kaser G, Ribstein P, Rivera A, Schneider C (2007) Current status of Andean glaciers. Glob Planet Chang 59:1–9

Caine N (1974) The geomorphic processes of the alpine environment. In: Ives JD, Barry R (ed) Arct and Alp Environ. Harper and Row, New York, NY

Chueca J, Julian A (2005) Movement of besiberris rock glacier, central pyrenees, Spain: data from a 10-year geodetic survey. Arct Antarct Alp Res 37:163–170

Degenhardt J, Giardino J (2003) Subsurface investigation of a rock glacier using ground-penetrating radar: implications for locating stored water on Mars. J Geophys Res 108:17-1–17-17

Eiken T, Hagen JO, Melvold K (1997) Kinematic GPS survey of geometry changes on Svalbard glaciers. Ann Glaciol 24:157–163

Fukui K, Sone T, Strelin JA, Torielli CA, Mori J, Fujii Y (2008) Dynamics and GPR stratigraphy of a polar rock glacier on James Ross Island, Antarctic Peninsula. J Glaciol 54:445–451

Giardino JR, Vick SG (1987) Geologic engineering aspects of rock glaciers. In: Giardino JR, Shroder F, Vitek JD (eds) Rock glaciers. Allen and Unwin, Boston, MA

Giardino M, Giordan D, Ambrogio S (2004) GIS technologies for data collection, management and visualization of large slope instabilities: two applications in the Western Italian Alps. Nat Hazards Earth Syst Sci 4:197–211

Haeberli W (1985) Creep of mountain permafrost: internal structure and flow of alpine rock glaciers. Mitt der Vers für Wasserbau, Hydrol und Glaziologie 77:142

Haeberli W (2000) Modern research perspectives relating to permafrost creep and rock glaciers: a discussion. Permafr Periglac Process 11:290–293

Hausmann H, Krainer K, Bruckl E, Mostler W (2007) Internal structure and ice content of Reichenkar rock glacier (Stubai alps, Austria) assessed by geophysical investigations. Permafr Periglac Process 18:351–367

Hofmann-Wellenhof B, Lichtenegger H, Collins J (1994) GPS theory and practice. Springer, New York, NY

Huggel C, Kääb A, Haeberli W, Teysseire P, Paul F (2002) Remote sensing based assessment of hazards from glacier lake outbursts: a case study in the Swiss Alps. Can Geotech J 39: 316–330

Humlum O (2000) The geomorphic significance of rock glaciers: estimates of rock glacier debris volume and headwall recession rates in West Greenland. Geomorphol 35:41–67

Ikeda A, Matsuoka N, Kääb A (2008) Fast deformation of perennially frozen debris in a warm rock glacier in the Swiss Alps: An effect of liquid water. J Geophys Res Earth Surf 113:(F1)

IPCC (Intergovernmental Panel on Climate Change) (2007a) Climate change 2007: the physical science basis. summary for policymakers, Brussels, Belgium

IPCC (Intergovernmental Panel on Climate Change) (2007b) Climate change 2007: impacts, adaptation and vulnerability. summary for policymakers, Brussels, Belgium

Isaksen K, Sollid JL, Holmlund P, Harris C (2007) Recent warming of mountain permafrost in Svalbard and Scandinavia. J Geophys Res Earth Surf 112:F02S04

Janke J, Frauenfelder R (2008) The relationship between rock glacier and contributing area parameters in the Front Range of Colorado. J Quat Sci 23:153–163

Janke JR (2001) Rock glacier mapping: a method utilizing enhanced TM data and GIS modeling techniques. Geocarto Int 16:5–15

Janke JR (2005a) Long-term flow measurements (1961–2002) of the Arapaho, Taylor, and Fair rock glaciers, Front Range, Colorado. Phys Geogr 26:313–336

Janke JR (2005b) Photogrammetric analysis of Front Range rock glacier flow rates. Geogr Ann Ser A Phys Geogr 87A:515–526

Johnson B, Bruce R (1991) Reconnaissance geologic map of parts of the Twin Peaks and Blanca Peak Quadrangles, Almaosa, Costilla, and Huerfano Counties, Colorado. Misc Field Stud Map. US Geological Survey

Kääb A (2002) Monitoring high-mountain terrain deformation from repeated air- and spaceborne optical data: examples using digital aerial imagery and ASTER data. ISPRS J Photogramm Remote Sens 57:39–52

Kääb A (2008) Remote sensing of permafrost-related problems and hazards. Permafr Periglac Process 19:107–136

Kääb A, Haeberli W, Gudmundsson GH (1997) Analyzing the creep of mountain permafrost using high precision aerial photography: 25 years of monitoring Gruben Rock Glacier, Swiss Alps. Permafr Periglac Process 8:409–426

Kääb A, Huggel C, Fischer L, Guex S, Paul F et al (2005) Remote sensing of glacier- and permafrost-related hazards in high mountains: an overview. Nat Hazards Earth Syst Sci 5:527–554

Kääb A, Vollmer M (2000) Surface geometry, thickness changes and flow fields on creeping mountain permafrost: automatic extraction by digital image analysis. Permafr Periglac Process 11:315–326

Kääb A, Weber M (2004) Development of transverse ridges on rock glaciers: Field measurements and laboratory experiments. Permafr Periglac Process 15:379–391

Kaufmann V (1998) Deformation analysis of the Doesen Rock Glacier (Austria). Proceedings of the 7th International Conference on Permafrost Nordicana, Yellowknife

Kaufmann V, Ladstädter R (2002) Spatio-temporal analysis of the dynamic behaviour of the Hochebenkar rock glaciers (Oetztal Alps, Austria) by means of digital photogrammetric methods. Proceedings of the 6th International Symposium on High Mt. Remote Sens Cartogry Institute of Geography and Regional Science, University of Graz, Addis Ababa

Kellerer-Pirklbauer A, Lieb GK, Avian M, Gspurning J (2008) The response of partially debris-covered valley glaciers to climate change: the example of the Pasterze Glacier (Austria) in the Period 1964 to 2006. Geogr Ann Ser A Phys Geogr 90A:269–285

Konrad SK, Humphrey NF, Steig EJ, Clark DH, Potter Jr N, Pfeffer WT (1999) Rock glacier dynamics and paleoclimatic implications. Geol 27:1131–1134

Krainer K, Mostler W (2000) Reichenkar rock glacier: a glacier derived debris-ice system in the Western Stubai Alps, Austria. Permafr Periglac Process 11:267–275

Krainer K, Mostler W (2006) Flow velocities of active rock glaciers in the Austrian Alps. Geogr Ann Ser A Phys Geogr 88A:267–280

Lambiel C, Delaloye R (2004) Contribution of real-time kinematics GPS in the study of creeping Mountain Permafrost: Examples from the Western Swiss Alps. Permafr Periglac Process 15:229–241

Leonard EM, Staab P, Weaver SG (2005) Kinematics of spruce Creek rock glacier, Colorado, USA. J Glaciol 51:259–268

Little JD, Sandall H, Walegur MT, Nelson FE (2003) Application of differential global positioning systems to monitor frost heave and thaw settlement in tundra environments. Permafr Periglac Process 14:349–357

Mark BG (2008) Tracing tropical Andean glaciers over space and time: some lessons and transdisciplinary implications. Glob Planet Chang 60:101–114

Monnier S, Camerlynck C, Rejiba F (2008) Ground penetrating radar survey and stratigraphic interpretation of the Plan du Lac rock glaciers, Vanoise Massif, northern French Alps. Permafr Periglac Process 19:19–30

Parson CG (1987) Rock glaciers and site characteristics of the Blanca Massif, Colorado, USA. In: Giardino JR, Shroder JF, Vitek JD (eds) Rock Glaciers. Allen and Unwin, Boston, MA

Paul F, Kääb A, Haeberli W (2007) Recent glacier changes in the Alps observed by satellite: Consequences for future monitoring strategies. Glob Planet Chang 56:111–122

Potter N, Steig EJ, Clark DH, Speece MA, Clark GM, Updike AB (1998) Galena Creek rock glacier revisited – New observations on an old controversy. Geogr Ann Ser A Phys Geogr 80A:251–265

Quincey DJ, Lucas RM, Richardson SD, Glasser NF, Hambrey MJ, Reynolds JM (2005) Optical remote sensing techniques in high-mountain environments: application to glacial hazards. Prog in Phys Geogr 29:475–505

Richardson S, Reynolds J (2000) An overview of glacial hazards in the Himalayas. Quat Int 65/66:31–47

Rivera A, Acuña C, Casassa G, Bown F (2002) Use of remotely sensed and field data to estimate the contribution of Chilean glaciers to eustatic sea-level rise. Ann Glaciol 34:367–372

Roessner S, Wetzel HU, Kaufmann H, Sarnagoev A (2005) Potential of satellite remote sensing and GIS for landslide hazard assessment in southern Kyrgyzstan (Central Asia). Nat Haz 35: 395–416

Saha AK, Arora MK, Gupta RP, Virdi ML, Csaplovics E (2005) GIS-based route planning in landslide-prone areas. Int J Geogr Inf Sci 19:1149–1175

Serrano E, San Jose JJ, Agudo C (2006) Rock glacier dynamics in a marginal periglacial high mountain environment: Flow, movement (1991–2000) and structure of the Argualas rock glacier, the Pyrenees. Geomorphol 74:285–296

Shroder JF, Bishop MP (1998) Mass movement in the Himalaya: new insights and research directions. Geomorphol 26:13–35

Sloan VF, Dyke LD (1998) Decadal and millennial velocities of rock glaciers, Selwyn Mountains, Canada. Geogr Ann Ser APhys Geogr 80A:237–249

Thies H, Nickus U, Mair V, Tessadri R, Tait D et al (2007) Unexpected response of high alpine lake waters to climate warming. Environ Sci Technol 41:7424–7429

Vitek JD, Deutch AL, Parson CG (1981) Summer Measurements of Dissolved Ion Concentrations in Alpine Stream, Blanca Peak Region, Colorado. Prof Geogr 33:436–414

Vitek JD, Giardino J (1987) Rock glaciers: a review of the knowledge base. In: Giardino JR, Shroder JF, Vitek JD (eds) Rock glaciers. Allen and Unwin, Boston, MA

Vonder Mühll D, Hauck C, Gubler H (2002) Mapping of mountain permafrost using geophysical methods. Prog Phys Geogr 26:643–660

Wangensteen B, Tonsberg OM, Kääb A, Eiken T, Ovehagen J (2006) Surface elevation change and high resolution surface velocities for advancing outlets of Jostedalsbreen. Geogr Ann Ser A Phys Geogr 88A:55–74

White SE (1971) Rock glacier studies in the Colorado Front Range, 1961 to 1968. Arct and Alp Res 3:43–64

White SE (1987) Differential movement across transverse ridges on Arapaho rock glacier, Colorado Front Range, U.S.A. In: Giardino JR, Shroder JF, Vitek JD (eds) Rock Glaciers. Allen and Unwin, Boston, MA

Williams MW, Knauf M, Caine N, Liu F, Verplank VL (2006) Geochemistry and source waters of rock glacier outflow, Colorado Front Range. Permafr Periglac Process 17:13–33

Williams MW, Knauf M, Cory R, Caine N, Liu F (2007) Nitrate content and potential microbial signature of rock glacier outflow, Colorado Front Range. Earth Surf Process Landf 32: 1032–1047

The World Bank (2004) Responding to climate change: proposed action plan for the world bank in Latin America. Latin America and the Caribbean Region, Sustain Development Working Paper 19

The World Bank (2009) Assessing the potential consequences of climate destabilization in Latin America. Latin America and the Caribbean Region, Sustain Development Working Paper 32

Chapter 6
Glacier Inventory: A Case in Semiarid Chile

Jorge Marín and José Araos

Abstract Glaciers are the most important water reservoirs found in the Andes. While the scientific community has conducted more extensive glaciological studies in southern Chile, it is only recently that attention has been focused on northern Chile. In the Chilean "Norte Chico" region, where glaciation is restricted to the highest summits, the sparse glacier network provides the majority of water to downstream users during dry years. Here the economy is based on mining and agriculture, both of which depend on an intensive and reliable water source. Given the importance of glaciers to supply this water, it is surprising that few detailed glaciological studies have been conducted in this region. Just as the glaciers recede to higher summits, making water availability less reliable, the economic activity in this region is increasing; thus, glacier inventory is needed to aid Chilean policy makers in the decision making process. This chapter examines how remotely sensed imagery (ASTER and aerial photos) is being used to develop baseline glacier data in Norte Chico and to provide policy makers with scientific data for decision making. Finally, the chapter shows how GIS technology can integrate remote sensing processing results into a georeferenced database with a broader range of users than the raw data.

Keywords Glaciers · Norte Chico · Chile · Glacier inventory · Water resources · GIS

6.1 Introduction

Glaciers in South America are critically important for water resources for domestic, agricultural and industrial uses, particularly in equatorial, tropical and subtropical latitudes (Casassa et al. 2007). In the northern region of Chile, the local economy depends on agriculture and mining, and both activities have high requirements of

J. Marín (✉)
Centro de Estudios Avanzados en Zonas Áridas (CEAZA), La Serena, Chile
e-mail: jorge.marin@ceaza.cl

N. Hoalst-Pullen, M.W. Patterson (eds.), *Geospatial Technologies in Environmental Management*, Geotechnologies and the Environment 3, DOI 10.1007/978-90-481-9525-1_6,

water during production. In fact, according to the 2002 Chilean National Census, more than two-thirds of local population works in these two economic sectors, with mining being the strongest and the agriculture the fastest growing rates in the recent years (INE 2002). During dry seasons, much of this water is provided by glacier melt water, and so understanding the quantity of water available now and robust predictions of water availability in the future are critical to determining the sustainability of the local economy.

The section of South America south of 30° latitude has an ice covered area of approximately 27,500 km^2, which contains about 89% of all glaciers located in the Andes (Casassa et al. 2006). These glaciers have shown a generalized retreat and wasting, in agreement with the global trend (Casassa et al. 2007). In the central Chilean Andes, nearly 1600 glaciers with a total ice area of ca. 1300 km^2 have experienced a total volume loss, due to thinning and retreat, of 46 ± 17 km^3 of water equivalent between 1945 and 1996 (Rivera et al. 2002; Casassa et al. 2006). Several studies about glacier-climate relationships undertaken in this region indicate that recent glacier variations are linked to increased atmospheric temperatures, increased rainfall variability, and a trend towards a reduction in the annual amount of precipitation (Rosemblüth et al. 1997; Carrasco et al. 2002; Rivera et al. 2002).

In northern Chile, where the glaciated area is sparse, the first glacier inventory was compiled by Garín in 1987 (Garín 1987) and included general approximations of the presence of glaciers, glacierets and temporary snow surfaces. Following this report, only partial updates have been completed, although these give a more detailed view of glacier covered area at a catchment scale. An example of these updates is the inventory of the upper Huasco catchment, which estimates an ice covered area of 16.8 km^2 based on ASTER images analysis (Nicholson et al. 2009).

Bearing in mind this context, there is a clear need of new studies about the state and variability of the cryosphere in arid and semi-arid regions under different climate change scenarios. Correspondingly, there is a need of integration to user friendly and compatible databases like GIS.

6.2 Concepts

Glacier inventories enable more complex investigations on the cryosphere and its interactions in the whole water resource and in geographical systems to be undertaken. This section will explain some basic concepts underpinning the development of glacier inventories.

Firstly, a glacier inventory is a "snapshot" from the state of cryosphere: glaciers, perennial snow patches, rock glaciers, and other cryospheric features, which may be created at different levels of sophistication (UNESCO 1970; Mueller 1976; Rau et al. 2005); and from different source materials, for example maps, photographs (aerial or terrestrial) and satellite imagery (Raup 2000).

A glacier classification system was introduced by UNESCO in 1970 as a contribution to the International Hydrological Decade. This system gives a classification scheme for perennial snow and ice masses. The aim was to provide a useful database of glacial observations in a standardized digital form. The system was designed to characterize the morphology of glaciers quickly and precisely (Rau et al. 2005). The development of such remote sensing techniques greatly improved the capability of observing glaciers in detail, and in this context, the Global Land Ice Measurements from Space (GLIMS) program was developed, which is the creation of a worldwide glacier inventory by means of satellite imagery (Rau et al. 2005).

6.3 Background

6.3.1 Glacier Inventory, State of the Art and Applications

Globally, much work has been undertaken on glacier inventories, which include inventories for the: Swiss Alps (Kääb et al. 2002); Former USSR (Suslov 1978); Antarctic Peninsula (Braun et al. 2008; Vaughan et al. 2003); Alaska and Canada (Young and Ommanney 1984; Miller 1965); and the Patagonian Ice fields (Aniya 1998; Aniya et al. 1999; Casassa et al. 2000; Casassa et al. 2002; Rignot 2003; Rivera and Casassa 2004) (see Fig. 6.1). Despite these important advances, there still are three important needs for glacier inventory development:

1. *More detailed scale glacier inventories:* Generally, inventories which record glaciers at a continent or country scale do not provide high spatial resolution data because of resource availability (for example people, data, and support). In

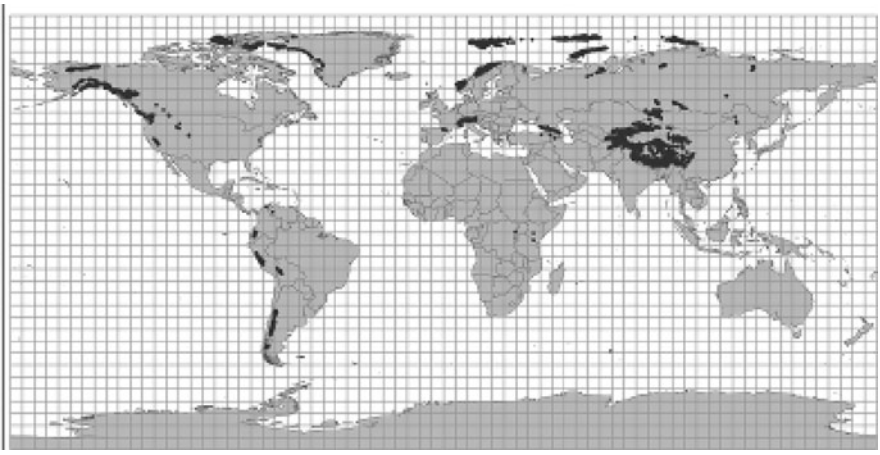

Fig. 6.1 World coverage of World Glacier Inventory

many applications, detailed inventories are a more useful tool for policy makers, public agencies, scientists, and private investors, because the analysis scale is more focused to catchments scale than administrative boundaries, which do not necessarily reflect the natural boundary.
2. *Current and historic data*: The addition of more recent information does not diminish the relevance of the existing information, in fact, historic data is a powerful input for methodological analysis, and perhaps more importantly, for monitoring glacier surface changes through time.
3. *Standardized, open-source information:* Cryosphere feature data analyses are being carried out throughout the world; and the collected data are obtained using methodologically robust means. The problem arises in that such data are not being added to world databases, and important aspect to glacial inventory.

To some extent, these needs are achieved through the remarkable work of World Glacier Inventory (WGI), which contains information of more than 100,000 glaciers throughout the world. The data for these glaciers are regularly updated and available via the internet (http://nsidc.org/data/g01130.html) (Fig. 6.1). The parameters for this inventory were made public in the late 1970s, as a first effort for compiling worldwide glacier inventory data. These parameters included geographical location's code and morphological classification features, among others (Mueller et al. 1977).

Despite the WGI, there is still a lack of information in semiarid areas glaciers, such as the Chilean North. This is beginning to change however, as the importance of glaciers as water reservoirs in this region is appreciated, and as the glaciers begin to respond to climate change.

6.3.2 Glacier Inventory Research in Chile

The most important information source for glacier inventory in Chile is Garín's inventory from 1987 between latitude 18 and 32°S. This work is considered a huge advancement to the field because it constitutes the first stage in glacier inventory creation in northern and central Chile, particularly information on both the area glaciated as well as the volume estimation derived from glacier surface area. However, earlier contributions from Louis Lliboutry in 1956 are considered invaluable. His findings resulted in the book *Nieves y Glaciares de Chile* (Snow and Glaciers of Chile); however, the focus was more in Central and Southern Chile and did not consider northern part of the country. Indeed, extensive glaciological works have been carried out in Patagonia, Chile and in Darwin cordillera, but in South and North Patagonian Icefields, there is still a need for updated and more detailed catchments-level inventory, using modern satellite imagery analysis techniques and GIS capabilities.

Another region with a well developed glacier inventory is central Chile, in which the Aconcagua Catchment has been updated in the recent years (Bown et al. 2008).

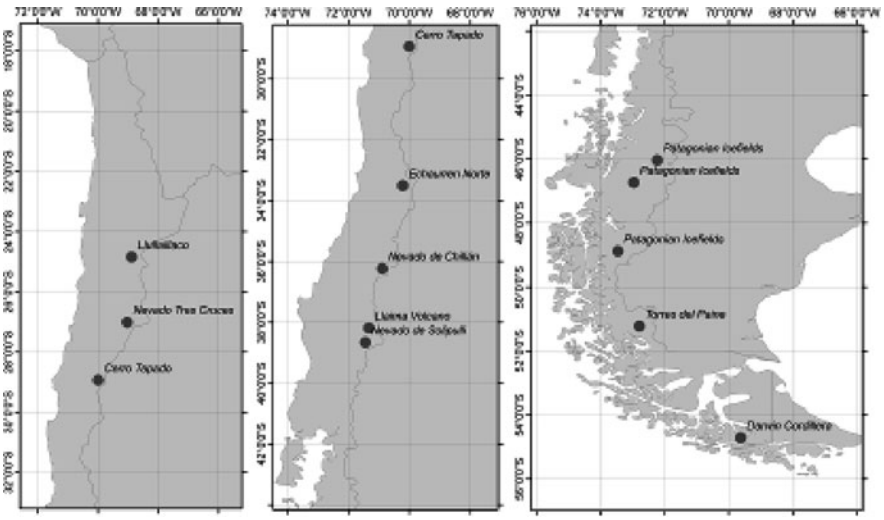

Fig. 6.2 Inventoried and updated glacier inventory and detailed glacier research in Chile

The most important work conducted by a Chilean is that carried out by Garín. He focused on all the country, but in particular on the Patagonian Icefields performing glacier inventory. Recent updates to his work can be seen in Fig. 6.2.

In the recent years, there has been an increase in the amount of glaciological studies conducted in Chile, predominantly from the Universidad de Chile and National Antarctic Institute (INACH). There are also three other Glaciology groups in research institutes namely Centro de Estudios de Cuaternario (CEQUA, based in Punta Arenas –53°S), Centro de Estudios Científicos (CECS, based in Valdivia –39°S) and Centro de Estudios Avanzados en Zonas Áridas (CEAZA, based in La Serena –30°S); in addition, the glaciology unit of DGA (National Water Direction), a government research unit. These research centers have engaged in more region-focused and applied research.

One of these regional and applied research lines has focused on glacier inventory. This inventory has been marked as one of the national priorities, as pertinent policies on natural resources must be based on scientific base data, including glacier inventory data.

6.4 Study Area

Huasco Catchment is located in the Atacama Region of Chile, which is part of the Norte Chico (27–33°S) (see Figs. 6.3 and 6.4). The southernmost edge of the catchment is known as the Arid Diagonal (Kull et al. 2002), and it extends over the

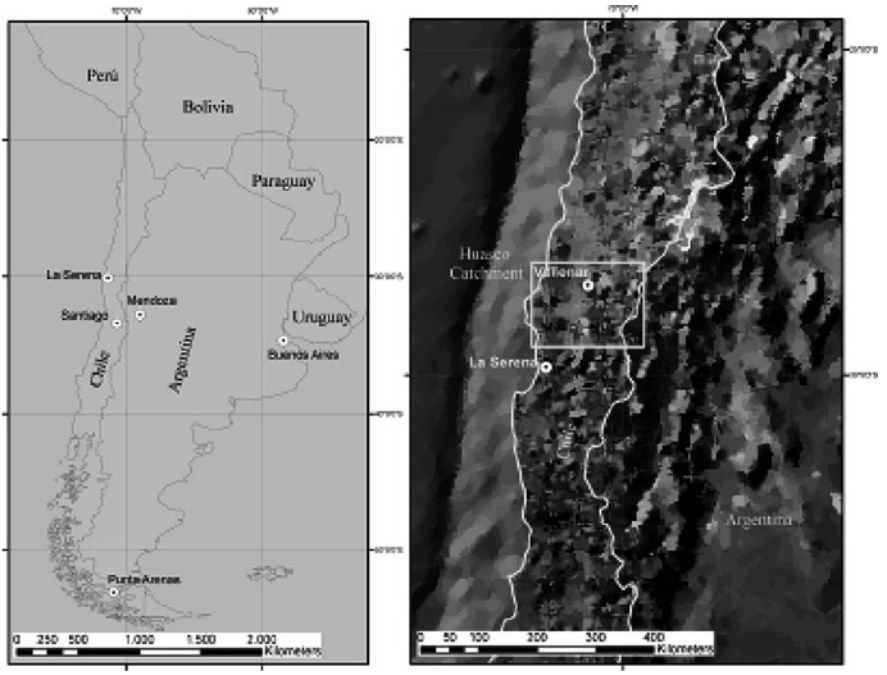

Fig. 6.3 Study area location map

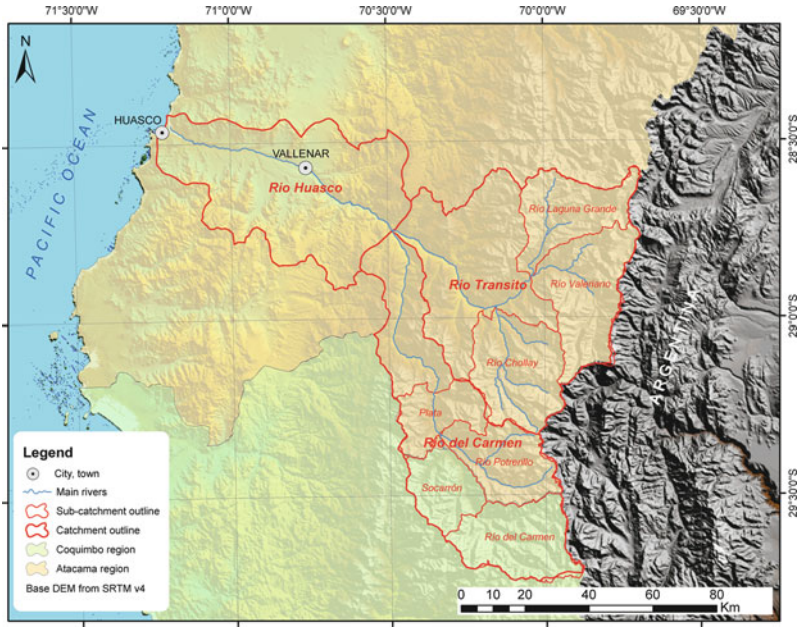

Fig. 6.4 Huasco catchment, glacier containing sub-catchment and tributaries

Freirina, Huasco, Vallenar and Alto del Carmen comunas. Huasco Valley is originated from the confluence of El Carmen and El Transito rivers, which converge together in Junta del Carmen area, 90 Km East from the sea (MOP 2004). The catchment has a mean orientation Southeast to Northwest, like many of Chilean Andes originated rivers (MOP 2004).

Precipitation in the region is characterized by strongly marked, winter precipitation, which is caused by Pacific cyclone activity, and the summer months are markedly dry, with exceptional convective showers (Kull et al. 2002; Ginot et al. 2001). Due to these climatic advantages, this region has earlier fruit production than others in the country, which has made the production of fresh fruit for export a very important economic activity in the last few decades (MOP 2004). The importance of water for the local economy with an increasing population (INE 2002) indicates a need for a detailed analysis of the behavior of snow and ice in this region (Pellicciotti et al. 2008). The glaciers in the Atacama region are not classical accumulation-ablation area glaciers, such that most behave either as a whole ablation or solely an accumulation area, with the exact form dependent on yearly climate variations (Rabatel et al. unpublished).

6.5 Materials and Methods

In the case of the Huasco catchment (see Fig. 6.4), there were three key data sets available: 1. A vector data set, generated from Chilean Military Geographical Institute (Instituto Geográfico Militar, IGM); 2. A satellite imagery source, in this case ASTER imagery, which allowed a DEM of the study area to be created; and 3. Aerial photographs, which were taken from Chilean Air Force's Photogrammetric Service (Servicio Aérofotogramétrico, SAF). A summary of used imagery and data can be seen in Table 6.1.

Vector files: The base vector files used were the Chilean IGM topographic maps in 1:50.000 scale. From this dataset the drainage network and the contours (with 25 m. equidistance) were obtained. In addition, vector files of the catchments boundaries, obtained from Chilean Dirección General de Aguas, DGA, were used. These boundaries had to be improved, because the original vectors were generated at a broad spatial resolution (1:250.000 scale), so has to be modified to fit the IGM map's contours.

Table 6.1 Upper Huasco Glacier Inventory, used data and imagery

Image/Material	Source	Year	Resolution or scale
ASTER	ASTER (Terra)	2002–2004	15 m pixel
Aerial photographs	GEOTEC flight	1999	1:50.000
Contour lines	Instituto Geográfico Militar (IGM)	Hycon flight, 1955	1:50.000
Drainage network	IGM	Hycon flight, 1955	1:50.000

In this case, data handling was made with ArcGIS software, and particularly consisted on two processes: In the first stage, digital topographic maps' were reprojected (from PSAD 56 to WGS 84); in a second stage, the vector files were gathered by each ASTER image, so all the vector data over the remotely sensed data were stored in the same folder. This processing and handling are relevant for the RASTER data orthocorrection and also for the vector data adjustment.

Aerial photographs: Aerial photographs used in this study were from a FONDEF flight in the late 1990s. The aerial photographs were used because they have a better resolution than satellite imagery, but also because photographs from years before the ASTER data are available can be used to "validate" what we can recognize as a glacier. This is necessary because for the inventory to be included in WGI/WGMS/GLIMS, the inventory must consider "every perennial snow and ice patch", so the photographs enable a multitemporal reference in order to confirm perennial characteristics.

Satellite imagery: ASTER data were chosen for this analysis, because of their spatial resolution (15 m), and also the possibilities for combining other studies carried by other research teams in the fields of biology, peat lands monitoring, highlands vegetation, primary productivity in mid altitude valleys, and hydrology. This remotely sensed data were also chosen because they enable the construction of a Digital Elevation Model (DEM) from the same datasets by the provider.

Raster data were obtained from ASTER imagery; such imagery has been well proven in cryosphere studies (Raup at al. 2000; Racoviteanu et al. 2008; Paul et al. 2002) and actually has been proposed as a base for GLIMS project (www.glims.org). Imagery data have been processed for all ASTER datasets, but in this specific case, only the very near infrared dataset (VNIR) has been considered. This is because the inventory at this stage has been carried out only using manual delineation. In spite of this, all images bands were processed. Also aerial photographs have been used in the process, however, the aerial photographs were not rectified, and only used to compare its area to the corresponding area from the already rectified and ortocorrected ASTER imagery. Also, DTM data, which have been used for the orthocorrection key process (Paul 2001), this process has been carried out with "ASTER DTM" application, developed by Brazilian company Sulsoft for ENVI software in an IDL created graphic user interphase (GUI). At a later stage, both raster data types (Imagery and DTM) have been combined for undertaking the orthocorrection process with the formerly mentioned software. In this process, raster and vector files are used. In the first stage, a vector file with a homogeneous presence in the selected imagery must be used. In this specific case, the drainage network from IGM (1:50,000) was used, as its coverage on the Chilean side is the most homogeneous, from the Chilean-Argentinean border to the mid-altitude that is located in the images. Also, DTM data, which has been used for the orthocorrection key process (Paul 2001), this process has been carried out with "ASTER DTM" application, developed by Brazilian company Sulsoft for ENVI software in an IDL created interphase.

6.6 Results

This research was carried out according to WGI guidelines (Mueller et al. 1977), and considers the most frequent cryosphere features existing in the Huasco upper catchment, which are in this case: Bare ice glaciers, debris covered glaciers and Rock glaciers, representing a total of 152 glaciers identified, of which 111 were bare ice glaciers, 1 was identified as having a debris-covered terminus and so was termed a debris-covered glacier and 40 were active rock glaciers.

From glacier inventory glaciations can be identified, according to their morphological and spatial shape, in this specific case, the authors (Marín et al. 2008; Nicholson et al. 2009) concluded that glaciation in upper Huasco is limited to small mountain glaciers, glacieretes and active rock glaciers, completing a total amount of 152 features, whose distribution within the whole catchment is shown in Table 6.2 and Fig. 6.5. An estimation of the water equivalent volume has been made considering former contributions; more than 87% of the mapped bare ice glaciers correspond to ice bodies which area is less than 0.1 square kilometer. Another important result

Table 6.2 Glacier areas in terms of WGI rank sizes, separated by sub-catchments (Fig. 4) and by glacier type

	Rank 1 (0.01–0.1 km^2)		Rank 2 (0.1–1 km^2)		Rank 3 (1–10 km^2)	
	Number	Area (km^2)	Number	Area (km^2)	Number	Area (km^2)
Bare ice glaciers (Debris covered)						
Laguna Grande	6	0.26	8	1.82	1	1.83
Valeriano	17	0.81	7	1.53		
Chollay	12	0.42	2	0.46	1	1.50
Plata						
Potrerillo	25	0.94	12 (1)	4.49 (0.19)	1	1.92
Carmen	17	0.58	1	0.10		
Socarrón	1	0.03				
All glaciers	78	3.03	30 (31)	8.40	3	5.24
Rock glaciers						
Laguna Grande	1	0.04	4	1.25		
Valeriano	5	0.29	3	0.96		
Chollay	9	0.35	9	2.42		
Plata			1	0.19		
Potrerillo	5	0.24	2	0.28		
Carmen			1	0.26		
Socarrón						
All rock glaciers	20	0.93	20	5.38		

Source: Nicholson et al. 2009
Note: There are no glaciers that apply Rank 4 which is greater than 10 km^2

Fig. 6.5 Map of the inventoried ice bodies in the Huasco upper catchment (Glaciers and Rock glaciers)

is a high frequency of "cornice glaciers", which are those glaciers wider than longer, and comprise 40% of all the glaciers mapped.

However glacier inventory is a baseline research. There have been some comparison with some of the climate scenarios proposed by IPCC, in this case, two scenarios were used: B2 and A2 Zero isotherm altitude (ZIA) scenarios. The result of this exercise was that in the case of B2 scenario, there would exist a loss of 65% of bare ice glaciers and a 70% loss of rock glaciers; in the A2 scenario, that would imply the loss of 95% of the current glacier area and a 91% of loss in active rock glaciers (Marín et al. 2008).

6.7 Scientific Data for Decision Makers

Glaciers and ice caps adapt to a change in climate conditions much more rapidly than does a large ice sheet, because they have a higher ratio between annual mass turnover and their total mass (Lemke et al. 2007). Despite the lack of data about deglaciation process in Norte Chico region, some examples about recent glacier variations in upper Huasco catchments and Tapado glacier demonstrates that ice bodies of the regions are decreasing, affecting the availability of water resources.

According to the study of climate variability in Chile for the XXI century (Departamento de Geofísica, Universidad de Chile 2006) it is expected that surface temperature shows positive changes, particularly in the Andean regions. It is further estimated that Norte Chico should experience an increase in rainfall in autumn and not in the winter. An important consequence of these changes would be the variations in the Andean catchments snow reserve. The rise of the isotherm 0°C may limit the availability of snow for the productive use particularly in the first 4 months of the calendar year.

Considering the economic situation in the Huasco Catchment, there appears to be a more complex scenario for water resource requirements. This includes the requirement for the Chilean "Valles transversales" (Copiapó, Huasco, Elqui, Limarí and Choapa valleys), which in the past has been very minor, but in recent years some big investments in export oriented agriculture has been developing in this formerly "underdeveloped" valley. This recent development means that mining is no longer the only viable activity in the valley, but now agriculture provides a real opportunity for wealth generation, which may eventually equal mining. It is not about deciding between exclusive economic sectors. However, the rise of the agricultural sector provides a more complex discussion scenario not only for the authorities, also for the private investors, who are now forced to see the whole integrated picture. In fact, the incorporation of glaciological research in the decision making process constitutes a new perspective, which has not been made in the region until now.

Since 2009, there has been a National Glacier Protection and Conservation Policy, which has been reviewed and discussed with national and international scientists, and was approved in April of 2009 by National Environment Commission's board (CONAMA) (La Tercera-Orbe 2009). This national policy does not just propose a new glacier inventory, but also proposes more Chilean based research in cryosphere science; an additional reach of this national policy is the contribution of common citizens to the proposed "Registro Nacional de Glaciares" (National Register or what can be also named a National Glacier Inventory). The National Glacier Inventory also satisfies the Chilean National strategy for facing Climate Change. Thus this national government initiative is not just an isolated one, but is also part of a holistic effort. Hence the research already carried out in the country acts as a powerful policy input and bodes well for glaciology and cryosphere research in Chile.

Despite the relevance of the national policy and legal efforts, is necessary to start thinking of a next stage in the cryosphere research. This includes an early warning system, which would allow decision makers at different levels, to carry on or to stop

projects located in the Andes that would affect ice bodies, and consequently impact local communities and their water supply, as rainfall diminishes and temperature raises (IPCC 2007).

This early warning system would become a very strong and important tool not just for government agencies or scientists, but also water users of this system which would allow them to have projections about water availability year to year, for irrigation, hydro electrical generation, and agricultural decisions.

6.8 Conclusion

Most of the glaciology and cryosphere science in Latin America and Chile in this context is made as "base" or "pure" science. However in this particular case, this glacier inventory is an innovative privately funded research project, which brings together private business, the Chilean government's responsibility for natural resources management and the scientific need for knowledge for cryospheric understanding in the semi arid region of Chile. This knowledge will allow these three stakeholder groups to interact and make decisions on the bases of scientifically obtained data. Hopefully this will generate discussion regarding the responsible management of natural resources and future development projects.

There are still some "gaps" in glacier inventory in Chile. Filling these gaps becomes more urgent given current climate change debates and the desire for more responsible natural resources management from Chilean State. In addition private investors are now considering the environment as one of the main factors prior to new investment projects related to natural resources and environment. This marks a change in the State's role, from a "laissez faire" state in the early 1980s.

These gaps are proposed to be addressed in the next few years. For example the national cryosphere baseline is proposed to be finished within a time horizon of 5, 10 and 20 years from the present (Barcaza 2009).

A key factor in this context is how "dynamic" these new data sets will be. Remote sensing data provide of large amounts of data, but process techniques and data representation should associated with a common language between different research institutes related to glaciological studies.

An important improvement in the knowledge about the current and future status of Chilean glaciers is also related to the modeling of water resources availability under different climate change scenarios. In this context Norte Chico region presents an interesting situation. An estimation (Nicholson et al. 2009) indicates that under B2 climate change scenario probably there will be a lost of glacier surface area close to 65–70%, and under a A2 scenario the estimation indicate a loss of glacier area around 91–95%. GIS modeling will play a key role in the administration and management of water resources under stress conditions that require an early warning system.

It is expected that this kind of study will be useful not only for scientific purposes, but will also represent information for regional synoptic approaches useful in the social and economic decision-making context.

Tools and applications like GIS platforms, through its connectivity and compatibility can allow decision makers, scientific community and local communities to have a better knowledge of their territory, to lead to a more sustainable natural resources management.

Acknowledgments Special thanks to N Hoalst Pullen, MW Patterson and S MacDonell for their invaluable comments on earlier drafts of this manuscript.

References

Aniya M (1988) Glacier inventory for the Northern Patagonia Icefield, Chile, and variations 1944/45 to 1985/86. Arct Alp Res 20:179–187

Aniya M, Naruse R, Casassa G, Rivera A (1999) Variations of Patagonian glaciers, South America, utilizing RADARSAT images. In: Proceedings of the international symposium on RADARSAT application development and research opportunity, Montreal, Canada, 13–15 Oct 1998

Barcaza G (2009) Unidad de Glaciología y Nieves. http://aprchile.cl/pdfs/ Presentacion_Gonzalo_Barcaza_Mayo_2009.pdf. Accessed 1 Aug 2009

Bown F, Rivera A, Acuña C (2008) Recent glacier variations at the Aconcagua basin, central Chilean Andes. Ann Glaciol 48:43–48

Braun M, Rau F, Simões J (2008) A GIS-based glacier inventory for the Antarctic Peninsula and the South Shetland Islands. A first case study on King George Island. Geosp Inf Sci 4(2):15–24

Carrasco J, Casassa G, Rivera A (2002) Meteorological and climatological aspects of the Southern Patagonia Ice Cap Patagonia. In: Casassa G, Sepulveda F, Sinclair R (eds) The Patagonian Icefields. A unique natural laboratory for environmental and climate change studies. Kluwer/Plenum, New York, NY

Casassa G, Rivera A, Aniya M, Naruse R (2000) Características glaciológicas del Campo de Hielo Patagónico Sur. An Inst Patagonia, Ser Cienc Nat 28:5–22

Casassa G, Rivera A, Aniya M, Naruse R (2002) Current knowledge of the Southern Patagonia Icefield. In: Casassa G, Sepulveda F, Sinclair R (eds) The Patagonian Icefields. A unique natural laboratory for environmental and climate change studies. Kluwer/Plenum, New York, NY

Departamento de Geofísica, Universidad de Chile (2006) Estudio de la variabilidad climática en Chile para el siglo XXI. http://www.dgf.uchile.cl/ACT19/COMUNICACIONES/OtrosTextos/articles-39442_pdf_Estudio_texto.pdf. Accessed 11 Jan 2010

Casassa G, Rivera A, Schwikowski M (2006) Glacier mass balance data for southern South America (30°S–56°S). In: Knight PG (ed) Glacier Science and Environmental Change, Blackwell, Oxford

Casassa G, Haeberli W, Jones G, Kaser G, Ribstein P, Rivera A, Schneider C (2007) Current status of Andean glaciers. Glob Planet Change 59:1–9

Garín C (1987) Inventario de Glaciares de los Andes Chilenos desde los 18° a los 32° de Latitud Sur. Revista Geogr Norte Gd 14:35–48

Ginot P, Kull C, Schwikowski M, Schotterer U, Gäggeler HW (2001) Effects of post-depositional processes on snow composition of a subtropical glacier (Cerro Tapado, Chilean Andes). J Geophys Res 106(D23):32375–32386

INE, Instituto Nacional de Estadísticas (2002) Censo Nacional de Población y Vivienda, Santiago, Chile

IPCC (2007) Summ for policymakers. In: Solomon S, Qin D, Manning M, Chen Z, Marquis M, Averyt KB, Tignor M, Miller HL (eds) Climate change 2007: the physical science basis. contribution of working group I to the 4th assessment report of the intergovernmental panel on climate change. Cambridge University Press, Cambridge

Kääb A, Paul F, Maisch M, Hoelzle M, Haeberli W (2002) The new remote sensing derived Swiss glacier inventory: II. First results. Ann Glaciol 34:362–366

Kull C, Grosjean M, Veit H (2002) Modelling modern and late pleistocene glacio-climatogological conditions in the North Chilean Andes (29°S–30°S). Clim Chan 52(3): 359–381

La Tercera-Orbe (2009) Consejo de ministros de Conama aprueba política nacional de glaciares. http://latercera.com/contenido/659_117909_9.shtml. Accessed 1 Aug 2009

Lemke P, Ren J, Alley R, Allison I, Carrasco J, Flato G, Fuji Y, Kaser G, Mote P, Thomas R, Zhang T (2007) Observations: changes in snow, ice and frozen ground. In: Solomon S, Qin D, Manning M, Chen Z Marquis M, Averyt KB, Tignor M, Miller HL (eds) Climate change 2007: the physical science basis. contribution of working group I to the 4th assessment report of the intergovernmental panel on climate change. Cambridge University Press, Cambridge

Lliboutry L (1956) Nieves y Glaciares de Chile Fundamentos de Glaciología, 1st edn. Ediciones de la Universidad de Chile, Santiago

Marín J, Nicholson L, Rabatel A, Castebrunet H, Garrido R, Novoa E (2008) Glacier inventory of the upper Huasco River Basin, Norte Chico, Chile. AVH4 Conference The Andes: challenge for geosciences. Santiago de Chile 24–28 Nov 2008

Miller M (1965) Inventory of terminal position changes in Alaskan Coastal Glaciers since the 1750's. Proc Am Philos Soc 108 (3):257–273

MOP, Ministerio de Obras Publicas (2004) Diagnóstico y Clasificación de los Cursos y Cuerpos de Agua según objetivos de calidad: Cuenca del Río Huasco. Santiago de Chile. http://www.sinia.cl/1292/articles-31018_Huasco.pdf. Accessed 13 Jan 2010

Müeller F, Caflish T, Müeller G (1976) Firn und Eis der Schweizer Alpen, Gletscherinventar, vdf-Verlag, Zürich

Mueller F, Caflisch T, Mueller G (1977) Instructions for the compilation and assemblage of data for a World Glacier Inventory. Temporary technical secretariat for the World Glacier Inventory. Zurich, ETH Zurich

Nicholson L, Marín J, Lopez D, Rabatel A, Bown F, Rivera A (2009) Glacier inventory of the upper Huasco valley, Norte Chico, Chile: glacier characteristics, glacier change and comparison to central Chile. Ann Glaciol 50(53):111–118

Paul F (2001) Evaluation of different methods for glacier mapping using Landsat TM. In eProceedings EARSeL Workshop on Remote Sensing of Land Ice and Snow, Dresden, 16.-17.6.2000. 1, 239–245

Pellicciotti F, Helbing J, Rivera A, Favier V, Corripio J, Araos J, Sicart JE, Carenzo M (2008) A study of the energy balance and melt regime on Juncal Norte Glacier, semi-arid Andes of central Chile, using melt models of different complexity. Hydrol Process 22:3980–3997

Rabatel A, Castebrunet H, Favier V, Nicholson L. Behaviour of cold glaciers in the semi-arid Andes of Chile (29°S), results of a 6-year monitoring program. Unpublished

Racoviteanu A, Williams M, Barry R (2008) Optical remote sensing of glacier characteristics: a review with focus on the Himalaya. Sensors 8:3355–3383

Rau F, Mauz F, Vogt S, Singh Khalsa SJ, Raup B (2005) Illustrated GLIMS glacier classification manual; glacier classification guidance for the GLIMS glacier inventory. GLIMS regional center Antarctic Peninsula Version 1.0. http://www.glims.org/MapsAndDocs/assets/GLIMS_Glacier-Classification-Manual_V1_2005-02-10.pdf. Accessed 11 Jan 2010

Raup B, Kieffer, Hugh H, Hare, Trent M, Kargel J (2000) Generation of data acquisition requests for the ASTER satellite instrument for monitoring a globally distributed target: glaciers. IEEE Trans Geosci Remote Sens 38(2):1105–1112

Rignot E, Rivera A, Casassa G (2003) Contribution of the patagonia icefields of South America to global sea level rise. Sci 302:434–437

Rivera A, Acuña C, Casassa G, Bown F (2002) Use of remotely sensed and field data to estimate the contribution of Chilean glaciers to eustatic sea-level rise. Ann Glaciol 34:367–372

Rivera A, Casassa G (2004) Ice elevation, areal, and frontal changes of glaciers from national park Torres Del Paine, Southern Patagonia icefiled. Arct Antarct Alp Res 36(4):379–389

Rosemblüth B, Casassa G, Fuenzalida H (1997) Recent temperature variations in southern south America. Intern J Climatol 17:67–85

Suslov VF (1978) Utilization of glacier inventory in the USSR water cadastre. http://iahs.info/redbooks/a126/iahs_126_0139.pdf. Accessed 13 Jan 2010

UNESCO (1970) Perennnial ice and snow masses. A guide for compilation and assemblage of data for a World Glacier Inventory: UNESCO/IAHS Technical Papers in Hydrol1

Vaughan D, Marshall G, Connolley W, Parkinson C, Mulvaney R, Hodgson D, King J, Pudsey C, Turner J (2003) Recent rapid regional climate warming on the Antarctic Peninsula. Clim Chan 60:243–274

Young G, Ommanney C (1984) Canadian glacier hydrology and mass balance studies; a history of accomplishments and recommendations for future work. Geogr Ann Ser A Phys Geogr 66(3):169–182

Part III
Wetlands and Watersheds

Chapter 7
Employing a Geographic Information System for Wetlands Management in Nebraska's Rainwater Basin

James W. Merchant and Patti R. Dappen

Abstract Wetlands are critical components of most ecosystems, providing a broad array of services including support for biodiversity, enhancement of water quality and flood abatement. In spite of their ecological importance, wetlands have been degraded and lost at alarming rates. In the Rainwater Basin (RWB) of south-central Nebraska, an internationally significant staging area for migratory water birds, the adoption of geographic information system (GIS) technology has been critical to managing wetlands. Efforts to employ GIS began with assemblage of dozens of geospatial datasets including digital elevation models, soils data, digital orthophotography, historic aerial photography and land ownership data. Land use and land cover data, which did not exist, were developed using satellite remote sensing. Subsequently, the Revised Universal Soil Loss Equation (RUSLE) was implemented via GIS to assess how sediment was impacting wetlands. All geospatial data, RUSLE modeling results, metadata and documentation were made available on a WWW site designed to facilitate both data download and mapping. During the past decade the RWB has developed an independent, robust and forward-looking program to exploit GIS and related technologies. Many new and improved datasets, including LiDAR data, have been developed, and increasingly sophisticated GIS-based models have been implemented for decision support. Examples includes models to establish priorities for wetlands management, to facilitate evaluation of eligibility of candidate sites for enrollment in programs such as the USDA Wetlands Reserve Program, and to assess the RWB landscape's capacity to provide food energy for migrating waterfowl.

Keywords Wetlands · Geographic information system (GIS) · Spatial modeling · Soil erosion

J.W. Merchant (✉)
Center for Advanced Land Management Information Technologies (CALMIT), School of Natural Resources, University of Nebraska, Lincoln, NE 68583, USA
e-mail: jmerchant1@unl.edu

N. Hoalst-Pullen, M.W. Patterson (eds.), *Geospatial Technologies in Environmental Management*, Geotechnologies and the Environment 3, DOI 10.1007/978-90-481-9525-1_7,

7.1 Introduction

Wetlands, though they cover less than 9% of the earth's land area, are critical components of most ecosystems, providing a broad array of services including support for biodiversity, enhancement of water quality, flood abatement, groundwater recharge and carbon sequestration (Zedler and Kercher 2005). In spite of their ecological importance, wetlands have been lost at alarming rates during the past two centuries, principally a result of drainage for intensive agriculture, infrastructure development and urbanization. It is estimated that barely 50% of global wetlands remain intact, and, in some regions, the loss has been much greater. Even remaining wetlands are often degraded by soil erosion and invasions of exotic species. Impacts on freshwater wetlands have been especially great (Zedler and Kercher 2005; Tiner 2003).

In recent decades, there has been substantial attention directed towards preserving, managing and restoring wetlands. These efforts have often been facilitated by new, innovative institutional structures such as "joint ventures" designed to marry the resources and expertise of public agencies with the interests and specialized knowledge of land owners, conservation organizations and other stakeholders. Geographic information technologies (GIS, GPS and remote sensing) have become increasingly important tools for inventory, mapping and monitoring of wetland resources and for predictive modeling (Lyon and McCarthy 1995). Especially when used in concert with the Internet, these technologies constitute a powerful means to provide decision support for joint ventures and other enterprises that seek to improve wetlands management.

In this chapter, we summarize the development and application of a comprehensive geographic information system designed for wetlands management in the Rainwater Basin of Nebraska, a project carried out in collaboration with the Rainwater Basin Joint Venture (http://www.rwbjv.org/). The principal objectives of the research were (1) to educate Rainwater Basin Joint Venture (RWBJV) partners about GIS and its applications in wetlands management, (2) to engage RWBJV partners in development of a comprehensive set of baseline geospatial data required for management of the Rainwater Basin region and (3) to transfer the data and technology to RWBJV technical staff so that they can continue to develop and use the GIS. All geospatial data and project results were delivered via a web site designed to demonstrate the value of on-line data access (http://www.calmit.unl.edu/rwb/).

7.2 Nebraska's Rainwater Basin

The Rainwater Basin (RWB), a region of approximately 6000 square miles in south-central Nebraska, is an internationally significant staging area for migratory water birds (Fig. 7.1). Located near where the Central Flyway narrows and crosses the Platte River, each spring the RWB attracts an estimated 10 million ducks and geese, and up to 300,000 shorebirds, to rest and feed before heading for northern breeding grounds. These include nearly 90% of the mid-continental population of greater

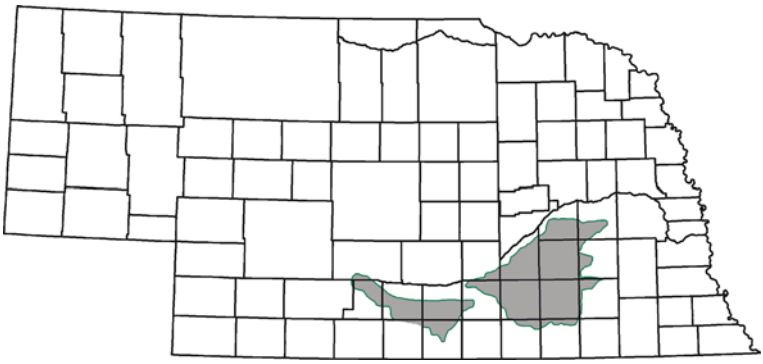

Fig. 7.1 The Rainwater Basin, located in south-central Nebraska, is an internationally significant staging area for migratory waterfowl

white fronted geese, approximately 50% of mid-continent mallards, about 30% of the continental breeding population of northern pintails and an increasing number (>1.5 million) of lesser snow geese. In addition, during a typical fall, approximately 2.6 million waterfowl migrate through the RWB (Rainwater Basin Joint Venture 2008a; USDA Natural Resources Conservation Service 2008; LaGrange 2005; Gersib et al. 1992). In addition to playing a critical role in supporting waterfowl, RWB wetlands are important habitat for other wildlife, and also provide services such as nutrient retention, floodwater storage and sediment trapping (LaGrange 2005; Tiner 2003).

Tiner (2003) characterizes the RWB wetlands as "geographically isolated," depressional wetlands created primarily by wind action on the nearly level silty loess plains of south-central Nebraska. Prior to European settlement in the 19th century, more than 200,000 acres of wetlands occurred in the RWB region, the majority ranging in size from <1 to 40 acres with a few as large as 1,000 acres. The wetlands derive most of their water from precipitation and surface runoff, however surface-water drainage in the RWB is poorly developed, so closed basins with internal drainage predominate (Tiner 2003).

Today, it is estimated that less than 20% of the original wetland area remains (about 34–37,000 acres), and most of the extant wetlands exhibit some form of degradation arising from siltation, fragmentation due to road construction and/or invasions of exotic plants (Rainwater Basin Joint Venture 2008a; USDA Natural Resources Conservation Service 2008; LaGrange 2005; Farrar 1982; Smith and Higgins 1990). The decreasing number and extent of wetlands have resulted in greater bird density and increased the risk of disease. For example, it is estimated that from 1975 to 1987 avian cholera killed more than 200,000 birds in the RWB (Tiner 2003; Smith and Higgins 1990).

The Rainwater Basin Joint Venture (RWBJV) was created in 1992 to address the problem of declining migratory waterfowl habitat. The principal goal of the RWBJV is to restore and permanently protect remaining high-quality wetlands to meet the habitat needs of waterfowl and other migratory birds (Rainwater Basin

Joint Venture 2008a). Most remaining RWB wetlands are privately-owned, although the region also includes 30 state-owned Wildlife Management Areas and 61 federal Waterfowl Production Areas (Rainwater Basin Joint Venture 2008a; USDA Natural Resources Conservation Service 2008). As a consequence, the RWBJV has made development of strong partnerships between private land owners, public agencies and non-governmental organizations a high priority. Wetlands management focuses on "wetland basins" that include associated uplands (primarily grasslands) and other lands surrounding, and draining into, a wetland.

Wetlands management, like other types of natural resources management, must be founded on comprehensive, up-to-date and easily-accessible data, and the tools to manage and use such data. Consequently, one of the first objectives of the RWBJV was to assemble key geospatial data for the region and to explore ways in which geotechnologies such as GIS and remote sensing might be employed to enhance, analyze and use these data for identifying and prioritizing areas of special concern, promoting collaborative decision-making, selecting target sites for restoration projects and developing long-term management plans.

7.3 Project Implementation

The RWBJV staff and project partners identified five major tasks upon which to focus. The first priority was to identify and assemble existing geospatial data scattered among a number of public agencies. Data covering the entire RWB were desired where possible, but detailed data were required for 87 wetland basins. Second, since existing data were known to have different formats, they would need to be reprojected, registered to one another and clipped to the RWB region and to the wetland basin boundaries. It was also deemed desirable to mosaic some datasets into seamless coverages for the entire RWB study area. Third, it was clear that some key data (e.g., land use and land cover) did not exist; consequently, new datasets would need to be developed using satellite remote sensing. In addition, it was considered important to explore how digital imagery, such as historical aerial photography, might be used to augment other geospatial data. Fourth, it was required that a study be undertaken to demonstrate how the geospatial datasets assembled could be used to implement models potentially useful in management. Finally, all datasets developed, modeling results and documentation needed to be easily accessible to RWBJV partners via the Internet.

7.3.1 Digital Database Assembly

The geospatial data assembled for the RWB wetlands and basins included:

- Wetlands basin boundaries
- USGS 1:24,000 quadrangle boundaries
- USGS 1:24,000 digital raster graphics

- 30 m digital elevation data, including slope and contours
- Digital orthophoto quarter quadrangles
- Digital soils data
- National Wetlands Inventory data
- Land ownership data
- Land cover and land use data
- Drainage structures
- Sediment sources
- Public Land Survey System data
- Historical aerial photography for selected wetland areas

Wherever feasible, geospatial data were obtained and/or developed at a scale of 1:24,000 (nominal spatial resolution of 30 m). All data were geo-referenced to the Universal Transverse Mercator Projection (UTM), zone 14, using the NAD83 datum and GRS 1980 spheroid. Data processing was accomplished using ArcGIS and ERDAS Imagine software.

7.3.1.1 Wetland Basin Boundaries

Wetland basin boundaries were identified by RWBJV staff, delineated on U.S. Geological Survey (USGS) 1:24,000 topographic quadrangle maps and subsequently digitized. The resulting vector coverages were buffered by 1 km and all associated data layers (see below) were clipped or generated to the 1 km boundary.

7.3.1.2 Digital Elevation Data

Digital elevation data were accessed from the USGS National Elevation Dataset (NED), a raster product having a resolution of one arc-second (approximately 30 m). The digital elevation data were subsequently used to calculate percent slope for the study area. Both the raw elevation data (in feet and meters), and the derived slope dataset were clipped to the RWB study area, the wetland basins and associated county boundaries.

7.3.1.3 Elevation Contours

Ten-foot elevation contours were obtained from the Nebraska Department of Natural Resources (NDNR) which produced them as a by-product of a cooperative USGS-NDNR project to develop digital orthophotos for Nebraska. The contour data were mosaicked into a seamless coverage of the entire RWB. Elevation contours were subset for the wetland basins and for individual counties.

7.3.1.4 Digital Raster Graphics

Digital Raster Graphics (DRGs) representing the USGS 1:24,000-scale topographic maps were obtained from USGS, clipped to remove overlapping areas and map

collars, and mosaicked to cover the entire RWB study area. Subsets were also provided for wetland basins and counties.

7.3.1.5 National Wetlands Inventory

The National Wetlands Inventory (NWI) data, describing the locations, characteristics and status of wetlands, were downloaded by USGS 7.5′ map tiles. These were mosaicked to form one coverage, then subset to the RWB region, the wetland basins and associated counties.

7.3.1.6 Land Ownership

Land ownership data were developed for publicly-owned wetland basins. Ownership boundaries were digitized on-screen from scanned and rectified plat maps provided by the Nebraska Game and Parks Commission. Plat maps were scanned at 300 dpi, converted to ERDAS Imagine files and rectified using USGS 1:24,000 digital raster graphics. Digital orthophoto quarter quadrangles (DOQQs) from 1993 were used to clarify field boundaries, roads and other land features. Land ownership coverages were considered useful for general planning purposes, but insufficiently accurate for use in legal or engineering applications.

7.3.1.7 Public Land Survey System and USGS Quadrangle Boundaries

Public Land Survey System (PLSS) township, range and section boundaries and USGS 1:24,000 topographic quadrangle boundaries were obtained from the University of Nebraska-Lincoln Conservation and Survey Division. Both PLSS and quadrangle boundary data were re-projected from Lambert Conformal Conic to Universal Transverse Mercator zone 14, NAD 83. The data were then subset to the RWB study area, the wetland basins and associated counties.

7.3.1.8 TIGER Line Files (Roads)

TIGER Line files, obtained from the U.S. Bureau of the Census, were used to represent the road and highway systems in the study area. TIGER Line data were clipped to the RWB study area, the wetland basins and associated county boundaries.

7.3.1.9 Digital Soils Data

The USDA Soil Survey Geographic Data Base (SSURGO) files were used as the primary source of data about the types and characteristics of soils found in the RWB. RWBJV staff selected the attribute fields required for wetlands management. Additional miscellaneous water and soil features (e.g., intermittent streams, ponds, canals, ditches) for wetland basins were digitized on-screen using SSURGO data as a guide. The SSURGO data were then clipped to the entire Rainwater Basin, wetland basins and associated county boundaries.

7.3.1.10 Detailed Hydrological Point and Line Features

To augment the SSURGO data, additional hydrologically-relevant point and line feature data were derived from information provided by the Nebraska Game and Parks Commission (NGPC). The data included access roads, culverts, un-grassed drainages, wells and water reuse pits. Aerial photography provided by NGPC portrayed hand-drawn features. These features were digitized on-screen using DOQQs as the base imagery.

7.3.1.11 Digital Orthophoto Quarter Quadrangles (DOQQs)

Digital Orthophoto Quarter Quadrangles (DOQQs), developed from 1993 National Aerial Photography Program (NAPP) aerial photos, were acquired from the Nebraska Department of Natural Resources. These orthophotos, having a nominal resolution of 1 meter, were originally developed by NDNR under a cooperative agreement with USGS. The image files were mosaicked to provide a seamless coverage for the RWB study area and clipped to the basin boundaries.

7.3.2 Development of Land Use/Land Cover Data

Land use and land cover (LULC) data that met RWBJV requirements for wetlands management were not available at the time of the project. Consequently, LULC data were developed via classification of satellite imagery. Fourteen classes of land cover were mapped at a nominal 30 m spatial resolution using Landsat-5 Thematic Mapper (TM) imagery and ancillary geospatial data (Table 7.1). In order to capture critical information on vegetation phenology, three dates of imagery obtained during the growing season (spring, summer and fall) were used in a classification strategy founded primarily on supervised methods (Dappen et al. 2008).

Ancillary data, such as National Wetlands Inventory (NWI) data, were used to augment the spectrally-based classification. USDA Farm Service Agency (FSA) reporting records, available for some parts of the RWB, were used to provide detailed information on crop type and field boundaries. These data were randomly split into two groups: one group used to determine training sites for specific crops, and a second group set aside for accuracy assessment.

LULC mapping accuracy was assessed using FSA reporting records that were set aside for that purpose. Random points were produced using a stratified random sampling design. The FSA "reference data" were compared, pixel by pixel, to the classification and the overall classification accuracy was estimated to be 87%.

7.3.2.1 Center Pivot Irrigation

Center pivot irrigated fields were identified using Landsat Thematic Mapper (TM) imagery. A summer date was selected so that the majority of crops would be at full canopy, allowing for easier identification of center pivots. The database was prepared by on-screen digitizing of pivot-irrigated fields. Center pivots were checked for accuracy using FSA reporting records.

Table 7.1 Land Use/Land Cover classes and characteristics

Land cover classes	General description
Corn	Includes corn used for grain or silage. Planted late April to early May with full cover by late July. Harvested September through November.
Soybeans	Planted in May, full cover by July. Harvested in September through October.
Sorghum	Includes sorghum for grain and silage as well as milo, sudan, and cane. Planted in May with full cover by July. Harvested September through October.
Potatoes	Planted in late April to early May. Harvested in September or October.
Alfalfa	Green-up during April and early May with first cut beginning in May. Harvested 3–4 times during the growing season ending in early October.
Small grains	Includes winter wheat, spring wheat, oats, barley, rye and millet. Winter wheat planted September of previous year with harvest beginning in early July. Oats and barley are generally planted in late March or early April and harvested in July.
Summer fallow	Cropland kept out of production during a cropping season to conserve moisture for the next season. It is common for wheat producers to rotate half their cropland to summer fallow each year.
Range/grass/pasture	Mostly range grasses and pasture, with some cultivated grass and hay. Includes brome grass and land in the Conservation Reserve Program. Green-up in spring and early summer. Grazing occurs at irregular intervals.
Urban land	Areas defined as towns or cities with a population greater than 300 people.
Open water	Lakes, streams, ponds, reservoirs. Water level varies due to irrigation draw down and evaporation.
Riparian forest and woodlands	Forested areas including areas next to streams, lakes and wetlands
Wetlands	Lands where saturation with water is the dominant factor determining the nature of soil development and plant and animal communities. This class may also include sub-irrigated grassland areas.
Other agricultural lands	Includes developed areas associated with farming, such as farmsteads, feedlots, etc.
Roads	Interstates, highways and county roads.

7.3.3 Additional Image-Based Data

Aerial and satellite imagery can serve a variety of purposes for wetlands management and analyses, including providing context for analyses, aiding revision of geospatial data (e.g., hydrography, roads) and documenting LULC change. In this project, as outlined above, Landsat TM imagery was used to provide LULC data for the RWB. In addition, it was deemed important to explore applications

Table 7.2 Historical aerial photography

Wetland name	County	Years collected
Green acres	Clay	1938, 1968, 1993
Moses hill	Phelps	1938, 1968, 1993
Straight water	Seward	1938, 1965, 1993

of two other types of imagery: IKONOS satellite imagery and historical aerial photography, respectively.

IKONOS, a commercial satellite operated by GeoEye, provides imagery having high spatial resolution (approximately 1 m), comparable to much aerial photography (http://www.geoeye.com). IKONOS imagery was available for 49 of the 87 targeted RWB wetland basins. Pan-sharpened images that combine the spatial detail of the IKONOS panchromatic channel with the spectral information of the 4 m multi-spectral sensor were obtained, mosaicked where required, clipped to the basin boundaries and converted to GeoTIFF format. The GeoTIFF files were then compressed using MrSID software using a 3:1 compression ratio.

Aerial photography has been collected over most of the U.S since about the mid-1930s. Historical photos provide valuable archival records of land use, land cover and land management. However, most are available only in paper format. In this project, for demonstration purposes, three dates of historical aerial photography were obtained for three wetland basins within the RWB study area (Table 7.2).

Paper prints of the photography were acquired from the Conservation and Survey Division archives at the University of Nebraska-Lincoln. The black and white photographs were scanned at 500 dpi, rectified using Digital Orthophoto Quarter Quadrangles, mosaicked and clipped to the wetland basin boundaries.

7.4 Modeling Potential Soil Erosion

Assemblage of a suite of key geospatial datasets, including demonstration of the value of remote sensing, were important achievements for the RWBJV. The partners recognized that these datasets can serve many needs in wetlands management, but a special interest was expressed in developing GIS-based models to aid in supporting management decisions and planning. In the RWB region, a particular concern is soil erosion because of the potential impacts of siltation on remaining wetlands. RWBJV staff need to be able to identify areas where soil erosion threatens wetlands, and prioritize time and funds to target the most endangered basins for rehabilitation and/or protection.

The Universal Soil Loss Equation (USLE), developed by Wischmeier and Smith (1965), has been widely used to estimate potential soil erosion. In this project, an updated implementation of the USLE, the Revised Universal Soil Loss Equation (RUSLE) was used to assess soil erosion for both individual wetland basins and for

the entire RWB study area (Renard et al. 1997). The RUSLE model is formulated as an equation that includes six factors:

$$A = R \times K \times LS \times C \times P \tag{7.1}$$

Where

A = soil loss in tons per acre per year
R = rainfall factor
K = soil erodibility factor
L = slope length factor
S = slope gradient factor
C = cropping management factor
P = conservation practice factor

In the RWB, the RUSLE model was implemented in raster mode using a 30 m cell.

7.4.1 Rainfall (R) Factor

The rainfall erosion factor provides a measure of the intensity of rainfall events. It is calculated from the annual summation of rainfall energy in every storm (correlated with raindrop size) times its maximum 30 min intensity. The *R* factors for Nebraska were obtained from the USDA Natural Resources Conservation Service.

7.4.2 Soil Erodibility (K) Factor

The soil erodibility factor measures the soil's ability to resist being dislodged and transported due to rainfall. The principal soil properties affecting the *K* factor are soil texture (including the amount of fine sand in addition to the usual sand, silt, and clay percentage used to describe soil texture), organic matter, structure and permeability of the soil profile. Lower values of the *K* factor value indicate higher susceptibility to erosion. The *K* factors were determined using SSURGO digital soils data.

7.4.3 Slope Length (LS) Factor

Slope length is defined as the horizontal distance from the origin of overland flow to the point at which either the slope gradient decreases enough that deposition begins, or runoff becomes concentrated in a defined channel (Wischmeier and Smith, 1965). The *LS* factor was derived from digital elevation data downloaded from the USGS National Elevation Dataset. *LS* values were estimated using computed percent slope

and maximum horizontal slope length augmented by values provided by the USDA Natural Resources Conservation Service.

7.4.4 Cropping and Management (C) Factor

The cropping and management factor values express the ratio of soil loss under a specific cropping and management system to the expected soil loss under a clean-till, continuous fallow system. The *C* factor represents the effect of land use on erosion. It is the single factor most easily changed and is the factor most often considered in developing a conservation plan. The land cover values used in this study were based on LULC data derived from Landsat TM imagery (see above) using coefficients provided by the USDA Natural Resources Conservation Service.

7.4.5 Conservation Practice (P) Factor

The conservation practice factor represents the reduction in soil erosion due to conservation measures such as contour farming, strip cropping and terracing. In the RWB, no information on the extent of conservation practices was available. Consequently, a *P* factor value equal to one was used. However, it was demonstrated that for future studies, using the DOQQs as a background image, terraces and contour strips could be on-screen digitized and used to modify *P* factor values.

7.4.6 RUSLE Implementation

Estimated soil loss in tons/acre/year was calculated in raster mode using ArcGIS software. The RUSLE estimates were mapped using a threshold value of soil loss greater than 5 tons/acre/year, as this value is considered indicative of locales that require additional conservation practices (Fig. 7.2). Output for selected basins was also depicted on DOQQs (Fig. 7.3). In ArcGIS, the wetland basin maps were overlaid with land ownership information to aid RWBJV staff in identifying fields and landowners who may require assistance to address conservation needs.

The RUSLE modeling exercise proved useful for demonstrating how GIS and remotely-sensed imagery can be used in concert to quickly produce information important for wetlands management. This effort had the additional benefit of increasing partners' awareness of possible shortcomings in both geospatial data and methods. For example, the estimates of soil loss are clearly related to the LULC existing in a specific year and to the annual average precipitation used in calculating the estimates. The LULC data in the RWB project did not reflect the impacts of conservation practices, since those data were not available. On the other hand, the utility of remote sensing for updating LULC data, and for future development of data on conservation practices was evident.

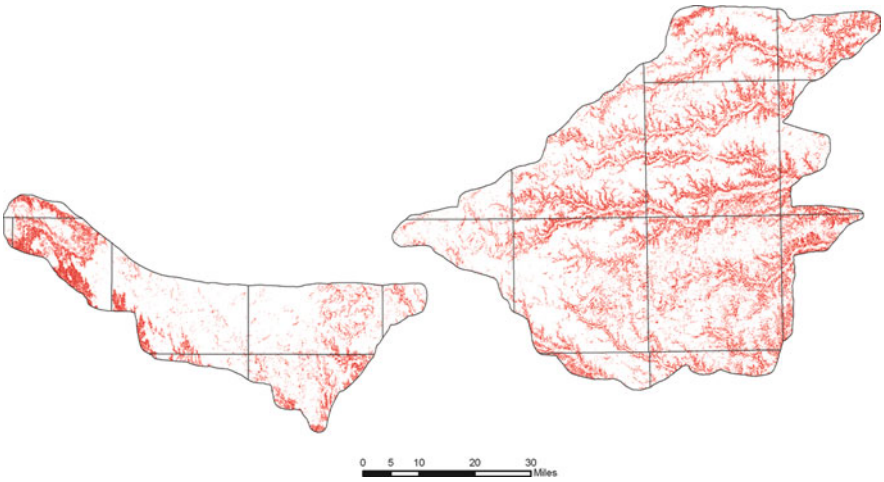

Fig. 7.2 The Revised Universal Soil Loss Equation (RUSLE) was used to estimate soil erosion in the Rainwater Basin. Red areas are those with predicted soil loss greater than 5 tons/acre/year

Fig. 7.3 RUSLE modeling results were overlaid on digital orthophotos to facilitate assessment of impacts on wetlands. This example portrays the Massie wetland basin (buffered to 1-km). Red areas are those with predicted soil loss >5 tons/acre/year

Limitations of modeling were also noted by RWBJV staff. Although the RUSLE model has been widely used and evaluated, the computed soil loss values are, nevertheless, based on average precipitation conditions; consequently, years with above or below-average precipitation will have different results. GIS technology, however, clearly provides opportunities to explore the utility of different models and scenarios.

7.5 Data Delivery and Project Operationalization

All geospatial data, including imagery, RUSLE modeling results, metadata and documentation were made available to RWBJV partners and staff via a Rainwater Basin GIS Internet site (http://www.calmit.unl.edu/rwb/). This site was designed to facilitate both data download, for those who had GIS software available and mapping functions that require users to have no additional software to visualize datasets (Fig. 7.4).

In the years since the initial project was completed, the RWBJV has made substantial progress in adopting and using both GIS and remote sensing technologies. An initial development was the establishment of a RWBJV GIS Steering Committee to foster enhancement of datasets, use of GIS for modeling and decision support, and interagency collaboration in seeking financial support through grants (Smith and Lucas 1998). One result of this collaboration has been a multiyear program to acquire 2-foot resolution color infrared aerial photography during spring to document the extent of wetlands and wetlands use by waterfowl. Recently, this program has been augmented by a cooperative project to acquire LiDAR data over the RWB. These data will be used to develop high resolution digital elevation models (2-foot contours) important for identifying hydrologic modifications such as surface drains and ditches and to better delineate wetland basins in this region of low relief (Merrick and Company 2009).

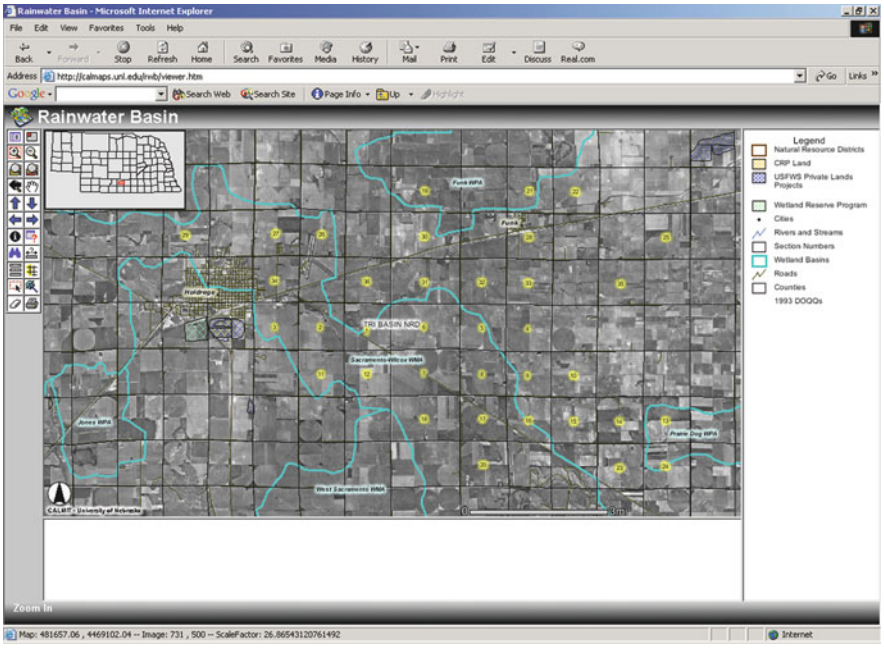

Fig. 7.4 All geospatial data, including imagery, RUSLE modeling results, metadata and documentation were made available to RWBJV partners and staff via the Internet (http://www.calmit.unl.edu/rwb/)

In 2004 the RWBJV joined with the Playa Lakes Joint Venture, the U.S. Fish and Wildlife Service and other public agencies to form the Great Plains GIS Partnership (Playa Lakes Joint Venture 2008; Rainwater Basin Joint Venture 2008b). Among other projects, this collaborative enterprise has developed a 2007 update of LULC based on Landsat data and National Agriculture Imagery Program (NAIP) aerial photography (Playa Lakes Joint Venture 2008).

Currently, new and improved geospatial datasets (e.g., an inventory of over 10,000 irrigation tailwater recovery pits) continue to be created by the RWBJV and partners, and are increasingly being used in the RWB for decision support. For example, RWBJV staff, working with the U.S. Fish and Wildlife Service Region 6 Habitat and Population Evaluation Team (HAPET), used a GIS-based model to establish priorities for wetlands management (USDA Natural Resources Conservation Service 2008). Areas that have a high density of functioning wetlands with optimal wetland juxtaposition between wetland types were identified as higher in priority for wetland acquisition, restoration and management activities. The RWBJV and HAPET have also collaborated to implement a model that facilitates evaluation of eligibility of candidate sites for enrollment in programs such as the USDA Wetlands Reserve Program. And, Bishop and Vrtiska (2008) have used GIS to model the RWB landscape's capacity to provide food energy for migrating waterfowl. They determined that the RWB needs to provide 24.1 billion kcal of energy for migratory waterfowl and that, although currently waste grain can meet caloric requirements, food resources other than waste grain are required to meet all waterfowl nutritional requirements such as essential amino acids, inorganic elements and vitamins (Bishop and Vrtiska 2008).

7.6 Conclusion

Today, geotechnologies are increasingly critical tools for management of wetlands. The Rainwater Basin project demonstrated that remote sensing, GIS and related technologies such as GPS, used in concert, are effective tools that can improve decision-making. Among other things, these technologies are useful to facilitate identification of important issues, establishment of priorities for allocation of funding and staff, development of interagency collaboration, public education and communication and assessment of management actions. Adoption of GIS by organizations such as the RWBJV is facilitated by pilot projects like that summarized above. The RWB project provided the foundation on which the RWBJV has developed an independent, robust and forward-looking program to exploit geotechnologies.

Acknowledgments Thanks are extended to the Rainwater Basin Joint Venture for providing the financial support that made this research possible. We also gratefully acknowledge the significant contributions of the following individuals: Marcus Tooze (GIS Workshop, Inc.), Michael Delvaux (U.S. Bureau of Reclamation), Ted LaGrange (Nebraska Game and Parks Commission), Steve Moran (Rainwater Basin Joint Venture) and Steve Scheinost (USDA Natural Resources Conservation Service).

References

Bishop AA, M Vrtiska (2008) Effects of the wetlands reserve program on waterfowl carrying capacity in the rainwater basin region of south-central Nebraska. ftp://ftp-fc.sc.egov.usda.gov/NHQ/.../RWB_WRP_Final%20Report.pdf. Accessed 1 Aug 2009

Dappen PR, Ratcliffe I, Robbins C, Merchant JW (2008) Mapping agricultural land cover for hydrologic modeling in the platte river watershed of Nebraska. Great Plains Res 18(1):39–52

Farrar J (1982) The rainwater basin – our vanishing wetlands. *Nebraskaland Magazine*. Nebraska Game and Parks Commission, Lincoln, NE

Gersib RA, Dinan KE, Kauffeld JD, Onnen MD, Gabig PJ, Cornely JE, Jasmer GE, Hyland JM, Strom KJ (1992) Looking to the future: an implementation plan for the rainwater basin joint venture http://www.rwbjv.org/pdf/Implementation_Plan_1992.pdf. Accessed 24 July 2009

LaGrange T (2005) Guide to Nebraska's wetlands and their conservation needs. Nebraska Game and Parks Commission, Lincoln, NE

Lyon JG, McCarthy J (1995) Wetland and environmental applications of GIS. CRC Press, United States. http://www.merrick.com/images/uploads/project_sheets/2509.pdf. Accessed 3 Aug 2009

Merrick & Company (2009) LiDAR collection and processing. http://www.merrick.com/images/uploads/project_sheets/2509.pdf. Accessed 3 Aug 2009

Playa Lakes Joint Venture (2008) GIS review. http://www.pljv.org/cms/gis-review. Accessed 3 Aug 2009

Rainwater Basin Joint Venture (2008a) Rainwater basin joint venture home page. http://www.rwbjv.org/. Accessed 15 July 2009

Rainwater Basin Joint Venture (2008b) Rainwater basin joint venture 2008 annual report. http://rwbjv.org/library.html. Accessed 3 Aug 2009

Renard KG, Foster GR, Weesies GA, McCool DA, Yoder DC (1997) Predicting soil erosion by water: a guide to conservation planning with the Revised Universal Soil Loss Equation (RUSLE). Agriculture Handbook No. 703. U.S. Department of Agriculture, Washington, DC

Smith BJ, Higgins KF (1990) Avian cholera and temporal changes in wetland numbers and densities in Nebraska's rainwater basin area. Wetl 10(1):1–5

Smith MS, Lucas J (1998) Rainwater Basin GIS effort. http://proceedings.esri.com/library/userconf/proc98/proceed/to200/pap182/p182.htm. Accessed 10 July 2009

Tiner RW (2003) Geographically isolated wetlands of the United States. Wetl 23(3):494–516

USDA Natural Resources Conservation Service (2008) The Wetlands reserve program supports migrating waterfowl in Nebraska's Rainwater Basin region. ftp://ftp-fc.sc.egov.usda.gov/NHQ/nri/ceap/rainwaterbasininsight.pdf. Accessed 3 Aug 2009

Wischmeier WH, Smith DD (1965) Predicting rainfall erosion losses from cropland east of the Rocky Mountains. Agriculture Handbook 282. U.S. Department of Agriculture, Washington, DC

Zedler JB, Kercher S (2005) Wetland resources: status, trends, ecosystem services, and restorability. Ann Rev Environ Resour 30:39–74

Chapter 8
The Effects of Land Cover Change: Increasing Watershed Imperviousness in Kentucky

Demetrio P. Zourarakis and Brian D. Lee

Abstract Imperviousness is recognized as a leading and trailing indicator of watershed health and one of critical importance in watershed management and planning. Quantitative evidence points to a close correlation between the increase in imperviousness and temporal land cover change. Drawing from baseline and temporal land cover change datasets generated for the state of Kentucky, U.S.A, this chapter presents two examples of geotechnology usage: remote sensing and geographic information systems (GIS) based modeling. Two methods are presented for calculating the increase in total impervious area (TIA) for a given watershed, by using a baseline imperviousness dataset and updates to the spatial distribution of land cover over time. Since as a spatial variable TIA can represent both categorical and continuous variation, considerations regarding data handling methods (i.e. resampling) to maintain original data accuracy while making the publically available data compatible to existing and planned datasets are considered. TIA increase and its implications for watersheds experiencing changes in urbanized areas, is explored in two temporal directions; the first, retrospective, and the second prospective, or updating. Finally, the potential consequences as a result of the findings are examined in the context of their impact on watershed based policies and management with a specific example relevant to an ongoing stormwater management conundrum.

Keywords Watershed imperviousness · Land cover · Change detection · Remote sensing · Landsat · Reprojection · GIS

D.P. Zourarakis (✉)
Kentucky Division of Geographic Information, Commonwealth Office of Technology, Frankfort, KY 40601, USA
e-mail: demetrio.zourarakis@ky.gov

N. Hoalst-Pullen, M.W. Patterson (eds.), *Geospatial Technologies in Environmental Management*, Geotechnologies and the Environment 3, DOI 10.1007/978-90-481-9525-1_8,

8.1 Introduction

The issue of protecting surface water from the impacts of stormwater across regions and in particular urbanized areas has potentially serious legal and monetary ramifications. This is on top of what some may feel as moral and/or ethical obligations because of its relationship to a higher quality of life. Geospatial technologies and data can be used to discover, model, and visualize environmental change with several opportunities for environmental resource managers. For example, the ability to improve watershed planning and management decisions is inextricably linked to impervious land cover. This chapter explores how two geotechnologies, remote sensing and GIS modeling, are used to help assess the potential impact of concomitant changes in land cover and imperviousness in the context of watershed management. Even though GIS is recognized as an essential element throughout the process of adaptive watershed management, substantial work remains to be done before its potential is fully realized and functionally and operationally integrated (Walker and Mostaghimi 2009).

Kentucky's complex and rich landscapes are changing as a result of both human interventions and natural fluctuations posing a challenge to measuring, monitoring and modeling such changes (Lee et al. 2009). In turn, the Commonwealth's watersheds and complex hydrologic networks are being impacted by temporal change – expressed as a change in land cover as well as land use. The link between water quality and watershed health and land cover/land use and their change over time becomes evident from the fact that Kentucky's section 303(d) list contains as many as 9,800 km of streams and 2,097 pollutant-water body combinations. This list is the official report to the Legislative Branch of government on the condition of water resources in Kentucky (Kentucky Division of Water 2008).

Using moderate resolution imagery and remote sensing methods to extract information is a cost and time effective solution to help quantify and spatially identify where the landscape is undergoing changes. Land cover change characterized using remote sensing-derived data layers can be correlated with trends in urbanization and changes in imperviousness (Bauer et al. 2005). Through two NASA-funded projects, the Kentucky Landscape Snapshot Project (KLS), and the Kentucky Landscape Census Project (KLC) Kentucky was able to be one of the first states to generate its portion of the 2001-era baseline land cover layer. Ultimately, this was the contribution to the 2001 National Land Cover Dataset (NLCD01) (Homer et al. 2007). Subsequently, the KLC produced the first, 2005 update to that dataset, with which estimates of land cover change become possible on a statewide basis during the intervening 4 years. An Anderson Level III for forested lands and wetlands for 2001, and a 2005-era Anderson Level II updates to NLCD01 are also now available because of these previous efforts. All these products are at a 30 m ground resolution (Harp et al. 2006; Kentucky Division of Geographic Information 2009a, b; Palmer 2007; Zourarakis and Palmer 2008). There are a number of applications that these previous efforts are now being used that have environmental resource management

implications such as watershed characterization, urbanization prediction, forest fragmentation, and characterization of large interior forest blocks in quantitative and spatial terms.

Over the 2001–2005 quadrennium, Kentucky experienced land cover class changes comprising about 1% of its total area – or over 98,100 ha. Such change represented for example a net loss of the forest cover class, and a net gain of urban development plus barren land cover classes of almost 62,000 ha and 11,600 ha, or about 42 and 8 ha/day, respectively. Inter-conversion of areas under different types of developed land is also evident (Table 8.1). Net forest loss estimates matched with similar gains in nonforested areas (barren, grassland/ herbaceous and scrub/shrub). Inspection of these changes indicates that some of it occurred as a result of surface mining activities which have its own environmental resource management implications. In contrast, urban development had a net gain rate of over 4 ha/day; the net loss rate for wetlands (woody and herbaceous) and agricultural land (hay/pasture and cultivated crops) was 1 and 2.5 ha/day, respectively, with small contributions from forested lands to urban areas (Zourarakis 2009).

Table 8.1 Land cover class change in Kentucky, 2001–2005

Land cover class (Class number) (Anderson level II)	Area lost (ha)	Area gained (ha)	Balance (ha)	Daily change (ha/day)
Open water (11)	159	643	484	0.3
Developed open space (21)	2,752	2,306	−446	−0.3
Developed low intensity (22)	904	4,852	3,948	2.7
Developed medium intensity (23)	456	2,377	1,921	1.3
Developed high intensity (24)	79	846	767	0.5
Barren (31)	9,455	14,831	5,377	3.7
Deciduous forest (41)	57,471	3	−57,468	−39.4
Evergreen forest (42)	2,825	4	−2,821	−1.9
Mixed forest (43)	1,510	0	−1,510	−1.0
Scrub/shrub (52)	1,400	36,733	35,333	24.2
Grassland/herbaceous (71)	12,728	35,058	22,330	15.3
Pasture/hay (81)	4,008	90	−3,917	−2.7
Cultivated crops (82)	2,813	170	−2,643	−1.8
Woody wetlands (90)	1,222	224	−998	−0.7
Emergent herbaceous wetlands (95)	356	0	−356	−0.2
Total	98,138	98,138	0	0

With these broad landscape scale changes identified in the state of Kentucky as a backdrop, this chapter's next four sections will provide environmental resource management examples specifically related to imperviousness analyses and its temporal changes with a focus on several parts of Kentucky's landscapes. The general approach is to extract estimates for total impervious area both as absolute and relative magnitudes, based on the NLCD01, subpixel imperviousness dataset

serving as baseline on which to compare changes. The second section continues with an analysis of the effects of spatial resampling methods on the distribution of imperviousness values and the geotechnogical implications in the context of environmental management and policy. Through a proposed method to estimate imperviousness based on developed land cover class data, an analysis of the rates of temporal change on imperviousness during the 1992–2005 time period follows as the third section. To conclude the chapter, some estimates of the spatial distribution of these temporal variations as aggregate areas and density analyses are presented. A discussion concerning the importance of these findings on stormwater policies and watershed management implications concludes this chapter.

8.2 Imperviousness: A Key Environmental Indicator for Watershed Management

Imperviousness is an important variable influencing hydrologic behavior and biological integrity (Arnold and Gibbons 1996; Miltner et al. 2004). This is reflected in multiple land cover and land use modifying processes and is utilized in several hydrologic models, and has often been implicated as a cause of water quality degradation (U.S. EPA 2008). Over time, changes in land cover are likely to alter the distribution of imperviousness in landscapes, bringing possible negative effects on watersheds due to degradation of water quantity and quality parameters (Schueler 1987, 1994; Booth and Reinelt 1993). The likely negative impact of imperviousness can drive the development, installation, and monitoring of stormwater management facilities and practices. Imperviousness can be characterized by GIS methods such as overlay and buffering operations of data layers extracted using either planimetric (e.g. subwatersheds, parcels, transportation network, and structures), or from remotely sensed information with methods such as sub-pixel classification, feature extraction or object-based analysis (Mid-Atlantic RESAC 2005; Obusek and Tribble 2006).

In Kentucky, the imperviousness data derived from 2001 epoch Landsat data is the only statewide, moderate spatial resolution source of information available (Kentucky Division of Geographic Information 2009c). Methods exist for estimating the total impervious area (TIA) based on GIS data which are proxies for imperviousness (Barber et al. 2002). Estimating TIA at the river basin scale is relatively simple when the classification of imperviousness for each pixel is binary: either the area represented by the pixel is 0 or 100% impervious. Another approach is to generate imperviousness or impervious cover data layers through subpixel classification approaches (Yang et al. 2002; Woods Hole Research Center 2007). A propagation method must be then used to estimate the TIA by utilizing this type of dataset. Calculation of "pooled" TIA by extracting subpixel contributions to imperviousness based on discrete percentage imperviousness classes (i.e. 101 classes: 0, 1%, etc. through 100%) can be determined by:

$$\text{TIA} = \sum p_j \, a_j / 100 \tag{8.1}$$

where,

TIA	total impervious area (ha)
p_j	sub-pixel percentage imperviousness for class j (%)
a_j	total surface area covered by imperviousness class j (ha)
j	imperviousness class (1,. . .,101)

This TIA calculation will be used throughout this chapter to present some spatial and temporal change trends in imperviousness, based on an existing sub-pixel impervious layer that can be used for developing environmental resource policy and management options.

8.2.1 The Effects of Resampling Method on Values and Distribution of Subpixel Imperviousness Classes

The 2001, 30 m imperviousness dataset is published and freely available for downloading as a raster dataset from a geospatial information provisioning system, the Seamless Data Distribution System (U.S. Geological Survey 2008). The imperviousness dataset inherited the coordinate system – USGS Albers Equal Area (ALB), of standard use in other USGS products such as the Landsat imagery used to generate it. Kentucky Single Zone in the State Plane Coordinate System (FIPS 1600) is the Commonwealth's official coordinate system (Kentucky Administrative Regulations 2009). For publication to the Kentucky Geography Network and subsequent spatial analysis procedures, data layers needed to be converted to, and clipped to the state boundary (Kentucky Division of Geographic Information 2009b) so that the impervious dataset could be more easily integrated with existing and planned geospatial data. Wall-to-wall impervious cover and land cover change datasets are available for Kentucky, except that post-processing of the data in order to be in a single recognized and compatible coordinate system could introduce distortions to the statistical estimates from the original dataset.

In order to make the USGS data more easily available to environmental managers in the state, a decision had to be made in terms of the resampling method to be used during reprojection from USGS's Albers Equal Area to Kentucky Single Zone. Subpixel imperviousness values range from 0 to 100% and it presents duality in that it can either be considered numerical (discrete or continual) or categorical, the effects of processing on spatial distribution of imperviousness were examined by using the nearest neighbor (NN) and the bilinear interpolation (BI) methods existent as utilities in ArcGIS/ArcInfo® 9.3.1 (ESRI 2009; Lillesand et al. 2007).

The Kentucky urban/rural interface can be characterized by an abundance of mixed use subwatersheds with a range of imperviousness. Therefore, ten 14-digit

Table 8.2 Percent (%) TIA and surface area distribution for 10 Lexington-Fayette County, KY 14-digit subwatersheds. Please see text for abbreviations

14-digit HUC	Subwatershed	%TIA (ALB)	Area (ha)
05100205-270-040	Steeles Run	1.0	11,806
05100205-270-030	South Elkhorn Creek – I	2.1	4,553
05100205-270-080	Town Branch – I	5.8	2,818
05100205-280-200	Cane Run	10.0	1,822
05100205-120-010	East Hickman Creek	10.8	2,236
05100205-270-010	South Elkhorn Creek – II	12.9	2,637
05100205-280-010	North Elkhorn Creek	17.7	3,492
05100205-120-040	West Hickman Creek	22.3	6,517
05100205-270-070	Wolf Run	28.2	5,792
05100205-270-060	Town Branch – II	44.5	5,458
	TOTAL	14.0	47,132

hydrologic unit code (HUC) subwatersheds corresponding to urban/suburban/rural areas falling primarily within the corporate city boundaries of Lexington-Fayette County, Kentucky were selected (Table 8.2; Fig. 8.1) (Kentucky Division of Geographic Information 2009d, e).

The post-reprojection results using the NN and BI methods were examined in three different ways in comparison to original USGS published data (ALB): (a) spatial distribution of imperviousness value; (b) overall frequency distributions by imperviousness numerical class; and (c) overall effects on %TIA.

As compared with the ALB data, contrast is lost by using BI due to smoothing effects, and even though general "crispness" is preserved, some geometric distortion of linear imperviousness features are introduced by using NN (Fig. 8.2). The BI method produced frequency distortions in the high pixel count classes, whereas the NN method preserved the relationship with the original pixel distributions (Fig. 8.3). The histogram shows that discrepancies in pixel value frequencies were of minor consequence overall (Fig. 8.4). As a result of this, and also possibly due to bias cancellation contributed to this agreement, when percent TIA was calculated for each of the ten 14-digit subwatersheds, both NN and BI produced similar results, in close agreement with the estimates from the original dataset (Fig. 8.5).

Therefore, in order to achieve the objective of making the existing USGS Seamless Data for imperviousness more readily integrated into existing and planned geospatial datasets while maintaining accuracy for environmental resource policymakers at the local and state levels as well as researchers, the decision was made to reproject the original USGS Albers Equal Area to Kentucky Single Zone using the NN method. The previous analysis shows how important this simple choice in software options/algorithms should not be taken lightly because of the implications of making a different choice would potentially have on estimating imperviousness in particular and land planning and management activities in general.

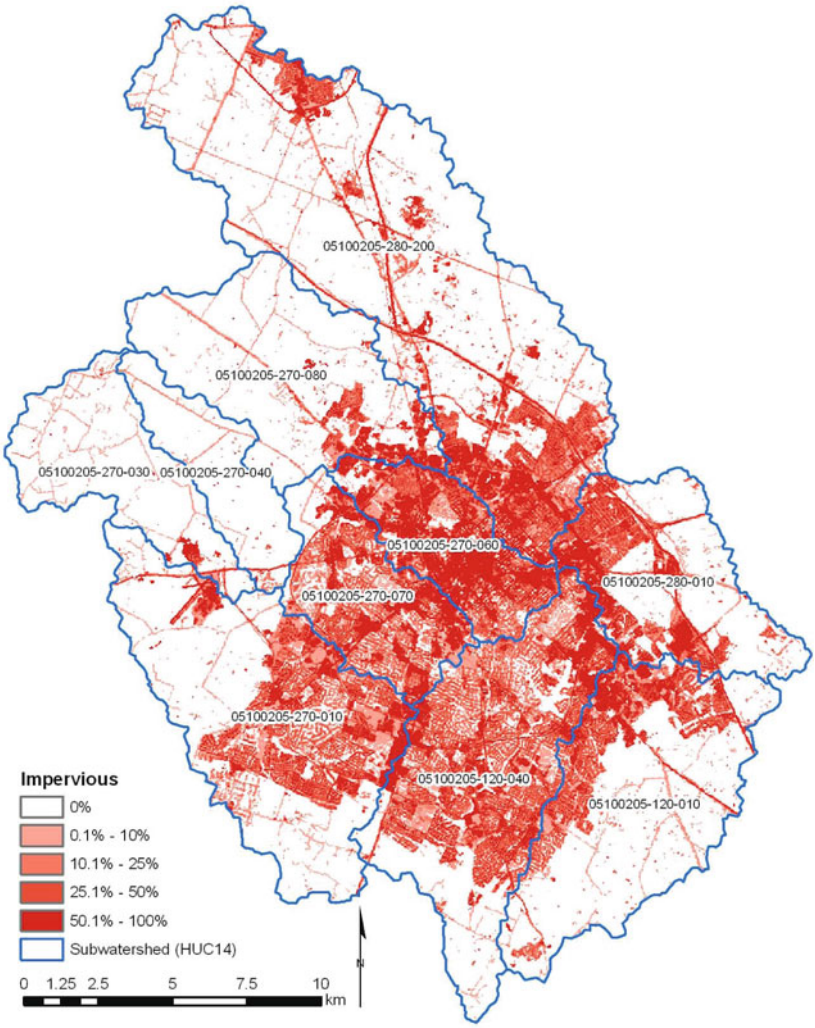

Fig. 8.1 Ten 14-digit hydrologic unit code subwatersheds representing mixed-use subwatersheds in a portion of Lexington-Fayette County, KY

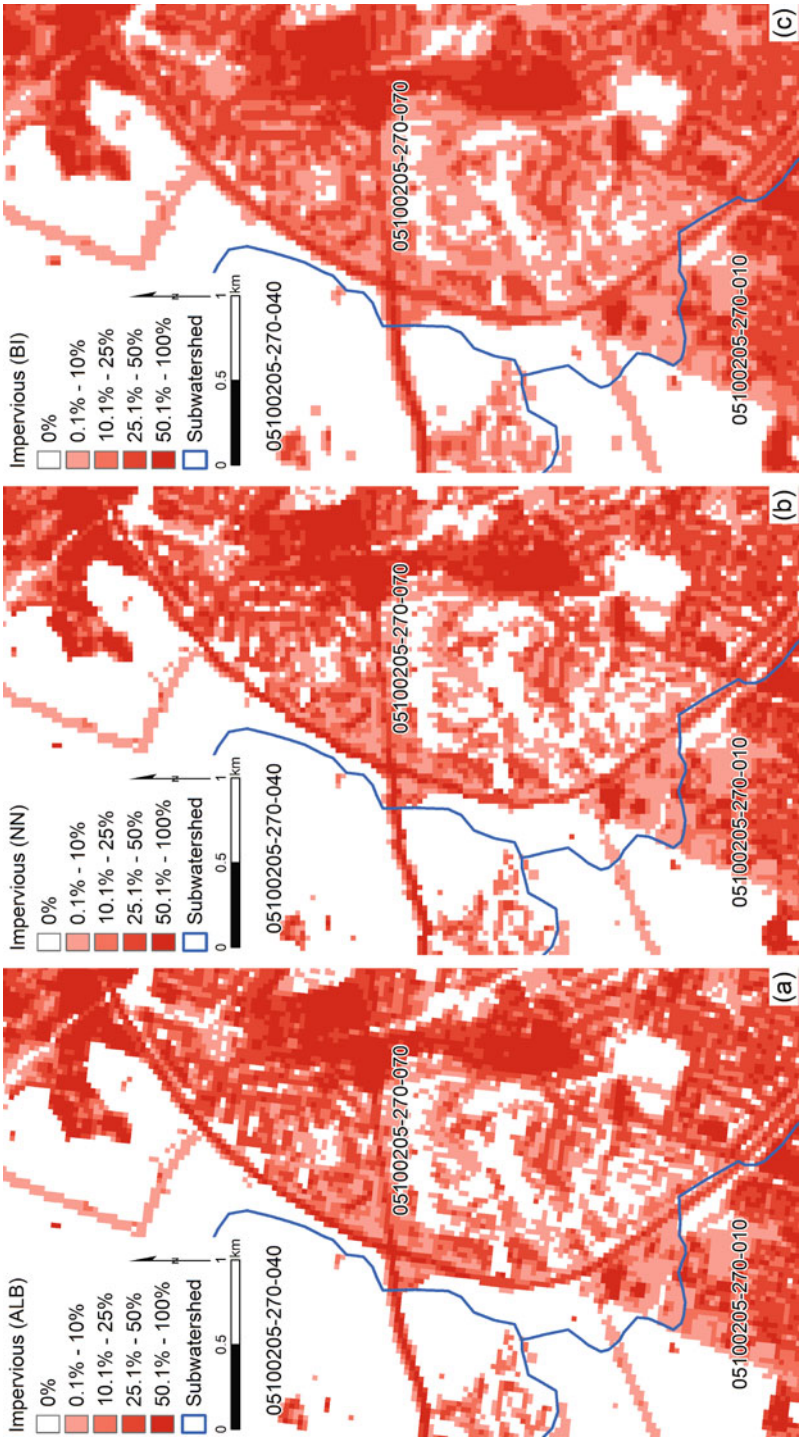

Fig. 8.2 Results from re-projection using different interpolation methods. (**a**) original imperviousness (USGS – Albers Equal Area); (**b**)nearest neighbor; (**c**) bilinear interpolation

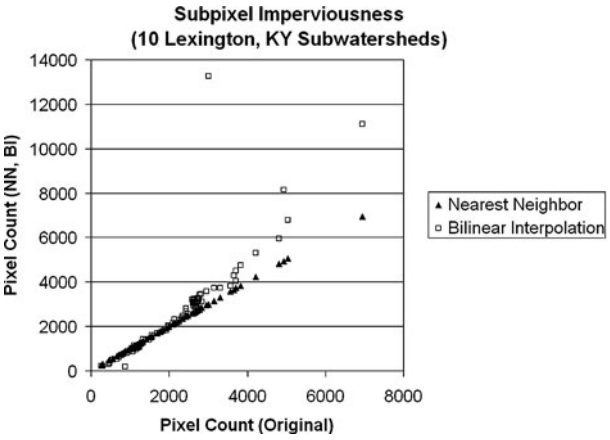

Fig. 8.3 Distortion in frequency distribution – class-to-class pairing; resampling by nearest neighbor and bilinear interpolation methods vs. original data (ALB)

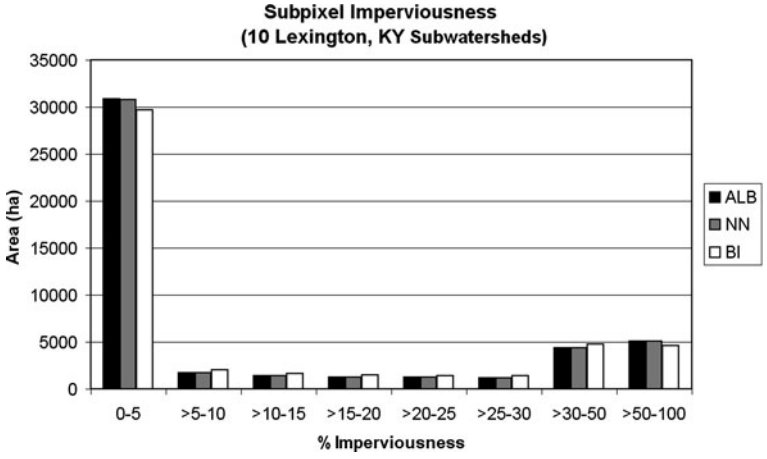

Fig. 8.4 Subpixel imperviousness comparison for two methods of resampling; all 10 subwatersheds

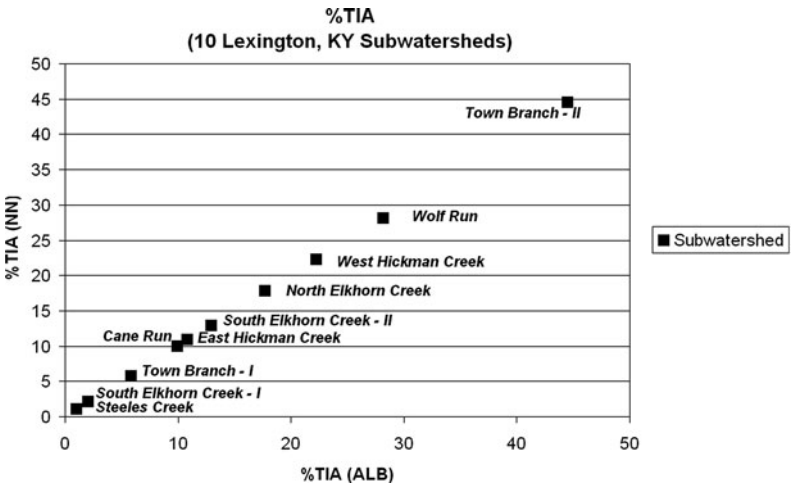

Fig. 8.5 Percentage of total impervious area (%TIA); all 10 subwatersheds

8.3 The Effects of Temporal Land Cover Change on Imperviousness

Landscapes are not static and are always changing. Impervious cover is a critical hydrologic factor for watershed management, but far be it from being a static property, the problem is often reduced to knowing where, how much, and when this landscape attribute changed. The increase in urban development across the state was demonstrated for the 2001–2005 period, but there is neither older nor more recent, specific imperviousness datasets, other than the "baseline" set for 2001. Newer data exist which are useful to look at more recent trends during what was considered to be an era of economic growth and urbanization in the region.

This section of the chapter will focus on two aspects of using geotechnologies and data for environmental resource management. First, a method to quantify spatial changes in imperviousness over time, covering a period between 1992 and 2005, while pivoting on the 2001 baseline imperviousness dataset is described. Next, an analysis addresses increases in imperviousness in the context of spatial overlap within the same subwatershed set. To provide temporal context to the land cover class changes and conversion rates resulting in added imperviousness to urban and suburban watersheds, information was used from two land cover change products, covering adjacent temporal windows – one quasi-decadal, the other quadrennial. The 2001–2005 temporal land cover change product for Kentucky has a documented accuracy and higher degree of class resolution (Anderson Level II vs. Level I) (Palmer 2007). Kentucky watersheds that had

experienced recent changes in developed land cover classes (i.e. "open" (Class 21), "low-intensity" (Class 22), "medium-intensity" (Class 23), "high-intensity" (Class 24)), based on the 2001–2005 change product, were identified and utilized to carry out both the retrospective (backward) (2001–1992) and prospective (forward) (2001–2005) imperviousness change analysis (Fry et al. 2009; Kentucky Division of Geographic Information 2009b). Subwatershed delineations were used (Kentucky Division of Geographic Information 2009d). Of a total of 9,109 subwatersheds comprising the state of Kentucky, 1,219 were utilized for this analysis (Fig. 8.6)

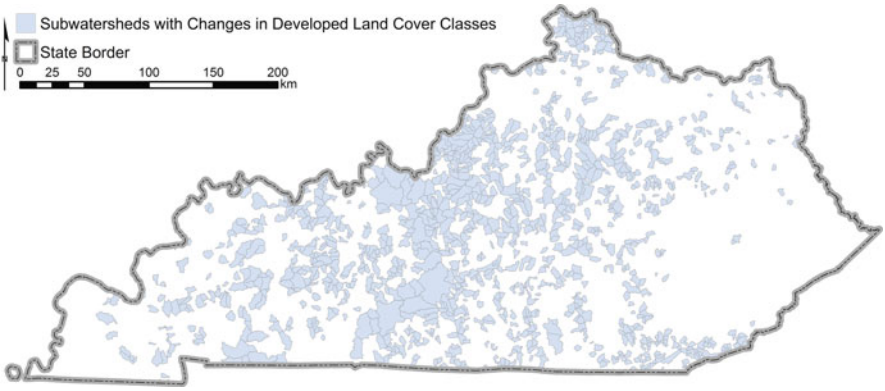

Fig. 8.6 Forward changes in developed land cover classes (i.e., NLCD01 Anderson Level II classes: 21, 22, 23, 24) was used to select subwatersheds for retrospective (1992–2001) and prospective (2001–2005) TIA analysis

8.3.1 Land Cover–Imperviousness Cross-walk: The 2001 Baseline Dataset

Imperviousness is correlated with and is utilized as an indicator of urban and suburban development (Bauer et al. 2005). With that relationship in mind, the use of the developed land cover class change information was explored as a way to extract information on increases in TIA. Conversion factors had to be estimated, in order to cross-walk categorical, developed land cover classes with the subpixel percent imperviousness which is a continuous variable. The relationship between subpixel imperviousness and Anderson Level II developed classes was very consistent, accounting for most if not all of the contribution to imperviousness, both for the statewide NLCD01 and the subset of 1,219 subwatersheds. This enabled the conversion of the increase in four developed land classes to increases in imperviousness, by using 0.07, 0.33, 0.64, and 0.88 as conversion factors (Table 8.3).

Table 8.3 Subpixel imperviousness and land cover class type on the selected 1,219 subwatersheds that exhibited developed land cover class change between 2001 and 2005

NLCD01 class	Pixel Count (no.)	Surface area (%)	Imperviousness mean (%)	Standard deviation. (%)	Standard error of the mean (%)
Open water	682,107	2.1	0.0102	0.6	0.0007
Developed, open space	1,963,787	6.1	7.8431	6.7	0.0048
Developed, low intensity	837,195	2.6	33.1667	10.2	0.0111
Developed, medium intensity	373,067	1.2	63.9875	11.4	0.0187
Developed, high intensity	164,961	0.5	88.5434	7.1	0.0174
Barren land	75,644	0.2	0.2378	4.2	0.0154
Deciduous forest	12,845,925	39.8	0.0016	0.17	0.0000
Evergreen forest	839,736	2.6	0.0023	0.2	0.0002
Mixed forest	422,418	1.3	0.0007	0.1	0.0001
Scrub/shrub	217,332	0.7	0.0104	0.5	0.0010
Grassland/herbaceous	997,511	3.1	0.0068	0.4	0.0004
Pasture/hay	9,138,486	28.3	0.0162	0.7	0.0002
Cultivated crops	3,391,482	10.5	0.0175	1.0	0.0005
Woody wetlands	240,994	0.7	0.0005	0.1	0.0002
Emergent herbaceous wetlands	117,958	0.4	0.0006	0.2	0.0006

The mean percentage imperviousness for the subwatersheds served as a basis to model TIA based on developed land class counts. For the 2001 data, a comparison of both methods was undertaken. TIA was calculated by propagating the subpixel imperviousness using expression (8.1) and by modeling it with land cover type by using the conversion factors derived from Table 8.3. When considering just the 1,219 subwatersheds, very close agreement was found between estimates of the total TIA yielded by the two methods, 73,721 and 73,482 ha respectively ($r = 0.999^{***}$; significant at the 0.001 level) (Fig. 8.7).

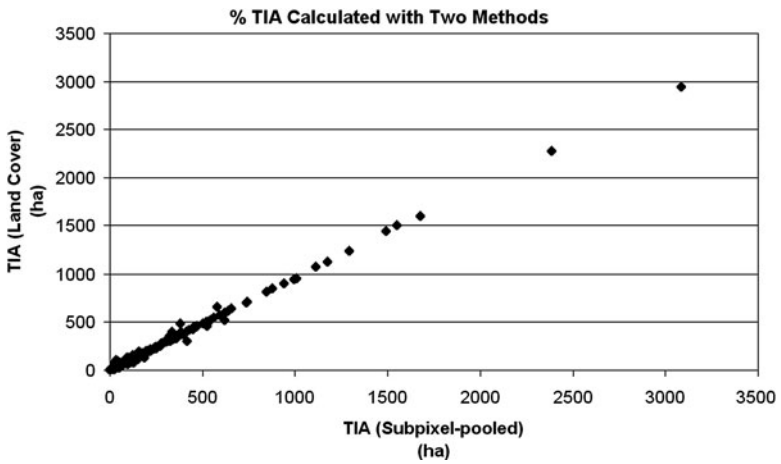

Fig. 8.7 Total impervious area calculated by two methods – the land cover class model and by subpixel formula (I); all subwatersheds

8.3.2 Rates of Change and Sources of Imperviousness (1992–2005)

A portion of the USGS's National Land Cover Dataset (NLCD) 1992/2001 Retrofit Land Cover Change Product (LCC9201) (MRLC 2009; Fry et al. 2009) was extracted and geoprocessed to the extent and boundary of Kentucky. In particular, three "from-to" – or "source-target" classes that are inherent in the LCC9201 data were extracted which included those labeled *"62"* (from agriculture to developed), *"42"* (from forest land to developed), and *"12"* (from water to developed). These classes represented 74.3, 23.4, and 1.9% of the added development, respectively. A "boundary clean" algorithm was utilized to eliminate single pixel change locations. A negative consequence of this operation is the loss of some linear change features, and some areas of less dense development (Fig. 8.8).

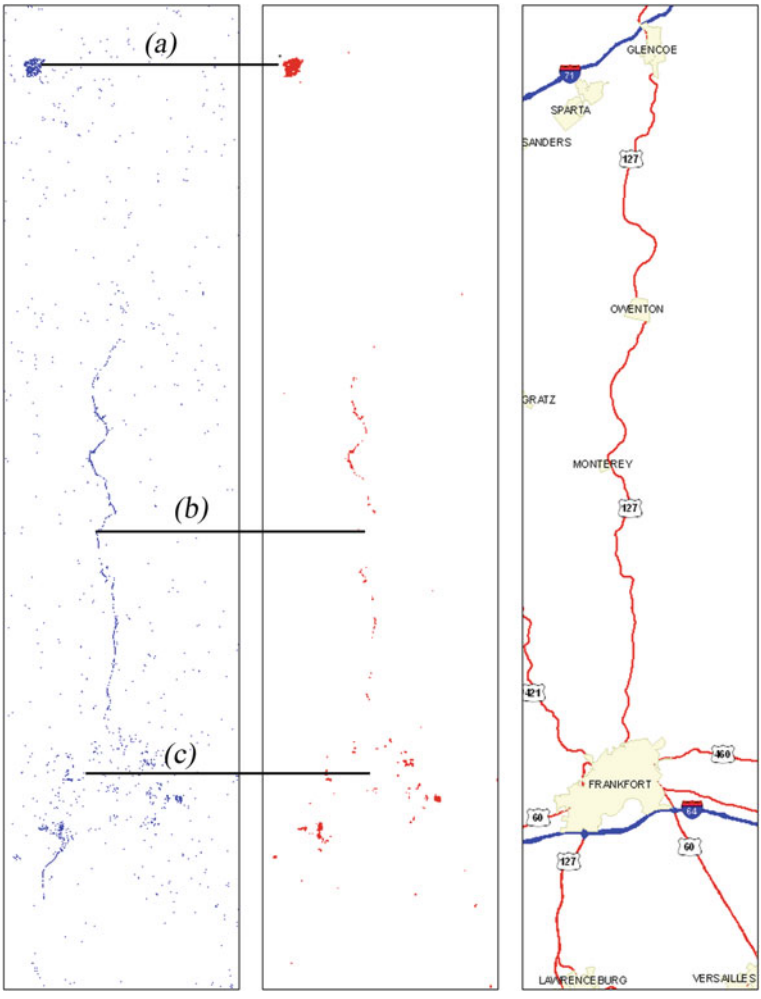

Fig. 8.8 Retention and loss of regions of change; (**a**) compact, (**b**) linear and (**c**) less dense and, respectively due to a generalization or "boundary clean" operation. Retrospective change (1992–2001). Map North is up. Approximate scale: 1:296,000

When compared with statewide change areas, the near-decadal change (1992–2001) occurring in the previously indicated subwatersheds, accounted for 80% of the statewide change, indicating a recurrence of land conversion in these subwatersheds. It is reasonable to expect that land cover change tends to happen near previous areas of land cover change and this has been shown in other studies. Change or urbanization begets more change (urbanization) which is important when planning for meeting clean water requirements at local, state, and national levels for environmental managers as it relates to policy implications and infrastructure implementation.

To examine the aggregation level of this new imperviousness, a region creation approach was used by applying a "queen contiguity" (8 neighbors) to the retrofit product (1992–2001) and the NLCD05 (2001–2005), followed by the boundary clean operation. Zonal statistics were calculated for the regions and regions attributed with their *majority* source class. The relative accuracy of the generalization method used can be assessed by the attribution of developed land to spurious classes, such as water, wetland, developed, etc., even though the amount of "contaminants" was minor. Forest and agriculture were the main contributors to the developed areas, with an apparent increasing contribution from the former, as indicated by their conversion ratios for each time period (1992–2001 and 2001–2005), 1.8 and 1.6 respectively. Total daily conversion rates appeared to double from 2.6 ha/day (1992–2001) to 4.9 ha/day (2001–2005), with agriculture and forestry also doubling from their daily rates of 0.9 and 1.6 ha/day, respectively, from the first to the second period. The contributions from all other land cover classes were negligible. For control purposes, the spatial overlap between the two time period generalizations was 107 ha – or 0.6% of the combined 1992–2001 and 2001–2005 change zones (excluding overlap).

8.3.3 Recurrent Addition of New, Compact, Impervious Areas in Subwatersheds

The distribution of 2001 baseline TIA (pooled method) relative to total area for those subwatersheds impacted by developed class change was assessed next. Based on Schueler's (1994) three major critical watershed imperviousness intervals (i.e., 0–10%, >10–25%, and >25–100%) it was found that nearly 14% of the approximately three million hectares (ha) in the study area fell in the impacted or threatened watershed categories. When compared with the 2001 land cover, the majority of the small relative increase in developed land observed four years later was represented by substantial growth in the low and medium intensity development classes (Table 8.4).

Using the land cover to calculate imperviousness conversion factors previously described, a *net* increase in TIA of 3,392 ha, resulted for the whole study area between 2001 and 2005. This represented an overall increase in TIA from 2.5–2.7% for the selected subwatersheds, highlighting the importance of both local concentration of imperviousness and its initial values (Figs. 8.9 and 8.10).

Table 8.4 Changes in developed land surface area from 2001 to 2005 for selected subwatersheds

Land Cover Class (Anderson Level II Class Number)	NLCD 2001 (ha)	NLCD 2005 (ha)	Difference (ha)	Increase (%)
Developed, Open Space (21)	176,741	177,323	582	7.7
Developed, Low Intensity (22)	75,348	79,512	4,165	55.4
Developed, Medium Intensity (23)	33,576	35,566	1,990	26.5
Developed, High Intensity (24)	14,846	15,628	781	10.4
Total	300,511	308,029	7,518	2.5

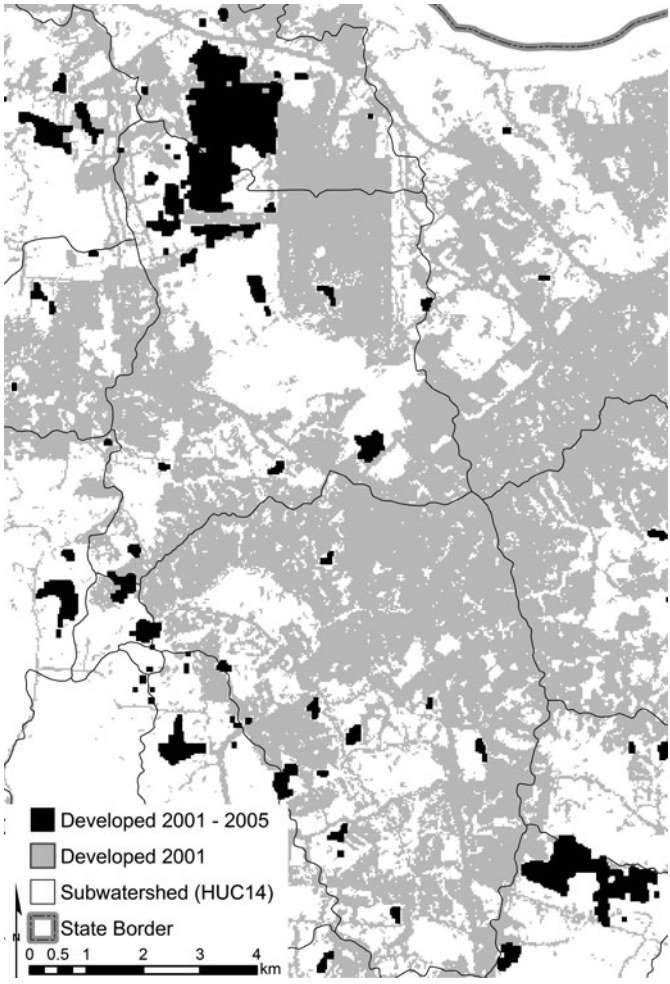

Fig. 8.9 Increase in developed classes with existing development in 2001 (*grey*) and added development from 2001 to 2005 (*black*) in selected subwatersheds

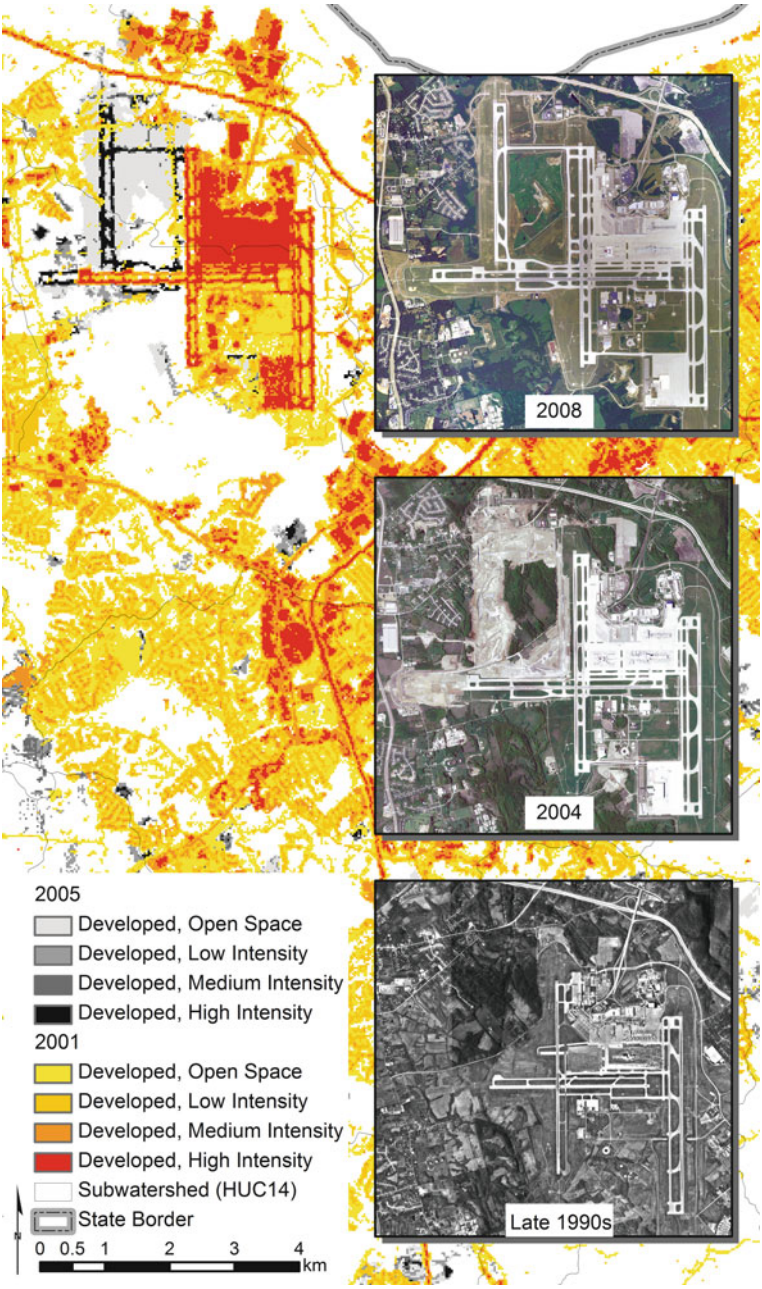

Fig. 8.10 Developed land cover classes (NLCD01) are indicated in *yellow* to *red* while the areas effectively added between 2001 and 2005 are indicated in *grey* to *black*. A time series of archival, aerial orthophotography is provided for comparison

The areas of developed land effectively added between 2001 and 2005 totaled 8,160 ha. A total of 6,178 regions were delineated using the same region-group algorithm as as described for the 1992–2001 data, grouping pixels into regions of continuous developed class increase (i.e. classes 21, 22, 23, and 24). The TIA was calculated by using individual areas of developed class, based on the contribution of each class to TIA (e.g. developed, open space). From preliminary visual verification and proximity analysis it became obvious that the surfaces effectively added were occurring in the vicinity of previously existent developed areas. The region group approach utilized created a very large proportion of regions less than 1 ha, accounting for 86% of the total count and for 15% of the total area added. In contrast, the total surface area for regions over 20 ha in surface area (n=74) totaled 2,838 ha. While information on diffuse (non-point) change may be lost by grouping and filtering by size, this type of generalization procedure allows for focusing environmental and watershed management efforts on areas of detected – but compact and extensive change.

Surprisingly, the mean %TIA was similar for all region size classes – 30–40%, thus each region's contribution to total increase in TIA is a proxy for its contribution to the total area, with a maximum of 35% for areas >20 ha – with 1% of total number of regions, and a minimum of 15% for areas between 0 and 1 ha – representing 86% of the total number of regions.

Centroids for contiguous developed areas effectively added in the two time periods, attributed with the total area developed. Using these, kernel densities were calculated, and mean densities (ha/ha) for each individual subwatershed were estimated. The kernel density procedure yielded similar range of values for the 1992–2001 and 2001–2005 analysis, with a maximum of 0.06 ha/ha (Fig. 8.11).

Not surprisingly, the subwatersheds affected by imperviousness increase were often in and around Kentucky's major metropolitan and peri-urban areas : 1.West Central KY (*Louisville-LaGrange-Shepherdsville-Shelbyville); 2.* East Central KY (*Lexington-Nicholasville-Georgetown; Lawrenceburg-Winchester-Richmond); 3.* Northern KY (*Florence-Covington-Independence- Alexandria; Warsaw-Sparta-Ghent)*; 4. South Central KY (*Somerset*) and 5. Western KY (*Bowling Green-Owensboro*).

Just in the four years intervening between 2001 and 2005, 7% of the study subwatersheds experienced added development densities of between 1 and slightly over 5%. Although these values translated into about 4% of the watersheds having an increase of %TIA of between 1 and 6%, a somewhat complex trend is revealed across mean %TIA classes (Fig. 8.12).

A recurrent or persistent densification of imperviousness in the selected subwatersheds was suggested by the relationship between kernel densities in the two consecutive time periods (Fig. 8.13).

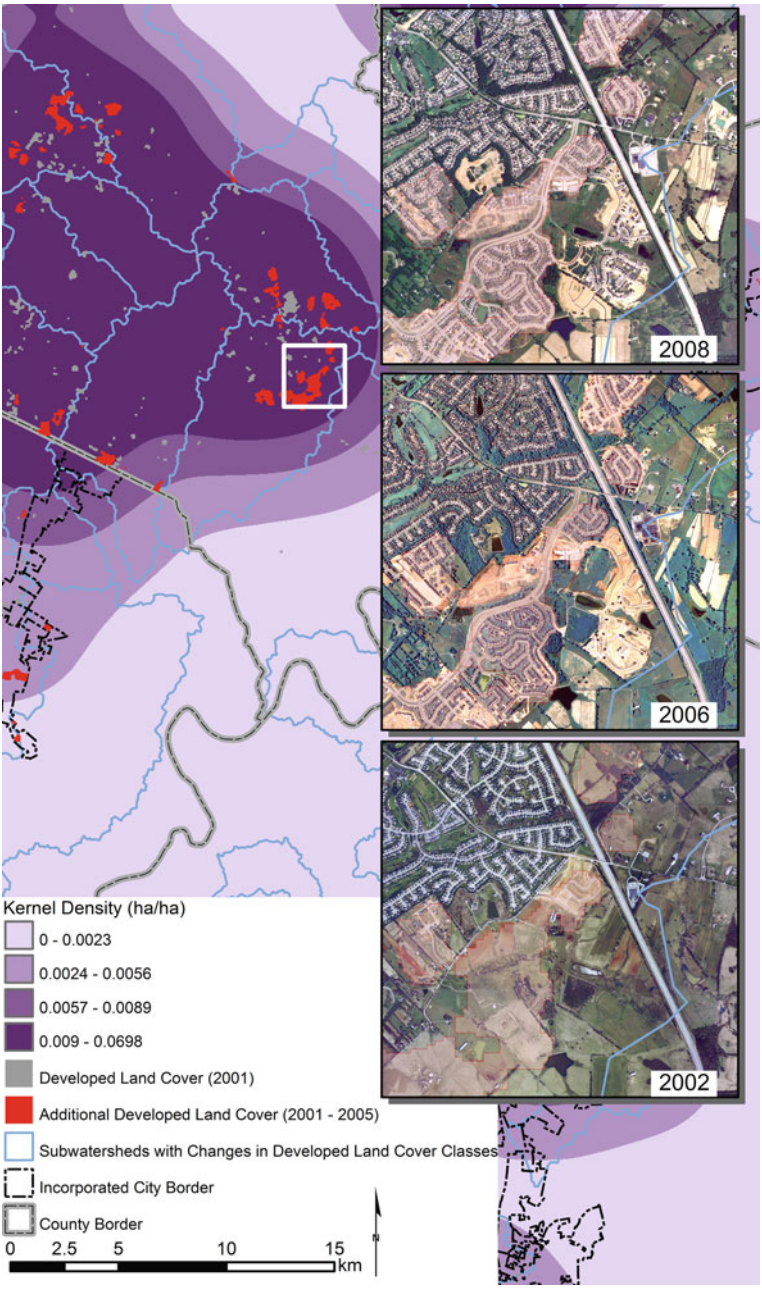

Fig. 8.11 Impacted subwatersheds, new developed areas (1992–2005), kernel density and corporate boundaries. A time series of archival, aerial orthophotography is provided for comparison

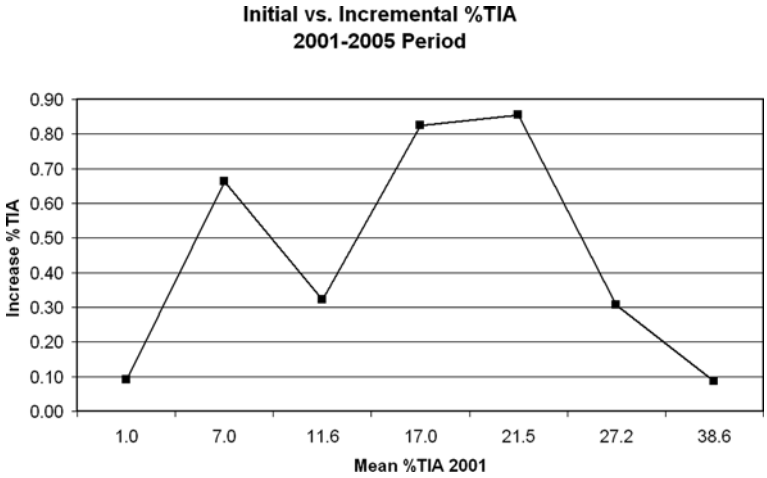

Fig. 8.12 Increment in %TIA as a function of initial value; values are means for the 5% TIA intervals (0–5%, 5–10%, etc.), except for the last one (30–50%)

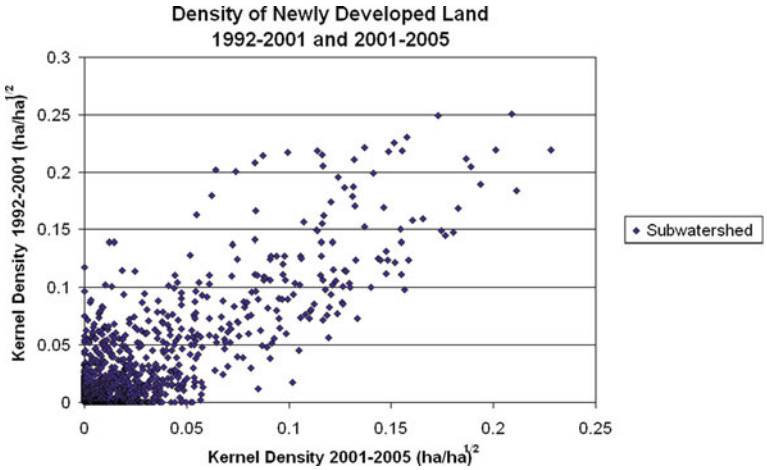

Fig. 8.13 Recurrent densification in developed land. Separate kernel densities for retrofit land cover product (1992–2001) and KLC (2001–2005)

8.4 Watershed Management and Policy Implications

The watershed management framework approach has been in existence in Kentucky since 1996 (Kentucky Division of Water 2009a, b). The importance of methods for the data collection, assessment of watersheds, and the detection of information gaps in the context of prioritization and targeting of basins or hydrologic units is one of

the core components of the effort. Imperviousness possesses both a dynamic and an "unplanned" nature in the sense that it results from land use and land cover change over a period of time from years to more than decades. The drivers, nature, and extent of these changes must be considered in the context of a state where 92% of its land area is under private ownership (Kentucky Department of Fish and Wildlife Resources 2009). This fact also strengthens the case for the use of remote sensing as the preferred way to measure changes in imperviousness in a routine, timely, and cost-efficient way to encompass large areas with relatively good accuracy data.

The implications of seemingly modest TIA increases such as the ones revealed by the previous analysis (about 5 ha/day in the 2001–2005 time interval) are obvious. Kentucky possesses a large and complex hydrologic surface network totaling 146,000 km (Kentucky Division of Water 2008), that drains a 30-year average annual precipitation of 1,242 mm (Kentucky Climate Center 2009). Examples of land development codes seeking to manage and mitigate increases in imperviousness at the subwatershed level exist in some parts of Kentucky (Louisville-Jefferson County Metro Government 2009). To further illustrate the public policy implications of increases in imperviousness and the time lag in the creation of watershed management infrastructure (e.g. stormwater sewers), the case of Lexington, Kentucky is used as an example.

Stormwater management in Central Kentucky has become an issue of public concern. For example, the Lexington-Fayette Urban County Government is involved with the US Environmental Protection Agency through a legal agreement to correct storm and sanitary sewer systems over the next decade or so with anticipated cost of several hundred million dollars (Lexington-Fayette Urban County Government 2008a).

The Lexington-Fayette Urban County Council approved a settlement agreement with state and federal governments that requires Lexington to fix problems with its storm and sanitary sewer systems over the next 11–13 years; outreach efforts to inform the population on the consequences and outlook of these developments are also on-going Lexington-Fayette Urban County Government (2008b, c).

In particular, the stormwater system is directly affected by the amount of imperviousness and the changing amount of imperviousness found in subwatersheds and portions of them. Therefore, the impact of imperviousness and its rate of increase in urban and mixed-use subwatersheds are of extreme relevance for communities trying to mitigate or ameliorate violations of the federal Clean Water Act and/or related Acts. This issue has dimensions of addressing current conditions as well as conditions that likely to be developing during future decades from now. If current conditions are mitigated but urbanization is allowed to continue following recent historic patterns and practices, forward progress is likely to be minimal if any is made since it appears the urbanization change begets urbanization change.

There are a variety of "carrot and stick" technological, economic, policy, and regulatory options that can help on several levels but are beyond the scope of how specifically geospatial technologies and data can be utilized in environmental resource management.

8.5 Summary and Conclusions

The importance of location and amount of changes in land cover, specifically imperviousness, as a leading and trailing indicator for watershed and stream health is commonly acknowledged. This chapter has demonstrated the possibilities that land cover change detection methods can provide for calculating indirect estimates of imperviousness over temporal periods. Therefore, environmental resource experts that utilize geospatial technologies and data for management and policy implantation recommendations should keep several things in mind that have been addressed in this chapter.

1. Using moderate resolution imagery is a most cost and time effective solution to help quantify and spatially identify where the landscape is undergoing changes when an entire state is involved.
2. Care in data handling is critical for efficient and accurate integration with existing and planned datasets during the reprojection process.
3. Landscapes are in a continual state of change. Identifying where, what, and the temporal trend of those changes are critical for proactive land use planning that has direct environmental and resulting ramifications for addressing stormwater management concerns.
4. In the absence of specific impervious data, but with a reliable baseline, reasonable retrospective and prospective impervious estimates can be made using new and complementary data.

Acknowledgments This work was partially supported by funding from NASA Cooperative Agreements NCC13-03010: "Taking GIS and Remote Sensing to the People of KY: Developing an Open GIS Data Viewing & Distribution System for Kentucky" (KLC); and NAG13-02024 "Monitoring and Assessment of Forest and Urban Resources in the Commonwealth of Kentucky" (KLS). Susan C. Lambert, Geographer, had the foresight to envision, design and procure funding for the Kentucky Landscape Snapshot, the Kentucky Landscape Census, and the Kentucky Watershed Modeling Information Portal projects.

References

Arnold Jr CL, Gibbons CJ (1996) Impervious surface cover: The emergence of a key environmental indicator. J Am Plan Assoc 62(2):243–258

Barber MC, Baca RM, Bird SL, Doherty J, Exum LR, Johnston JM, Lassiter RR, Rashleigh B, Cyterski MJ, Colarullo S, Loux NT, Prieto LM, Wright CJ (2002) Regional assessment of fish health: a prototype methodology and case study for the Albemarle Pamlico River Basin, North Carolina. EPA/600/R-02/067. http://www.epa.gov/athens/publications/reports/EPA_600_R02_067.pdf Accessed 31 July 2009

Bauer ME, Loeffelholz B, Wilson B (2005) Estimation, mapping and change analysis of impervious surface area by landsat remote sensing. Proceedings pecora 16 global priorities in land remote sensing 23–27 October 2005 Sioux Falls, South Dakota

Booth D, Reinelt L (1993) Consequences of urbanization on aquatic systems: measured effects, degradation thresholds, and corrective strategies. In: Proceedings of Watershed 93: A National Conference on Watershed Management

ESRI ArcGIS 9.3 [CD-ROM] (2009) Redlands, CA: Environmental Systems Research Institue.
Fry JA, Coan MJ, Homer CG, Meyer DK, Wickham JD (2009) Completion of the national land cover database (NLCD) 1992–2001 land cover change retrofit product: US Geol Surv Open File Rep 2008–1379. http://pubs.usgs.gov/of/2008/1379/. Accessed 31 July 2009
Harp GR, Zourarakis DP, Brenner A, Palmer M, Boggs R (2006) Kentucky landscape snapshot final performance report. Monitoring and assessment of forest and urban resources in the commonwealth of Kentucky. Coop Agreem NAG13-02024 http://kygeonet.ky.gov/metadataexplorer/full_metadata.jsp?docId=%7BCB1F6AFD-C652-4414-AC48-7AA90D200EE0%7D. Accessed 31 July 2009
Homer C, Dewitz J, Fry J, Coan M, Hossain N, Larson C, Herold N, McKerrow A, VanDriel J, Wickham J (2007) Completion of the 2001 national land cover database for the conterminous United States. Photogramm Eng Remote Sens 73(4):337–341
Kentucky Administrative Regulations (2009) 10KAR 5:010. The Kentucky single zone coordinate system of 1983. http://www.lrc.ky.gov/kar/010/005/010.htm. Accessed 31 July 2009
Kentucky Department of Fish and Wildlife Resources (2009). Kentucky wildlife action plan. Vol I. Append 1.4. http://fw.ky.gov/kfwis/stwg/Appendix/1.4%20public%20land%20ownership.pdf. Accessed 31 Jan 2010
Kentucky Division of Geographic Information (2009a) Kentucky NLCD01. http://kygeonet.ky.gov/metadataexplorer/full_metadata.jsp?docId=%7B0484AA9B-4633-4A36-B212-0C8EC1BE686D%7D. Accessed 31 July 2009
Kentucky Division of Geographic Information (2009b) Kentucky land cover change detection 2001–2005 Anderson level II. http://kygeonet.ky.gov/metadataexplorer/full_metadata.jsp?docId=%7B65E31366-1A04-4BE4-8128-0324E6C672F0%7D. Accessed 31 July 2009
Kentucky Division of Geographic Information (2009c) Kentucky imperviousness 2001 – national land cover database. http://kygeonet.ky.gov/metadataexplorer/full_metadata.jsp?docId=%7BB0CF6969-C67A-4A92-AFF6-4F29860B9AF5%7D. Accessed 31 July 2009
Kentucky Division of Geographic Information (2009d) 14-digit hydrologic units. http://kygeonet.ky.gov/metadataexplorer/full_metadata.jsp?docId=%7BBE9E665C-5A2C-4390-BF58-CD19553EA756%7D. Accessed 31 July 2009
Kentucky Division of Geographic Information (2009e) Corporate boundary polygons of Kentucky. http://kygeonet.ky.gov/metadataexplorer/full_metdata.jsp?docId=%B59F7D0A6-12C1-48AB-9D13-AB52EB736E60%7D. Accessed 31 July 2009
Kentucky Division of Water (2008) Integrated report to congress on water quality in Kentucky. Rep 305(b). http://www.water.ky.gov/NR/rdonlyres/1A883375-82DB-46AD-A0DB-3A8BA43EE959/0/2008IntegratedReporttoCongressonWaterQualityinKetucky Vol1.pdf. Accessed 31 July 2009
Kentucky Division of Water (2009a) Watershed framework statewide schedule. http://www.watersheds.ky.gov/framework/wapro4/. Accessed 31 Jan 2010
Kentucky Division of Water (2009b) Watershed framework document chapter 2. http://www.watersheds.ky.gov/NR/rdonlyres/576CB533-3CA7-4F16-AA4B-CBDA47BECF24/0/Chapter_2.pdf. Accessed 31 Jan 2010
Kentucky Climate Center (2009) Kentucky precipitation monthly observations. http://kyclim.wku.edu/indexTables.htm. Accessed 31 July 2009
Lee BD, Hanley CD, Zourarakis DP (2009) Mapping and monitoring land resource change: bridging the geospatial divide for decision making May 20–21 2008 Lexington, Kentucky. http://kygeonet.ky.gov/metadataexplorer/full_metadata.jsp?docId=%7BF5E3B018-3902-453A-8BCF-4BB00F265870%7D. Accessed 31 July 2009
Lexington-Fayette Urban County Government (2008a) EPA consent decree. http://www.lexingtonky.gov/index.aspx?page=840. Accessed 31 Jan 2010
Lexington-Fayette Urban County Government (2008b) Consent decree at a glance. http://www.lexingtonky.gov/Modules/ShowDocument.aspx?documentid=3573. Accessed 31 Jan 2010
Lexington-Fayette Urban County Government (2008c) Mayoral remarks concerning approval of consent decree with Us Environmental Protection Agency and Commonwealth of Kentucky.

http://www.lexingtonky.gov/Modules/ShowDocument.aspx?documentid=3574. Accessed 31 Jan 2010

Lillesand TM, Kiefer RW, Chipman JW (2007) Remote sensing and image interpretation. Appendix C. Sample coordinate transformation and resampling. Wiley, Hoboken, New Jersey

Louisville-Jefferson County Metro Government (2009) Land development code http://www.louisvilleky.gov/PlanningDesign/ldc/LDCMarch2006.htm. Accessed 31 Jan 2010

Mid-Atlantic RESAC (2005) (Mid-Atlantic Regional Earth Science Applications Center) Subpixel estimates of impervious cover from Landsat TM image. http://www.geog.umd.edu/resac/impervious2.htm. Accessed 31 July 2009

Miltner RJ, White D, Yoder C (2004) The biotic integrity of streams in urban and suburbanizing landscapes. Landsc Urban Plan 69:87–100

Multi-Resolution Land Characteristics Consortium (MRLC) (2009) National land cover database (NLCD) 1992/2001 Retrofit Land Cover Change Product Multi-zone download site. http://www.mrlc.gov/multizone.php. Accessed 31 Jan 2010

Obusek F, Tribble T (2006) Final project report: vertical integration of local, commercial, and NASA produced geospatial data to identify and characterize impervious surfaces. NASA Grant NAG13-02020. http://www.cgia.state.nc.us/Portals/0/documents/cgia-nasa_finalreport.pdf. Accessed 31 July 2009

Palmer M (2007) Kentucky landscape census: accuracy assessment report. http://kygeonet.ky.gov/metadataexplorer/full_metadata.jsp?docId=%7B0D96DCC1-5DBF-4496-8C5E-38F1EA48B4FD%7D. Accessed 31 July 2009

Schueler T (1987) Controlling urban runoff: a practical manual for planning and designing urban best management practices. Metropolitan Washington Council of Governments. Washington, DC. Publ No 87703. http://dnrweb.dnr.state.md.us:8080/FullDisp?itemid=00000103. Accessed 2 September 2010

Schueler T (1994) The importance of imperviousness. Watershed Prot Tech 1(3):100–111. http://www.stormwatercenter.net/Library/Practice/13.pdf. Accessed 2 September 2010

US Environmental Protection Agency (2008) EPA's 2008 report on the environment (Final Report. EPA/600/R-07/045F (NTIS PB2008-112484). http://oaspub.epa.gov/eimscomm.getfile?p_download_id=473171. Accessed 31 July 2009

US Geological Survey (2008) seamless data distribution system. http://seamless.usgs.gov/index.php. Accessed 21 Jan 2010

Woods Hole Research Center (2007) Impervious surfaces. http://www.whrc.org/midatlantic/mapping_land_cover/products/impervious_surfaces.htm. Accessed 31 July 2009

Yang L, Huang C, Homer C, Wylie B, Coan M (2002) An approach for mapping large-area impervious surfaces: synergistic use of Landsat 7 ETM+ and high spatial resolution imagery. Can J Remote Sens 29(2):230–240

Walker S, Mostaghimi S (2009) Chapter 4: Watershed-Based Systems. In: Moore KM (ed) The sciences and art of adaptive management: innovating for sustainable agriculture and natural resource management. Ankeny, IA: Soil and Water Conservation Society. http://www.swcs.org/en/publications/the_sciences_and_art_of_adaptive_management/ Accessed 2 September 2010

Zourarakis DP (2009) Land cover change entropy: the 2001–2005 quadrennium in Kentucky. Proceedings MultiTemp 2009-The 5th international workshop on the analysis of multi-temporal remote sensing images. 28–30 July 2009 Groton, Connecticut

Zourarakis DP, Palmer M (2008) Accuracy analysis of the 2005 Kentucky land cover dataset update. Proc. 2008 annual meeting. Lexington KY. J Ky Acad of Sci 69(1):80

Chapter 9
Exploring the Spatially Varying Impact of Urbanization on Water Quality in Eastern Massachusetts Using Geographically Weighted Regression

Jun Tu

Abstract The impact of urbanization on water quality might vary over space because watershed characteristics, pollution sources, and land use patterns are not the same in different places. However, the spatially varying impact is usually not considered using conventional statistical methods, such as ordinary least squares regression (OLS) and Spearman's rank correlation analysis. This study applies a geospatial statistical technique, geographically weighted regression (GWR), to analyze the relationships between urbanization and water quality indicators across watersheds with varied urbanization levels in eastern Massachusetts, USA. The study finds that the relationships between water quality and urbanization indicators vary across the urbanization gradient in the studied watersheds. Percentage of developed land and population density are more strongly related to concentrations of water pollutants in less-urbanized areas than in highly-urbanized areas. The adverse impact of urbanization on water quality is more substantial in less-urbanized suburban areas than highly-urbanized central cities, which is associated with the dominant pattern of urbanization in the study area: urban sprawl. The study suggests that GWR is a useful geospatial technology for policy makers, regional and local agencies, and researchers to unveil the local pollution causes, to improve the understanding of local pollution status, and to adopt appropriate environmental and land use planning policies suitable to the local watershed conservation and management.

Keywords Geographically weighted regression · Water quality · Urbanization · Urban Sprawl

J. Tu (✉)
Department of Geography and Anthropology and the Interdisciplinary Program of Environmental Studies, Kennesaw State University, Kennesaw, GA 30144, USA
e-mail: jtu1@kennesaw.edu

N. Hoalst-Pullen, M.W. Patterson (eds.), *Geospatial Technologies in Environmental Management*, Geotechnologies and the Environment 3, DOI 10.1007/978-90-481-9525-1_9,

9.1 Introduction

Over decades, urban sprawl has been the dominant urbanization pattern throughout much of the United States. Urban sprawl is the land-consumptive pattern of suburban development characterized by increasing scattered, low-density residential and commercial areas outside of city centers caused by population growth, rising incomes, decreasing commuting costs, and dependent on extensive automobile use (Wilson et al. 2003; Interlandi and Crockett 2003; Robinson et al. 2005). Many studies have found that urban sprawl has an adverse impact on varied aspects of social and natural environment, including community development, public health, forests, and stream systems (Zhang 2001; Ewing et al. 2003; McGrath et al. 2004; Wheeler et al. 2005). The main reason has been attributed to the low-density development pattern of urban sprawl since per capita land use, energy consumption, and pollution generation are higher in low-density suburban areas than in high-density central cities.

An increasing concern about the impact of urban sprawl is stream degradation due to the increasing impervious surfaces and human activities in the process of urbanization in watersheds. (Bowen and Valiela 2001; Finkenbine et al. 2001; Tong and Chen 2002; Interlandi and Crockett 2003; Hatt et al. 2004; Aichele 2005; Brett et al. 2005; Deacon et al. 2005; Schoonover et al. 2005). The impact is usually studied through relationship analysis of urbanization and water quality indicators using conventional statistical methods, such as ordinary least squares regression (OLS) and Spearman's rank correlation analysis. Generally positive correlations exist between concentrations of water pollutants and percentages of developed lands (i.e. urban lands, as used in many studies) including commercial, residential, and industrial lands. In other words, higher concentrations of water pollutants are related to higher percentages of developed lands. For example, Tong and Chen (2002) examined the relationships of land use and water quality on regional scale in the watersheds of the Ohio State, USA. They found that TN (total nitrogen), TP (total phosphorus), conductivity, and fecal coliform were significantly positively related to commercial and residential lands. However, a relationship between an urbanization indicator and a water quality parameter found in one study might not be true, or even opposite in other studies. For instance, a study in the Ipswich River watershed, Massachusetts, USA found that TN and TP had no significant correlations with urban lands (Williams et al. 2005). Therefore, the relationships between urbanization and water quality indicators are not constant because watershed characteristics and pollution sources are not the same in different watersheds. Especially for the regions under rapid urban sprawl, the relationships between urbanization and water quality indicators might vary substantially over space because great differences in land development pattern exist between low-density suburbs and high-density central cities. However, the potential different impact of urbanization on water quality between suburban areas and central cities has been seldom studied and reported. One of the reasons might be due to the fact that the conventional statistical methods used in previous studies are global statistics, which analyze the average situation for

the whole study area, so it is not easy to use them to explore local variations in the impact of urbanization on water quality.

In recent years, a simple but powerful statistical method named geographically weighted regression (GWR) has been developed to explore the spatial non-stationarity among spatial variables (Brunsdon et al. 1998; Fotheringham et al. 2002). Spatial non-stationarity means that the relationships between independent and dependent variables are not constant over space (Fotheringham et al. 2002). Unlike OLS that generates a set of regression results applied to all the regression points, GWR can calculate a set of local regression results for each regression point. In other words, the model parameters (e.g. regression coefficients and R^2) from GWR might be different at different sampling points. The local model parameters can be mapped using visualization (e.g. GIS) so that local spatial variation in the regression relationships can be investigated. GWR is an increasing widely used spatial statistical method that is an important geospatial technology along with GIS and remote sensing (Fotheringham et al. 2002). Therefore, GWR provides a useful geospatial tool to explore the spatially varying relationships among spatial variables, such as population density, land uses, water quality, and climate variables, which usually change over space. This technique has been applied in some fields, such as ecology (Shi et al. 2006), social studies (Fotheringham et al. 2001), and urban studies (Yu 2006), which are all good examples of the application of geospatial technology. However, GWR is seldom used in water resources research.

This study applied the GWR technique to examine the spatially varying relationships between urbanization and water quality indicators in eastern Massachusetts, USA. GWR is an exploratory spatial data analysis (ESDA) technique. Thus, the objective of this study is not so much to study mechanism of water pollution, but to explore how the relationships between urbanization and water quality indicators change across space and to compare the influence of urbanization on water quality among watersheds with different degrees of urbanization distributed from central city to suburbs.

9.2 Study Area

An area covering fifteen river basins in eastern Massachusetts as defined by the U.S. Geological Survey (USGS) and the Massachusetts Department of Environmental Managements (MADEM) has been chosen for this study. The study area contains metropolitan Boston and its surrounding areas up to 80 km away from Boston in eastern Massachusetts (Fig. 9.1). The area is about 10,000 km^2. The population in year 2000 is about 5.2 million. This area is more densely populated, urbanized and industrialized than most parts of New England. Most of lands in metropolitan Boston and the City of Worcester are highly developed, including residential, commercial, and industrial lands. The rest of the study area is mainly covered by forest. A small amount of agricultural land also exists in some places outside

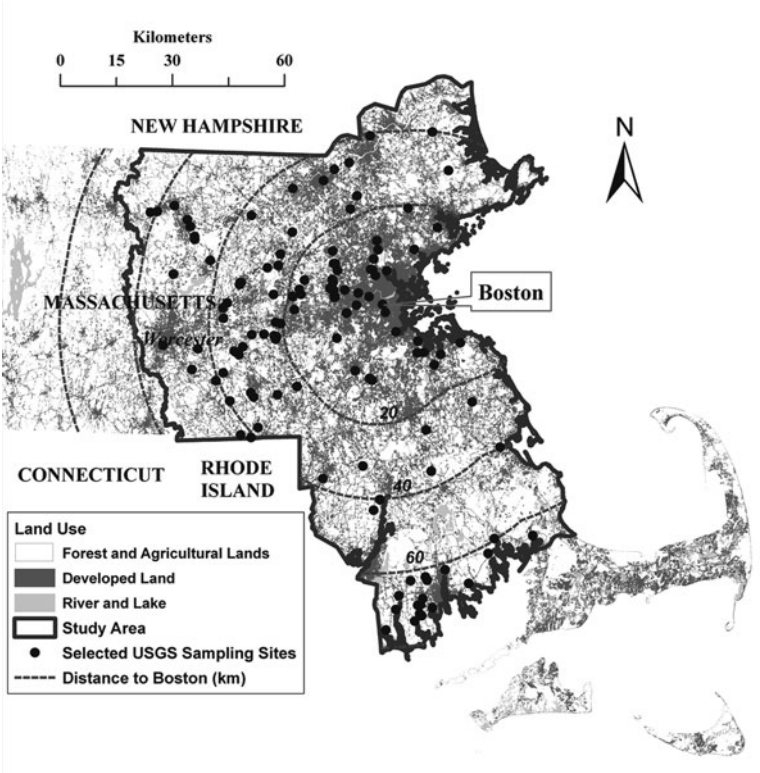

Fig. 9.1 Location of study area and water quality sampling sites

the metropolitan area. Different parts of the study area are currently with different levels of urbanization, which generally decreases from the City of Boston to outside.

Over the past several decades, the study area has being experienced substantial urban sprawl, characterized by population decline and stable land use change in central city but rapid population growth and land development in suburban and rural areas (Tu et al. 2007). The rapid urban sprawl is continuing to cause the fast conversion of undeveloped land, mainly forest, into developed lands, especially residential land. Urban sprawl is continuing to put great pressure on the undeveloped land (i.e. forest and agricultural lands) and the ecosystem in the study area, especially in the interface of rural and urban areas (i.e. suburban areas). To evaluate the impact of urban sprawl on water quality is very important for regional land use and watershed management. In addition, the different levels of urbanization across the study area might result in spatially varying local water pollution sources and watershed characteristics, and thus relationships between urbanization and water quality indicators might change across the urbanization gradient. As a result, it is quite appropriate

to apply GWR in this area, and this study can become a valuable pilot study for spreading GWR techniques to water resources research.

9.3 Data Sources and Methods

9.3.1 Water Quality Indicators

Water quality data during the period of 1990–2005 were extracted on-line from the USGS National Water Information System Web (NWISWeb; URL http://waterdata.usgs.gov/nwis/). The NWISWeb is a very important and widely used public water quality and streamflow data source for research, education, and administration in the US. It contains water quality data collected by various projects. The accuracy of the water quality data provided to the public is insured by the USGS. Based on data availability, 129 water quality sampling sites were selected, excluding the sites with part of upstream drainage area extending outside of the study area (Fig. 9.1). The mean values of 14 water quality parameters during the period of 1990–2005 were calculated. The water quality parameters are specific conductance (SC), dissolved solid (residue on evaporation, DS), calcium (Ca), magnesium (Mg), sodium (Na), potassium (K), chloride (Cl), sulfate (SO_4), ammonia nitrogen (NH_3–N), nitrite nitrogen (NO_2–N), ammonia plus organic nitrogen (also known as kjeldahl nitrogen, KN), nitrate plus nitrite nitrogen (NO_3–N + NO_2–N), phosphorus (P), and orthophosphate phosphorus (PO_4–P). SC is a measure of the ability of water to conduct electrical current and reflects the concentrations of dissolved ions or solids in water. Dissolved ions, solid, and nutrients are the pollutants that affect aquatic ecosystem and can be contributed by human activities associated with urbanization. Anthropogenic sources of dissolved ions and solid include runoff from roads treated by deicers, discharges of residential, municipal, and industrial sewage, and mining. High concentrations of dissolved ions and solid are toxic to freshwater organisms and cause death of aquatic life. Dissolved nutrients might come from fertilizer and pesticide use in urban and residential lawns, dumping of raw and treated sewage and industrial discharges, and phosphate detergents. High concentrations of dissolved nutrients can cause algal blooms, death of fish, and reduction of diversity and growth of aquatic life (Enger and Smith 2010). Therefore, all the above water quality parameters are good indicators to assess water quality degradation affected by urbanization.

9.3.2 Urbanization Indicators

Percentage of developed land (PDLU) and population density (PD) were used as urbanization indicators. Developed land consists of residential, commercial, industrial, transportation, and recreational lands. The land use data for 1999 and population data by census block for 2000 were obtained from the website of the

Massachusetts Geographic Information System (URL http://www.mass.gov/mgis/). The land use data were originally interpreted from 1:25,000 aerial photographs by the Resource Mapping Project at the University of Massachusetts, Amherst (MassGIS 2005).

The drainage area (watershed) for each sampling site was delineated from digital elevation data provided by the USGS National Elevation Dataset (NED) 1 Arc Second (about 30 m resolution, URL http://seamless.usgs.gov/ website/Seamless/) using ArcGIS spatial analysis tools, and then used for the calculation of urbanization indicators.

PDLU and PD for each sampling site were calculated in ArcGIS by overlapping land use and population layers to the drainage area layer. PDLU for a sampling site was calculated by dividing the amount of the developed lands within the watershed of the site by the total area of the watershed. PD for a sampling site was calculated by dividing the total population within the watershed of the site by the total area of the watershed. It is always a challenge for geospatial technologies application to link a variable limited by administrative boundaries (e.g. population density) to another that derived from natural features (e.g. land cover, soil, climate, etc.). To estimate the total population within a watershed, the proportion of each census block that fell within the watershed was calculated, and then multiplied by the population in the entire census block. Obviously, this will introduce some error in population density of watersheds because the calculation assumes that population is evenly distributed over a census block. However, census blocks are the smallest spatial units for the population data available in the study area. Compared with other spatial units for population data (e.g. municipalities and counties), the error was relatively small. This method has been widely used to derive population variables in many previous studies (Ahearn et al. 2005; Alberti et al. 2007; Xian et al. 2007). Through these steps, a linkage of water quality for points to urbanization indicators for areas was established. They were used for further statistical and spatial analyses.

The temporal discrepancy between the water quality data (1990–2005), and the land use data (1999), and population data (2000) might raise some doubt about the comparability of the water quality and urbanization indicators. Temporal agreement was not vital with respect to the land use and population data since they did not normally change dramatically over a short time period. As for the water quality indicators, they might change daily or hourly. However, for this study that takes advantage of geospatial technologies to analyze data from dozens of water quality sampling sites on a regional scale at once, it is infeasible to set up many sampling sites with multiple water quality indicators over this study area during a short time period (e.g. 1999 or 2000). In addition, the purpose of this study is to test the general pattern in the spatially varying relationship between water quality and urbanization, not to explore their temporal relationship (i.e. how water quality changes over time affected by urbanization). The water quality data from 1990 to 2005 is used to represent the average situation of water quality at different sampling sites associated with different urbanization levels. The spatial relationship between water quality and urbanization can have implication for their temporal relationship. Therefore, as

a pilot study of applying GWR in water resources research, the temporal discrepancy won't distort the results.

9.4 Methods

Because most of the urbanization and water quality indicators were not normally distributed checked by the Kolmogorov-Smirnov test and visual interpretation of histogram and Q–Q plots, appropriate methods such as natural log and square root were applied to transform the non-normally distributed variables to meet the condition of normal distribution for further analyses.

The spatially varying relationships between urbanization and water quality indicators were analyzed by using GWR. In a GWR model, a water quality indicator was dependent variable, and either PDLU or PD was independent variable. There were two urbanization indicators and fourteen water quality indicators. Therefore, the relationships for 28 pairs of water quality and urbanization indicators were analyzed. GWR analyses were conducted using GWR 3 software package (Fotheringham et al. 2002).

Afterwards, the outputs from the GWR models, including the values of *t*-test on the local parameter estimates and the local R^2 values, were mapped to give a clear visualization of the spatial variations in the relationships between urbanization and water quality and the abilities of the urbanization indicators to explain water quality. All mappings and GIS analyses were performed using ArcGIS 9.2.

The detailed description of the model design in this study can be found in Tu and Xia (2008). Detailed description of GWR technique can be found in some literatures (Brunsdon et al. 1998; Fotheringham et al. 2002). Thus, theoretical background of GWR is only briefly introduced here.

GWR is an extension of the traditional standard regression framework (e.g. OLS) by allowing local rather than global parameters to be estimated (Fotheringham et al. 2001). A GWR model can be stated as:

$$y_j = \beta_0(u_j, v_j) + \sum_{i=1}^{p} \beta_i(u_j, v_j) x_{ij} + \varepsilon_j \tag{9.1}$$

where u_j and v_j are the coordinates for each location (spatial data point) j, $\beta_0(u_j, v_j)$ is the intercept for location j, $\beta_i(u_j, v_j)$ is the local parameter estimate for independent variable x_i at location j, ε is the error term.

GWR assumes that every data point is more affected by nearby data points than those further away. Thus, GWR is calibrated by weighting all data points around a regression point using a distance decay function to produce local parameter estimates.

The weighting function is an exponential distance decay form:

$$w_{ij} = \exp(-d_{ij}^2/b^2) \tag{9.2}$$

where w_{ij} is the weight of data point j for point i, d_{ij} is the distance between i and j, b is the kernel bandwidth. When the distance is greater than the kernel bandwidth, the weight rapidly approaches zero.

By using this weighting function to calibrate the model, GWR produces a set of local regression results including local parameter estimates, the values of t-test on the local parameter estimates, the local R^2 values, and the local residuals for every spatial data point (water quality sampling site in this study).

The local statistics obtained from the GWR analyses were interpreted and discussed to examine the spatially varying relationships between urbanization and water quality indicators in the following sections.

9.5 Results

9.5.1 Spatial Variations in Urbanization Indicators

The spatial patterns of the urbanization indicators can be identified from Fig. 9.2. Most sites within the 20-km buffer of Boston have PDLU higher than 80%, so these sites are within highly-urbanized central city areas. Most sites between the 20-km and 40-km buffers have PDLU below 40%. A value of PDLU less than 20% is observed for many sites outside the 40-km buffer of Boston. Therefore, the watersheds beyond 20-km buffer are considered as less-urbanized suburban and rural areas. Likewise, the highest PD values (>2000 people/km^2) are found at many sites inside the 20-km buffer, the highly-urbanized metropolitan Boston area; the PD values for some sites in this area even reach 5000 people/km^2. PD below 500 people/km^2 is observed for most of sites between the 20 and 40-km buffers, while most sites outside the 40-km buffer have the lowest PD (<200 people/km^2; Fig. 9.2). Thus, a clear urbanization gradient exists from Boston to outside of the metropolitan area.

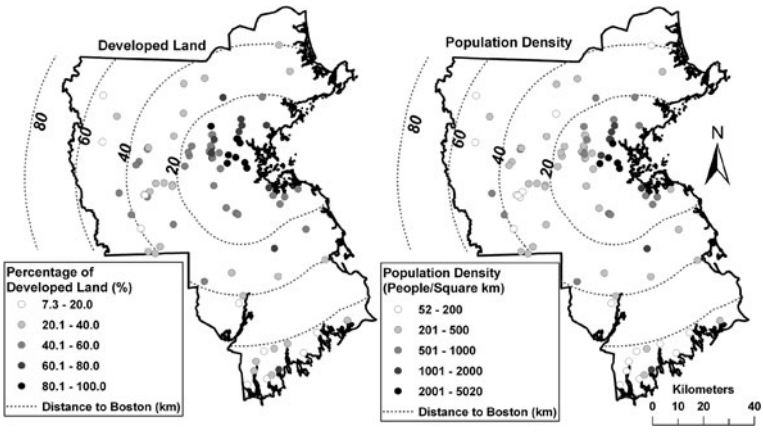

Fig. 9.2 Spatial patterns of urbanization indicators

The watersheds with different levels of urbanization in the study area are good for examining how the impact of urbanization on water quality varies across the urbanization gradient. Furthermore, the great spatial variability in urbanization indicators suggests that the significant spatial non-stationarity might exist in the relationships between urbanization and water quality variables over the study area, so GWR is a more appropriate method than traditional regression techniques, which is already confirmed by model evaluation (Tu and Xia 2008).

9.5.2 Relationships Between Developed Land and Water Quality

Because of space considerations, not all the maps of parameter estimates and local R^2 values from the GWR models can be presented here. The ranges of local parameter estimates and R^2s are summarized in Table 9.1. Parameter estimates for an independent variable actually reflect the correlations between the independent

Table 9.1 Ranges of local parameter estimates and R^2 from GWR models

		Local parameter estimates		Local R^2	
Water quality indicator		% developed land	population density	% developed land	population density
SC	Min	0.200	–0.462	0.293	0.210
	Max	0.374	2.022	0.644	0.973
NH_3–N	Min	0.596	1.188	0.272	0.414
	Max	1.024	1.684	0.624	0.710
NO_2–N	Min	15.18	10.90	0.349	0.309
	Max	25.75	88.96	0.655	0.928
KN	Min	−0.040	−0.040	0.344	0.099
	Max	0.100	1.372	0.999	0.997
NO_3–N +	Min	0.001	0.240	0.317	0.194
NO_2–N	Max	0.032	0.980	0.630	0.791
P	Min	0.006	−0.410	0.130	0.110
	Max	0.059	3.280	0.380	0.918
PO_4–P	Min	−2.25	−17.68	0.140	0.077
	Max	0.51	51.13	0.501	0.890
Ca	Min	0.017	−0.280	0.511	0.243
	Max	0.122	1.690	0.996	0.935
Mg	Min	0.014	0.100	0.364	0.312
	Max	0.021	0.710	0.664	0.931
Na	Min	0.011	0.100	0.172	0.438
	Max	0.065	1.270	0.992	0.996
K	Min	−0.007	0.131	0.243	0.370
	Max	0.024	0.234	0.999	0.650
Cl	Min	0.060	0.940	0.203	0.246
	Max	0.270	4.400	0.972	0.841
SO_4	Min	0.006	0.040	0.345	0.345
	Max	0.045	0.790	0.991	0.991
DS	Min	0.0001	0.001	0.302	0.147
	Max	0.0023	0.032	0.998	0.945

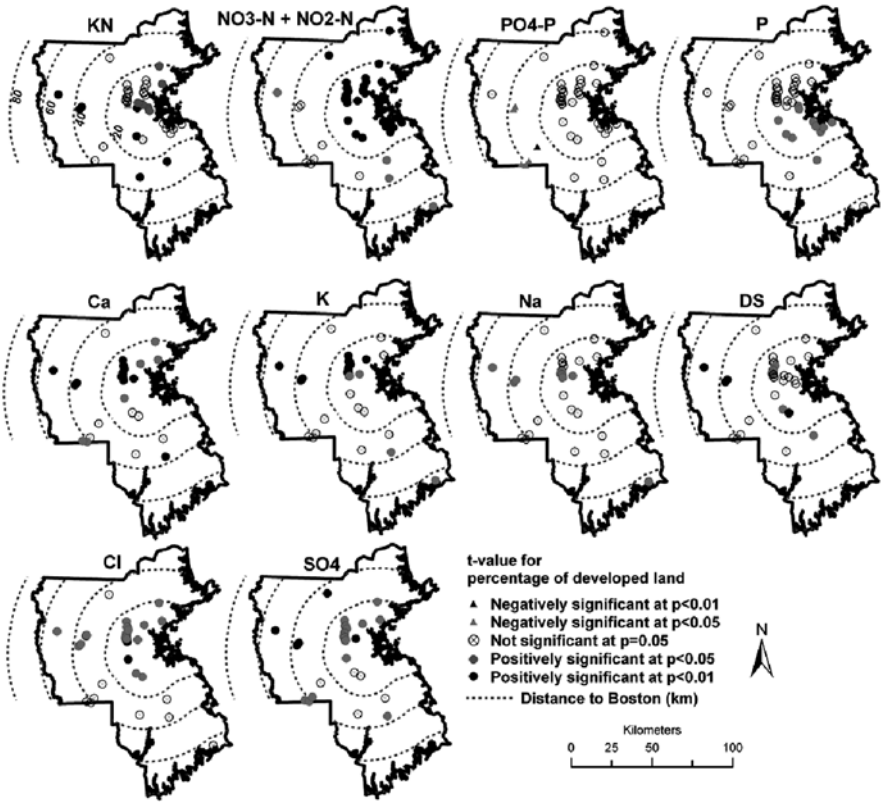

Fig. 9.3 Results of t-test on the parameter estimates for developed land from the GWR models (The *t*-values for NO_2–N, NH_3–N, SC and Mg are positively significant at $p<0.005$ at all sampling sites)

variable and dependent variable at different sampling sites. Thus, in a GWR model for a water quality indicator and an urbanization indicator, the local parameter estimates for the urbanization indicator are used to describe the relationships between the water quality indicator and the urbanization indicator at different sampling sites. In addition, the local R^2 values from the GWR model reflect the abilities of the urbanization indicator to explain the spatial variance in the water quality indicator at different sites.

Figure 9.3 shows the values of *t*-test on the local parameter estimates for PDLU obtained from the GWR models. Positive correlations are found between developed land and most water quality indicators at all the sampling sites (Table 9.1 and Fig. 9.3). They are significant for SC, NO_2–N, NH_3–N and Mg in the whole study area and for other water quality indicators at many sampling sites (Fig. 9.3). This result indicates that higher percentage of developed land is associated with higher concentrations of most water quality indicators.

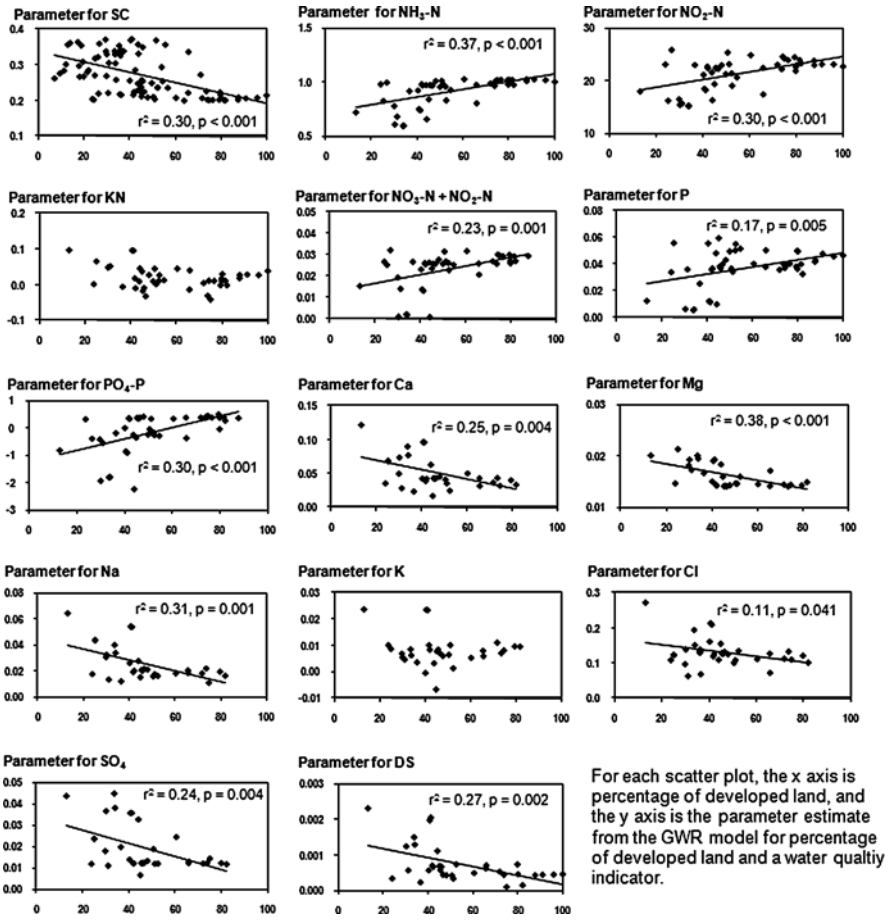

Fig. 9.4 Scatter plots of urbanization levels of watersheds and parameter estimates from the GWR models for developed land and water quality. For each Scatter plot, the *x* axis is percentage of developed land, and the *y* axis is the parameter estimate from the GWR model for percentage of developed land and a water quality indicator

No clear spatial pattern can be identified from the maps of *t*-value (Fig. 9.3). In order to more clearly understand how the relationships change across space in response to urbanization level, percentage of developed land (PDLU) is used as an indicator of urbanization level in watersheds, and then make a scatter plot of PDLU and the parameter estimate from each of GWR models (Fig. 9.4). Thus, the scatter plot reflects how the correlations (reflected by parameter estimates) between developed land and each water quality indicator vary across the urbanization gradient. The scatter plots show that the relationships between developed land and water quality indicators are significantly associated with the urbanization level in the watersheds (Fig. 9.4). The parameter estimates for SC, DS, and most of dissolved

ions have significant negative correlations with PDLU. In other words, the relationships between developed land and these water quality indicators decrease as the urbanization level of watershed increases. On the contrary, the parameter estimates for most of dissolved nutrient parameters have significant positive correlations with PDLU, indicating that the relationships between developed land and dissolved nutrient parameters increase as the urbanization level of watershed increases. Therefore, a clear spatial pattern exists in the study area: the correlations of developed lands with SC, DS, and dissolved ions are stronger in less-urbanized areas, while the correlations with dissolved nutrients are stronger in highly-urbanized areas.

This spatial pattern is also observed in the maps of local R^2 value (Fig. 9.5). The local R^2 values show great spatial non-stationarity. SC, DS, and most dissolved ions, such as Na, Cl, and Mg, have higher local R^2 values at many sampling sites outside the 20-km buffer, but lower local R^2 values inside the 20-km buffer (Fig. 9.5). In contrast, the local R^2 values for dissolved nutrient indicators, including NH_3–N, NO_2–N, and NO_3–N + NO_2–N, are lower at many sites outside the 20-km buffer, but higher inside the 20-km buffer (Fig. 9.5). However, the higher local R^2

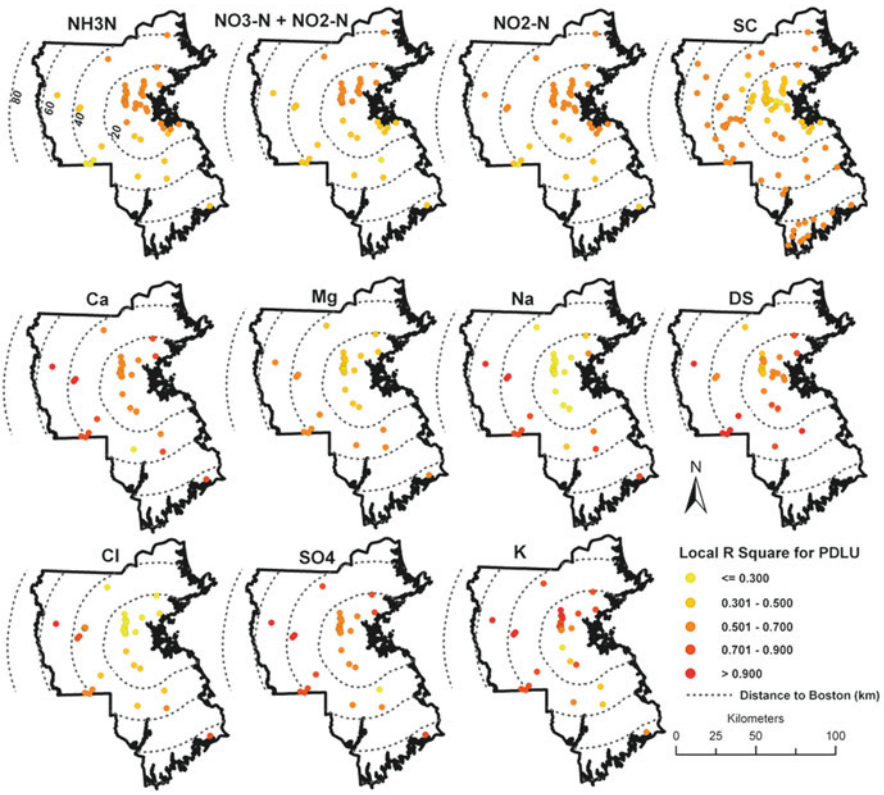

Fig. 9.5 Local R^2 values for the GWR models of developed land and water quality

values for these dissolved nutrients are generally lower than those for dissolved ions and solid (Table 9.1). The result indicates that although the ability of PDLU to explain the spatial variation in dissolved ions and solid vary greatly across the study area, PDLU exhibits stronger abilities to explain the variance in dissolved ions and solid than to explain the variance in dissolved nutrients, especially in less-urbanized areas. Therefore, the results suggest that developed land has more adverse impact on water quality, especially on the concentrations of dissolved ions and solid, in less-urbanized watersheds than in highly-urbanized watersheds. Same amount of increase in percentage of developed land may cause higher increase in concentrations of dissolved ions and solid in less-urbanized areas than in highly-urbanized areas.

9.5.3 Relationships Between Population Density and Water Quality

Figure 9.6 shows the values of *t*-test on the local parameter estimates for population density obtained from the GWR models. Although negative correlations are found between population density and some water quality indicators at some sites, none of them are significant (Table 9.1 and Fig. 9.6). Significant positive correlations

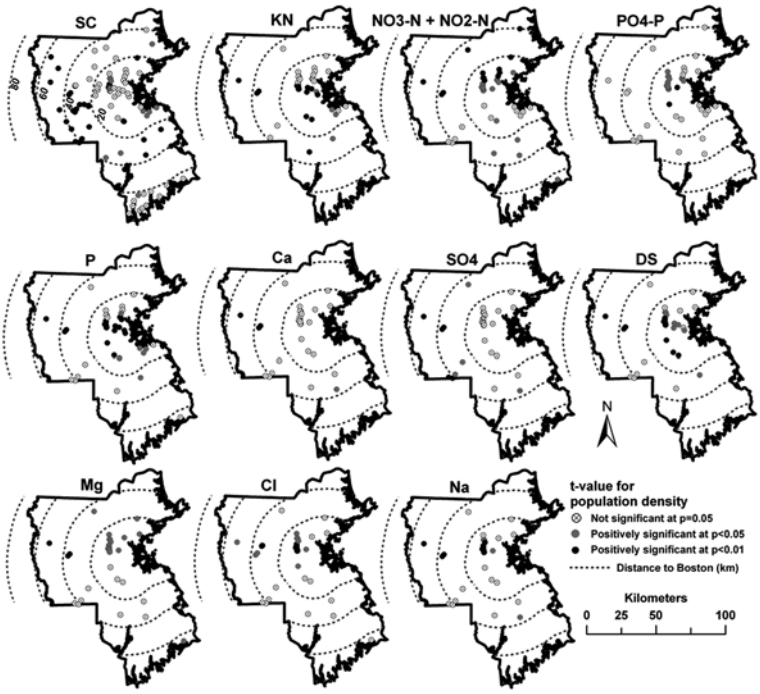

Fig. 9.6 Results of *t*-test on the parameter estimates for population density from the GWR models (The *t*-values for NH_3–N and K are positively significant at $p<0.05$ at all sampling sites; the *t*-value for NO_2–N are positively significant at $p<0.05$ at most sampling sites)

are found for K and NH_3–N in the whole study area, for NO_2–N at most of the sampling sites, and for other water quality indicators at some sites (Fig. 9.6). The significant positive correlations indicate that higher PD is associated with higher concentration of water quality indicators. The significant positive correlations for SC, Ca, and SO_4 are mainly distributed outside the 20-km buffer, while that for PO_4–P are concentrated inside the 20-km buffer, and no clear spatial pattern can be identified from the maps of *t*-value for other water quality indicators (Fig. 9.6).

However, the scatter plots of urbanization level and the parameter estimate from the GWR models show that the relationships between population density and water quality indicators are significantly associated with the urbanization level in the watersheds (Fig. 9.7). The parameter estimates for most water quality indicators

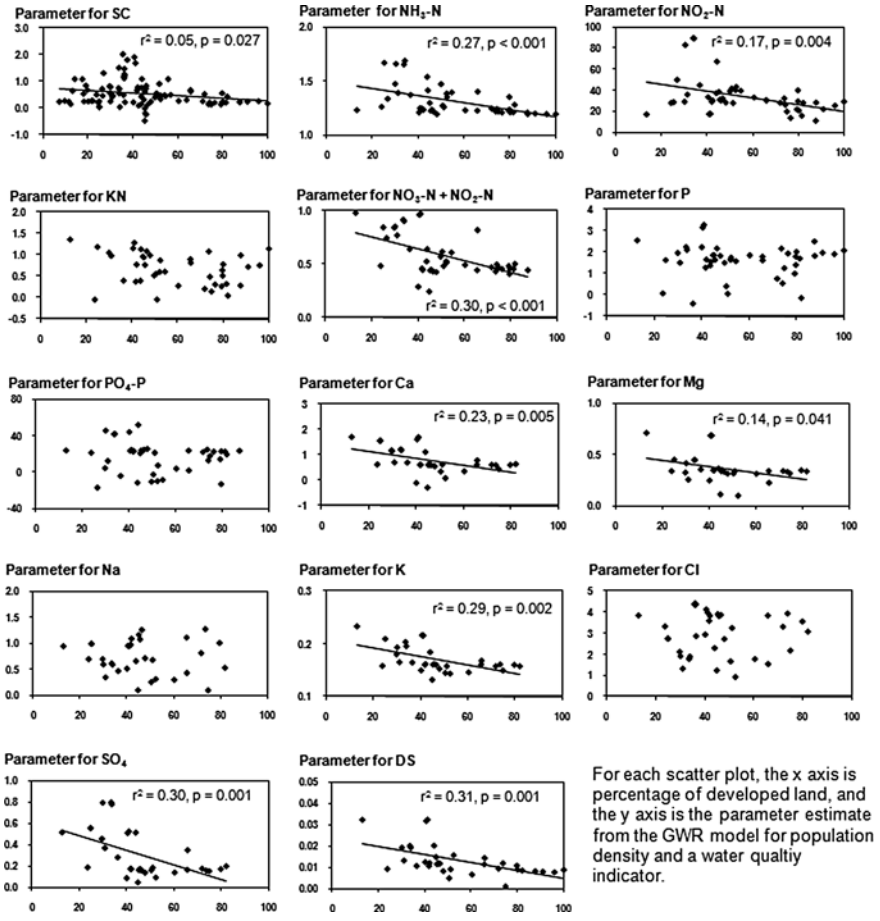

Fig. 9.7 Scatter plots of urbanization levels of watersheds and parameter estimates from the GWR models for population density and water quality. For each Scatter plot, the *x* axis is percentage of developed land, and the *y* axis is the parameter estimate from the GWR model for population density and a water quality indicator

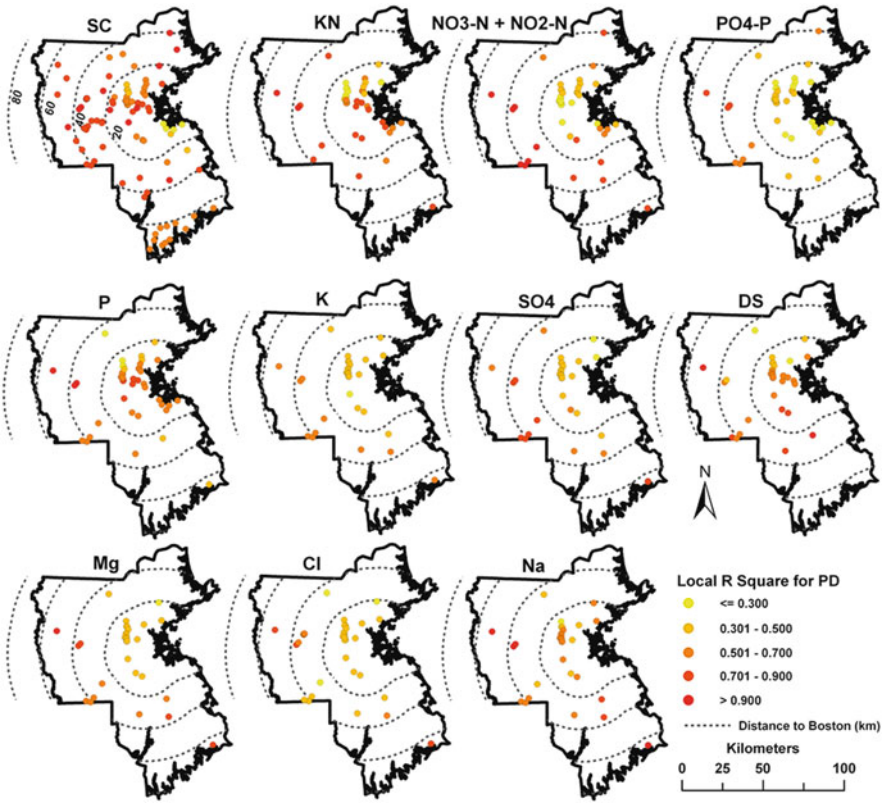

Fig. 9.8 Local R^2 values for the GWR models of population density and water quality

have significant negative correlations with the urbanization level. In other words, the relationships between population density and these water quality indicators decrease as the urbanization of watershed increases.

A clear spatial pattern in the ability of PD to explain the variance in water quality can also be identified from the maps of local R^2 values from the GWR models (Fig. 9.8). Lower R^2 values are mainly concentrated inside the 20-km buffer of Boston, where PD explains low variance in the concentrations of most water quality indicators (Table 9.1 and Fig. 9.8). In contrast, high R^2 values are usually observed outside the 20-km buffer. The R^2 values generally increase as the sampling sites move away from Boston metropolitan area (Fig. 9.8). The highest R^2 is close to 1 for some water quality parameters, such as SC, KN, Na, and SO_4, at some sites outside the 20-km buffer (Fig. 9.8 and Table 9.1). Like the finding for PDLU, this result indicates that population density is a better predictor to explain the spatial variance in water quality indicators in less-urbanized areas than it in highly-urbanized areas. Same degree of increase in population density may cause higher increase in concentrations of water pollutants in less-urbanized suburban areas,

which are usually experiencing fast land development, than in highly-urbanized central cities, where the land use changes and population growth are relatively stable.

9.6 Discussion

Urbanization is usually related to water degradation caused by various human activities, including discharges of residential, municipal, and industrial sewage, fertilizer and pesticide use in lawns, and applications of road deicers, so higher percentage of developed land is always associated with higher concentrations of water pollutants in different watersheds around the world (Bowen and Valiela 2001; Finkenbine et al. 2001; Tong and Chen 2002; Interlandi and Crockett 2003; Hatt et al. 2004; Aichele 2005; Brett et al. 2005; Deacon et al. 2005; Schoonover et al. 2005; Tu et al. 2007). Likewise, in the present study, higher concentrations of water pollutants are significantly related to higher percentage of developed land and higher population density. Nevertheless, the application of GWR finds that the correlations vary over space and differ among different urbanization and water quality indicators and the correlations are not significant at all the sampling sites. Considerable spatial differences in the correlations are observed between less- and highly-urbanized areas.

The correlations of PDLU with dissolved solid and ions become stronger as the urbanization level of watersheds decreases, while the correlations with nutrients are stronger in highly-urbanized areas. The different correlations with PDLU between dissolved nutrients and other parameters might be explained by the different sources of pollutants. Compared to dissolved ions and solid, which are contributed mainly by human activities associated with urbanization, such as urban runoff, road deicers use, and discharges of residential, municipal, and industrial sewage, dissolved nutrients are also largely contributed by agricultural activities, such as fertilizer application and animal waste, besides urban sources. Thus, the sources of dissolved nutrients might differ largely between highly- and less urbanized areas. In highly-urbanized areas without agricultural sources, dissolved nutrients are only contributed by urban sources, and thus significant positive relationship exists between dissolved nutrients and PDLU. On the contrary, dissolved nutrients in less-urbanized areas are contributed by both agricultural and urban sources, and thus relatively weaker relationships were found between dissolved nutrients and PDLU. Unlike dissolved nutrients, dissolved ions and solid are mainly contributed anthropogenically by urban sources in both highly- and less- urbanized areas. Their correlations with PDLU are not affected by agricultural sources and even get stronger in less-urbanized areas.

The correlations of PD with most water quality indicators get stronger as the urbanization level of watersheds decreases. In other words, same amount of increase in developed land or population density causes more increase in concentrations of water pollutants in less-urbanized areas than highly-urbanized areas, especially for dissolved solid and ions. This result might be attributed to the low-density

development in suburban areas but high-density land use in central cities associated with urban sprawl.

After World War II, since the building of interstate highways, urban sprawl is the dominant development pattern throughout much of the US. Over the past several decades, populations have moved away from central cities to surrounding areas. During the 1970s and 1980s, over 95% of US population growth happened in suburban areas. Sprawl is converting forestland, agriculture land and wetlands into developed area including residential, commercial, industrial, and transportation uses. Low-density development tends to occupy far more land than higher-density urban centers (Robinson et al. 2005). As a result, more impact might be caused by land development on natural environment including water quality in low-density less-urbanized suburban areas than high-density highly-urbanized cities, which is proved by the results of this study.

Considering the stronger adverse impact of urbanization on water quality in less-urbanized suburban areas than highly-urbanized central cities associated with urban sprawl, "smart growth" might be a better development pattern. Smart growth is an urbanization pattern that urban development is concentrated in the center of a city to avoid urban sprawl, and compact, transit-oriented, walkable, and bicycle-friendly land use is encouraged (Miller and Hoel 2002; Shore 2006). The goal of "smart growth" includes "better coordinated planning with input from the public, providing multiple transportation and housing choices, providing green space to make communities attractive, using mixed-use development, and infill strategies (new construction within the urban core of cities and the inner suburbs)" (Miller and Hoel 2002). Under smart growth, less-density development in suburbs is limited, and high-density development is kept in central cities. Thus, the adverse impact of urbanization on water quality in suburbs found in this study might be controlled. Clearly, this study provides an evidence for policy makers to oppose urban sprawl and to support smart growth.

In addition, this study extended the application of GWR to water resources research. Conventional statistical techniques are not able to explore the spatially varying correlations between urbanization and water quality indicators, and unable to examine the spatially varying abilities of urbanization indicators to explain water quality change. GWR can also unveil previously unknown information on the local pollution sources. For instance, this study found that the impact of developed land on dissolved nutrients is stronger in highly-urbanized areas than less-urbanized areas using GWR. This result can lead environmental scientists to find varying sources of dissolved nutrients across space. In highly-urbanized areas, they are mainly contributed by urban sources. However, in less-urbanized areas, more sources might be responsible for dissolved nutrients, which bring mixed effect on the relationship of developed land and nutrients, causing weaker relationship, and so non-urban sources (e.g. agricultural activities) should also get attention. If conventional statistical techniques were used, no different pollution sources would be detected since the relationship between water quality and land use was the same for the whole study area. GWR is also able to find which specific water pollutants at certain sampling sties are more affected by human activities than others, which can also help

scientists and environmental protection agency to trace specific pollution sources. Thus, GWR provides a useful tool for policy makers, regional and local agencies, and researchers to unveil the local pollution causes, and to adopt appropriate urbanization indicators based on the dominant pollutant appearing at the local sampling sites to better assess the pollution status and improve watershed conservation and management.

9.7 Conclusions

This chapter interprets the results from the application of GWR to analyze the relationships between two urbanization and fourteen water quality indicators in eastern Massachusetts. Most of water quality indicators, including SC, dissolved ions and solid, and dissolved nitrogen parameters have significant relationships with percentages of developed land and population density. This result indicates that water pollution is associated with urbanization. Nevertheless, the impact of urbanization on water quality changes over space in response to the urbanization levels of watersheds. The relationships of the two urbanization indicators and most of water quality indicators increase as the urbanization levels of watersheds decrease. Thus, the adverse impact of urbanization on water quality is more substantial in less-urbanized areas than it in highly-urbanized areas. The same degree increase in population density and developed land have more adverse impact on water quality in less-urbanized suburban areas than highly-urbanized central cities.

This result might be caused by the dominant development pattern in US. Urban sprawl, the land-consumptive pattern of suburban development over decades in the US, encourages low-density land development in less-urbanized suburban areas. Under this development pattern, per capita land use, energy consumption, and pollution generation are all higher in suburban areas than central cities, and so the adverse impact of urbanization on natural environment is assumed to be more significant in suburban areas. The more significant adverse impact of urbanization on water quality in suburban areas than central cities found by this study provides an important evidence to prove the above assumption. To control or reduce the impact of urbanization on water quality, an alternative urbanization pattern, smart growth, which promotes compact, transit-oriented, walkable, and bicycle-friendly land development in central cities, should be encouraged. The redevelopment in central cities, which is already highly-urbanized, has lower adverse impact on water quality than new development in less-urbanized suburbs as indicated by the results of this study. Thus, this study provides an additional evidence for policy makers to oppose urban sprawl and to support smart growth, and can have important implications on environmental policy and management.

This study also proves that GWR can be a very useful geospatial technology for environmental research, policy, and management. GWR is able to detect the spatially varying relationships between urbanization and water quality indicators, the changing abilities of urbanization indicators to explain water quality change over

space, the local situation and causes of water pollution, and the spatial differences in the impact of urbanization on water quality between watersheds with different urbanization levels. All these information detected by GWR are important for watershed conservation and management.

This study suggests that GWR can also serve as a useful geospatial tool for environmental research and management in other fields than water environment. Environmental protection agencies and researchers are all concerned with how natural environment affected by varied natural and anthropogenic factors, such as soil, climate, topography, vegetation, land use, economic activities, and policies, and try to understand the interrelations between these factors and environment. However, all these factors are not uniform across space, and so spatial non-stationarity might exist in the relationships between these factors and environment, which can be examined by GWR technique. The spatially varying relationships found by GWR can help analyze and detect different situations and causes of environmental issues for different specific local areas, and then local environmental protection agencies and policy makers will be able to adjust environmental policies and techniques to fit the local environment. Thus, GWR can serve as a useful geospatial tool for policy makers, regional and local agencies, and researchers to unveil the local pollution causes, to improve the understanding of local pollution status, and to adopt appropriate environmental policies suitable to the local environment issues.

References

Ahearn DS, Sheibley RW, Dahlgren RA, Anderson M, Johnson J, Tate KW (2005) Land use and land cover influence on water quality in the last free-flowing river draining the western Sierra Nevada California. J Hydrol 313:234–247

Aichele SS (2005) Effects of urban land-use change on streamflow and water quality in Oakland County, Michigan, 1970–2003, as inferred from urban gradient and temporal analysis. US Geol Surv Sci Investig Rep 2005–5016

Alberti M, Booth D, Hill K, Coburn B, Avolio C, Coe S and Spirandelli D (2007) The impact of urban patterns on aquatic ecosystems: An empirical analysis in Puget lowland sub-basins. Landsc Urban Plan 80:345–361

Bowen JL, Valiela I (2001) The ecological effects of urbanization of coastal watersheds: historical increases in nitrogen loads and eutrophication of Waquoit Bay estuaries. Can J Fish Aquat Sci 58:1489–1500

Brett MT, Arhonditsis GB, Mueller SE (2005) Non-point-source impacts on stream nutrient concentrations along a forest to urban gradient. Environ Manag 35:330–342

Brunsdon C, Fotheringham S, Charlton M (1998) Geographically weighted regression-modeling spatial non-stationarity. Stat 47:431–443

Deacon JR, Soule SA, Smith TE (2005) Effects of urbanization on stream quality at selected sites in the seacoast region in New Hampshire, 2001–2003. US Geol Surv Sci Investig Rep 2005–5103

Enger ED, Smith BF (2010) Environmental science, 12th edn. McGraw-Hill, New York, NY

Ewing R, Schmid T, Killingsworth R, Zlot A, Raudenbush S (2003) Relationship between urban sprawl and physical activity, obesity, and morbidity. Am J Health Promot 18:47–57

Finkenbine JK, Atwater JW, Mavinic DS (2001) Stream health after urbanization. J Am Water Resour Assoc 36:1149–1160

Fotheringham AS, Charlton ME, Brunsdon C (2001) Spatial variations in school performance: a local analysis using geographically weighted regression. Geogr Environ Model 5:43–66

Fotheringham AS, Brunsdon C, Charlton M (2002) Geographically weighted regression: the analysis of spatially varying relationships. Wiley, Chichester

Hatt BE, Fletcher TD, Walsh CJ, Taylor SL (2004) The influence of urban density and drainage infrastructure on the concentrations and loads of pollutants in small streams. Environ Manag 34:112–124

Interlandi S, Crockett CS (2003) Recent water quality trends in the Schuylkill River, Pennsylvania, USA: a preliminary assessment of the relative influences of climate, river discharge and suburban development. Water Res 37:1737–1748

MassGIS (2005) Massachusetts land use datalayers and land use summary statistics http://www.mass.gov/mgis/landuse_stats.htm. Accessed 19 Sep 2005

McGrath DA, Evans JP, Smith CK, Haskell DG, Pelkey NW, Gottfried RR, Brockett CD (2004) Mapping land-use change and monitoring the impacts of hardwood-to-pine conversion on the Southern Cumberland Plateau in Tennessee. Earth Interact 8:1–24

Miller JS, Hoel LA (2002) The "smart growth" debate: best practices for urban transportation planning. Socioecon Plan Sci 36:1–24

Robinson L, Newell JP, Marzluff JM (2005) Twenty-five years of sprawl in the Seattle region: growth management responses and implications for conservation. Landsc Urban Plan 71:51–72

Schoonover JE, Lockaby BG, Pan S (2005) Changes in chemical and physical properties of stream water across an urban-rural gradient in western Georgia. Urban Ecosyst 8:107–124

Shi H, Laurent EJ, LeBouton J, Racevskis L, Hall KR, Donovan M, Doepker RV, Walters MB, Lupi F, Liu J (2006) Local spatial modeling of white-tailed deer distribution. Ecol Model 190: 171–189

Shore WB (2006) Land-use, transportation and sustainability. Technol Soc 28:27–43

Tong STY, Chen W (2002) Modeling the relationship between land use and surface water quality. J Environ Manag 66:377–393

Tu J, Xia ZG, Clarke KC, Frei A (2007) Impact of urban sprawl on water quality in eastern Massachusetts, USA. Environ Manag 40:183–200

Tu J, Xia ZG (2008) Examining spatially varying relationships between land use and water quality using geographically weighted regression I: model design and evaluation. Sci Total Environ 407:358–378

Wheeler AP, Angermeier PL, Rosenberger AE (2005) Impacts of new highways and subsequent landscape urbanization on stream habitat and biota. Rev Fish Sci 13:141–164

Williams M, Hopkinson C, Rastetter E, Vallino J, Claessens L (2005) Relationships of land use and stream solute concentrations in the Ipswich River basin, Northeastern Massachusetts. Water Air Soil Pollut 161:55–74

Wilson EH, Hurd JD, Civco DL, Prisloe MP, Arnold C (2003) Development of a geospatial model to quantify, describe and map urban growth. Remote Sens Environ 86:275–285

Xian G, Crane M, Su J (2007) An analysis of urban development and its environmental impact on the Tampa bay watershed. J Environ Manag 85:965–976

Yu D (2006) Spatially varying development mechanisms in the greater Beijing area: a geographically weighted regression investigation. Ann Reg Sci 40:173–190

Zhang T (2001) Community features and urban sprawl: the case of the Chicago metropolitan region. Land Use Policy 18:221–232

Part IV
Human Health and the Environment

Chapter 10
Application of GIS in Evaluating the Potential Impacts of Land Application of Biosolids on Human Health

Kevin P. Czajkowski, April Ames, Bhuiyan Alam, Sheryl Milz, Robert Vincent, Wendy McNulty, Timothy W. Ault, Michael Bisesi, Brian Fink, Sadik Khuder, Teresa Benko, James Coss, David Czajkowski, Subramania Sritharan, Krishnakumar Nedunuri, Stanislov Nikolov, Jason Witter, and Alison Spongberg

Abstract This chapter describes the development and use of a geographic information system (GIS) in an environmental health investigation of the application of Class B biosolids (sewage sludge) on agricultural fields. The research project is broad-based including field observations and modeling to investigate the presence of microorganisms, metals, and pharmaceutical and personal care products (PPCPs) in biosolids applied agricultural fields and the associated runoff. These data has been linked with remote sensing imagery and added to GIS layers for Wood, Lucas and Greene Counties in Ohio. Specifically, this project describes the way in which a GIS was developed and utilized with a mailed, epidemiological health survey to investigate the potential impact of biosolids application to agricultural fields in relation to self-reported human health symptoms, acute diseases and chronic diseases among groups of individuals living specified distances from fields where biosolids were permitted and applied. For Wood County, of the 24 symptoms in the survey, six were statistically higher near biosolids permitted fields and of the 29 diseases in the survey, five were statistically higher near biosolids permitted fields. The Lucas and Greene County surveys are still being analyzed. Our future work includes refinement of the spatial analysis and health survey to include the application of biosolids and the constituents of the biosolids to fields, distances to any farm field and to other potential relationships to health effects.

Keywords Epidemiology · Biosolids · Agriculture · Pharmaceuticals and Personal Care Products · Heavy Metals · Human Pathogens

K.P. Czajkowski (✉)
Department of Geography and Planning, The University of Toledo, Toledo 43606, OH, USA
e-mail: kevin.czajkowski@utoledo.edu

N. Hoalst-Pullen, M.W. Patterson (eds.), *Geospatial Technologies in Environmental Management*, Geotechnologies and the Environment 3, DOI 10.1007/978-90-481-9525-1_10,

10.1 Introduction

Sewage sludge, also known as biosolids, is defined in the Code of Federal Regulations, Title 40, as the solid, semi-solid, or liquid residue generated during the treatment of domestic sewage in a wastewater treatment plant (WWTP) (USEPA 1994). In the United States, a significant proportion of biosolids are disposed of through application to agricultural fields. There are anecdotal reports of illness and in one case death after application of biosolids. This is a very politically-charged issue in part due to public perception and concerns over health and safety having resulted in lawsuits.

In July 2002, the National Research Council (NRC) issued a report expressing concern over the practice of applying biosolids to farm fields in the United States (Renner 2002). In the 2002 report, the NRC states:

> There is no documented scientific evidence that the Part 503 rule has failed to protect public health. However, additional scientific work is needed to reduce persistent uncertainty about the potential for adverse human health effects from exposure to biosolids. There have been anecdotal allegations of disease, and many scientific advances have occurred since the Part 503 rule was promulgated. (NRC 2002)

Across the United States as well as in many other countries, policy makers are faced with the question of whether biosolids should be land applied or not. In this chapter, we will give background on biosolids application in the United States focusing on Ohio, discuss what is known on the potential environmental health impacts of land application of biosolids, and show a recent study in which a geographic information system (GIS) is being used to investigate those potential effects.

10.2 Biosolids Application in the United States

Biosolids became a disposal issue after the Clean Water Act was enacted in 1972 which laid out regulations for waste water treatment. Since then, land application of biosolids from WWTPs, to agricultural fields has become commonplace in the United States. Over 50% of biosolids produced in the United States are land-applied with the remaining placed in landfills or incinerated (USEPA 2004). The Clean Water Act section 405 amendment in 1987 required EPA to set biosolids regulations for minimizing environmental and health risks of identified toxic pollutants while maximizing the use of biosolids (NRC 2002).

Part 503, effective in 1993, was established by the U.S. Environmental Protection Agency to oversee the national biosolids program and established treatment and use requirements of biosolids, land application management practices, and concern concentration limits and loading rates of chemicals. Apart from regulating human pathogens, USEPA has adopted what it calls a “risk-based” approach to regulating ten heavy metals in biosolids: arsenic, cadmium, chromium, copper, lead, mercury, molybdenum, nickel, selenium, and zinc. Table 10.1 shows the ceiling

Table 10.1 Maximum allowable concentrations for different metals in soils

Metals	Maximum allowable concentrations (mg/Kg dry weight basis)
Arsenic	75
Cadmium	85
Copper	4300
Lead	840
Mercury	57
Molybdenum	75
Nickel	420
Selenium	100
Zinc	7500

concentrations of each of these metals allowed by the USEPA, which are considered safe for human contact (OEPA 2002). Chromium was later removed from the list due to a lack of evidence of human toxicity (McBride 2003). On the other hand, pathogen levels are not risk based. Instead, through treatment and use limitations, pathogens are limited through requirements to reduce their incidence and resultant potential exposure (NRC 2002). The Part 503 establishes criteria for classification of biosolids as Class A or B dependent on the level of treatment.

10.2.1 Class A Biosolids

Biosolids that have gone through extensive treatment to reduce pathogens below detectable levels and enhance vector attraction reduction (VAR) are termed Class A biosolids, also known as exceptional quality (EQ) biosolids. Biosolids must meet both prescribed densities of either *Salmonella* sp. or fecal coliform and treatment-process control requirements to be classified as Class A. EQ biosolids can be bagged and are deemed safe to sell to the public given that they meet these requirements. They can also be applied to land if there are no pathogen-related restrictions attached to the application site. The WWTPs distributing EQ biosolids need only a facility permit for land application, not a land permit. The WWTPs are not required to keep records of land sites to which EQ biosolids are applied. EQ biosolids can be applied to land under the same restrictions of other soil amendment products or fertilizers (NRC 2002).

10.2.2 Class B Biosolids

Class B biosolids are treated, but may still contain measurable levels of live bacteria and active viruses after treatment. That means Class B biosolids contain more pathogens than Class A biosolids. Class B biosolids must meet the organism control requirements of Part 503 in at least one of seven alternatives: fecal coliform limitation, aerobic digestion, anaerobic digestion, lime stabilization, air drying, composting, or equivalent process to significantly reduce pathogens. Unlike Class

A biosolids, Class B biosolids require land permits from the EPA for application. There are several restrictions for use of this type of biosolids. It cannot be given away in bags and cannot be sold. It is also prohibited to be used at sites that are open to the public, lawns, and home gardens. However, it can be applied to mine reclamation sites, forests, and agricultural sites in bulk quantities if the biosolids meet criteria for pollutants control, pathogen requirements, vector attraction reduction, and other applicable requirements of Part 503 (NRC 2002). Pathogenic microorganisms have been found in Class B biosolids, including harmful coliform bacteria, *Esherichia coli* (*E. coli*), poliomyelitis viruses, *Shigella sonnei*, fecal streptococci, and others (Lewis et al. 2002; Brooks et al. 2005a, b; Borjesson et al. 2009).

Part 503 mandates isolation distances between the Class B applied agricultural fields and houses, waterways and drinking water supplies (Table 10.2) to reduce potential exposure to humans and animals.

In Ohio, biosolids are applied through splash method or direct injection and can vary in moisture content from 3% solids, a liquid or up to 40% solids, which is often called cake. Splashing is the most common and least costly method for biosolids application while the injection method is more costly. Injection is often used to reduce VAR. Figure 10.1 shows an injection application of Class B biosolids in Oregon, Ohio. In 2006, in Ohio, approximately 20% of biosolids (in dry tons) were disposed of in landfills, 36% were incinerated while 46% were applied to agricultural land – 35% was Class A biosolids while the remaining 65% was Class B biosolids (OEPA 2006).

Land application of biosolids is considered a beneficial use of the material. Farmers use it because it is a free source of soil conditioner relative to providing nutrients (i.e. fertilizer) and it improves soil structure. It is an innovative way to recycle biosolids derived from municipal WWTPs. Land application supplies necessary nutrients, including all of the phosphorous and part of the nitrogen needed for crop growth. It also provides trace elements such as copper and zinc among others. It is reported to increase agricultural productivity by improving soil structure, mainly due to increased stable organic matter (Eberle et al. 1994). The stable

Table 10.2 Ohio EPA set isolation distances for surface and injection applications of Class B biosolids

Land use type	Isolation distances for surface applications	Isolation distances for injection applications
Bedrock	3 ft	3 ft
Medical care facility	1000 ft	300 ft
Occupied buildings	300 ft	100 ft
Private potable water source	300 ft	100 ft
Waters of the state (excludes ground)	33 ft	33 ft
Sinkhole or UIC class V drainage	300 ft without grass buffer, 100 ft with grass buffer	300 ft without grass buffer, 100 ft with a grass buffer

Source: Ohio EPA (2002)

Fig. 10.1 Biosolids application in Oregon, OH. The left picture is the tractor and applicator and the right picture shows the field after the application

organic matter is predominantly in the form of the complex polyphenolic humic and fulvic acids. In Ohio, the typical application is in late summer after winter wheat has been harvested. The following year, corn is most often planted on the amended fields.

10.3 GIS and Human Health

Health effects basically function at the level of the individual, although research concerned with the environmental impacts (the natural, social, and built settings experienced by individuals) on health can be analyzed as area-level effects. The health of the population in relationship to the environment can be plotted to determine the presence of patterns, a potential spatial relationship between health and physical proximity to particular phenomena spatial analysis. Historically, Dr. John Snow, a British physician, was one of the first to investigate an environmental health problem in a geographical context. During a Cholera outbreak in 1854, Snow plotted the cases of Cholera on a map of London. He then identified a cluster of residences, which accounted for most of the deaths, around a public water pump. Once the pump was disabled, the incidence of cholera dropped (Schultz 2007).

The role of geography in epidemiology and public health in the present is much more robust. Within environmental health, disease ecology, and public health, GIS has become an indispensable tool. Contributing to the acceptance and expanding use of GIS within health sciences is the availability of large amounts of environmental data as well as GIS internet functionality (Kistemann et al. 2002). The greatest potential of GIS lies in its ability to clearly show the results from complex research through maps (Mullner et al. 2004).

10.3.1 Biosolids and Human Health

Due to the lack of existing substantiated studies, scientists differ in opinion on the nature and intensity of impacts of biosolids application. Some argue that US and state EPAs have arbitrarily chosen toxicity thresholds and therefore, the impacts

of biosolids application cannot be validated with adequate scientific knowledge. In contrast, others opine that the impacts found by field studies are substantial because the current practice of biosolids application is strictly regulated by federal and state laws that are based on multiple procedures (Düring and Gath 2002).

Although biosolids are high in more stable organic content and plant nutrients and make a good soil amendment, they can also contain metals, organic pollutants, and pathogens. Although processing biosolids attempts to limit the number of pathogens present, previous studies have shown that pathogenic bacteria often survive the treatment process (Lewis et al. 2002; Brooks et al. 2005a,b; Borjesson et al. 2009). Direct contact of waters contaminated by runoff from nearby land application sites is one potential mode of human exposure to pathogens present in land-applied biosolids (USEPA 1999). Since infection by resistant pathogens poses a unique treatment challenge, the off-site movement of pathogens, especially those expressing antibiotic resistance, is of particular public health importance. With repeated land application over time, heavy metals can accumulate to levels that may damage agricultural soils. Arsenic, cadmium, copper, lead, mercury, molybdenum, nickel, selenium, and zinc can be present in biosolids and are regulated in the Part 503 regulations. Both pathogens and some heavy metals are known to cause illness (ATSDR 1999; 2003; 2004; 2005; 2007; 2008).

The studies that are most commonly cited are those of STP workers (Brugha et al. 1998; Weldon et al. 2000; Trout et al. 2000; Gregersen et al. 1999; Rylander et al. 1977; Lundholm and Rylander 1983; Elia et al. 1983; Clark et al. 1984) and WWTP workers (Melbostad et al. 1994; Khuder et al. 1998). However, there are few studies on biosolids applicators and residents living in close proximity to biosolids applied fields.

Varying conclusions are present in epidemiological studies of disease in wastewater workers. Retrospective epidemiological studies have found that wastewater work presents an increased risk for a variety of symptoms. Melbostad et al. (1994) found in a study of 24 wastewater workers at Norwegian wastewater treatment facilities that workers who were exposed to rod-shaped bacteria reported significantly higher rates of tiredness after work, headache during work, nausea and respiratory symptoms. Khuder et al. (1998) found in a retrospective epidemiological study of 204 wastewater workers in Ohio that they had a significantly higher prevalence of gastroenteritis, gastrointestinal symptoms, abdominal pain and headache compared to workers in other occupations.

In the 2002 NRC report, the information from 14 studies of sewage treatment plant workers was gathered. Two studies showed that Hepatitis A increased (Brugha et al. 1998; Weldon et al. 2000) while one study showed no increase in Hepatitis A (Trout et al. 2000). Additionally, an outbreak of Pontiac Fever, which is caused by a bacteria transmitted through water, was confirmed (Gregersen et al. 1999). Among general complaints were increases in nasal irritation, tiredness, and diarrhea which are compatible with exposures to some bacterial endotoxin (Rylander et al. 1977). Increased rates of skin disorders, diarrhea, and gastrointestinal symptoms have also been reported (Lundholm and Rylander 1983). A study by Elia et al. (1983) provided evidence of pesticide absorption without reporting any health

effects. However, Clark et al. (1984) reported no differences in illness rates and no isolation of viruses or bacteria.

While studies of WWTP workers and sewage plant workers suggest or document some health effects that may be related to exposure to sewage and/or biosolids, those of biosolids applicators vary. Tanner et al. (2008) estimated occupational risks through the collection of microorganism levels in air immediately downwind of land application operations. Risks from aerosolized microorganisms at biosolids land application sites were lower compared to wastewater treatment plants. Robinson et al. (2006) developed and performed a pilot test of a health survey for WWTP workers, and although eight reported at least one potentially associated symptom, personal protective equipment (gloves, goggles, respirators) were not always worn to protect from potential exposure. Workers associated with biosolids land application activities were interviewed in a study by Burton and Trout (1999) and all five had reported at least one instance of gastrointestinal illness after working with biosolids at the WWTP or during application, while four of the five reported at least one symptom of various gastrointestinal symptoms or repeated intermittent headache. However, the site in question did not comply with EPA regulations, and at times before the study, had applied biosolids that exceeded the EPA fecal coliform upper limit for Class B biosolids (NIOSH 2002).

Community exposure to biosolids has been evaluated, although findings indicate further study is needed. Dorn et al. (1985) performed a 3-year prospective epidemiologic study in three geographic areas of Ohio on families of biosolids receiving farms and control farms. No significant differences were found in general symptoms or digestive or respiratory illness between the families. Lewis et al. (2002) surveyed 48 residents in eight states reportedly affected by ten biosolids land application sites although no control group was included. Results indicated at least 25% of participants reported coughing, burning throat or burning eyes within 1-h of exposure.

10.4 Methodology

In 2004, researchers from the University of Toledo and Bowling Green State University along with collaborators from Central State University, Kent State Unviersity, Cleveland State University, Youngstown State Univeristy, the University of Michigan, Oregon, Ohio WWTP and Bowling Green, Ohio WWTP developed a project to evaluate potential impacts of land application of Class B biosolids on human health using a geographic information system (GIS). This ongoing project is very comprehensive and seeks to analyze the potential pathways in which pathogens and heavy metals, through aerosols and transport of contaminants in runoff away from application fields, could result in human exposures and cause associated health problems. Field observations and modeling were utilized to investigate the fate of pathogens, heavy metals and pharmaceutical and personal care products (PPCPs) and the pathways of these constituents off of the fields. We have identified

approximately 50 compounds in wastewater influent, effluent and biosolids that are classified as caffeine, antibiotics, anti-depressants, and other pharmaceuticals, etc. (Spongberg and Witter 2008; Wu et al. 2008a,b; Wu et al. 2009a,b). Samples were analyzed for PPCPs within a GIS and PPCPs were detected on the sludge amended fields, from water exiting tile drains and in ditches downstream of applied fields (Wu et al. 2009a). We have determined the source of *E. coli* bacteria in runoff water from biosolids applied fields using DNA sequencing (Kassem et al. 2008; Esseili et al. 2008). Remote sensing has been used to identify biosolids application from satellite imagery as well as to estimate phosphorus concentrations in biosolids applied soils (Sridhar et al. 2009). Aerosol sampling has been performed using both direct reading instruments and integrated sampling in an effort to characterize farm fields during major field activities including application of biosolids. We are developing a predictive screening model to determine the concentration and risk due to aerosols released into the air on nearby residents.

This project led to the publication of an epidemiological study conducted in Wood County of people living near agricultural fields permitted to receive biosolids (Khuder et al. 2007). The GIS described herein was developed in ArcGIS in support of the Khuder et al. (2007) epidemiological study.

10.4.1 GIS Layer Development

GIS databases were created for Lucas, Wood, Greene, Mahoning, Portage and Trumbull Counties in Ohio (Fig. 10.2). A standardized state plane, Ohio North

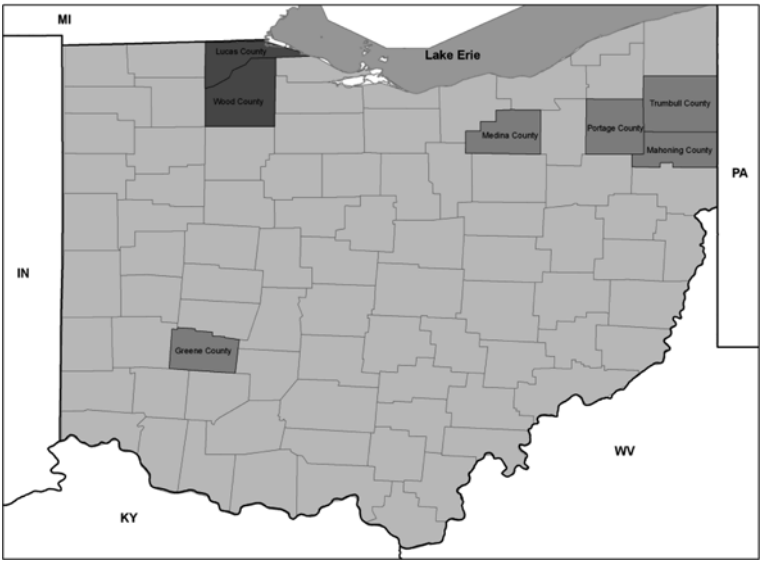

Fig. 10.2 Counties in Ohio in which the GIS and epidemiological surveys have been developed and performed

Table 10.3 Data layers and sources for the county GIS

Parcels	County auditors
Roads, railways, bike trails	ESRI, Inc. & Census TIGER files
Township boundaries	Census TIGER files
Demographic information	Census TIGER files
Soils	NRCS USDA Geospatial data gateway: http://datagateway.nrcs.usda.gov/
Hydrology	USGS NHD http://nhd.usgs.gov/
Septic tanks	County health department
Land cover	USGS/NLCD http://www.mrlc.gov/nlcd.php

(feet) coordinate system was used with the Lambert Conformation Conic projection and datum of NAD 83. Thus far, the epidemiological survey has been performed in Wood, Lucas and Greene Counties.

A base map layer was the first layer to be developed and includes parcel information, roads, railways, bike trails, schools, forests, zip codes, census tracts, township boundaries, waste water treatment plants, sewer districts, septic tanks (if available), soil classifications, hydrology, and hydrogeology (Table 10.3). Multiple sources of data were needed to collect this information including Census TIGER files, ESRI Inc. data set, County Auditors, County Engineers, and County Health Departments. After the base map, the permitted fields for Class B biosolids application were added. For the epidemiological study, permitted field locations were used to generate addresses that surveys were sent to for Wood and Lucas Counties. For Greene County, a further step was taken to attach the application information to the fields prior to generation of the addresses. This further refined the survey results and removed a confounding factor, a permitted field that never had biosolids applied, from the analysis.

10.4.2 Mapping Permitted Fields

A shapefile was created to identify the location of Class B permitted fields in each participating county. The location of Class B biosolids permitted fields (hereinafter referred to as "permitted fields") were collected from plat maps on file at the Northwest District Office of the Ohio Environmental Protection Agency for Wood and Lucas Counties and from the Dayton WWTP and local hauler for Greene County. Polygon shapes to represent the permitted fields were initially drawn freehand (Fig. 10.3). At times the description of the field was used to find the correct location of the field when plat maps were not available. Issues with polygons were observed such as overlapping of fields, the inclusion of forested areas and fields outside of parcel boundaries. A set of rules were developed to provide more accurate

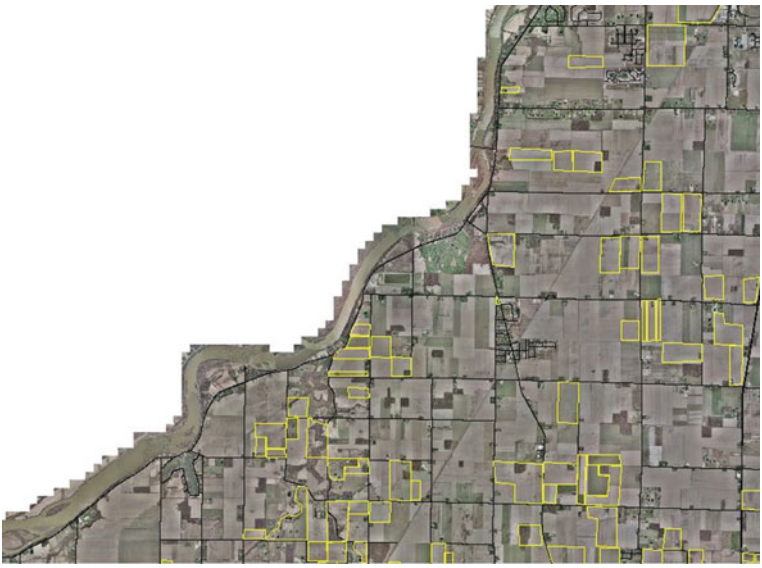

Fig. 10.3 Permitted field polygons were hand drawn from paper plat maps provided by the local EPA office over an aerial photograph. (Source: McNulty 2005)

locations and a cleaner topology of the permitted fields. The following steps were taken to ensure better accuracy.

- Aerial photographs were analyzed to verify the shape of the permitted field polygons. Heads-up digitizing was performed to match the shape of the permitted field polygon to the shape of the field.
- Permitted field polygons were compared with the parcel layer polygons provided by county auditor's offices to verify that it was within the parcel boundaries.
- Overlap of permitted field polygons with forested polygons was adjusted such that a permitted field did not include any forested area.
- A comparison of permitted field acreage listed on the EPA reports was compared to the measured acreage of the polygons produced. Substantial difference indicated an issue and the field was subsequently resolved.
- A comparison of farmer/owner name to the name listed on the parcel by the auditor was used to verify the location of the fields. Differences in owner name indicated a potential issue and the field was subsequently resolved.

The permitted fields are designated with a number and letter by the OEPA that represents the township that the permitted field is in (Fig.10.4). This leads to some confusion because a single county can have two or more fields with the same designation such as 27j. In addition, a field may be designated 27j in more than one county. The parcel ID was used as a unique identifier instead of the permitted field designation.

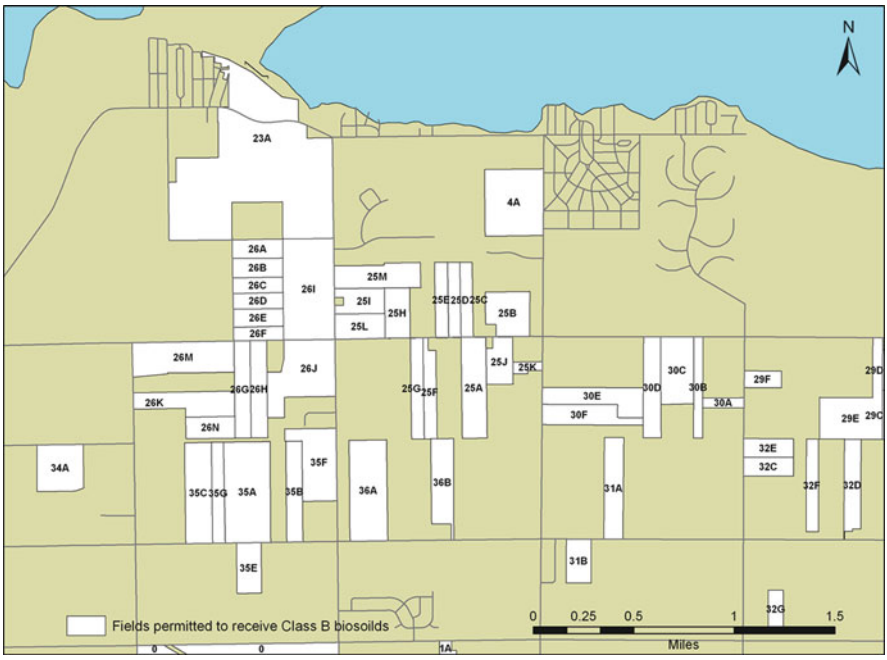

Fig. 10.4 Permitted fields in Oregon, Ohio showing the OEPA number and letter designations

After the original list of permitted fields was created for Wood County the database was continually updated in an attempt to include new permitted fields. Subsequently, the Wood County methodology was followed to develop the permitted field shape file for the other counties. The permitted fields for Wood, Lucas and Greene Counties respectively are show in Figs. 10.5, 10.6 and 10.9. The epidemiological study for Wood and Lucas Counties was performed using permitted fields only (Khuder et al. 2007).

10.4.3 Mapping Biosolids Applications

Not all fields that are permitted to receive biosolids actually have biosolids applied. Therefore, the epidemiological study in Wood and Lucas Counties had a potential confounding factor if permitted fields did not have biosolids applied to them. For Greene County, fields with known biosolids applications were used in the epidemiological study. Paper copies of submitted biosolids application reports were obtained through the Northwest District Office of OEPA for Lucas and Wood Counties and from the Dayton WWTP and sludge hauler for Greene County. Data were hand entered into data tables and joined to the parcel layer in the GIS using the parcel ID as the unique identifier. WWTPs are required to keep application reports as Part II of most NPDES permits issued to POTW and include detailed information about

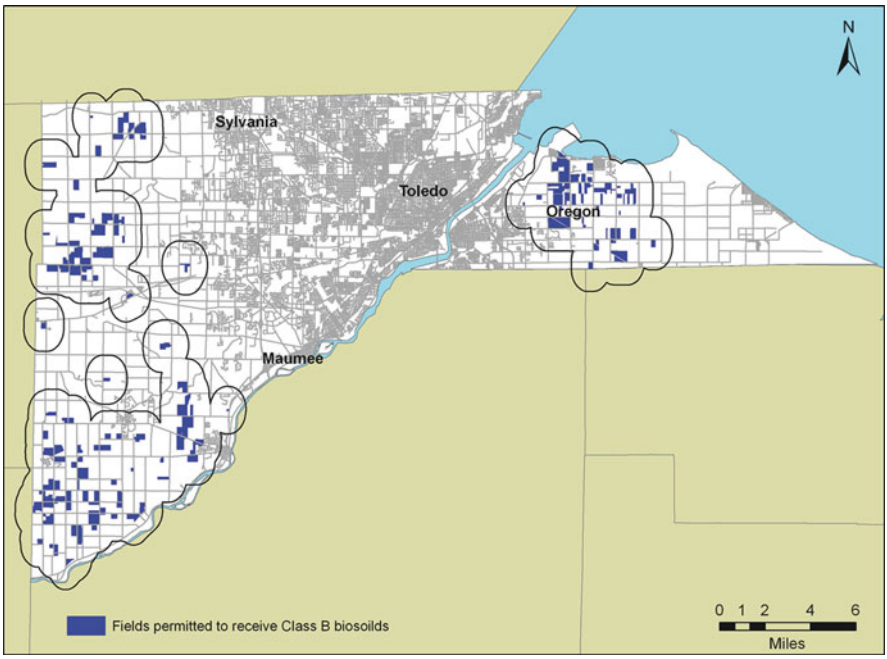

Fig. 10.5 Lucas County fields: a 1 mile buffer around permitted fields

the application site. Individual site reports vary by WWTP but often include the size of the field, gallons or dry tons applied to the field, percent solids of the biosolids, owner name, and location of the site.

The application information depicts the amount of application by year, geographic region, and amount of historical application (Table10.4). The fields that have received biosolids between 1990 and 2003 are shown in Figs. 10.5 (Lucas County), 10.7(Wood County) and 10.9 (Greene County). Once all of the data has been added, maps of the applications can be produced specifically showing the application rate of heavy metals and nutrients from the biosolids.

10.4.4 Address Generation for Epidemiological Study

The ability to look at spatial relationships was integral to the epidemiological portion of the project. The epidemiology study focused on potential health effects of residents in each county in relation to the households distance from a permitted or applied field. Households were selected to receive a mailed survey based on the distance of the house from permitted fields (Wood and Lucas Counties) or from applied fields (Greene County). A list of all households in Wood County by distance from permitted fields was created using the developed permitted fields shapefile. A

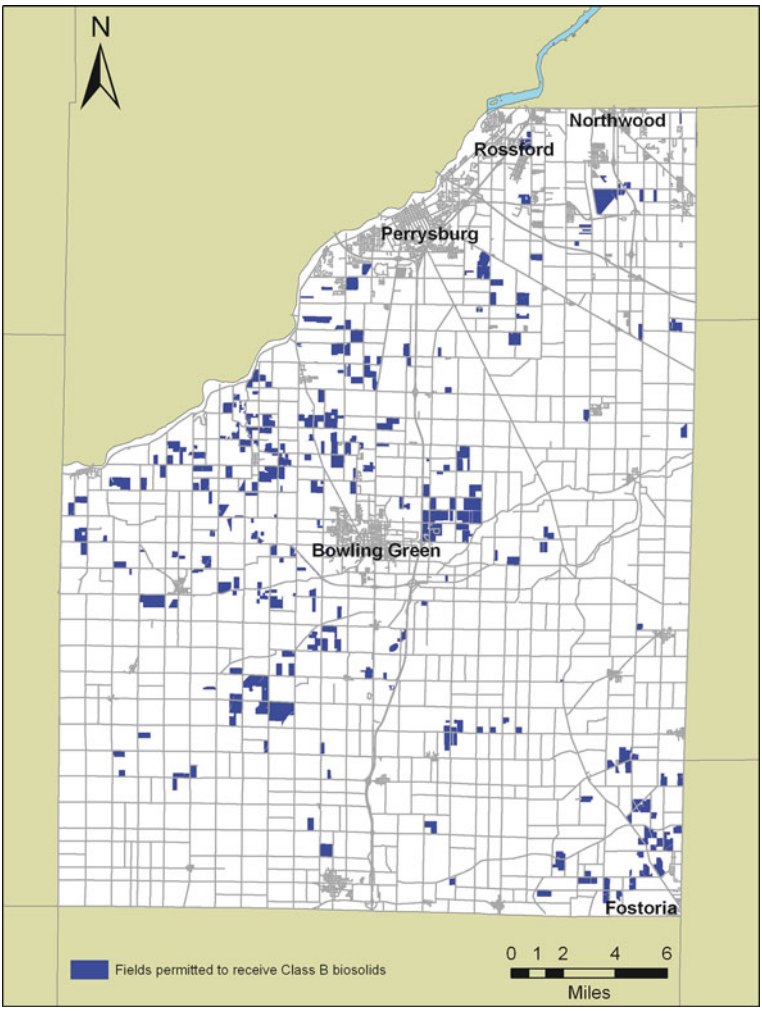

Fig. 10.6 Wood County fields permitted to receive Class B biosolids

distance buffer was generated from the edges of the permitted fields. The buffers were categorized as:

- on field,
- within 1 mile of the field,
- greater than 1 mile and within 2 miles of the field,
- greater than 2 miles and within 3 miles of the field,
- greater than 3 miles and within 4 miles of the field,
- greater than 4 miles and within 5 miles of the field, and
- greater than 5 miles of the field.

Table 10.4 Data variables recorded on biosolids application data forms

Basic information			
Date	Site	Site size	Site location
Application information			
Liquid volume applied	Percent solids	Dry lbs. material applied	Total dry tons material applied
Tons per acre	–	–	–
Nutrients (mg/Kg)			
Organic nitrogen	Ammonia nitrogen		Phosphorus
Metals (mg/Kg)			
Arsenic	Cadmium	Copper	Lead
Mercury	Nickel	Zinc	Molybdenum
Selenium	–	–	–

Participating households were selected from within these buffers. Since more health effects would be expected in areas with closer proximity and possibly higher exposure, (i.e., closest to permitted fields) all houses located on permitted fields were selected for inclusion. A similar number of houses were randomly selected from the houses within 1 mile of a permitted field and another group of houses were randomly selected from the houses greater than 1 mile of a permitted field, of which 51% were between 1 and 2 miles and 49% were between 2 and 3 miles of a permitted field. Houses more than 3 miles from a permitted field were excluded from the study due to the small number of houses in those buffers. Ultimately, the respondents were put into two groups, households up to one mile from a field and households greater than one mile from a field. These same two distance groups were used in all three studies. Figures 10.5, 10.8 and 10.9 depict a one mile buffer around the permitted fields for Lucas and Wood Counties and around confirmed applied fields for Greene County.

Survey groups for the epidemiological study were partitioned into households that were within one mile of several permitted fields (heretofore the exposed group) and households that were further than one mile away from any permitted field (heretofore the unexposed group). Epidemiological surveys were sent to the addresses chosen randomly from the generated lists. The use of GIS in the selection of survey households allowed for a random selection sample rather than a convenience sample of potentially exposed populations living near biosolids permitted fields and eventually biosolids applied fields. A convenience sample would not have guaranteed potentially exposed respondents. Additionally, the ability to verify the presence of a household on a property prior to mailing reduced the potential for returns due to bad addresses. This was especially true with dealing with agricultural areas as many properties have addresses but no one resides on the property. In addition, for Wood and Lucas Counties, many surveys were returned without delivery with *Address Unknown* on the envelope. In the process of generating addresses for the survey, we did not check to see if there was a house on the parcel. For Greene County, prior to household inclusion, a visual inspection of aerial photographs was performed to ensure that a residence was present on the parcel.

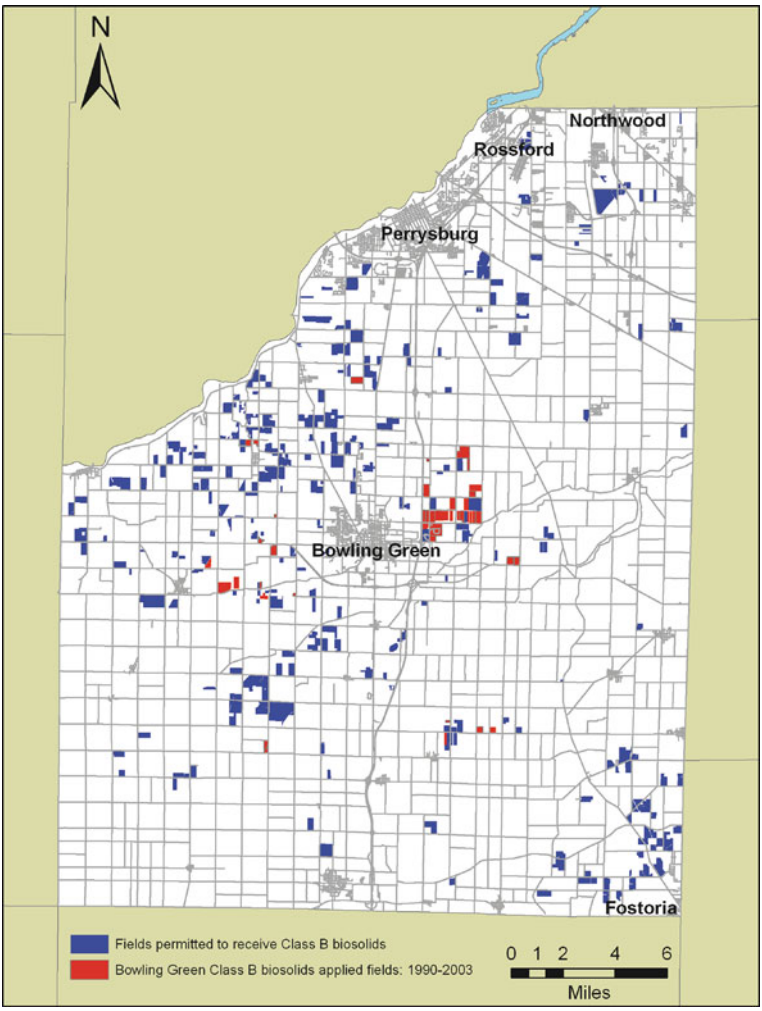

Fig. 10.7 Wood County fields that had biosolids applied between 1990 and 2003

Similar processes were used for Lucas and Greene Counties as were used for Wood County. Similar numbers of surveys were sent out for each county. The most significant difference was that fields that had biosolids applied were used for Greene County to set up the buffer (Fig. 10.9).

In the surveys, respondents were asked if they had any symptoms from a list and/or had been diagnosed with a disease by a physician. Survey respondents were asked to indicate the frequency of the following symptoms: headache, fever, excessive secretion of tears, cough, sneezing, sore throat, chest pain or discomfort, abdominal pain, abdominal bloating, nausea, vomiting, diarrhea, constipation, jaundice, skin rash, ulcer on the skin, muscle spasm, chills, dehydration, loss of appetite,

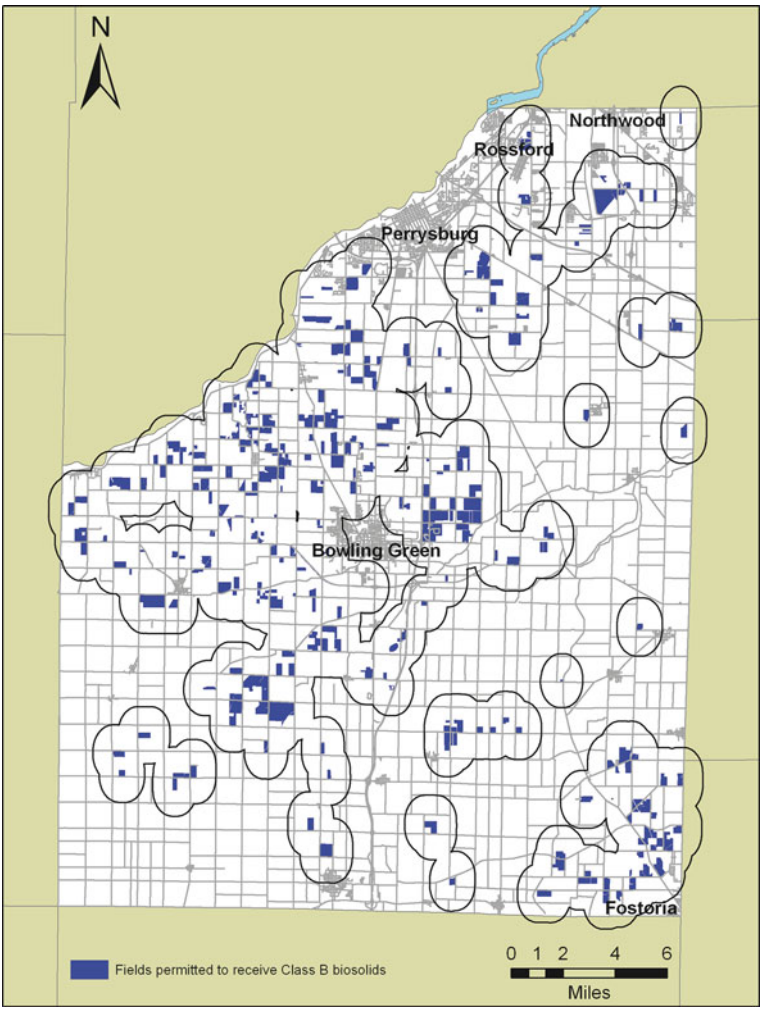

Fig. 10.8 Wood County fields a 1 mile buffer around permitted fields

weight loss, insomnia, fatigue, weakness, and general ill feeling. Respondents were asked to indicate on the questionnaire if they had been diagnosed with chronic diseases by a physician: asthma, emphysema, Crohn's disease, migraine headache, ulcerative colitis, chronic bronchitis, irritable bowel syndrome, allergies, multiple sclerosis, Parkinson's disease, scleroderma, skin disease, poliomyelitis, autism, skin cancer, and, arthritis/osteoarthritis. Lastly, physician diagnosed acute diseases listed on the questionnaire included: leptospirosis, salmonellosis, shigellosis, typhoid fever, hepatitis A, poliomyelitis, amoebiasis, bronchitis, pneumonia, upper respiratory infection, lower respiratory infection, cold, giardiasis, and gastroenteritis.

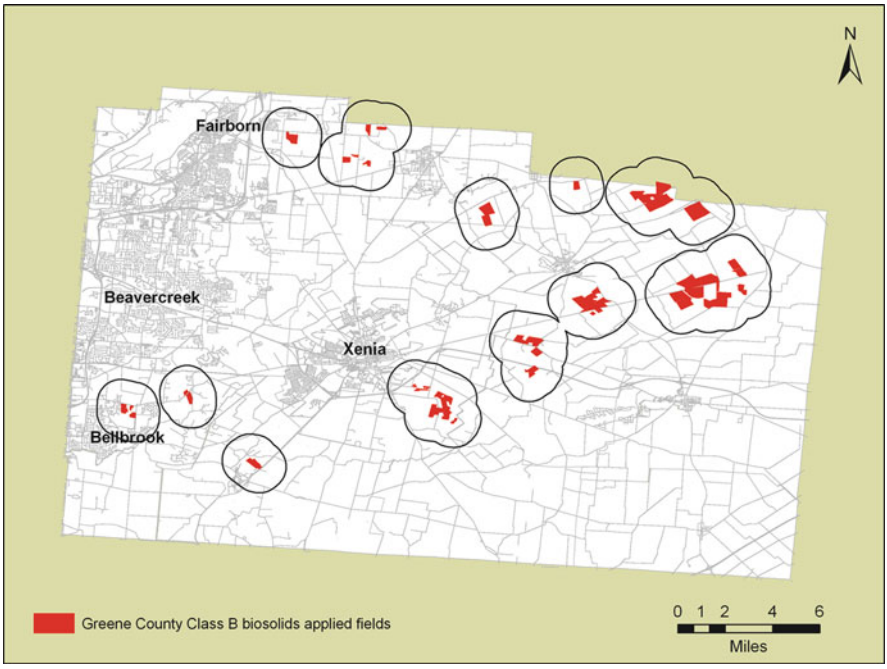

Fig. 10.9 Greene County fields a 1 mile buffer around applied fields

10.5 Results

Exposure determination in Wood County was based strictly on the distance the household was located from a permitted field. Originally, the study was designed with the intent to show a dose-response relationship, if one existed. In other words, more health effects were expected closer to the permitted fields with the number of health effects decreasing with each successive buffer zone away from the permitted fields. However, the results did not support this assumption. The symptoms and diseases self-reported from the on-field group and those reported from residents of houses within 1 mile of a permitted field were not statistically different and were combined to comprise the potentially exposed group. The control group was the sample of houses between 1 mile and within 3 miles of a permitted field. The "n" was 437 respondents from 178 households from within a mile of the permitted fields and an "n" of 176 respondents from 80 households from greater than one mile of the permitted fields.

A synopsis of the results is highlighted here with the rest of the results available from Khuder et al. (2007). Of the survey participants, there was no significant difference with regard to age, gender, length of time living on the farm, percentage of time each spent at the address, high-risk occupations, and smoking status between the participants near the permitted fields and those greater than one mile

away. The findings suggest that residents living near biosolids permitted fields may be at an increased risk for certain respiratory, gastrointestinal, and other diseases. Of the 25 symptoms on the survey, seven were significantly higher for the respondents living near the fields than away from the fields at a α=0.05 confidence level including excessive secretion of tears, abdominal bloating, jaundice, ulcer on the skin, dehydration, weight loss and weakness. Of the sixteen chronic diseases surveyed, only emphysema was statistically higher in the group near the fields. Of the 14 acute diseases surveyed, bronchitis, upper respiratory infection and Giardiasis were significantly higher in the group close to the permitted fields. The findings show that there is some correlation between illness and proximity to permitted fields for biosolids application in Wood County, Ohio, but it is not proof that biosolids were the cause of the illnesses. This study suggests that additional research is needed.

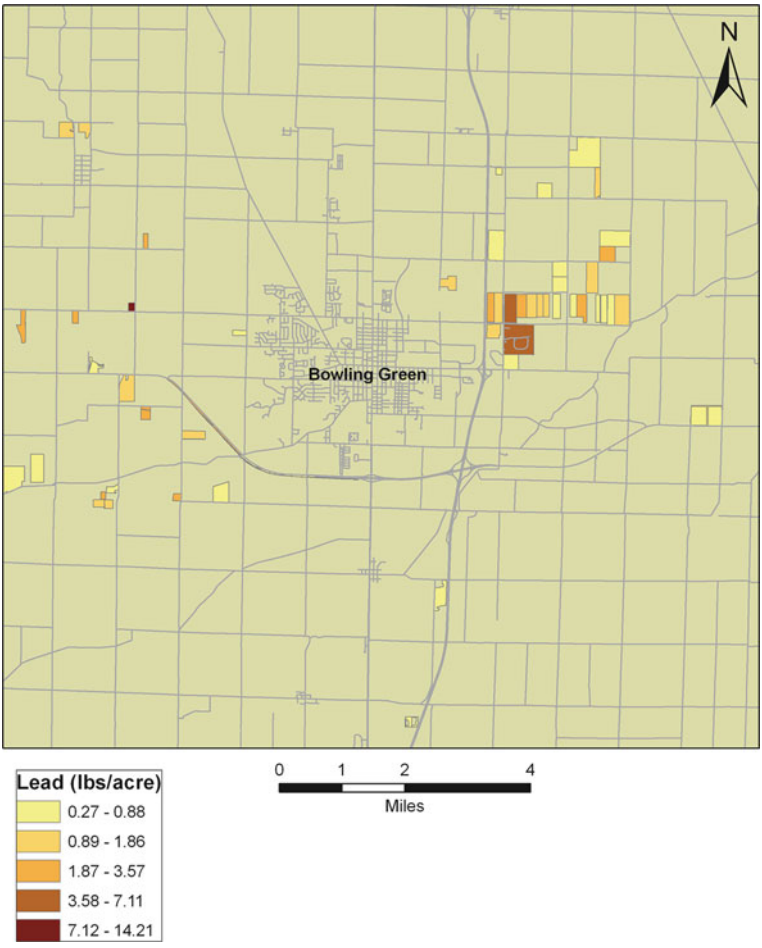

Fig. 10.10 Mass of lead applied to biosolids amended fields through 2003 in Wood County

Since the Wood County results were published, two additional health surveys have been performed in Lucas and Greene Counties in Ohio. These surveys were implemented using methods improved from the Wood County surveys. Wood County potential exposure status was defined purely by distance of the household from permitted fields. In Lucas County, the potentially exposed group was improved by selecting all of the households closest to the permitted fields. For the control households, the same procedure was used as in Wood County, a distance buffer of more than one mile but less than three miles from the nearest permitted field.

In an effort to further strengthen the epidemiological study in Greene County, the Class B biosolids application data were mapped first and then the addresses generated (Fig. 10.9). The exposed group then became the closest households to the

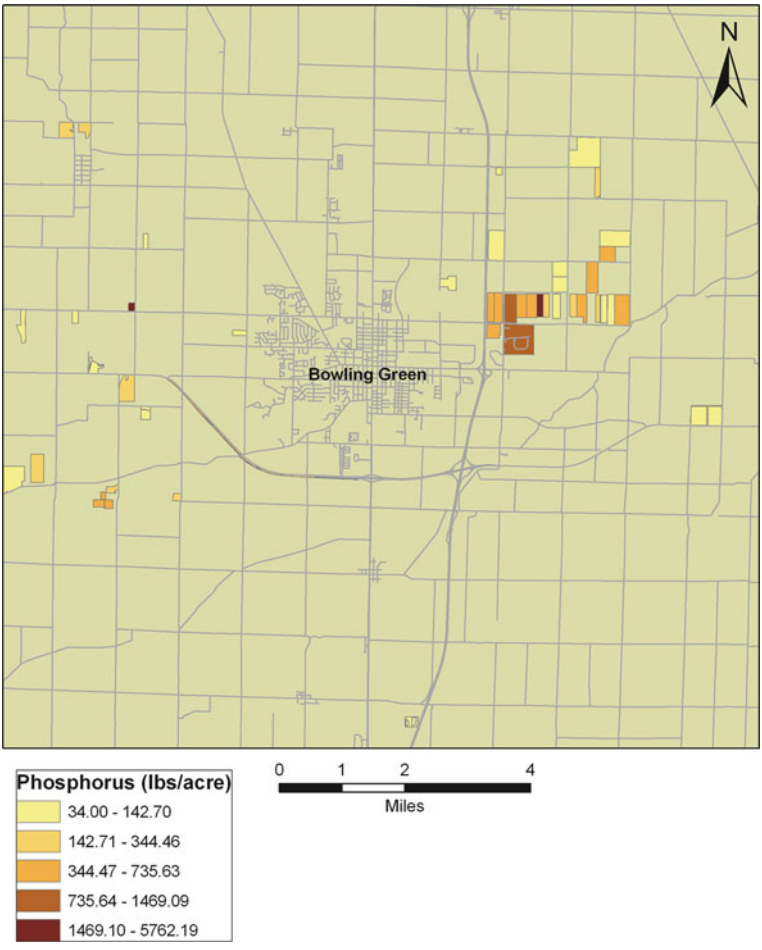

Fig. 10.11 Mass of phosphorus applied to biosolids amended fields through 2003 in Wood County

applied fields. A distance buffer was again generated, but for Greene County this buffer was set up from the edges of applied fields. The control households were then located more than 1 mile but less than three miles from the applied fields, matching the distances used in Wood County.

10.5.1 Conclusions and Future Directions

The results showed that there is some statistical correlation between illness and proximity to permitted biosolids fields in Wood County, Ohio, but it does not show a cause and effect relationship between biosolids applications to farm fields and illnesses. More work is need to further refine the epidemiological health survey data, including spatial analysis. In our study, counties that were surveyed prior to obtaining the application data will be evaluated using the obtained historical application data for a focus on biosolids applied fields, in addition to permitted fields. Application reports from WWTPs have generally been archived. Often WWTPs retain specific application information including heavy metals including arsenic, cadmium, copper, lead, mercury, molybdenum, nickel, selenium, zinc and nutrients including phosphorus and nitrates (Figs. 10.10 and 10.11). Comparison of the survey responses with application data has the potential to clarify the potential cause and effect relationship between biosolids and illnesses. These steps will allow for further examination of potential environmental exposure to contaminants from biosolids and relationships to human health effects.

Acknowledgments *Funding for this work was provided by the* United States Department of Agriculture (USDA) Cooperative State Research, Education, and Extension Service (CSREES) Program under Grant Nos. 2004-06227, 2005-06223, 2006-06255.

References

Agency for Toxic Substances and Disease Registry (ATSDR) (1999) Toxicological profile for Mercury Atlanta, GA: US Department of Health and Human Services, Public Health Service

Agency for Toxic Substances and Disease Registry (ATSDR) (2003) Toxicological profile for Selenium Atlanta, GA: US Department of Health and Human Services, Public Health Service

Agency for Toxic Substances and Disease Registry (ATSDR) (2004) Toxicological profile for Copper Atlanta, GA: US Department of Health and Human Services, Public Health Service

Agency for Toxic Substances and Disease Registry (ATSDR) (2005) Toxicological profile for Zinc Atlanta, GA: US Department of Health and Human Services, Public Health Service

Agency for Toxic Substances and Disease Registry (ATSDR) (2007) Toxicological profile for Lead Atlanta, GA: US Department of Health and Human Services, Public Health Service

Agency for Toxic Substances and Disease Registry (ATSDR) (2008) Toxicological profile for Cadmium (Draft for Public Comment) Atlanta, GA: US Department of Health and Human Services, Public Health Service

Borjesson S, Melin S, Matussek A, Lindgren PE (2009) A seasonal study of the mecA gene and Staphylococcus aureus including methicillin-resistant S aureus in a municipal wastewater treatment plant. Water Res 43:925–932

Brooks JP, Tanner BD, Gebra CP, Haas CN, Pepper IL (2005a) A national study on the residual impact of biological aerosols from the land application of biosolids. J Appl Microbiol 99:310–322

Brooks JP, Tanner BD, Gebra CP, Haas CN, Pepper IL (2005b) Estimation of bioaerosols risk of infection to residents adjacent to a land applied biosolids site using an empirically derived transport model. J Appl Microbiol 98:397–405

Brugha, R, Heptonstall J, Farrington P, Andren S, Perry K, Parry J (1998) Risk of hepatitis a infection in sewage workers. Occup Environ Med 55(8):567–569

Burton NC, Trout D (1999) Biosolids land application process. NIOSH Health Hazard Eval Rep HETA 98-0118-2748:1–16

Clark CS, Bjornson HS, Schwartz-Fulton J, Holland JW, Gartside PS (1984) Biological health risks associated with the composting of wastewater treatment plant sludge. J Water Pollut Control Fed 56(12):1269–1276

Dorn CR, Reddy CS, Lamhere DN, Gaeuman JV, Lanese R (1985) Municipal sewage sludge application on Ohio farms: health effects. Environ Res 38(2):332–359

Düring RA, Gäth S (2002) Utilization of municipal organic wastes in agriculture: where do we stand, where will we go? J Plant Nutr Soil Sci 165:544–556

Eberle WM, Whitney DA, Powell GM (1994) Sewage sludge use on agricultural land. Cooperative Extension Service, Kansas State University, Manhattan 29

Elia VJ, Clark CS, Majeti VA, Gartside PS, MacDonald T, Richdale N, Meyer CR, Van Meer GL, Hunninen K (1983) Hazardous chemical exposure at a municipal wastewater treatment plant. Environ Res 32(2):360–371

Esseili M, Sigler V, Kassem I (2008) Optimization of DGGE community fingerprinting for characterizing Escherichia coli communities associated with fecal pollution. Water Res 42:4467–4476

Gregersen P, Grunnet K, Uldum SA, Andersen BH, Madsen H (1999) Pontiac fever at a sewage treatment plant in the food industry Scandinavian. J Work Environ Health 25(3):291–295

Kassem I, Sigler V, Esseili M (2008) Occurrence of mecA in nonstaphylococcal pathogens in surface waters. J Clin Microbiol 46:3868–3869

Khuder SA, Arthur T, Bisesi M, Schaub EA (1998) Prevalence of diseases and associated symptoms in wastewater treatment workers. Am J Ind Med 33:571–577

Khuder S, Milz S, Bisesi M, Vincent R, McNulty W, Czajkowski K (2007) Health survey of residents living near biosolids permitted farm fields. Arch Occup Environ Health 62:5–11

Kistemann T, Dangendorf F, Schweikart J (2002) New perspectives on the use of geographical information systems (GIS) in environmental health sciences. Int J Hyg Environ Health 205:169–181

Lewis D, Gattie D, Novak M, Sanchez S, Pumphrey C (2002) Interactions of pathogens and irritant chemicals in land applied sewage sludges (biosolids). BMC Public Health 2:11

Lundholm M, Rylander R (1983) Work related symptoms among sewage workers. Br J Ind Med 40(3):325–329

McBride MB (2003) Toxic metals in sewage sludge-amended soils: has promotion of beneficial use discounted the risks? Adv Environ Res 8:5–19

Melbostad E, Eduard W, Skogstad A, Sandven P, Lassen J, Sosstrand P, Heldal K (1994) Exposure to bacterial aerosols and work-related symptoms in sewage workers. Am J Ind Med 25:59–63

McNulty WS (2005) The creation of a GIS database and the determination of sludge's spectral signature in an agricultural setting (master's thesis). Bowling Green State University, Department of Geology

Mullner R, Chung K, Croke K, Mensah E (2004) Geographic information systems in public health and medicine. J Med Syst 28(3):215–221

National Research Council (NRC) (2002) Committee on toxicants and pathogens in biosolids applied to land: advancing standards and practice. National Academy Press, Washington, DC

National Institute of Occupational Safety and Health (NIOSH) (2002) Guidance for controlling potential risks to workers exposed to class B biosolids. NIOSH Publ 2002-149, Cincinatti, OH

Ohio Environmental Protection Agency (2002) State of Ohio sewage sludge rules. Adm Code Ch 3745:40

Ohio Environmental Protection Agency (2006) Sewage sludge use or disposal in Ohio, Annu Rep CY 2006

Renner R (2002) NRC targets pathogens in sludge for research. Environ Sci Technol 36(17):338A

Robinson C, Robinson K, Tatgenhorst C, Campbell D, Webb C (2006) Assessment of wastewater treatment plant workers exposed to biosolids. Am Assoc Occup Health Nurses 54(7):301–306

Rylander R, Andersson K, Belin L, Berglund G, Bergstrom R, Hanson L, Lundholm M, Mattsby I (1977) Studies on humans exposed to airborne sewage sludge. Schweiz Med Wochenschr 107(6):182–184

Schultz SG (2007) From a pump handle to oral rehydration therapy: a model of translational research. AJP Adv Physiol Educ 31(4):288–293

Spongberg AL, Witter JD (2008) Pharmaceutical compounds in the wastewater process stream in northwest Ohio. Sci Total Environ 397:148–157

Sridhar BBM, Vincent RK, Witter JD, Spongberg AL (2009) Mapping the total phosphorus concentration of surface soils using LANDSAT TM remote sensing imagery. Sci Total Environ 407:2894–2899

Tanner BD, Brooks JP, Gerba CP, Haas CN, Josephson KL, Pepper IL (2008) Estimated occupational risk from bioaerosols generated during land application of class B biosolids. J Environ Qual 37(6):2311–2321

Trout D, Mueller C, Venczel L, Krake A (2000) Evaluation of occupational transmission of hepatitis A virus among wastewater workers. J Occup Environ Med 42(1):83–87

US Environmental Protection Agency (1994) 40 CFR Part 503 Standards for use and disposal of sewage sludge. Final rule Fed Regist 59:9095–9100

US Environmental Protection Agency (1999) Environmental regulations and technology: control of pathogens and vector attraction in sewage sludge under 40 CFR part 503

US Environmental Protection Agency (2004) Primer for municipal wastewater treatment systems. EPA 832-R-04-001

Weldon M, VanEgdom MJ, Hendricks KA, Regner G, Bell BP, Sehulster LM (2000) Prevalence of antibody to hepatitis a virus in drinking water workers and wastewater workers in Texas from 1996 to 1997. J Occup Environ Med 42(8):821–826

Wu C, Spongberg AL, Witter JD (2008a) Use of solid phase extraction and liquid chromatography-tandem mass spectrometry for simultaneous determination of various pharmaceuticals in surface water. Int J Environ Anal Chem 88:1033–1048

Wu C, Spongberg AL, Witter JD (2008b) Determination of the persistence of pharmaceuticals in biosolids using liquid-chromatography tandem mass spectrometry. Chemosphere 53:511–518

Wu C, Witter JD, Spongberg AL, Czajkowski K (2009a) Monitoring pharmaceutical and personal care products in an agricultural landscape, western lake Erie basin. Water Res 43:3407–3416

Wu C, Spongberg AL, Witter JD (2009b) Adsorption and degradation of triclosan and triclocarban in soils and biosolids amended soils. J Agric Food Chem 57:4900–4905

Chapter 11
Remote Sensing, Public Health & Disaster Mitigation

Gilbert L. Rochon, Joseph E. Quansah, Souleymane Fall, Bereket Araya, Larry L. Biehl, Thierno Thiam, Sohaib Ghani, Lova Rakotomalala, Hildred S. Rochon, Angel Torres Valcarcel, Bertin Hilaire Mbongo, Jinha Jung, Darion Grant, Wonkook Kim, Abdur Rahman M. Maud, and Chetan Maringanti

Abstract The authors review advances in applications for geotechnologies, specifically earth-observing satellite remote sensing, geo-positioning (i.e. USA's Global Positioning System (GPS), Russia's Global'naya Navigatsionnaya Sputnikovaya Sistema (GLONASS), Europe's Galileo and China's Beidou/Compass) and selected geo-spatial modeling software for public health and disaster management applications, with an emphasis on environmental health and environmental sustainability. Specific applications addressed include the use of remote sensing for infectious disease vector habitat identification and ecologically sustainable disease vector population mitigation, as well as the integration of GPS into mobile CD4 testing devices for HIV/AIDS. Public domain software models described include the Spatio-Temporal Epidemiological Modeler (STEM) and the Hydrologic Engineering River Analysis System (HEC-RAS) for flood modeling. Examples of regional, national and global real-time data acquisition and near-real-time data product development and distribution for time-critical events are offered, specifically through the Purdue Terrestrial Observatory (PTO), the United States Geological Survey (USGS) supported AmericaView and the International Charter – Space & Major Disasters.

Keywords Remote Sensing · Public Health · Infectious Disease Vector Habitat · Environmental Health · Climate Change · Africa · Cytometry for Life · C4L · IndianaView · AmericaView · Purdue Terrestrial Observatory · Disasters · Sustainability · Geotechnologies

11.1 Advances in Remote Sensing and Geo-Positioning

There has been demonstrable progress in the global deployment of earth observing satellites, telecommunications satellites and geo-positioning satellite constellations.

G.L. Rochon (✉)
Purdue Terrestrial Observatory, Rosen Center for Advanced Computing, Information Technology at Purdue (ITaP), Purdue University, Lafayette, IN 47907, USA
e-mail: rochon@purdue.edu

N. Hoalst-Pullen, M.W. Patterson (eds.), *Geospatial Technologies in Environmental Management*, Geotechnologies and the Environment 3, DOI 10.1007/978-90-481-9525-1_11,

Such progress is particularly evident within the developing nations of Africa, Asia and Latin America. Although these inter-disciplinary technologies have applicability to a wide array of sectors, the primary focus of this review will be the extent to which space-based technologies have contributed thus far to the public health and disaster management sectors. In this context, the range of "Public Health and Disaster Management" related applications of orbiting sensors encompasses environmental risk assessment, chronic disease mapping, infectious disease vector habitat identification and monitoring (Rejmankova et al. 1995), early warning for famine (Verdin et al. 2005), for specific disease outbreaks (Cuevas et al. 2007), as well as determining populations' vulnerability to biogenic and anthropogenic disasters, thereby facilitating both emergency response and subsequent post-catastrophe recovery (Rochon et al. 2008).

The application of remote sensing, in combination with in situ measurements and epidemiological data, to Environmental Health, particularly within the industrialized countries, has concentrated on monitoring the impact of atmospheric pollution and particulates on respiratory ailments, the downstream impact of urban effluent (e.g. residue from auto emissions, road salts, sewage, industrial hazardous wastes) and agricultural runoff (e.g. pesticides, fertilizers, hormones, fecal material from confined animal feeding operations (CAFOs)) on drinking water quality and subsequent acute and chronic morbidity, as well as the increased vulnerability to stomach, duodenal, esophageal and lung cancers, associated with proximity to petro-chemical facilities or other sources of industrial emissions.

Within the developing countries, there has been a greater emphasis on deploying remote sensing for food security issues, including famine early warning and monitoring the desert locust, *Schistocerca gregaria,* as well as identification and mitigation of infectious disease vector habitat. Even in this instance, environmental considerations are becoming more prominent, specifically the quest for more sustainable means for disease vector population reduction. Broad spectrum pesticides not only wreak havoc on entire ecosystems; but also impact benign species, such as the honey bee (*Apis mellifera*). With the increase in industrialization without concomitant environmental protections in megacities within the developing countries (e.g. Cairo, Egypt; Shanghai, China; Mexico City, Mexico; Sao Paolo, Brazil; Mumbai, India, etc.), the same air quality and water quality issues that began plaguing Europe and the United States prior to environmental safeguards are now manifested in urban centers in Africa, Asia and Latin America.

As recent catastrophic earthquake events in Port au Prince, Haiti have demonstrated, poverty significantly increases vulnerability to natural disasters, to food insecurity, to infectious diseases and to the ability to recover during the aftermath of a major calamity. As the response to Hurricane Katrina in New Orleans, Louisiana also demonstrated, enclaves of poverty in the highly industrialized countries also inhibit timely response to evacuation orders, even when early warning systems are supposedly in place. It is ironic that the first satellite data available depicting the flooding of New Orleans consequent to Hurricane Katrina was captured by NigeriaSat 1. The recent proliferation of earth observing satellites by developing countries is a harbinger of a growing awareness that space-based technologies are

becoming an essential adjunct to sustainable development in the "Third World" (See Table 11.1).

In addition to the satellites launched by developing countries, data from numerous other satellites, launched by the highly industrialized countries, have been utilized specifically for public health, environmental impact and disaster management applications (Rochon et al. 2009; Beck et al. 2000). In particular, a consortium of the major global owners of earth observing satellites have formed the International Charter-"Space & Major Disasters," http://www.disastercharter.org/, a vehicle for rapid dissemination and free distribution to approved disaster managers of near-real-time satellite data, in the event of a declared major biogenic or anthropogenic disaster.

Since the inception of its first activation on February 2, 2002 through the January 13, 2010 activation for the Haitian earthquake, the Charter has been activated 222 times for a wide array of disasters, including flooding, earthquakes, landslides, hurricanes, cyclones, tornadoes, typhoons, tsunamis, volcanic eruptions, fires, oil spills, oil slicks, snow disaster, a chemical tanker accident and a train wreck. To date, the Charter has not been activated for famine, drought, an epidemic *or an* epizootic; however, the potential for such activation still exists. The current member agencies of the International Charter and their respective earth observing satellite assets are listed in Table 11.2.

A global surveillance program, in anticipation of a potentially pandemic influenza outbreak, has been initiated by the World Health Organization (WHO) http://www.who.int/csr/disease/influenza/pandemic/en/, as well as early warning for a wide range of other infectious diseases (i.e. WHO Global Alert and Response (GAR) http://www.who.int/csr/en/). Similar initiatives are sponsored by the Centers for Disease Control (CDC), (i.e. Early Warning Infectious Disease Surveillance (EWIDS) Program http://www.bt.cdc.gov/surveillance/ewids/) and the Department of Defense Global Emerging Infections System (Pavlin et al. 2003). Methods employed in surveillance programs, for example, as relates to avian influenza, include combining ecological variables and in situ inspections with remote sensing for monitoring migratory bird movements, as well as domestic poultry production (Xiao et al. 2007).

11.2 Geopositioning

The georeferencing of satellite data is propaedeutic to development of an effective spatial/temporal database, otherwise referred to as a Geographic Information System (GIS). Such georeferencing enables the accurate fusion of multiple data layers (e.g. elevation, soil type, landcover, landuse, health care facilities, population density, specific disease prevalence/incidence, transportation routes, disaster vulnerability mapping, etc.). The early constellations of geo-positioning satellites included *Global'naya Navigatsionnaya Sputnikovaya Sistema* (GLONASS), launched by the Soviet Union and currently maintained and enhanced by the Russian Federation, and the Global Positioning System (GPS), launched by the USA.

Table 11.1 Earth observing satellites: Latin America, Asia and Africa

Earth observing satellites	Continent	Satellites	Launch date	References
Brazil and China	Asia and Latin America	SCD-1	2/09/93	INPE : National Institute for Space Research (http://www.inpe.br/)
		SCD-2	10/23/98	
		Aqua	5/4/02	
		CBERS-2B	9/19/07	
Argentina	Latin America	SAC-A	12/04/98	CONAE : National Space Activities Commission (http://www.conae.gov.ar/)
		SAC-B	11/04/96	
		SAC-C	11/21/00	
Turkey	Euro/Asia	TurksSat 1	1/24/94	TÜBITAK UZAY : Space Technologies Research Institute (http://www.uzay.tubitak.gov.tr/)
		EurasiaSat	1/10/01	
		Bilsat-1	9/27/03	
		RASAT	5/1/10	
Thailand,	Asia	THEOS	10/01/08	GISDA : Geo-Informatics and Space Technology Development Agency (http://www.gistda.or.th/en/)
Korea	Asia	KOMPSAT-1	12/21/99	KARI : Korea Aerospace Research Institute (http://new.kari.re.kr/english/)
		KOMPSAT-2	7/28/06	
		COMS	6/26/10	
Japan	Asia	TRMM	11/28/97	JAXA : Japan Aerospace Exploration Agency (http://www.jaxa.jp/)
		Terra	12/18/99	
		Aqua	5/04/02	JMA : Japan Meteorological Agency (http://www.jma.go.jp/)
		MTSAT-1R	2/26/05	
		ALOS	1/24/06	
		MTSAT-2	2/18/06	
		GOSAT	1/23/09	
China	Asia	Fengyun-1D	5/15/02	
		Fengyun-2C	10/19/04	
		Beijing-1	10/27/05	
		Fengyun-2D	12/8/06	

Table 11.1 (continued)

Earth observing satellites	Continent	Satellites	Launch date	References
		Fengyun-3A	5/27/08	CAST : Chinese Academy of Space Technology (http://www.cast.cn/CastEN/) NRSCC : National Remote Sensing Centre of China (http://www.nrscc.gov.cn)
		Fengyun-2E	12/26/08	
India	Asia	IRS-1D	9/29/97	ISRO : Indian Space Research Organization (http://www.isro.org/)
		INSAT-2E	4/3/99	
		OCEANSAT-1	5/26/99	
		TES	10/22/01	
		KALPANA-1	9/12/02	
		INSAT-3A	4/4/03	
		RESOURCESAT-1	10/17/03	
		CARTOSAT-1	5/5/05	
		CARTOSAT-2	1/10/07	
		IMS-1	4/28/08	
		RISAT-2	4/20/09	
		OCEANSAT-2	9/24/09	
Nigeria	Africa	NigeriaSat-1	9/27 /03	NASRDA : National Space Research and Development Agency (http://www.nasrda.net/)
		NigeriaSat-2	9/1/10	
Algeria	Africa	AlSAT-1	11/28/02	ASAL : Algerian Space Agency (http://www.asal-dz.org)
Morocco	Africa	Zarkae Al Yamama (Maroc-Tubsat)	12/10/01	CRTS : Royal Centre for Remote Sensing (http://www.crts.gov.ma/)
South Africa	Africa	SunSat	2/23/99	SANSA : South African National Space Agency (http://www.space.gov.za/)
		SumbandilaSat	9/18/09	
Egypt	Africa	Egyptsat 1	4/17/07	NARSS : National Authority for Remote Sensing and Space Sciences (http://www.narss.sci.eg/)
Taiwan	Asia	FORMOSAT 3 A–F	4/15/06	NSPO : National Space Organization (http://www.nspo.org.tw/2008e/)

Table prepared by Bereket Araya and Wonkook Kim (Purdue Terrestrial Observatory)

Table 11.2 Current international charter members

International charter members	Space resources
European Space Agency (ESA)	ERS, ENVISAT
Centre national d'études spatiales (CNES)	
Spotimage	SPOT
NSPO	Formosat
Canadian Space Agency (CSA)	RADARSAT
Indian Space Research Organization (ISRO)	IRS
National Oceanic and Atmospheric Administration (NOAA)	POES, GOES
Argentina's Comisión Nacional de Actividades Espaciales (CONAE)	SAC –C
Japan Aerospace Exploration Agency (JAXA)	ALOS
United States Geological Survey (USGS)	Landsat
Digital Globe	Quickbird
GeoEye	GeoEye-1
DMC International Imaging (DMC)	
Centre National des Techniques Spatiales (Algeria)	ALSAT-1
National Space Research and Development (Nigeria)	NigeriaSat
Tübitak-BILTEN (Turkey)	BILSAT-1
BNSC/Surrey Satellite Technology Limited (UK)	UK-DMC
BNSC/Qinetiq (UK)	TopSat
China National Space Administration (CNSA)	FY, SJ, ZY satellite series

Source: International Disaster Charter: http://www.disasterscharter.org/participants_e.html

These constellations have more recently been joined by the European Union's geo-positioning constellation, Galileo, and by China's Beidou Satellite Navigation and Positioning System, also known as Beidou-2 or Compass.

It is envisioned that future handheld or mounted receiving devices may be able to interchangeably access any satellite signals from these four constellations, in order to quickly obtain highly accurate latitude/longitude or Universal Transverse Mercator (UTM) coordinates, as well as elevation data. With the demise of "Selective Availability," a deliberate distortion of the GPS signal instituted by the US Department of Defense, a practice terminated during the presidency of William Jefferson Clinton, the advent of dual base station/rover receivers with post-correction capability, and subsequent signal enhancement, contemporary geo-positioning systems have achieved centimeter-level accuracy.

Within the United States, several states have initiated high spatial resolution ortho-photography over-flights. Data from these missions, while lacking the temporal and spectral resolution of satellite data, have demonstrated their utility in contributing to accurate base maps, user-friendly graphical interfaces and to broad distribution either directly by state governments or by academic institutions for heterogeneous applications. Additionally, real-time satellite ground stations for acquisition, processing and distribution of near-real-time data products have been established at selected universities, primarily to address time-critical phenomena.

As a case in point, Purdue University's Purdue Terrestrial Observatory (PTO) (http://www.itap.purdue.edu/pto/) disseminates image data through several different avenues. The near real-time image data collected by the PTO are distributed

via a subscription service for users called PRESTIGE (http://www.purdue. teragrid.org/prestige). Archival satellite image data for Indiana, including the Landsat Thematic Mapper (TM) and Multispectral Scanner (MSS) data, ASTER, EO1 Hyperion and ALI, as well as some declassified Corona data, are distributed via a portal developed by the IndianaView program (http://www.indianaview.org/ glovis/). Moreover, this portal contains a link to the digital orthographic images that have been collected for Indiana in the last 10 years. These data are made available over the Indiana Spatial Data Portal, managed by Indiana University. Users can also obtain image data by means of a portal developed under the auspices of the National Science Foundation (NSF) sponsored TeraGrid program (http://www.purdue.teragrid.org/portal/). This portal contains the basics to allow a user to search for data sets, but does not include a graphical clue to indicate where the data originates. The portal does include access to the NEXRAD (Next Generation Radar) data that are collected by all National Weather Service (NWS) Doppler stations throughout the United States. Image data sets are available in a heterogeneous manner; the work involved in doing this is divided across many different portals operated by diverse governmental and university institutions. A key element is to provide cross-links and obvious help cues and messages, so as to guide the user to the appropriate data and data products for each specific task.

IndianaView is a consortium of ten universities and four non-profit agencies engaged in remote sensing research, instruction and services within Indiana and is a component of AmericaView (AV), a non-profit corporation. AV is a nationwide program that focuses on satellite and aerial remote sensing data and technologies, in support of applied research, K-16 education, workforce development, and technology transfer. AV was developed through a partnership between the U.S. Geological Survey (USGS). The AmericaView Program is the outgrowth of a research and education pilot project initiated in the State of Ohio by the USGS in 1998. The objective of OhioView was to create a prototype system for high-speed processing and rapid delivery of remotely sensed data to state and local users. The AmericaView Consortium is comprised of university-led, state-based consortia working together to build a nationwide network of state and local users. The Consortium is actively working with the USGS and universities across the country to expand participation in the AV Program to all 50 states; currently there are 36 state-view programs. Each state-view makes image data available from their state freely available to all.

For many local, city and county agencies, the digital orthographic image data that many states have now been able to collect becomes very important for satisfying spatial needs. These data usually represent spatial resolutions of .15 m (6 inches) to 1 m. This becomes crucial for identifying utilities, buildings, transportation infrastructure, streams, rivers, etc. These data sources provide a very visual presentation when overlaid with other demographic data in Geographic Information Systems (GIS). The Information Technology (IT) infrastructure has grown in recent years to be much faster, easier to network with other users and application developers, more affordable and able to handle the terabytes of data that are now available. The orthographic image data that were collected for the entire state of Indiana in 2005 represents over 10 terabytes of data that are easily accessible from the Indiana University Spatial Data Portal.

11.3 Infectious Disease Vector Habitat Identification and Monitoring

The potential utility of such resources to public health and safety is significant. Studies using satellite data to investigate the spatial and seasonal dynamics of infectious disease transmission were mostly initiated in the late 1970s and the 1980s. Most of these studies focused on utilization of satellite data to identify habitats and breeding sites of disease vectors, as well as other environmental parameters affecting health (Barnes and Cibula 1979; Wagner et al. 1979; Jovanovic 1987; Linthicum et al. 1987; Hugh-Jones 1989). Conclusive results from these early studies revealed the significant potential of remote sensing applications for disease vector monitoring and related epidemiological applications in a wide array of site-specific geographic locations.

Over the past three decades, the use of remote sensing techniques in epidemiological studies has evolved significantly due to two factors: (i) the rapid development in spatial information technologies (i.e. remote sensing, Geographical Information Systems and Geo-positioning Systems) and (ii) the development of disease ecology (Thomson et al. 1996), a sub-discipline of epidemiology, which investigates the biological, physical and anthropogenic links between the environment and disease, consequently accounting for spatial variation in transmission (Graham et al. 2004). As shown in a number of comprehensive reviews on the use of remote sensing and GIS for epidemiological applications (e.g. Thomson and Connor 2000; Hay et al. 2000; Kalluri et al. 2007), a growing number of epidemiologists are now taking advantage of the reductions in cost and increased ease of access.

A variety of techniques ranging from simple correlations to complex combinations with models have been used to link satellite-derived variables to vector biology. A typical approach involves classifying remotely sensed images into habitats for disease vectors (Rogers 2000; Randolph 2000; Guo et al. 2005; Lacaux et al. 2007; Leblond et al. 2007) and creating environmental and land use maps associated with vector-borne diseases (Hay et al. 2006). Such methods often use the satellite-derived Normalized Difference Vegetation Index (NDVI) to estimate the amount of green biomass, which is an indicator of not only the abundance of vectors (Rogers and Randolph 1991; Malone et al. 2001; Wu et al. 2002; Odiit et al. 2005; Peterson et al. 2005; Raso et al. 2006), but also of other environmental factors such as moisture, soil type, slope and elevation (Boone et al. 2000). Among other commonly used satellite-derived variables linked to vector biology are the modified soil-adjusted vegetation index (MSAVI), the land surface temperature (LST) derived from the Advanced Very High Resolution Radiometer (AVHRR) channels 4 and 5, the middle infrared band derived from AVHRR channel 3 (detection of hot regions associated with forests), the near-surface air temperature derived from LST and vegetation index measurements, atmospheric and near-surface humidity, vapor pressure deficit, and various precipitation indexes. For example, Rogers (2000) found a good correlation between the satellites derived index of LST and monthly mortality rates and used the index as input for tsetse population models for the Yankari Game

Reserve (Nigeria) and in Gambia. A detailed review of satellite-derived variables and their use in public health is given by Hay (2000) and Goetz et al. (2000).

More complex methods involve using statistical models that relate various components of the transmission of parasites to satellite data for the description, explanation and prediction of vector-borne diseases. Remote sensing data are used as inputs to drive (i) spatial models of transmission risk (Danson et al. 2006), (ii) hydrological models that aim to describe or predict disease transmission in catchment basins (Spear et al. 1998), and (iii) climate based parasite forecast models that reveal hotspots of disease occurrences and predict the risk area and intensity of diseases (Zhou et al. 1998, 1999).

Epidemiological studies have taken advantage of the steady improvement of satellite sensors. In some instances, investigators used aerial color-infrared photography (Welch et al. 1989); however, passive satellite sensor data have been used most commonly for epidemiological studies (Rogers et al. 2002): Landsat MSS (Barnes and Cibula 1979); AVHRR (Baylis et al. 1999; Brooker et al. 2002; Estrada-Peña and Venzal 2006; Mendelsohn and Dawson 2008); Landsat TM (Pope et al. 1992; Hugh-Jones et al. 1992; Brown et al. 2008); Landsat ETM (Brooker et al. 2004; Goossens et al. 2006); ASTER (Tatem et al. 2004); MODIS (Raso et al. 2006; Gilbert et al. 2007); METEOSAT (Hay et al. 1998; Hay et al. 2006); SPOT (Tran et al. 2002; De La Rocque et al. 2004); IKONOS (Mushinzimana et al. 2006); QuickBird (Ratana et al. 2005). While earth observing satellites have a higher spatial resolution (e.g. 1–4 m for IKONOS, 60–70 cm for panchromatic, 2–4 m and 2–8 m for multispectral QuickBird; 10–20 m for SPOT), meteorological satellites, despite their lower resolution, have the major advantage of a high temporal resolution (two images are collected every day by AVHRR and one image every 30 min by the geostationary satellite, Meteosat). Recent studies have focused on the use of active remote sensing for epidemiology applications. Kaya et al. (2004) used RADARSAT-1 and RADARSAT 2 for vector-borne disease risk mapping.

Remote sensing methods have been employed for a wide range of diseases over various regions worldwide: e.g. Dengue fever in Argentina (Carbajo et al. 2001; Rotela et al. 2007); onchocerciasis in West and Central Africa (Thomson et al. 2000); Rift Valley fever in Kenya (Linthicum et al. 1987), Yemen (Abdo-Salem et al. 2006), Senegal (Lacaux et al. 2007); schistosomiasis in Africa (Brooker 2007) and China (Zhou et al. 1998; Guo et al. 2005); cholera in Bangladesh (Lobitz et al. 2000); tick-borne encephalitis in the Baltic States (Šumilo et al. 2006); visceral leishmaniasis in Sudan (Elnaiem et al. 1998) in India (Sudhakar et al. 2006) and in Southwestern Asia (Cross et al. 1996); human trypanosomiasis in Africa (Rogers and Randolph 1994; Rogers et al. 1996; Kitron et al. 1996; Rogers 2000); helminth infections in Cameroun (Brooker et al. 2002); human tick-borne encephalitis infection in the Czech Republic (Daniel et al. 2006); lyme disease in Wisconsin (Kitron and Kazmierczak 1997). A massive body of remote sensing-based studies focus on malaria in various parts of the world, including the Western Kenyan highlands (Mushinzimana et al. 2006), Mexico (Beck et al. 1997), Southern France (Tran et al. 2008), China (Liu and Chen 2006); Belize (Achee et al. 2006); Philippines (Leonardo et al. 2005); India (Srivatsava et al. 2001); Bangladesh (Rahman et al.

2006); Indochina Peninsula (Nihei et al. 2002); continental Africa (Rogers et al. 2002) and Korea (Ratana et al. 2005).

Remote sensing applications for modeling and forecasting vector-borne diseases are still an emerging field, but epidemiologists and biologists benefit from increasing satellite coverage, a growing number of higher resolution sensors and the development of hyperspectral imagery, combined with GIS and statistical software packages that are available within an affordable desktop computing environment (Kalluri et al. 2007). However, besides these opportunities, epidemiologists face challenges: Disease patterns are closely linked to poverty and social inequalities, which cannot be inferred from remote sensing techniques alone. In addition, population growth and climate change make the dynamics of disease spread more complex. In order to develop accurate disease early-warning systems, it is necessary to find an efficient way of incorporating the social component, to better understand transmission dynamics (Rogers et al. 2002) and to implement an automation of satellite data processing, so that remotely sensed environmental variables will be processed and made available to epidemiologists in near-real-time. This will ensure the generation of vital information relevant to potential disease outbreaks and transmission (e.g. near-real-time risk maps), thus enabling the initiation of rapid response strategies.

11.4 Cytometry for Life (C4L)

Vector-borne disease mitigation is not the only public health beneficiary of space-based technologies, as evidenced by an initiative of the Purdue University Cytometry Laboratory (PUCL), specifically Cytometry for Life (C4L), under the leadership of Dr. J. Paul Robinson, Director, PUCL and Gary Gurack of i-Cyt, Inc. The C4L initiative centers on the need for affordable, reliable, and manageable CD4 T-lymphocyte cell testing in Africa. The aim for the C4L initiative is to create a low cost, low maintenance, portable CD4 Counter that will test, and only test, the amount of CD4 T-lymphocyte cells in humans efficiently and accurately. Many of the flow cytometers that are currently in use are large, expensive, require trained technicians and numerous resources to operate and maintain them. The components used to effectively accommodate bulky cytometers are scarce in most of Africa, which translates into the majority of the HIV/AIDS infected population not receiving critical testing that would result in antiretroviral treatment that would be life-prolonging (Willyard 2007; Robinson et al. 2007).

The current model for CD4 testing in Africa for the past 7–8 years is to create central labs that house expensive, mostly automated equipment, and train technicians to operate the machines and its complex software. Samples are taken from all over Africa to be tested in central labs and then sent back to the remote areas from which the samples came. The patient must therefore spend a great deal of time waiting, due to the lengthy process of receiving the results. This model is based on the philosophy of Western health care systems, which rely on heavy infrastructure

and centralized networks; only the main populated sites in Africa can assimilate this model. The downfalls of using the centralized model is that it forces the people in the rural parts of Africa to travel from their homes to the central labs to receive testing, which make thereby making CD4 testing exclusive to large cites and areas that support the infrastructure. Also, since CD4 testing is high in demand, the central lab systems become overloaded, due to frequent testing, therefore creating a need for more system automation (Willyard 2007; Robinson et al. 2007).

The low cost, low maintenance, portable CD4 counter with full optical and fluidic assembly will be housed in a high impact plastic, contain powerful electronic components that are user friendly, and will need no computer attachments or additional software and/or interfaces. The CD4 counter will also include GPS capabilities, cell phone based data transmission, battery operation, CD4 T-cell single line readout, and a gravity-feed low-volume sheath fluid system. These features will allow the CD4 counter to become very robust and durable, thus having the capability to adapt to any situation that may present itself in Africa. With the addition of GPS, other than the ability to track the portable devices, the CD4 Counter will have the ability to transmit epidemiological data; this feature can provide vital information on the geographical regions of Africa with higher incidence of HIV/AIDS and of antiretroviral resistant strains of HIV/AIDS and facilitating prompt and accurate decisions with respect to HIV therapy distribution to highly infected areas (Willyard 2007).

11.5 Modeling for Epidemics, Biogenic and Anthropogenic Disasters

Modeling tools that have been developed to facilitate projections of the impact of epidemics, storms, flooding, oil/chemical spills, earthquakes and fires have a long history. Thomson et al. (2006) evaluated the utility of environmental models, incorporating Normalized Difference Vegetation Index (NDVI) and Cold Cloud Duration (CCD) for prediction of meningitis epidemics in Africa. Early integrated model entrants included the Federal Emergency Management Agency's (FEMA) Integrated Emergency Management Information System (IEMIS) for a wide array of disasters (e.g. conflagration, storms, gaseous effluent release, spills), FEMA's HAZUS-MH (Multi-Hazard) modeling tool for flooding, hurricanes and earthquakes (Porter and Eeri 2009; Scawthorn et al. 2006; Tralli, et al. 2007; Vickery and Lin 2006; Vickery and Skerlj 2006), as well as ALOHA, CAMEO and MARPLOT, for emergency response to oil and hazardous chemical spills, utilized by the United States Coast Guard (USCG), the US Environmental Protection Agency (EPA) and the National Oceanic and Atmospheric Agency (NOAA). (http://www.epa.gov/emergencies/content/cameo/what.htm) Two such specific modeling tools are briefly discussed in the following:

11.6 Spatio-Temporal Epidemiological Modeler (STEM)

The public domain Spatiotemporal Epidemiological Modeler (STEM) tool, initially released by IBM, is designed to help scientists and public health officials create and use spatial and temporal models of emerging infectious diseases. These models could aid in understanding and potentially preventing the spread of such diseases. Policymakers responsible for creating strategies to contain diseases and prevent epidemics need an accurate understanding of disease dynamics and the likely outcomes of preventive actions. In an increasingly connected world with extremely efficient global transportation links, the modes of infection can become quite complex. STEM facilitates the development of advanced mathematical models, the creation of flexible models involving multiple populations (species) and interactions between diseases, and a better understanding of epidemiology.

The STEM application has built-in Geographical Information System (GIS) data for almost every country in the world. It comes with data about country borders, populations, shared borders (neighbors), interstate highways, state highways, and airports. These data come from various public sources. STEM is designed to make it easy for developers and researchers to plug in their own models.

It comes with spatiotemporal Susceptible/Infectious/Recovered (SIR) and Susceptible/Exposed/Infectious/Recovered (SEIR) models pre-coded with both deterministic and stochastic engines. The parameters in any model are specified in XML configuration files. Users can easily change the weight or significance of various disease vectors (such as the weights of highways, shared borders, airports, etc.). Users can also create their own unique vectors for disease. Further details are available in the user manual and design documentation. Download and installation information is provided at the STEM Eclipse Setup webpage (http://wiki.eclipse.org/index.php/STEM_Eclipse_Setup). Once STEM is installed on the computer, a sample scenario gives more information about how diseases are modeled in STEM (http://wiki.eclipse.org/Creating_a_STEM_Scenario).

11.7 Hydrologic Engineering Center River Analysis System (HEC-RAS)

Hydrologic Engineering Center River Analysis System (HEC-RAS) is a river hydraulic tool created by the U.S. Army Corps of Engineers (USACE) in 1994. HEC-RAS is a next generation (NextGen) hydraulic successor of the HEC-2 water surface program. The model can be linked to a geographic information system (GIS), thereby greatly facilitating the prediction and monitoring of flooding through visual and spatial analysis.

HEC-RAS is a one-dimensional, steady flow, water surface profiling program (U.S. Army Corps of Engineers 2002); it is capable of modeling a full network of channels, a dendritic system, or a single river reach. HEC-RAS requires the input of geometric data in order to plot water surface profiles for subcritical, critical, and

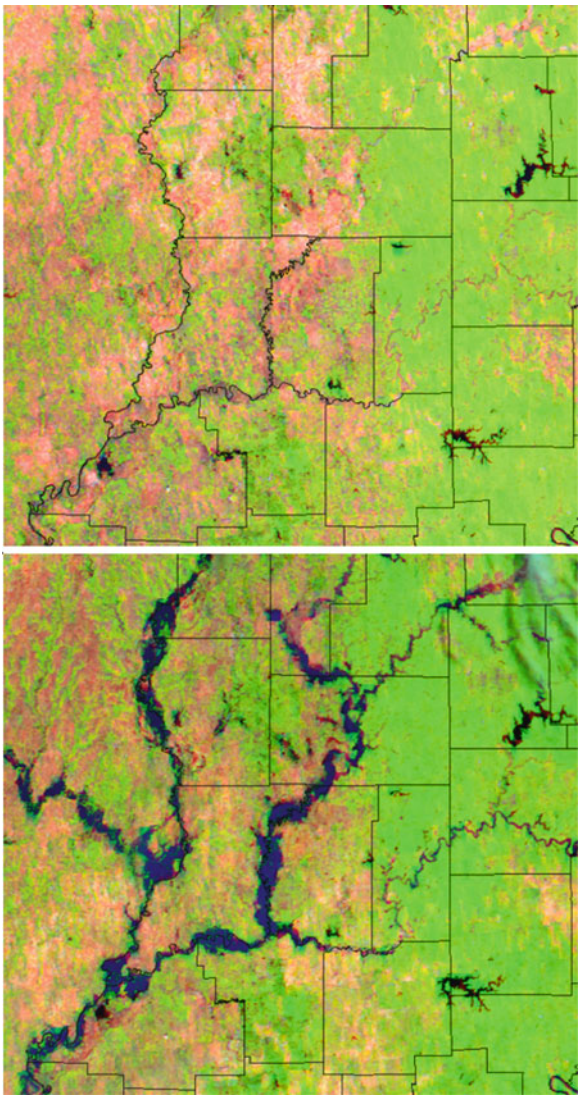

Fig. 11.1 (**a**) May 28, 2008–before Indiana flood and (**b**) June 11, 2008 –after Indiana flood (Larry Biehl, Systems Manager, PTO-Purdue)

supercritical steady flows in channels of any cross-sectional configuration (McLin et al. 2001). The geometric data needed are built with the Hydrographic Modeling System (HEC-HMS), also developed by USACE; the parameters are cross-sections, left and right banks of the river. HEC-HMS output data are combined with a digital elevation model (DEM) and river network to simulate the inundation basin. The result from hydraulic analysis can be displayed in the GIS to show the floodplain extent and evaluate flood depth (Knebl et al. 2005).

Flooding is one of the costliest and most destructive natural disasters. In order to minimize the impact, an optimal predictive model is critical. The HEC-RAS model has been successfully applied to predict the extent of flooding in the United States and Europe. The immediate destruction of properties and human casualties are the more noticeable consequences of catastrophic flooding; but flood events can also have long-lasting consequences. After catastrophic flooding, outbreaks of water borne diseases (e.g. cholera, typhoid fever), water-based diseases (e.g. schistosomiasis, Guinea worm), water-related vector-borne diseases (e.g. malaria, Dengue fever, lymphatic filariasis, trypanosomiasis, leismaniasis, onchocerciasis) may occur because the flood plain facilitates intensified breeding for the disease vectors associated with malaria (*Anopheles gambiae), with Dengue fever (Aedes aegypti & A. albopictus), with lymphatic filiariasis (i.e. Culex quinquefaciatus, Anopheles funestus, An. gambiae, Aedes scapularis, Ae. pseudoscutellaris, Ae. ploynesiensis, etc.), with trypanosomiasis (Glossina morsitans), with leishmaniasis (Phlebotomus paptasi & P. duboschi)* and with onchocerciasis (*Semulium damnosum)*. HEC-RAS can potentially be used as a powerful tool in public health in the prediction of future epidemics, particularly in combination with remote sensing and in situ monitoring (Manguin and Boussinesq 1999).

Researchers at Purdue University-West Lafayette and the Polis Center of Indiana University/Purdue University at Indianapolis (IUPUI), together with other academic partners participated in a FEMA initiative for 100 year flood modeling for 2000 counties in the USA, utilizing FEMA's HAZUS-MH modeling software. The Purdue Terrestrial Observatory also deployed remotely sensed data from NASA's Moderate Resolution Imaging Spectroradiometer (MODIS) Channels 6, 2 & 1, to acquire before and after images of the June 6–7, 2008 flood after a rainfall of 7–11 inches ravaged the Southern Indiana (Fig. 11.1).

11.8 Climate Change and Public Health

Space-based technologies are not solely limited in their applicability to immediate quotidien emergencies. They have been applied, as well, to longer term potentially disastrous events, such as climate change (Patz et al. 2005). The application of satellite data to climate change research is despite the fact that climatic perturbations occur over time scales that long predate the advent of the earliest earth observing satellites. Data from the military spy satellites, CORONA, LANYARD and ARGON, launched during the presidency of Dwight David Eisenhower and declassified in 1995 by President William Jefferson Clinton, now offer the earliest known earth observing data from orbital platforms for the period 1960–1972, with 6–8 ft. spatial resolution. Tappan, et al. (2000) deployed declassified data from two of these satellites, in addition to Landsat data, for change detection in land resources over a 30 year period in West-Central Senegal.

In contrast, long-term global climate change trends have been observed through more traditional methodologies, such as dendrochronology, polar ice coring and

limnology. Tree ring analysis methods, including dendrochronology and dendrochemistry, provide records up to the age of the oldest known tree, Bristlecone pine (*Pinus longaeva)*, dated to be over 4,700 years old (Flanary and Kletetschka 2005) and both pollen analysis and macrofossil analysis of Norway spruce (*Picea abies*), found in Sweden, provide data exceeding 8,000 years (Segerström and von Stedingk 2003). Petit et al. in their article published in Nature (1999) traced 420,000 years of climatic and atmospheric history from the Vostok ice core in Eastern Antarctica. Limnology cores from Lake Baikal in Eastern Siberia have recorded long-term climate cycles over the past 12 million years (Kashiwaya et al. 2001).

Nonetheless, given events such as a rapid escalation in polar ice melts and 40 years of multispectral data collected from NOAA's Advanced Very High Resolution Radiometer (AVHRR) and Landsat, specific applications of remote sensing have proven to have utility for contributing to climatology. As a case in point, (Green and Hay 2002) evaluated data from NOAA's AVHRR as a source for "surrogate climatic variables across Africa and Europe for epidemiological applications."

The Intergovernmental Panel on Climate Change (IPCC 2007) asserts, "Human beings are exposed to climate change through changing weather patterns (for example, more intense and frequent extreme events) and indirectly through changes in water, air, food quality and quantity, ecosystems, agriculture, and economy. At this early stage the effects are small but are projected to progressively increase in all countries and regions". Moreover, according to the World Health Organization, "Changes in climate are likely to lengthen the transmission seasons of important vector-borne diseases, and to alter their geographic range, potentially bringing them to regions that lack population immunity and/or a strong public health infrastructure" (WHO 2007). IPCC (2007) projects that the global population at risk from vector-borne malaria will increase within a range of 220 million to 400 million, in the next century. Most of the increase is predicted to occur in Africa; but Britain, Australia and Portugal are expected to experience some increased risk.

Climate change as a result of both natural and anthropogenic activities could result in environmental dynamics and conditions favorable to the outbreak and spread of chronic diseases. Climate change conditions, such as severe heat waves, flooding, drought and extreme weather events (Ebi 2007; Hajat and Kosatsky 2009), have direct impact on agriculture, water resources, air pollution (Chauhan and Johnston 2003) and the environment (e.g. coastal zones, forest and biodiversity). Adverse health effects include loss of life, respiratory illness (e.g. allergies, asthma, and lung cancer) from air pollution, the spread of vector borne diseases, as well as hunger related diseases, due to the loss of agricultural productivity (Patz et al. 2000). Most waterborne and airborne disease parasites require specific range of meteorological conditions, with respect to temperature, precipitation and relative humidity in order to thrive in breeding and transmission. Climate change enables extreme variability that may intensify breeding habitat and the outbreak of vector borne diseases (Anyamba et al. 2001).

To understand and quantify the potential impact of climate change on public health, health risk assessment models, incorporating climate change related remote sensing products, experimental field data and ranges of climatic and socioeconomic

scenarios are used to simulate adverse health implications, with respect to trends, timing, intensity, regional vulnerability and specific population groups at risk (Casimiro et al. 2006). Regional climate change impact models such as PROMES, developed at the Universidad Complutense de Madrid (Gallardo et al. 2001) and HadRM2, developed at the Hadley Centre in the United Kingdom (Jones et al. 1997), have been used to simulate potential future air pollution levels (e.g. nitrogen dioxide and tropospheric ozone), as well as vector borne diseases and transmission risk assessments. Health models integrated with hydrologic and agricultural models also allow the simulation of climate change impacts, relating drought and agriculture to public health (Ebi 2007).

11.9 Conclusion and Recommendations

The exact impacts of climate change on public health are not completely known; however based on recorded mortality and morbidity from injuries and diseases, according to some model projections, millions of people will be at increased future risk (McMichael et al. 2004). While regional climate change models may contribute to understanding potential health risk factors at regional scales, such models offer only limited benefit for localized analysis. There is the need for more research with localized (small scale) models to optimize climate change impact predictions for localized areas, so as to enable enhanced mitigation measures. Advances in remote sensing technologies are likely to improve monitoring of climatic conditions, epidemiological modeling and the understanding of the quantitative and qualitative impacts of climate change on public health, as well as on biogenic and anthropogenic disaster mitigation; however greater disaggregation of data collection and dissemination, particularly by multi-lateral agencies, is imperative in order to capture the site-specific nuances required for climate change mitigation and adaptation.

The prudent intergenerational management of natural resources and ecosystem services that are prerequisite to achieving environmental sustainability, particularly in countries with substantially impoverished populations, will certainly require more than technological advances in satellite remote sensing, geopositioning constellations, enhanced spatial data infrastructure, telecommunications and high performance computing (Rochon et al. 2004). (Ahmed et al. 2009) in an August 20, 2009 article in *Environmental Research Letters* presented their findings, based on a review of thirteen countries, indicating that one impact of volatile climate changes in developing countries is an increase vulnerability to poverty. The poor are likewise more vulnerable to malnutrition, infection and natural disasters. Consequently, best management practices (BMPs) that focus exclusively upon technological advance or technology transfer from bi-lateral or multi-lateral donors without provision of adequate safeguards for the wellbeing and ultimate prosperity of the lowest socio-economic strata are unlikely to be efficacious (Herbreteau et al. 2007; Rochon et al. 2010; Rochon 2009). Poverty eradication is a fundamental and ineluctable objective

in the struggle to achieve and maintain sustainable development and environmental sustainability. The major challenge transcending the complexities of technological innovation is the task of innovatively and optimally utilizing such space-based and computational technologies in the service of sustainably improving the lives, the health and wellbeing the people most in need of poverty alleviation.

In sharp contrast to the proliferation of weapons of mass destruction, the proliferation of earth observing satellites is an extremely beneficial and promising development. Enabled by such technologies, developing countries are enhancing their capabilities with respect to environmental sustainability, meteorological forecasting, crop forecasting, famine & drought early warning, urban planning, transportation planning, sustainable natural resource management, quantification of biodiversity loss, disaster mitigation, mapping vulnerability to epidemics and epizootics and delineation of populations at risk for further impoverishment.

In the aftermath of officially declared biogenic and anthropogenic disasters, the global near-real-time archive of satellite data assets is potentially available to affected regions. This *ex post facto* response, however, while laudable is quite insufficient. What is needed is a global spatial data infrastructure that would facilitate the free access of earth observational data throughout the life cycle of disasters (i.e. from vulnerability assessment and early warning through emergency response and post disaster recovery) and the enhancement of indigenous academic institutions so as to provide state-of-the science training for the next generation of geospatial scientists and technicians.

Moreover, the empowerment of people to elect leaders who are committed to sustainable development and environmental sustainability is even more crucial than advances in geotechnologies; since, in the absence of such committed political leadership, optimal technological deployment and associated environmentally enlightened policy formulation and implementation cannot occur.

Acknowledgments The authors wish to acknowledge support from AmericaView, Inc., NATO Science for Peace Program, and Purdue University's Information Technology at Purdue (ITaP) – Rosen Center for Advanced Computing.

References

Abdo-Salem S, Gerbier G, Bonnet P, Al-Qadasi M, Tran A, Al-Eryni G, Roger F (2006) Descriptive and spatial epidemiology of Rift Valley fever outbreak in Yemen 2000–2001. Ann NY Acad Sci 1081:240–242

Achee NL, Grieco JP, Penny M, Richard AG, Donald RR, James T, Ireneo B, Russell K, Eliska R (2006) Use of remote sensing and geographic information systems to predict locations of Anopheles darlingi-positive breeding sites within the Sibun River in Belize, Central America. J Med Entomol 43(2):382–392

Ahmed SA, Diffenbaugh NS, Hertel TW (2009) Climate volatility deepens poverty vulnerability in developing countries. Environ Res Lett 4(3):004.1–8. doi:10.1088/1748-9326/4/3/034004.8 pp

Anyamba A, Linthicum KJ, Tucker CJ (2001) Climate-disease connections: Rift Valley fever in Kenya. Cadernos Saude Publ 17:133–140

Barnes C, Cibula W (1979) Some implications of remote sensing technology in insect control programs including mosquitoes. Mosq News 39:271–282

Baylis M, Meiswinkel R, Venter GJ (1999) A preliminary attempt to use climate data and satellite imagery to model the abundance and distribution of Culicoides imicola (Diptera: Ceratopogonidae) in Southern Africa. Tydskr South Afr Vet Ver 70(2):80–89

Beck LR, Lobitz BM, Wood BL (2000) Remote sensing and human health: new sensors and new opportunities. Emerg Infect Dis 6:217–226

Beck LR, Rodriguez MH, Dister SW, Rodriguez AD, Washino RK, Roberts DR, Spanner MA (1997) Assessment of a remote sensing-based model for predicting malaria transmission risk in villages of Chiapas, Mexico. Am J Trop Med Hyg 56(1):99–106

Boone JD, McGwire KC, Otteson EW, DeBaca RS, Kuhn EA, Villard P, Brussard PF, St. Jeor SC (2000) Remote sensing and geographic information systems: Charting Sin Nombre Virus infections in deer mice. Emerg Infect Dis 6:248–258

Brooker S (2007) Spatial epidemiology of human schistosomiasis in Africa: risk models, transmission dynamics and control. Trans R Soc Trop Med Hyg 101(1):1–8

Brooker S, Hay SI, Tchuenté LT, Ratard R (2002) Using NOAA-AVHRR data to model human helminth distributions in planning disease control in Cameroon, West Africa. Photogramm Eng Remote Sens 68(2):175–179

Brooker S, Clarke S, Njagi JK, Polack S, Mugo B, Estambale B, Muchiri E, Magnussen P, Cox J (2004) Spatial clustering of malaria and associated risk factors during an epidemic in a highland area of western Kenya. Trop Med Int Health 9(7):757–766

Brown HE, Diuk-Wasser MA, Guan Y, Caskey S, Fish D (2008) Comparison of three satellite sensors at three spatial scales to predict larval mosquito presence in Connecticut wetlands. Remote Sens Environ 12(5):2301–2308

Carbajo AE, Schweigmann N, Curto SI, de Garin A, Bejarán R (2001) Dengue transmission risk maps of Argentina. Trop Med Int Health 6:170–183

Casimiro E, Calheiros J, Santos FD, Kovats S (2006) National assessment of human health effects of climate change in Portugal: approach and key findings. Environ Health Perspect 114(12):1950–1956

Chauhan AJ, Johnston SL (2003) Air Pollution and Infection in Respiratory Illness. Br Med Bull 68:95–112

Cross ER, Newcomb WW, Tucker CJ (1996) Use of weather data and remote sensing to predict the seasonal distribution of Phlebotomus papatasi in southwestern Asia. Am J Trop Med Hyg 54:530–536

Cuevas LE, Jeanne I, Molesworth A, Bell M, Savory EC et al (2007) Risk mapping and early warning systems for the control of meningitis in Africa. Vaccine 25:A12–A17

Daniel M, Zitek K, Danielová V, Kríz B, Valter J, Kott I (2006) Risk assessment and prediction of Ixodes ricinus tick questing activity and human tick-borne encephalitis infection in space and time in the Czech Republic. Int J Med Microbiol 296(1):41–47

Danson FM, Giraudoux P, Craig PS (2006) Spatial modeling and ecology of Echinococcus multilocularis transmission in China. Parasitol Int 55(1):S227–S231

De La Rocque S, Michel V, Plazaneta D, Pinc R (2004) Remote sensing and epidemiology: examples of applications for two vector-borne diseases. Comp Immunol Microbiol Infect Dis 27(5):331–341

Ebi KL (2007) Using health models to prepare for and cope with climate change. Clim Change 88(1):1–3

Elnaiem DA, Connor SJ, Thomson MC, Hassan MM, Hassan HK, Aboud MA, Ashford RW (1998) Environmental determinants of the distribution of Phlebotomus orientalis in Sudan. Ann Trop Med Parasitol 92(8):877–887

Estrada-Peña A, Venzal JM (2006) High-resolution predictive mapping for Boophilus annulatus and B. microplus (Acari: ixodidae) in Mexico and Southern Texas. Vet Parasitol 142(3–4):350–358

Flanary BE, Kletetschka G (2005) Analysis of telomere length and telomerase activity in tree species of various life-spans, and with age in the bristlecone pine Pinus longaeva. Biogerontol 6(2):101–111

Gallardo C, Arribas A, Prego JA, Gaertner MA, de Castro M (2001) Multi-year simulations using a regional-climate model over the Iberian Peninsula: current climate and double CO_2 scenario. Quat J R Meteorol Soc 127:1659–1681

Gilbert M, Xiao X, Chaitaweesub P, Kalpravidh W, Premashthira S, Boles S, Slingenbergh J (2007) Avian influenza, domestic ducks and rice agriculture in Thailand. Agric Ecosyst Environ 119:409–415

Goetz S, Prince S, Small J (2000) Advances in satellite remote sensing of environmental variables for epidemiological applications. Adv Parasitol 47:289–307

Goossens B, Mbwambo H, Msangi A, Geysen D, Vreysen M (2006) Trypanosomosis prevalence in cattle on Mafia Island (Tanzania). Vet Parasitol 139:74–83

Graham AJ, Atkinson PM, Danson FM (2004) Spatial analysis for epidemiology. Acta Trop 91(3):219–225

Green RM, Hay SI (2002) The potential of pathfinder AVHRR data for providing surrogate climatic variables across Africa and Europe for epidemiological applications. Remote Sens Environ 79(2–3):166–175

Guo J, Vounatsou P, Cao C, Jürg U, Zhu H, Daniel A, Zhu R, He Z, Li D, Hu F, Chen M, Marcel T (2005) A geographic information and remote sensing based model for prediction of Oncomelania hupensis habitats in the Poyang Lake area, China. Acta Trop 96(2–3):213–222

Hajat S, Kosatsky T (2009) Heat-related mortality: a review and exploration of heterogeneity. J Epidemiol Community Health. doi:10.1136/jech.2009.087999 (Accepted for publication). Available as Online First article: http://jech.bmj.com/content/early/2009/09/01/jech.2009.087999.abstract

Hay SI, Tatem AJ, Graham AJ, Goetz SJ, Rogers DJ (2006) Global environmental data for mapping infectious disease distribution. Adv Parasitol 62:37–77

Hay SI, Snow RW, Rogers DJ (1998) Prediction of malaria seasons in Kenya using multi-temporal meteorological satellite sensor data. Trans R Soc Trop Med Hyg 92:12–20

Hay SI (2000) An overview of remote sensing and geodesy for epidemiology and public health application. Adv Parasitol 47:1–35

Hay SI, Randolph SE, Rogers DJ (2000) Remote sensing and geographical information systems in epidemiology. Academic, London

Herbreteau V, Salem G, Souris M, Hugot JP, Gonzalez JP (2007) Thirty years of use and improvement of remote sensing applied to epidemiology: from early promises to lasting frustration. Health Place 13:400–403

Hugh-Jones M (1989) Applications of remote sensing to the identification of the habitats of parasites and disease vectors. Parasitol Today 5(8):244–251

Hugh-Jones M, Barre N, Nelson G, Wehnes K, Warner J, Garvin J, Garris G (1992) Landsat-TM identification of Amblyomma variegatum (Acari: Ixodidae) habitats in Guadeloupe. Remote Sens Environ 40:43–55

Intergovernmental Panel on Climate Change (IPCC) (2007) Climate change 2007: impacts, adaptation, and vulnerability. Cambridge University Press, Cambridge

Jones RG, Murphy JM, Noguer M, Keen AB (1997) Simulation of climate change over Europe using a nested regional-climate model. II: comparison of driving and regional model responses to a doubling of carbon dioxide. Quat J R Meteorol Soc 123:265–292

Jovanovic P (1987) Remote sensing of environmental factors affecting health. Adv Space Res 7(3):11–18

Kalluri S, Gilruth P, Rogers D, Szczur M (2007) Surveillance of arthropod vector-borne infectious diseases using remote sensing techniques: a review. PLoS Pathog 3(10):1361–1371

Kashiwaya K, Ochiai S, Sakai H, Kawai T (2001) Orbit-related long-term climate cycles revealed in a 12-Myr continental record from Lake Baikal. Nat 410:71–74

Kaya S, Sokol J, Pultz TJ (2004) Monitoring environmental indicators of vector-borne disease from space: a new opportunity for RADARSAT 2. Can J Remote Sens 30:560–565

Kitron U, Kazmierczak JJ (1997) Spatial analysis of the distribution of Lyme disease in Wisconsin. Am J Epidemiol 145:558–566

Kitron U, Otieno LH, Hungerford LL, Odulaja A, Brigham WU, Okello OO, Joselyn M, Mohamed-Ahmed MM, Cook E (1996) Spatial analysis of the distribution of tsetse flies in the Lambwe Valley, using Landsat TM satellite imagery and GIS. J Anim Ecol 65(3): 371–380

Knebl MR, Yang ZL, Hutchinson K, Maidment DR (2005) Regional scale flood modeling using NEXRAD rainfall, GIS, and HEC-HMS/RAS: a case study for the San Antonio River Basin Summer 2002 storm event. J Environ Manag 75(4):325–336

Lacaux JP, Tourre YM, Vignolles C, Ndione JA, Lafaye M (2007) Classification of ponds from high-spatial resolution remote sensing: application to Rift Valley fever epidemics in Senegal. Remote Sens Environ 106(1):66–74

Leblond A, Sandoz A, Lefebvre G, Zeller H, Bicout DJ (2007) Remote sensing based identification of environmental risk factors associated with West Nile disease in horses in Camargue, France. Prev Vet Med 79(1):20–31

Leonardo LR, Rivera PT, Crisostomo BA, Sarol JN, Bantayan NC, Tiu WU, Bergquist NR (2005) A study of the environmental determinants of malaria and schistosomiasis in the Philippines using Remote Sensing and Geographic Information Systems. Parassitologia 47(1):105–114

Linthicum KJ, Bailey CL, Davies FG, Tucker CJ (1987) Detection of Rift Valley fever viral activity in Kenya by satellite remote sensing imagery. Sci 235(4796):1656–1659

Liu J, Chen X (2006) Relationship of remote sensing normalized differential vegetation index to Anopheles density and malaria incidence rate. Biomed Environ Sci 19(2):130–132

Lobitz B, Beck L, Huq A, Wood B, Fuchs G, Faruque AS, Colwell R (2000) Climate and infectious disease: use of remote sensing for detection of Vibrio cholerae by indirect measurement. Proc Natl Acad Sci USA 97(4):1438–1443

Malone JB, Yilma JM, McCarroll JC, Erko B, Mukaratirwa S, Zhou X (2001) Satellite climatology and the environmental risk of Schistosoma mansoni in Ethiopia and East Africa. Acta Trop 79:59–72

Manguin S, Boussinesq M (1999) Remote sensing in public health: applications to malaria and other diseases. Med Mal Infect 29(5):318–324

McLin SG, Springer EP, Lane LJ (2001) Predicting floodplain boundary changes following the Cerro Grande wildfire. Hydrological Processes 15(15):2967–2980

McMichael AJ, Campbell-Lendrum D, Kovats S, Edwards S, Wilkinson P, Wilson T, Nicholls R, Hales S, Tanser F, LeSueur D, Schlesinger M, Andronova N (2004) Global climate change. In: Ezzati M, Lopez A, Rodgers A, Murray C (eds) Comparative quantification of health risks: global and regional burden of disease due to selected major risk factors. World Health Organization, Geneva

Mendelsohn J, Dawson T (2008) Climate and cholera in KwaZulu-Natal, South Africa: The role of environmental factors and implications for epidemic preparedness. Int J Hyg Environ Health 211(1–2):156–162

Mushinzimana E, Munga S, Minakawa N, Li L, Feng C, Bian L, Kitron U, Schmidt C, Beck L, Zhou G, Githeko AK, Yan G (2006) Landscape determinants and remote sensing of anopheline mosquito larval habitats in the western Kenya highlands. Malar J 5:13

Nihei N, Hashida Y, Kobayashi M, Ishii A (2002) Analysis of malaria endemic areas on the Indochina Peninsula using remote sensing. Jpn J Infect Dis 55(5):160–166

Odiit M, Bessell PR, Fèvre EM, Robinson T, Kinoti J, Coleman PG, Welburn SC, McDermott J, Woolhouse ME (2005) Using remote sensing and geographic information systems to identify villages at high risk for rhodesiense sleeping sickness in Uganda. Trans R Soc Trop Med Hyg 100(4):354–362

Patz JA, McGeehin MA, Bernard SM, Ebi KL, Epstein PR, Grambsch A, Gubler DJ, Reiter P, Romieu I, Rose JB, Samet JM, Trtanf J (2000) The potential health impacts of climate variability and change for the United States: executive summary of the report of the health sector of the U.S. national assessment. Environ Health Perspect 108(4):367–376

Patz JA, Campbell-Lendrum D, Holloway T, Foley JA (2005) Impact of regional climate change on human health. Nat 438(17):310–317

Pavlin JA, Mostashari F, Kortepeter MG, Hynes NA, Chotani RA, Mikol YB, Ryan MAK, Neville JS, Gantz DT, Writer JV, Florance JE, Culpepper RC, Henretig RM, Kelley PW

(2003) Innovative surveillance methods for rapid detection of disease outbreaks and bioterrorism: results of an interagency workshop on health indicator surveillance. Am J Public Health 93(8):1230–1235

Peterson AT, Martínez-Campos C, Nakazawa Y, Martínez-Meyer E (2005) Time-specific ecological niche modeling predicts spatial dynamics of vector insects and human dengue cases. Trans R Soc Trop Med Hyg 99(9):647–655

Petit JR, Jouzel J, Raynaud D, Barkov NI, Barnola J, Basile I, Bender M, Chappellaz J, Davisk M, Delaygue G, Delmotte M, Kotlyakov VM, Legrand M, Lipenkov VY, Lorius C, Pépin L, Ritz C, Saltzmank E, Stievenard M (1999) Climate and atmospheric history of the past 420,000 years from the Vostok ice core, Antarctica. Nat 399(3):429–436

Pope KO, Sheffner EJ, Linthicum KJ, Bailey CL, Logan TM, Kasischke ES, Birney K, Njogu AR, Roberts CR (1992) Identification of central Kenyan Rift Valley fever virus vector habitats with Landsat TM and evaluation of their flooding status with airborne imaging radar. Remote Sens Environ 40:185–196

Porter K, Eeri M (2009) Cracking an open safe: HAZUS vulnerability functions in terms of structure-independent spectral acceleration. Earthq Spectra 25(2):361–378

Rahman A, Kogan F, Roytman L (2006) Short report: Analysis of malaria cases in Bangladesh with remote sensing data. Am J Trop Med Hyg 74(1):17–19

Randolph SE (2000) Ticks and tick-borne disease systems in space and from space. Adv Parasitol 47:217–243

Raso G, Vounatsou P, Singer BH, N'Goran EK, Tanner M, Utzinger J (2006) An integrated approach for risk profiling and spatial prediction of Schistosoma mansoni–hookworm coinfection. Proc Natl Acad Sci USA 103(18):6934–6939

Ratana S, Lee WJ, Ugsang DM, Linthicum KJ (2005) Identification and characterization of larval and adult anopheline mosquito habitats in the Republic of Korea: potential use of remotely sensed data to estimate mosquito distributions. Int J Health Geogr 4(17)

Rejmankova E, Roberts DR, Pawley A, Manguin S, Polanco J (1995) Predictions of adult Anopheles albimanus densities in villages based on distances to remotely-sensed larval habitats. Am J Trop Med Hyg 53:482–488

Robinson JP, Rochon HS, Rochon GL (2007) Cytometry for life (C4L) CD4 diagnostic device for HIV/AIDS. Co-sponsors: Purdue University Cytometry Laboratories, ICYT, Parker Life Sciences, Wealthy Consults and convoy of Hope International. Transcorp Hilton Hotel, Abuja, Nigeria, 14 March 2007

Rochon GL (2009) Space-based technologies and high performance computing in support of environmental sustainability in developing countries. Clean Technol Environ Policy 11(3): 251–252

Rochon GL, Niyogi D, Fall S, Quansah JE, Biehl L, Araya B, Maringanti C, Valcarcel AT, Rakotomalala L, Rochon HS, Mbongo BH, Thiam T (2010) Best management practices (BMPS) for corporate, academic and governmental transfer of sustainable technology to developing countries. Clean Technologies & Environmental Policy 12(1):19–30, February, 2010. Springer. doi:10.1007/s10098-009-0218-3. http://www.springerlink.com/content/103074/?Content+Status=Accepted&sort=p_OnlineDate&sortorder=desc&v=expanded

Rochon GL, Niyogi D, Chatturvedi A, Madhavan K, Arangarasan R, Biehl L, Quansah J, Fall S (2008) Adopting multisensor remote sensing datasets and coupled models for disaster management. In: Nayak S, Zlatanova S (eds) Remote sensing and GIS technologies for monitoring and prediction of disasters. Springer, Heidelberg

Rochon GL, Johannsen C, Landgrebe D, Engel B, Harbor J, Majumder S, Biehl L (2004) Remote sensing for monitoring sustainability. In: Sikdar SK, Glavič P, Jain R (eds) Technological choices for sustainability. Springer, Berlin, Heidelberg

Rogers DJ, Myers MF, Tucker CJ, Smith PF, White DJ, Backenson PB, Eidson M, Kramer LD, Bakker B, Hay SI (2002) Predicting the distribution of West Nile fever in North America using satellite sensor data. Photogramm Eng Remote Sens 68:112–114

Rogers DJ, Randolph SE (1991) Mortality rates and population density of tsetse flies correlated with satellite imagery. Nat 351:739–741

Rogers DJ (2000) Satellites, space, time and the African trypanosomiases. Adv Parasitol 47: 129–171

Rogers DJ, Randolph SE (1994) Satellite imagery, tsetse flies and sleeping sickness in Africa. Sistema Terra Year III:40–43

Rogers DJ, Randolph SE, Snow RW, Hay SI (2002) Satellite imagery in the study and forecast of malaria. Nat 415:710–715

Rogers DJ, Hay SI, Packer MJ (1996) Predicting the distribution of tsetse flies in West Africa using temporal Fourier processed meteorological satellite data. Ann Trop Med Parasitol 90: 225–241

Rotela C, Florence F, Mario L, Phillipe S, Virginia I, Mario Z, Scavuzzo C (2007) Space–time analysis of the dengue spreading dynamics in the 2004 Tartagal outbreak, Northern Argentina. Acta Trop 103(1):1–13

Scawthorn C, Blais N, Seligson H, Tate E, Mifflin E, Thomas W, Murphy J, Jones C (2006) HAZUS-MH flood loss estimation methodology. I: Overview and flood hazard characterization. Nat Hazards Rev 7(2):60–71

Spear RC, Gong P, Seto E, Zhou Y, Xu B, Liang S, Davis D, Gu X (1998) Remote Sensing and GIS for schistosomiasis control in mountainous areas in Sichuan, China. Geogr Inf Syst 4(1–2):14–22

Segerström U, von Stedingk H (2003) Early-Holocene spruce, Picea abies (L.) Karst., in west central Sweden as revealed by pollen analysis. Holocene 13(6):897–906

Srivatsava A, Nagpal BN, Saxena R, Subbarao SK (2001) Predictive habitat modeling for forest malaria vector species An. Dirus in India – A GIS based approach. Curr Sci 80:1129–1134

Sudhakar S, Srinivas T, Palit A, Kar SK, Battacharya SK (2006) Mapping of risk prone areas of kala-azar (visceral leishmaniasis) in parts of Bihar State India: an RS and GIS approach. J Vector Borne Dis 43:115–122

Šumilo D, Bormane A, Asokliene L, Lucenko I, Vasilenko V, Randolph S (2006) Tick-borne encephalitis in the Baltic States: identifying risk factors in space and time. Int J Med Microbiol 296(1):76–79

Tappan G, Hadj A, Wood E, Lietzow R (2000) Use of argon, corona, and Landsat imagery to assess 30 years of land resource changes in west-central Senegal. Photogramm Eng Remote Sens 6:727–735

Tatem AJ, Goetz SJ, Hay SI (2004) Terra and Aqua: new data for epidemiology and public health. Int J Appl Earth Obs Geoinf 6(1):33–46

Thomson MC, Obsomer V, Dunne M, Connor SJ, Molyneux DH (2000) Satellite mapping of Loa Loa prevalence in relation to ivermectin use in West and Central Africa. The Lancet 356(9235):1077–1078

Thomson MC, Connor SJ (2000) Environmental information systems for the control of arthropod vectors of disease. Med Vet Entomol. 14:227–244

Thomson MC, Connor SJ, Milligan PJM, Flasse SP (1996) The ecology of malaria seen by earth-observation satellites. Ann Trop Med Parasitol 90:243–264

Thomson MC, Molesworth AM, Djingarey MH, Yameogo KR, Belanger F, Cuevas LE (2006) Potential of environmental models to predict meningitis epidemics in Africa. Trop Med Int Health 11(6):781–788

Tran A, Ponçon N, Toty C, Linard C, Guis H, Ferré J-B, Seen DL, Roger F, Rocque S, Fontenille D, Baldet T (2008) Using remote sensing to map larval and adult populations of Anopheles hyrcanus (Diptera: Culicidae) a potential malaria vector in Southern France. Int J Health Geogr 7:9 doi:10.1186/1476-072X-7-9. Open access: http://www.ij-healthgeographics.com/content/7/1/9

Tralli DM, Blom RG, Fielding EJ, Donnellan A, Evans DL (2007) Conceptual case for assimilating interferometric synthetic aperture radar data into the HAZUS-MH earthquake module. IEEE Trans Geosci Remote Sens 45(6):1595–1604

Tran A, Gordon J, Weber S, Polidori L (2002) Mapping disease incidence in suburban areas using remotely sensed data. Am J Epidemiol 156:662–668

US Army Corps of Engineers (USACE) (2002) HEC-RAS: river analysis system. hydraulic reference manual, version 3.1. Hydrologic Engineering Center, Davis, CA

Verdin J, Funk C, Senay G, Choularton R (2005) Climate science and famine early warning. Philos Trans R Soc Lond Biol Sci 360(1463):2155–2163

Vickery PJ, Lin J, Skerlj PF, Twisdale LA Jr, Huang K (2006) HAZUS-MH hurricane model methodology. I: hurricane hazard, terrain, and wind load modeling. Nat Hazards Rev 7(2): 82–93

Vickery PJ, Skerlj PF, Lin J, Twisdale LA Jr, Young MA, Lavelle FM (2006) HAZUS-MH hurricane model methodology. II: damage and loss estimation. Nat Hazards Rev 7(2):94–103

Wagner VE, Hill-Rowley R, Narlock SA, Newson HD (1979) Remote sensing: a rapid and accurate method of data acquisition for a newly formed mosquito control district. Mosq News 39: 282–287

Welch JB, Olson JK, Hart WG, Ingle SG, Davis MR (1989) Use of aerial color-infrared photography as a survey technique for Psorophora columbiae oviposition habitats in Texas ricelands. J Am Mosq Control Assoc 5:147–160

Willyard C (2007) Simpler tests for immune cells could transform AIDS care in Africa. Nat Med 13(10):1131

World Health Organization (2007) Fact sheet N°266, Geneva

Wu W, Davis GM, Liu H, Seto E, Lu S, Zhang J, Hua Z, Guo J, Lin D, Chen H, Gong P, Feng Z (2002) Application of remote sensing for surveillance of snail habitats in Poyang Lake, China. Chin J Parasitol 20:205–208

Xiao X, Gilbert M, Slingenbergh J, Lei F, Boles S (2007) Remote sensing, ecological variables, and wild bird migration related to outbreaks of highly pathogenic H5N1 Avian Influenza. J Wildl Dis 43(3):S40–S46

Zhou X, Hu X, Sun N, Hong Q, Sun L, Lu G, Fuentes M, Malone JB (1999) Application of geographic information systems on schistosomiasis surveillance II. Predicting transmission intensity. Chin J Schistosomiasis Control 11:66–70

Zhou XN, Hu XS, Sun NS, Hong QB, Sun LP, Fuentes M, Malone JB (1998) Application of geographic information systems on schistosomiasis surveillance I. Application possibility of prediction model. Chin J Schistosomiasis Control 10:321–324

Index

N. Hoalst-Pullen, M.W. Patterson (eds.), *Geospatial Technologies in Environmental Management*, Geotechnologies and the Environment 3, DOI 10.1007/978-90-481-9525-1,